Lower Kuiseb River sediments and their control on dust emission

In partial fulfilment towards a Masters in Philosophy of Environmental, Society and Sustainability

Johanna RC von Holdt

VHLJOH002

Supervisor: Dr Frank Eckardt

December 2013

Abstract

Previous studies, using remote sensing, have identified the Kuiseb River in Namibia as the dustiest river in Southern Africa. Dust plumes detected from this basin are mostly associated with the Lower Kuiseb River, between the end of the bedrock canyon at Natab and the Kuiseb Delta towards the Atlantic Ocean. The purpose of this study was to examine the surface materials of the Lower Kuiseb River and establish their potential towards dust production, leading to such plumes. This investigation focused predominantly on the size characteristics of 153 surface sediment samples collected from the Kuiseb main channel, its terraces, delta, gravel plain surfaces and tributaries, dunes and interdune, all of which were analysed using a Malvern Mastersizer 2000 laser diffractometer. In addition, other sediment characteristics such as mineralogy, organic matter content, soluble salts; and selected surface roughness elements were also considered. Furthermore MODIS satellite imagery was used to assess the dust emission activity from each of the geomorphological units sampled in the field for the period from 2005 to 2013.

This study has demonstrated surface sediments suitable for dust production to increase towards the coast with particular "dusty" floodplain surfaces between Swartbank and Rooibank, as well as the Kuiseb Delta. It appears that silt crusts formed as the flood water dissipate, provide a main source of appropriately sized material for deflation. The crusts consist entirely of silt and clay sized material, with a maximum of 97% <63µm, 39% <10µm and 6% <2µm. Dust producing surfaces of the gravel plain include the gravel plain drainage, which has the largest quantity of clay sized material (maximum of 11% <2µm). Anthropogenic disturbances of the surface are likely playing a role in the production of dust, with livestock farming causing a fragmentation of crusts in the river valley, and mining and off-road driving disturbing the gravel plain.

Table of Contents

Acknowledgements

I am very grateful for the opportunity to have been part of the MPhil programme at UCT. It has been an incredible learning experience. I was fortunate to attend the SAAG conference in September 2012 at Gobabeb. This fortuitously provided the opportunity to consult a number of Namib and dust experts in person. I thank them all for willingly sharing their knowledge.

My sincere gratitude to the staff at the Gobabeb Training and Research Centre for all their assistance in conducting this research, especially Sebedeus Swartbooi, Lahja Tjilumbu and Dr Mary Seely. A thank you also to Peter Bridgeford of Walvis Bay for taking me into the delta on one of the wettest days in recorded history. His knowledge and experience as a veteran of the area proved to be of great use. Dankie aan Oom Willie Korumeb vir die huur van sy donkie kar vir die ekspedisie in die delta, asook sy gewilligheid om sy kennis van die area met my te deel.

Thank you to Dr Frank Eckardt who patiently helped me turn randomness into order. Thank you for all your guidance, time and expertise.

Thank you to Dr Lesego Khomo and Scott Yammin for their assistance with the field work and sampling conducted in September, 2012. Thank you to Dr Khomo for sharing his knowledge, opinions and laboratory.

Thank you also to Kate Vickery for her knowledge and assistance (sometimes from far away).

Thank you to Prof Mike Meadows who afforded me the opportunity to go to Gobabeb and also acquired the Malvern Mastersizer, which formed a vital part of this study.

Thank you to Martin Turner, Esbe van Assen and Prof Pat Harris who taught me a lot and continue to do so enthusiastically.

Lastly, a huge thank you to my family for supporting me during the last two years. To my husband, Chris and two kids, Catherine and William, thank you for your patience and understanding. My children have loved this research as much as I have.

List of Figures

List of tables

List of Abbreviations

AASHTO: American Association of State Highway and Transportation Officials

ISO: International Organisation for Standardisation

MODIS: Moderate Resolution Imaging Spectroradiometer

USDA: United States Department of Agriculture

1 Introduction

The ephemeral lower Kuiseb River in the Namib Desert has been identified as one of the dustiest rivers in Southern Africa, which in part is a response to summer floods (Eckardt et al., 2005; Vickery et al., 2013). These originate in the headwaters situated in the Khomas Hochland and terminate in the lower Kuiseb River. As water dissipates, sediments brought from upstream are deposited. This supply of sediments to the downstream reaches of the river has been suggested to be the dominant source of the dust which is produced during high magnitude winds that occur in winter (Eckardt et al., 2005).

Prospero et al. (2002) maintain that most of the world's dust emission sources are situated in arid regions, in topographic lows or adjacent to topographic highs and that all such sources are associated with fluvial activity. For some dust sources, the fluvial activity plays an active role in the dust activity of the system at present. For others, the fluvial activity occurred in the past and served to build up a reserve of supply sediment that under present conditions is available for deflation. The Bodélé depression in Chad is one example of a system that accumulated a supply of lacustrine sediment in Paleolake Megachad before it dried out about a thousand years ago (Bristow et al., 2009). Under the present hyper-arid conditions devoid of vegetation, the supply source of diatomite is extremely erodible and currently makes the Bodélé depression one of the largest sources of dust in the world (Washington et al., 2006).

One of the reasons that the Bodélé depression is regarded as the largest global source of dust is the consistency of its surface features. The supply of sediment for deflation is permanently present and available, waiting for the transport capacity of the wind to pick it up and blow it away. Most dust sources around the world do not show this consistency and rely on the opening of specific spatial and temporal windows for the system to emit dust. The majority of dust-source areas around the world produce dust on an intermittent basis, when there is a supply of appropriate sediment that is available for deflation and once the wind energy is sufficient to entrain the sediment. Dust emission takes place when the driving forces of dust emission are larger than the resistive forces (Gillies, 2013).

The surface features of a system are an important controlling force of dust activity, capable of both driving and resisting deflation. These features include surface moisture content, soil characteristics (including texture and mineralogy) and roughness elements, including vegetation. The dust source areas identified globally consist of a number of different

geomorphological units made up of a wide range of surface features. The surfaces associated with dust emission are dynamic, and deflation mechanisms from these surfaces are complex and often not well understood.

The Kuiseb River basin comprises many geomorphological units and a large variety of surface features, many of which are associated with fluvial activity, both past and present. Aeolian activity for this region has been identified with MODIS satellite imagery and is associated with the lower river, the delta and to a lesser extent the gravel plain (Vickery et al., 2013). Dust activity for this region occurs on an intermittent basis, similar to other global source areas. The surface features of the geomorphological units or landforms of the Kuiseb River basin will be an important factor in the dustiness of the area, capable of being either a resisting or a driving force (Gillies, 2013). The influence of these surface features on dust activity within the area has not been subject to ground based studies.

Aeolian or windblown dust has a significant influence on earth processes. In the last two decades there has been a surge in research efforts surrounding aeolian dust. This is a result of the realisation of the magnitude of the impact of dust on both past, present and probably most importantly future land, atmospheric and ocean processes. Two important components of the research into dust are how dust affects humans and how dust generation is affected by humans. The Lower Kuiseb River falls within the Erongo region in Namibia and this region has seen a significant increase in anthropogenic activities over the last few decades, specifically in the form of mining and tourism. It has yet to be determined to what extent these activities have affected the dustiness of the Kuiseb River area.

2 Literature review

2.1 Characteristics of dust and dust emission

Windblown (also referred to as aeolian) sediments are entrained, transported and deposited by the wind (McTainsh et al., 2013). The mode by which sediments are moved by the wind generally depends on the size of the sediment and the power of the wind. Larger-sized particles, such as coarse sand (>500 µm), generally undergo creep, whereby particles are rolled along the surface. Fine- to medium-sized sand particles (100-500 µm) undergo saltation, which entails moving in short hops horizontally along the surface. Conversely, dust particles undergo suspension within the flow of air. Particles that undergo suspension are generally regarded as being <100 µm (McTainsh et al., 2013). The size of the particles undergoing the three different modes of movement can vary substantially depending on the strength of the wind. Figure 1 from Pye (1987) provides a graphical representation of the three modes of movement, with additional detail for each mode.

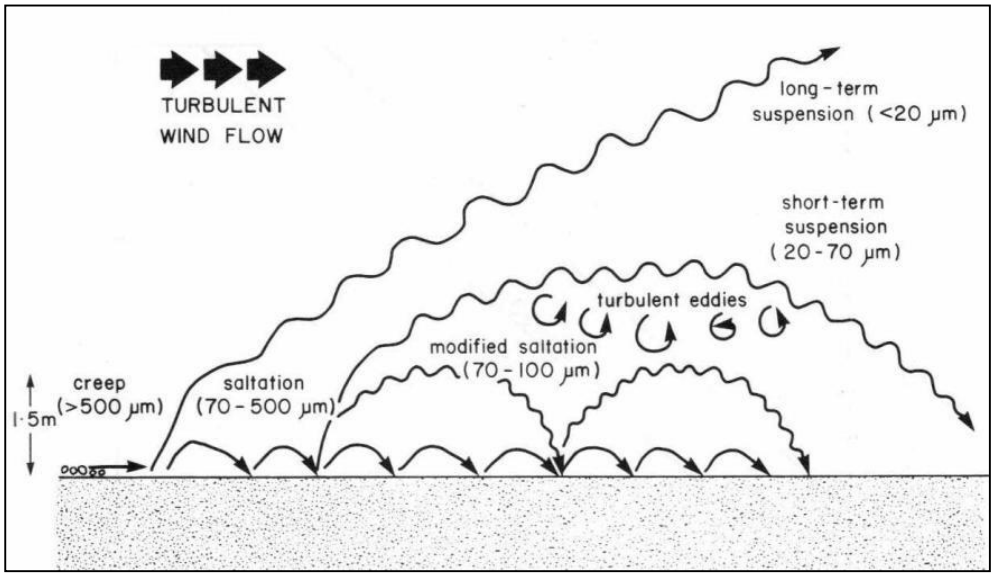

Figure 1 Modes of particle transport by wind (Pye, 1987)

Aeolian dust research generally regards the clay and silt sized fractions as having the potential to become entrained by suspension in the wind (Goossens et al., 2002). Depending on which classification system is used, the cut off for silt can be either at 50 µm (e.g. AASHTO and

USDA) or 63 µm (e.g. ISO-14688-1 and Wentworth). For the purposes of this study the size classes will be as follows: clay: <2 µm; silt: 2-63 µm; sand: 63-2000 µm.

The deposition of the entrained sediments can either be local, regional or global depending on the distance from the sediment source area. Lawrence et al. (2009) compiled a data set of dust observation studies from research published in peer-reviewed literature. For the purposes of their study, the authors classified dust emission observations as local if deposition was located between 0-10 km from the source area, regional if deposition took place between 10-1000 km and global if deposition occurred >1000 km from the source area. By looking at the particle size distributions of the dust for each of these areas, Lawrence et al. (2009) concluded that local dust deposition consists predominantly of coarse silts and/or fine sands, with 10-60% of the particles being >20 µm (by mass). Local dust also contains large fractions of fine silt (25-60%) and clay, making up about 10-40%. Regional dust on the other hand consists of less coarse silt and fine sands and a larger proportion of fine silt, but it has a clay content similar to local deposition. Global deposition was found to consist entirely of silts and clays. Figure 2 from Lawrence et al. (2009) provides a summary of the particle sizes coupled with the distance to deposition described above. The authors highlight that silt-sized particles appear to be the most suited for atmospheric transport at all scales and that larger particles (>10µm) play a significant role.

Deposition class	*n*	Distance from source	Deposition rate	Particle size
		km	g m^{-2} yr^{-1} (mean)	% clay, silt, sand
Local	11	0–10	50 – 500 (200)	20, 50, 30
Regional	28	10–1000	1 – 50 (20)	25, 60, 15
Primary			25 – 50	
Secondary			1 – 25	
Global	13	>1000	0 – 1 (0.4)	30, 70, 0

The deposition range of the regional class is further divided by source region strength (primary or secondary).

Figure 2 Particle size characteristics of three categories of distance to deposition from Lawrence et al. (2009).

A number of studies have highlighted the importance of saltation and sandblasting for dust emission from a soil surface, initially identified by Bagnold (1941). The saltation of sand sized particles with sufficient wind velocity bombards the soil surface and is able to dislodge the finer silt and clay particles. The entrainment of the silt and clay particles is extremely difficult

to achieve with the aerodynamic force of the wind alone due to the strong cohesive bonds between these small particles (Houser et al., 2001). Despite the majority of studies pointing to the importance of the presence of appropriately sized saltators to release fine material from a soil surface (Shao et al., 1993; Cahill et al., 1996; Houser et al., 2001), there have been studies that observed the entrainment of fine sediment in the absence of saltation (Kjelgaard et al., 2004; Baddock et al., 2011).

Equally important is the erodibility of particles within the 70-125 µm size range. Several studies have concluded that sediment within this size range is most easily entrained by the wind (Pye et al., 1990; Bagnold, 1941; Goossens et al., 2002). In addition to the velocity of the wind and the presence of sand sized particles, the strength of the surface being bombarded will influence the quantity and particle size distribution of the entrained dust. Dust emission from an area therefore depends on a complex interplay between the transport capacity of the wind, the supply of appropriately sized sediment and the availability of the sediment to be entrained. The Kuiseb River floods deposit large amounts of silt-sized sediments in the lower sections of the river (Jacobson et al., 2000). The suitability of the flood sediment for deflation, as well as the extent and availability of the sediment supply, still has to be determined. In addition, the dune fields of the Namib Sand Sea provides an unlimited supply of appropriately sized saltators. However, it is not known if these sediments will be available in all the geomorphological units of the basin.

2.2 Forces of dust emission: driving and resistive

The distribution of dust in time and space varies and is determined by one of the following components within a system (Bullard et al., 2011):

a) Supply: the supply of appropriately sized sediment to areas where it can be entrained, i.e. deltas, floodplains.
b) Availability: the sediment is present within the system but is not readily available for entrainment due to the surface characteristics, for example the presence of vegetation and surface soil moisture.
c) Transport: sufficient wind energy to entrain the sediments if they are present.

A dust producing area can be controlled by a combination of these components.

The transport capacity is primarily controlled by the frequency and magnitude of the winds capable of entraining particles. For many dust producing areas, the transport capacity controls the temporal variation of the dust activity. For instance, the dust activity from the Namib Desert coastline takes place predominantly in winter, from April to August, as a result of the high-magnitude, low-frequency north-easterly winds (Vickery et al., 2013).

The availability is mainly dependent on the surface features of the area, which can in turn be identified at two levels: small-scale surface characteristics on one level and surface roughness on the other (Gillies, 2013). Small-scale surface characteristics entail mostly particle-to-particle interactions that inhibit entrainment by the wind. These particle interactions involve the interparticle bonds between the particles present in the sediment. The binding energy between particles is affected by particle size distribution (soil texture), moisture content, mineralogy (specifically salt and clay content) and organic matter (Webb et al., 2011; Gillies, 2013). An important surface characteristic for dust emission that has been the focus of many research studies are surface crusts (Gillette et al., 1982; Belnap et al., 1997; Goossens, 2004; Baddock et al., 2011). Surface crusts are normally divided into two broad categories: physical and biological crusts (Strong et al., 2004). Physical crusts are again divided into structural crusts, which are formed by the impact of raindrops, and depositional crusts, which are formed when fine particles suspended in water are moved and deposited some distance away. Biological crusts are formed by biological activity at the surface, including cyanobacteria, fungi, mosses, algae and lichens (Zhang, 2005). The strength of the surface crusts to withstand erosion by the wind is dependent on the composition of the crusts and the binding forces between the different components, e.g. salt, clay, organic matter, and so forth.

The surface roughness is another aspect that controls the availability of sediment and hence dust activity. Its effects can be either aerodynamic or physical (Gillies, 2013). Aerodynamic effects are due to the alteration of the flow properties of the wind by the roughness elements, whereas physical effects are due to the interaction of moving sediment with the roughness elements. Roughness is the variability of surface elevation and varies from the millimetre to kilometre scale (Sankey et al., 2011). At a micro-scale, the roughness can be as a result of elements such as salt crusting or a gravel overlay. At the meso-scale, the roughness incorporates vegetation, ranging from grasses to shrubs to trees. Topographical roughness starts playing a role at the macro-scale and can involve landscape elements such as hills, dunes and rocky outcrops. The relationship between dust emission and roughness is complex. Whether the roughness enhances or reduces emission from a given surface will vary depending

on the scale of the roughness elements and also on the distribution of the roughness elements. At the micro-scale, aerodynamic roughness lengths (Z_0) of more than 0.1 cm have the potential to significantly reduce dust emission by increasing the threshold friction velocity of the surface (Gillette, 1999). On the other hand, Sankey et al. (2011) demonstrated that a positive relationship exists between dust emission and surface roughness at the sub-meter spatial scale, in the absence of non-erodible roughness elements such as vegetation. By contrast, Sankey et al. (2010) concluded that an inverse relationship exists between erosion and surface roughness at the meter-kilometre scale.

The influence of vegetation on dust emission is due to the protection it affords the soil surface from the wind either by sheltering the surface or by the momentum extracted from the wind. Vegetation can also trap the deflated soil particles and thereby act as a deposition site for sediments (Okin et al., 2006). Traditionally, vegetation as a roughness element has been quantified by a parameter called lateral cover, λ. Lateral cover gives an indication of the plant cover and is calculated by the relationship: $\lambda = NA_p$, where N = the number density of the plants and A_p = the area of each plant projected onto a plane perpendicular to the surface or, otherwise stated, the area of the plant when viewed in profile (Okin, 2008). Although this parameter provides a fairly simple means of accounting for the vegetation of an area, it does not take into account the distribution of the vegetation. To illustrate the consequences of using this parameter, we use what Okin (2008) called the "telephone" problem. Both surfaces in Figure 3 will have the same lateral cover.

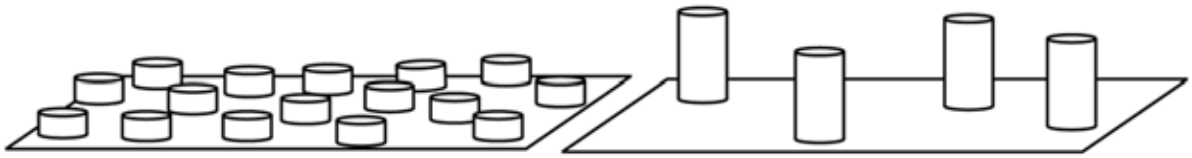

Figure 3 Lateral cover, λ, as a measure of representing vegetation. Both surfaces have the same lateral cover. From Okin (2008).

Lateral cover has been used as a measure of representing non-erodible roughness elements in aeolian research since the 1970s (Okin, 2008). More recent research has illustrated that dust emission from an area exhibits a strong relationship with vegetation distribution and that areas in between vegetated patches could experience increased dust deflation (Gillette et al., 2006; Okin et al., 2006). Okin (2008) maintains that wind erosion and the resultant dust emission can

occur at relatively high lateral cover and suggests a new model incorporating the size and distribution of the unvegetated gaps to characterise the surface.

Dust emissions are predominantly related to surface characteristics such as soil texture, moisture content and mineralogy as well as to roughness elements and could therefore potentially be important resistant forces against the driving force of the wind. The interplay between the resistant and driving forces is complex and controls the emission of dust from a source area (Gillies, 2013). Webb et al. (2009) provide a useful summary of the controls of the erodibility of soil. These controls operate at various scales. In addition to the surface characteristics and roughness of an area, land use and management can also have important consequences for the dust activity of an area on a regional scale.

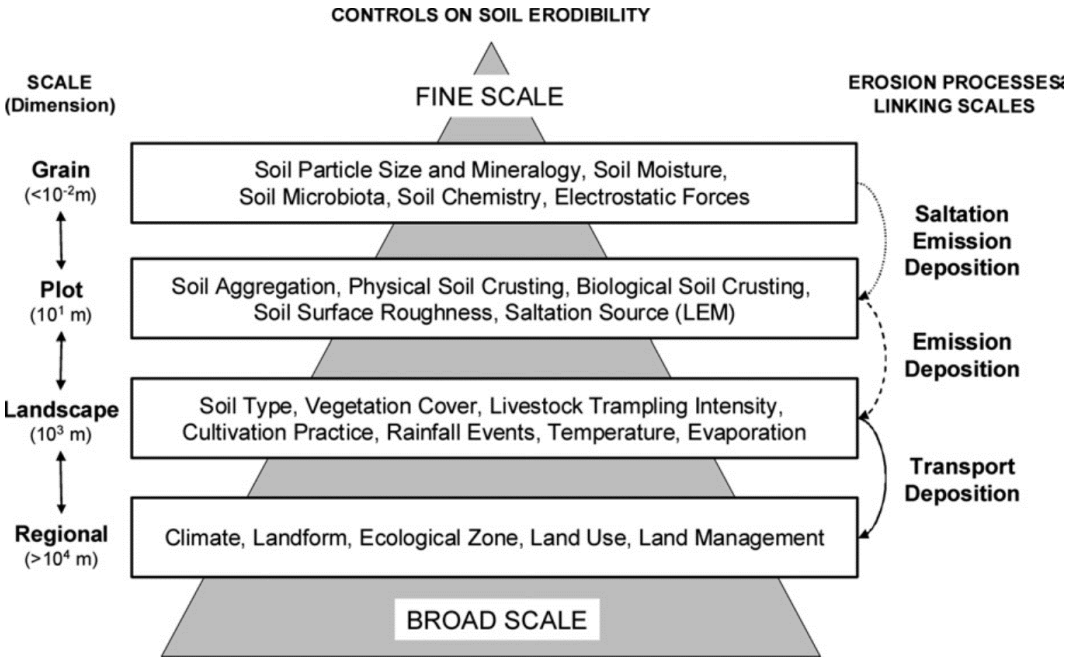

Figure 4 Controls on soil erodibility from Webb et al., 2011

2.3 Disturbance mechanisms and the anthropogenic factor

Disturbance of the surface characteristics and roughness could substantially modify the dust activity of a region by altering the resistive forces of the system. Very often such disturbances are linked to human activities. These disturbances can be direct and result in the destruction of the physical bonds between particles, making more sediment available for deflation (Gillies,

2013). Disturbances of this nature include tracks made by off-road vehicles, trampling by livestock and wildlife, and mining and its associated exploration activities.

There are also various disturbances that indirectly affect the dust emission capacity of an area. Indirect disturbances do not directly result in the breaking of bonds between particles but instead affect the surface characteristics and roughness, as a result of a change in the components of the system other than the supply sediment. Such disturbances could be as a result of a change in vegetation cover, which could either reduce or enhance dust activity. A reduction in vegetation could be as a result of overgrazing by livestock or overharvesting of plants by humans. The abstraction and diversion of water can also have consequences for the availability of dust. The desiccation of the Aral Sea was as a result of the diversion of water for large-scale agricultural activities from the 1960s and 1970s. The extremely large dried up lake area is the source of exposed saline sediment, which makes this area a famous (or rather infamous) saline dust field of the world (Abuduwaili et al., 2010).

2.4 The landscape of deflation

Rivers have been associated with dust emission in many parts of the world, mostly in low-slope internally draining environments, where the low-energy flow is conducive to deposition of sediments (Koven et al., 2008). The creation of these dust sources can be due to past fluvial processes or active ephemeral rivers (Koven et al., 1997). The dominant source areas of dust are in most instances not the riverbed or terraces. Instead, the river provides a pathway for fluvial sediment transported to downstream source areas of dust; including deltas, lakes and dune fields. Some examples are the inland delta formed by the Niger River in Mali (McTainsh et al., 1997), the Heihe River in north-western China (Wang et al., 2004), the ephemeral river systems of the Lake Eyre and Murray-Darling basins in Australia (Bullard et al., 2003), Owens River draining into Owen (dry) Lake in California (Cahill et al., 1996) and the ephemeral channels draining into Etosha Pan (Bryant, 2003). The lower Kuiseb River is an active ephemeral river for which the river channel, together with the delta and playas, have been proposed as a potential source area of dust (Vickery et al., 2013). This research study will assess the potential of the various geomorphologies or landforms present within the Kuiseb River basin to act as dust sources. This investigation will include the river terraces and riverbed.

Several researchers have attempted to assess the emission potential of different landforms within the larger dust producing regions using a variety of methods. Sweeney et al. (2011)

measured dust emissions from eight common desert landforms within the eastern Mojave Desert, USA. Wang et al. (2005) studied the surface sediments of five representative geomorphological ground surfaces in an attempt to identify the potential source areas of dust in the Badain Jaran Desert in North-western China. Bullard et al. (2008) attempted a sub-basin scale investigation of the Lake Eyre Basin in Australia by looking at the five main potential source geomorphologies found within this region. These studies highlight the different roles that sub-basin geomorphologies or landforms play in the dust emission potential of a region.

2.4.1 Geomorphological units associated with deflation

The three different research studies mentioned above investigated the potential of the different desert landforms present within each study area to act as a source area of dust. The three studies were situated in different parts of the world and also employed different methods to assess the potential dust emission from the various landforms. Wang et al. (2005) studied five landforms extensively distributed in the Badain Jaran Desert and its margin in North-western China. This study used surface samples analysed for particle size distribution (laser diffraction), mineral composition (SEM and XRF) and elemental composition (ICP-AES) to evaluate the dust potential of each landform. Sweeney et al. (2011) used a PI-SWERL (Portable In-Situ Wind Erosion Lab) to measure the dust emission from eight common landforms in the eastern Mojave Desert in California, USA. The PI-SWERL measures wind erosion and dust emission potential by the rotation of a ring that produces adjustable shear stress to entrain particles at different friction velocities. The concentration of particles <10 μm (mg m^{-3}) is measured and converted to emission flux (mg m^{-2} s^{-1}) (Sweeney et al., 2011).

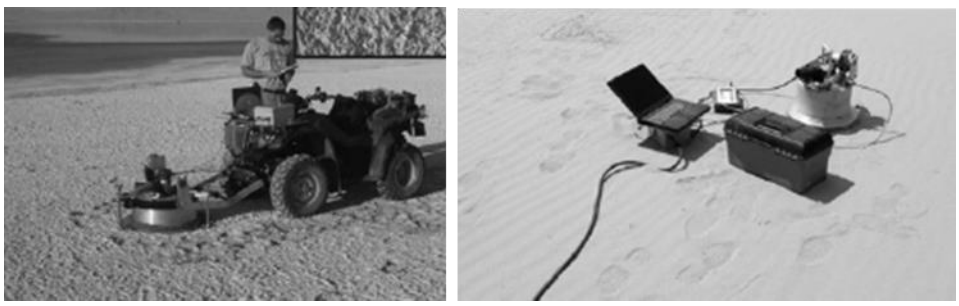

Figure 5 Two versions of the PI-SWERL used by Sweeney et al., 2011.

Bullard et al. (2008) conducted a sub-basin scale analysis of the Lake Eyre Basin in Australia using MODIS imagery to identify the major dust source landforms. The different landforms or geomorphological units investigated in each of these studies are summarised in Table 1:

Table 1 Landforms investigated by three different studies in three different parts of the world with different methods.

Wang et al., (2005)	Sweeney et al., 2011	Bullard et al., 2008
1. Gobi desert	1. Desert pavement	1. Gibber – stone covered plains
2. Lacustrine sediment	2. Distal alluvial fans	2. Alluvial channels and deposits
3. Mobile dune	3. Dry ephemeral washes	3. Ephemeral lakes, playas and claypans
4. Shrub dune	4. Playas with silt crust	4. Aeolian sand deposits – divided into sand sheets and dunes (divided into sand dunes with sandy interdunes and sand dunes with interdune pans)
5. Deteriorated land	5. Playas with silt-clay crust	5. Plains and low hills, including bedrock and duricrust
	6. Playa margin	
	7. Sand dunes	
	8. Beaches	

Sweeney et al. (2011) identified dry, ephemerally active washes as the largest dust emitters within the study area due to the large particle size range found within the channels, including loose sand, which bombards the silt-rich sediment. Other large dust emitters included vegetated, stabilised dunes, distal alluvial fans and playa margins. The lowest emitters were desert pavements protected by gravel overlays (with a gravel cover >75%), playas with salt crust caused either by soil moisture or by the presence of hard surface crusts, and playas with silt-clay crusts. The salt crusts are, however, able to act as a short-term source of dust. A mechanism proposed for dust emission from salt-crusts is the suspension of efflorescent salts

directly from the surface (Reynolds et al., 2007). In addition, the playas with silt-clay rich crusts are able to emit large quantities of dust when there are loose particles (specifically from mud cracks) and saltating sand to dislodge silt-clay particles from the crusted surfaces (Sweeney et al., 2011). An important finding from this study was not only the potential for dust emission of the different landforms, but also the variation in dust emission within each landform. Figure 6 shows the variation in results obtained from the PI-SWERL for each of the landforms tested and highlights the diverse dust emission potentials of a specific surface type under different conditions and in different states.

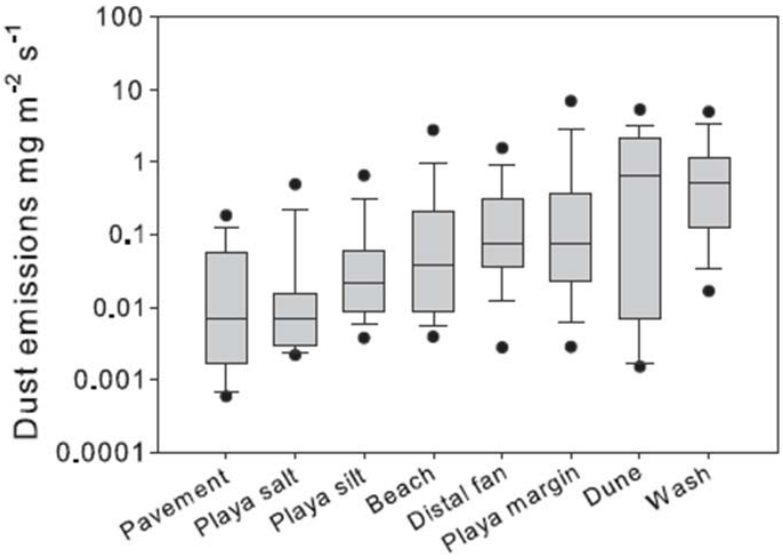

Figure 6 Dust emissions as measured with the PI-SWERL by Sweeney et al. (2011).

The portable size of the PI-SWERL enables it to measure potential dust emission from a variety of different landforms at the sub-meter scale. An important limitation of the PI-SWIRL is that it does not take into account the total possible size distribution of dust (Formenti et al., 2011).

Bullard et al. (2008) classified dust plumes evident on MODIS images as a point source (narrow if ≤10 km across or broad if >10 km across but still with sharp upwind edge) or a zonal source (>10 km with soft upwind margin). This study concluded that for the study period aeolian deposits, alluvial deposits/floodplains and ephemeral lakes were the dominant sources of dust. Gibber and plain areas accounted for the least dust activity (stony desert areas in Australia are referred to as Gibbers). The study by Bullard et al. (2008) emphasised the annual variation in dust plume sources. For the study period from 2003 to 2006, each year showed a

different geomorphology as the dominant dust source for the basin. Table 2 shows the percentage of plumes originating in each of the top three dust emitting geomorphologies.

Table 2 Percentage of plumes detected in each landform type within the Lake Eyre Basin from MODIS images from 2003-6 (Bullard et al., 2008).

	Aeolian deposits %	Ephemeral lakes %	Alluvial deposits %
2003/4	51.5	21.5	19.6
2004/5	30.8	37.3	27.3
2005/6	35.6	19.5	33.3

This inter-annual variation was ascribed to the response of each landform to different environmental conditions, such as variations in rainfall and wildfires. The high dust activity from aeolian deposits in 2003/4 followed extensive wildfires in 2001 and very low rainfall in 2001/2. This study also pointed to the influence of anthropogenic activities, such as livestock grazing, which can lead to a reduction in vegetative cover, which in turn leads to the reactivation of dunes.

The last study by Wang et al. (2005) concluded that lacustrine sediment, shrub dune, gobi desert and deteriorated land are the most likely sources of dust emission within the study area. They base their findings on the characteristics of the surface samples taken within each geomorphological unit. One of the characteristics measured were the fractions <50 μm, and their results are reproduced in Table 3.

Table 3 Percentages of particles <50 μm for each geomorphological unit from the study by Wang et al., 2005.

Alluvial and lacustrine sediments %	Gobi deserts %	Shrub dunes %	Mobile dunes %	Deteriorated land %
37-99	5-7	0.26-36	0.05-0.4	51-62

The Kuiseb River's geomorphological units can be investigated using a similar approach to the studies discussed above. Vickery et al. (2013) used MODIS imagery to identify potential source areas within the Kuiseb River region. As for the study by Bullard et al. (2008), this method lends itself to the identification of dust plumes on a scale of approximately 10 km and greater.

A ground-based study looking at the surface features of the potential source areas within the geomorphological units identified with MODIS is necessary to develop an understanding of the landforms that emit dust and the factors that make them emissive. The studies conducted by Sweeney et al. (2011) and Wang et al. (2005) are examples of such ground-based studies.

2.5 The significance of deflation

Aeolian dust has been shown to have various impacts on the earth's systems. The impact of the windblown dust can vary from local to global, depending on the transport capacity of the system. In addition, the physico-chemical properties of the dust such as size distribution, shape and composition will also influence the impact of the dust (Formenti et al., 2011). Dust from some source regions has the ability to travel great distances: dust deposits have been traced over 10,000 km from the Taklamakan Desert in China to Hawaii (Livingstone et al., 1996). It has also been hypothesised that dust from the Sahara could have an effect on the nutrient budgets of forest ecosystems in Ghana and the Amazon (McTainsh et al., 2007).

Knowledge of the different size fractions present in dust emissions could be useful when considering the impacts of dust. One has to bear in mind that the size distribution of the sediments has the ability to evolve dramatically once entrained by the wind (Formenti et al., 2011). The size fractions <30 µm and <50 µm have a significant influence on the biogeochemical cycles of the ocean and terrestrial systems (Xuan et al., 2002). Deposition of atmospheric dust often supplies large quantities of micro-nutrients to these systems. The influence of iron-rich dust on marine phytoplankton activity has also been proposed and is known as the "iron hypothesis" (McTainsh et al., 2007). Soderberg et al. (2007) found that mineral dust particles provide important nutrients to fynbos of the Cape Floristic Region in South Africa. Aeolian dust could have an effect on soil integrity, development and fertility at both the source and sink regions (Bullard et al., 2011).

The <10 µm dust has the ability to scatter and absorb solar and infrared radiation and hence has an influence on the earth's energy budget and climate (Xuan et al., 2002). The shape of the dust particles can have a significant influence on the scattering of radiation, with deviations from a spherical shape having a pronounced effect on the dust optical properties and hence the ability to scatter light (Formenti et al., 2011). Dust can also affect rainfall patterns by providing dust derived cloud condensation nuclei (McTainsh et al., 2007). Formenti et al. (2011)

emphasise that the ability for dust particles to act as cloud condensation nuclei is predominantly influenced by mineralogical composition, particularly the calcite content of the dust. Moreover, the <10 μm fraction can also have adverse effects on people's health, in particular causing respiratory ailments and infections and cardiovascular events (Griffin et al., 2004). Mineral dust components, such as quartz, are known to cause respiratory disease in highly exposed persons. Kanatani et al. (2010) confirmed in a study in Japan that mineral dust exposure is associated with an increased risk of hospitalisation for asthmatics. Increasingly, research indicates that atmospheric dust has the ability to transport bacteria, fungi, viruses and chemical contaminants from source to sink (and within the transport pathway). Chen et al (2010) investigated the long-range transport of influenza and avian influenza (H5N1) by dust storms. The authors concluded that the concentration of ambient influenza viruses was significantly higher during Asian dust storm days compared to background days.

Numerous other interactions between aeolian dust and global to local physical, chemical and biogeochemical processes have been suggested. Investigating the characteristics of the sediments of the Kuiseb River will assist in developing an understanding of the possible atmospheric, oceanic and terrestrial systems the dust could have an impact on. These characteristics include mineralogy and particle size.

2.6 Southern African dust sources

Vickery (2010) conducted a detailed study of the location of dust sources within Southern Africa using both MODIS and MSG satellite imagery. In addition to the Makgadikgadi and Etosha pans, traditionally regarded as the main Southern African source areas (Prospero et al, 2002; Washington et al, 2003), the Namibian Coast was identified as one of the most active sources within the region (Figure 7). This is in agreement with work done by Eckardt et al (2005).

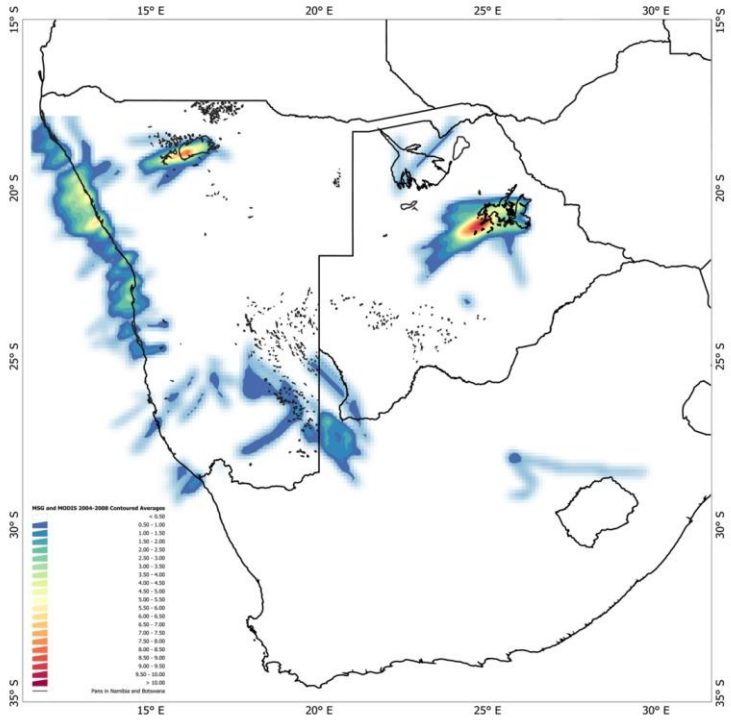

Figure 7 Dust plume activity over Southern Africa between 2005 and 2008 as identified by MODIS and MSG satellite imagery (Vickery, 2010).

Vickery et al. (2013) identified over 70 unique sources of dust along the Namibian coastline, all of which originated from ephemeral rivers and coastal pans. A total of 203 plumes were identified during the four-year study period, with 22 originating from the Kuiseb River catchment. This confirms earlier work done by Eckardt et al. (2005), who identified 150 dust plumes with the aid of SeaWiFS images for a three-year period from 1998. A total of 42 sources were identified, with 12 plumes originating from the Kuiseb River catchment. The Kuiseb River acted as one of the most active dust sources in both studies for the time periods under investigation.

There are 12 major ephemeral rivers situated along the Namibian Coastline (Figure 8). All these rivers originate in the higher rainfall highlands and drain west towards the Atlantic Ocean, at which point rainfall becomes insignificant (approximately 10 mm/year). River flow is isolated to a few times per year during the summer rainy season (and will reach the lower reaches of the rivers if enough rainfall occurs to generate floods that can overcome the transmission losses along the river course (Morin et al., 2009). All the West Coast Rivers deflate, as established by Vickery (2010), and this is often the only way sediments will reach

the ocean. Dust deflation occurs from the lower reaches of these rivers as they flow through the Namib Desert for the last hundred or so kilometres before reaching the Atlantic Ocean.

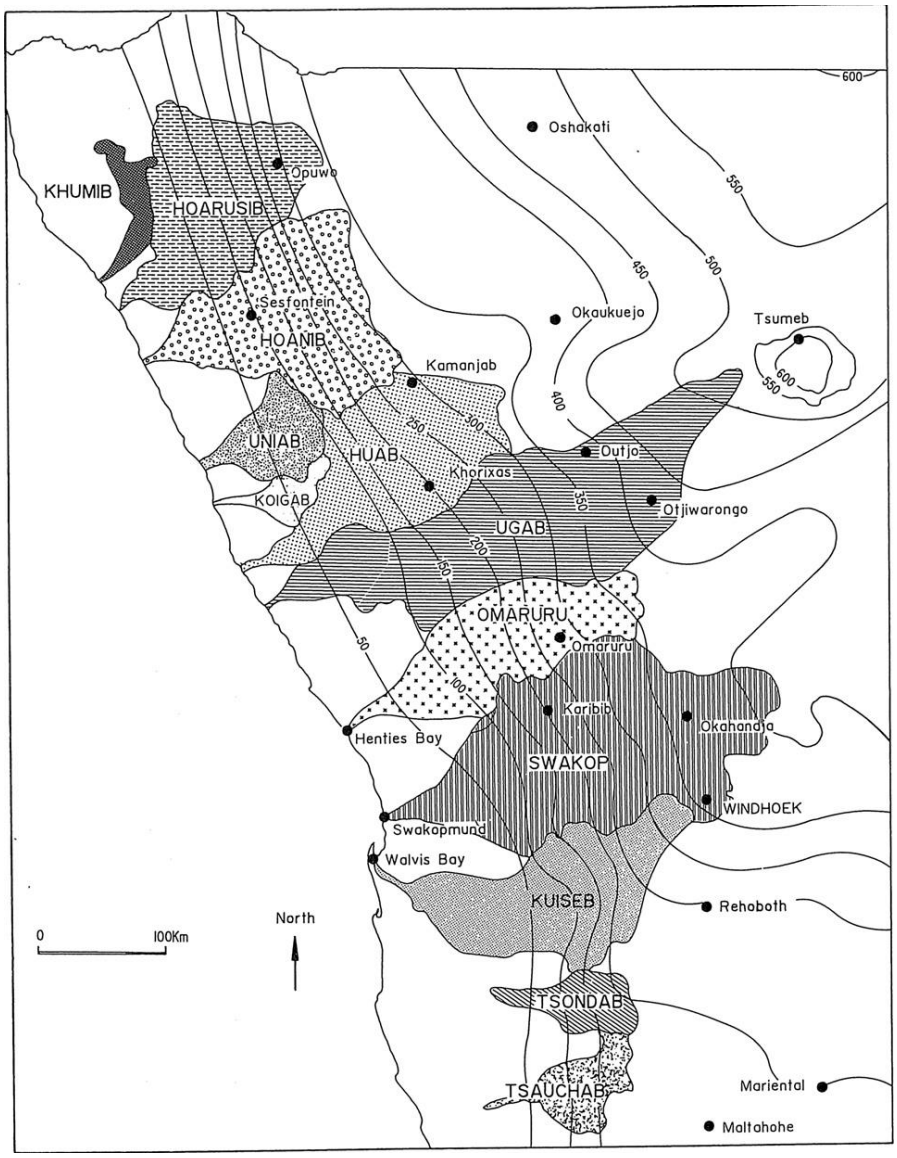

Figure 8 Major ephemeral catchments and mean rainfall isohyets (mm). Jacobson et al., 1995.

Several of the dust sources identified by Vickery (2010) were also associated with salt pans and salt flats. Along the length of Namib Desert a distinction is made between inland salt pans or playas and coastal salt flats or coastal sabkhas (Eckardt et al., 2001). The dust activity from the ephemeral rivers, playas and coastal sabkhas is highly visible on a MODIS true colour image used by Vickery (2010) to identify dust sources within Southern Africa (Figure 9). The ephemeral rivers of the Namib Desert are not regarded as the most important global sources of dust, but are nevertheless important regional dust sources in the Southern Africa context.

Figure 9 MODIS image for 17 June 2010 from the Terra satellite. Available from http://lance-modis.eosdis.nasa.gov/imagery/subsets/?subset=Namibia.

2.7 The Kuiseb River

2.7.1 Kuiseb River geomorphological units

The major geomorphological units of the Lower Kuiseb River include the main river, including channel and floodplain; the delta; the gravel plain; and Sand Sea, including dune fields and interdune areas (Figure 10).

Figure 10 The lower Kuiseb River and its geomorphological units. Image from Google Earth.

2.7.1.1 River

The headwater of the Kuiseb River is situated in the Khomas Hochland Mountains just to the west of Windhoek at approximately 2000 masl. The rainfall in the headwaters (250-350 mm/year) generates the flow that produces the floods downstream. The river flows down the escarpment in the Kuiseb River Canyon through schist bedrock, which can be up to 200 m deep and 35 m wide at the foothills (Morin et al., 2009). From the end of the canyon, the river morphology changes to a sandy alluvial channel. The rainfall drops significantly from approximately 150 mm/year at the top of the canyon to <25 mm/year as the river flows towards the delta. Figure 11 shows the annual total rainfall recorded at Gobabeb from 1962 to 2011, with an average rainfall at Gobabeb of 25 mm/yr for the period (Eckardt et al., 2012).

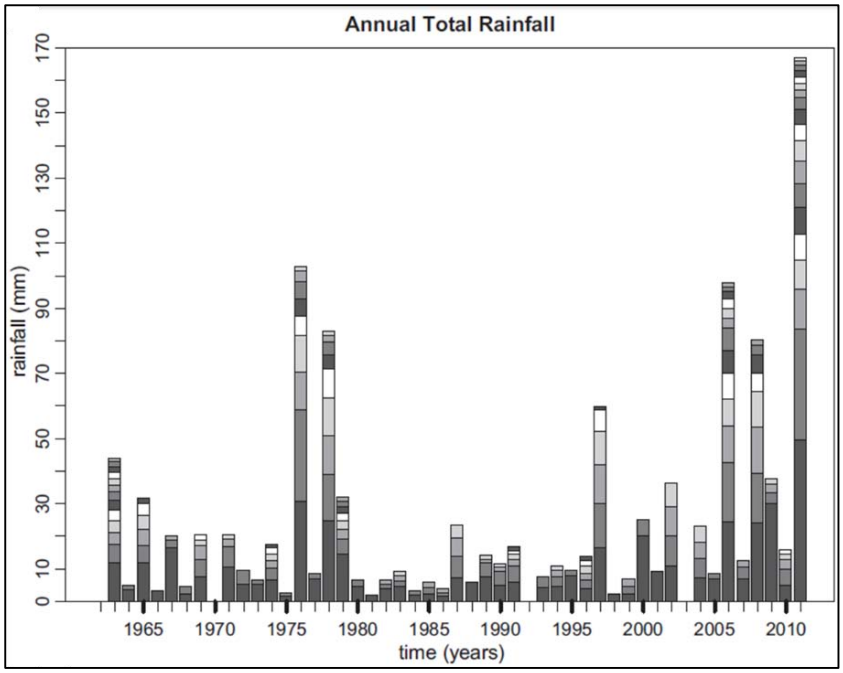

Figure 11 Annual total rainfall from 1962 to 2011 at Gobabeb taken from Eckardt et al. (2012). Different shading of the bars depict different rainfall days and associated accumulation amounts per day.

The Lower Kuiseb River has often been described as a linear oasis, with lush riparian vegetation situated within the river channel and/or on the floodplain (Huntley, 1985). The vegetation within the river plays an important role in the survival of many wildlife species within the area. The aquifer situated within the alluvium of the Kuiseb River enables the survival of the lush vegetation along the course of the river in this otherwise arid environment. The vegetation on the river results in high concentrations of particulate and dissolved organic matter that are transported and deposited when the river floods. The dissolved organic matter (DOM) concentration of the lower Kuiseb River is amongst the highest recorded for any aquatic system, averaging 82mg/L at peak discharge versus 10mg/L for the global average of rivers and streams (Jacobson et al., 2012).

The lower river flowing through the Namib Desert can be divided into three main sections based on river morphology and vegetation, after Huntley (1985) and Theron et al. (1985). The first section is referred to as the Upper Riverine Woodland and stretches from Harubes, where the Gaub River flows into the Kuiseb, to approximately Soutrivier (Figure 10). At Harubes the river aggrades and the channel becomes sandy with occasional terraces. At this point the river flows within a deeply incised canyon. At Homeb the height of the canyon becomes less severe and the river floodplain becomes increasingly wider. This section of the river is characterised by a sandy, meandering active channel and dense woodland of predominantly large *F. Albida*

trees on the relatively narrow floodplains. The Middle Riverine Woodland section stretches from Soutrivier to Swartbank. In this section the floodplain becomes wider, whereas the active channel remains relatively narrow. The wider floodplain results in *A. Erioloba* becoming the dominant woody species (Theron et al., 1985). This section is characterised by rock outcrops and relatively thin alluvium of about 2-3 m. The Lower Riverine Woodland section stretches from Swartbank to Rooibank. In this section the river becomes braided and the floodplain widens considerably (>1 km in places) (Figure 12). The vegetation becomes less dense and more spread out compared to the two upstream sections. The decrease in density of the vegetation is evident from the baseline study conducted by Theron et al. (1985). The average number of woody plants per hectare decreases significantly from the upper section to the lower section (Table 4). Although the baseline study is old, it makes it possible to compare the vegetation characteristics of the different sections of the river. Such a detailed study on the vegetation in the river has not been conducted since. Water abstraction had already commenced at that stage and any increase in abstraction since then would affect the section from Swartbank to Rooibank the most.

Figure 12 The Kuiseb River in flood. On the south the river is bordered by the Namib Sand Sea and to the north by the gravel plain. Photo courtesy of www.mariesworldtour.com. Available at URL: http://www.mariesworldtour.com/2011/05/flying-over-sossusvlei.html.

Table 4 Average number of woody plants per hectare in 1978.

Species	Upper	Middle	Lower
Faidherbia albida	178	138	40
Acacia erioloba	110	189	122
Euclea pseudebenus	136	60	3
Tamarix usneoides	297	162	26
Total	721	549	191

2.7.1.2 Delta

A few kilometres downstream of Rooibank the delta area starts and the river meanders through coastal sand dunes towards the Atlantic Ocean, occasionally flushing through the lagoon at Walvis Bay. It has been recorded that floods have reached this section of the river only 16 times between 1837 and 2009 (Morin et al., 2009). The delta river channel used to consist of a northern and southern arm, but a flood diversion wall built in the early 1960s blocked off the flow to the northern river channel. The wall was built by the South African government to protect Walvis Bay from flooding and has resulted in a dramatic reduction of the distribution of !Nara fields, a plant used traditionally by the Topnaar people living along the Kuiseb River (Ito, 2005).

The river maintains an identifiable channel bordered by nebkha dunes on either side for several kilometres past the start of the delta. At this point the southern arm of the delta fans out and becomes indistinct, bordered by linear dunes to the south and flowing between crescentic and nebkha dunes. *F. Albida* trees become rare, but the shrub form of *A. Erioloba* and *Tamarix usneoides* is still present. In addition to the woody plants, there are also shrubs and grasses mostly associated with the nebkha dunes. Between the dunes and the sea lies a large, unvegetated salt flat, also referred to as a sabkha.

2.7.1.3 Sand Sea: dune field and interdunes

The lower reaches of the river are bordered by the Namib Sand Sea to the south, which has been slowly encroaching northward in the lowest segment of the river, as revealed by Quaternary geologic records (Ward, 1987). The dunes' slow movement to the north-east is prevented by the scouring action of the floods in the river and the subsequent deposition of the

sand downstream within the most downstream section of the river. The dunes are sparsely vegetated, but there is grass found within the interdune areas.

2.7.1.4 Gravel plain

To the north of the river lies the rock desert or gravel plain, which consists essentially of a relatively smooth planation surface consisting of granite and schist variably covered by a gravel overlay, gypcrete and calcrete (Huntley, 1985; Eckardt et al., 1999). It has been proposed that these desert pavements form by the accumulation of dust that result in the upward growth of the soil profile (McFadden, 2013). This is fundamentally different to the traditional A/B/C soil profile development model. The stone pavement is intersected by drainage channels with several playas situated within the drainage network. Shrubs and grasses are mostly found within the channels (Huntley, 1985), with grass present on the stone pavement mainly after rainfall events. Although stone pavements are generally not regarded as dust sources, research have pointed to the fact that the dust emission from these surfaces could be significant (Xuan et al., 2002; Wang et al., 2012).

2.7.2 Groundwater

From where the river exits the bedrock canyon, the alluvial deposits become deep enough for a shallow local aquifer to develop along the river course (Morin et al., 2009). From Gobabeb onwards, the water storage capacity of the aquifer greatly increases as the alluvial fill increases. The recharge of the aquifer is dependent on the intermittent summer floods originating in the headwaters. Recharge to the aquifer does not take place in dry years, during which the river does not flood, and there have been periods where the river did not flood for several consecutive years (Figure 13).

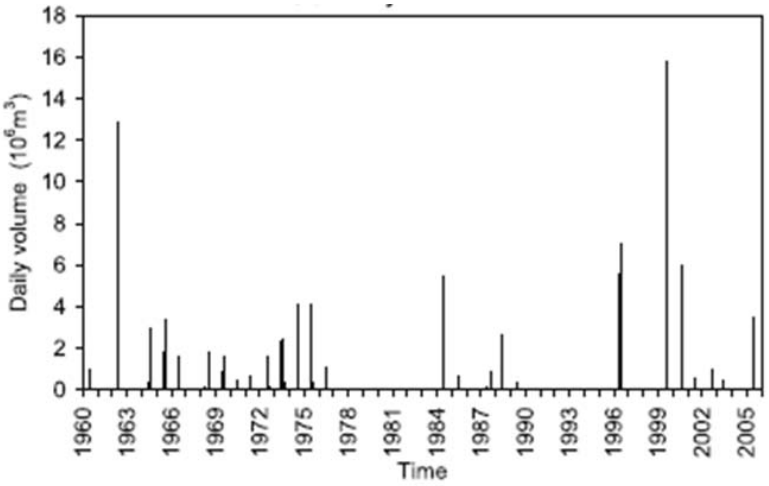

Figure 13 Daily flow volume at Rooibank from 1960 to 2005 from Morin et al., 2009.

Groundwater is not only associated with the active channel alluvium: it is also present under the gravel plain and the Sand Sea. Five paleochannels incised into Tsondab Sandstone have been identified under the Sand Sea to the south of the river with magnetic, electromagnetic (AEM) and radiometry methods (Sengpiel et al., 2000). The paleochannels extend from Natab just upstream of Gobabeb to Sandwich Harbour and the delta (Figure 14) and are between 20 and 65 km in length, with a width of between 0.5 and 5 km (Klaus et al., 2008).

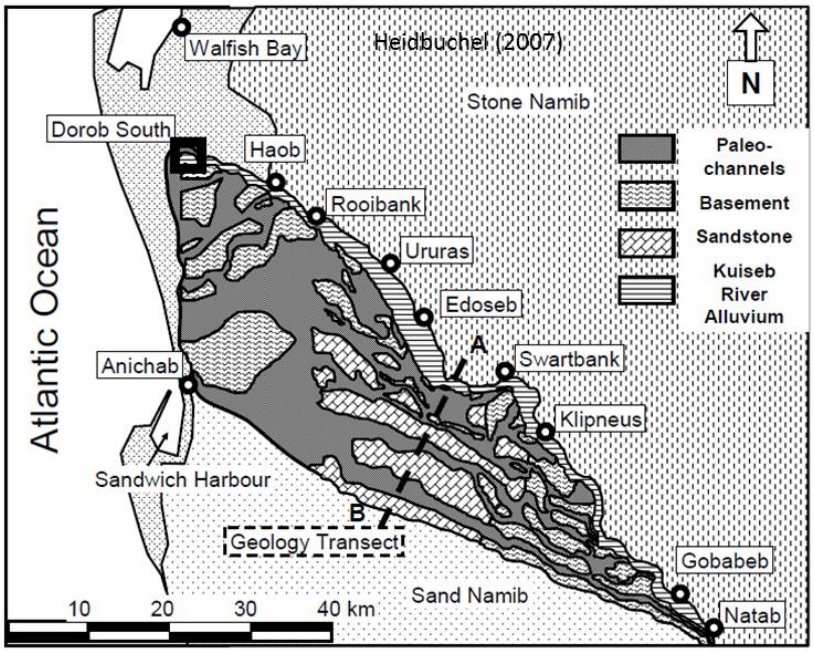

Figure 14 Paleachannels under the Namib Sand Sea identified by magnetic, electromagnetic and radiometry methods (Sengpiel, 2000). This representation of the paleochannels is from Heidbuchel, 2007.

In addition, the gravel plain also has a network of groundwater channels that follows the low gradient of the terrain itself (1%). The groundwater channels are saline, shallow and consequently of low volume; they therefore do not offer any storage capacity (Eckardt et al., 2012). There are numerous areas of groundwater discharge in the form of springs, seeps and pans (Viles et al., 2013). These areas of groundwater discharge, also referred to as playas, are often characterised by salt crusts due to the saline nature of the water (Eckardt et al., 2001).

The last feature indicative of the presence of groundwater is the coastal sabkhas. There are more than 20 sabkhas situated between Meob Bay (just south of Conception Bay) and Cape Fria (100 km south of the border with Angola) over a distance of about 700 km (Eckardt et al., 2001). The coastal sabkha of the Kuiseb delta covers an extensive area and is recharged by groundwater flow from the Kuiseb. The different groundwater units (Sand Sea paleochannels, gravel plain channels, delta sabkha and river active alluvium) are all linked, and flow and recharge between them does occur (Klaus et al., 2008).

2.7.3 Dust activity

Dust emission from the Lower Kuiseb River basin for the period 2005 to 2008 seemed to mainly originate from the delta and river channel (19 out of 22 plumes). Only three plumes were identified as originating from the drainage network of the gravel plain. Figure 8 shows the location of the origin points of dust events from 2005-2008, as identified by Vickery (2010) with the aid of MODIS imagery.

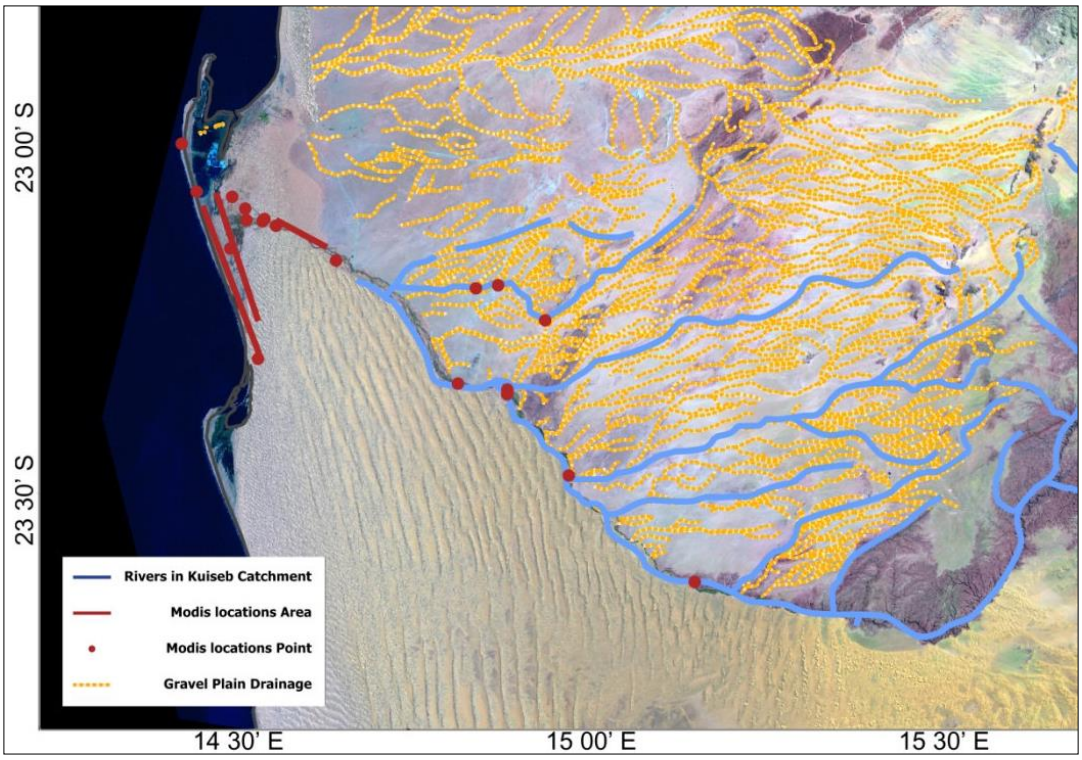

Figure 15 Source points and areas for dust events from 2005-2008 from the Kuiseb River basin, identified with the aid of MODIS imagery by Vickery (2010). From Vickery (2010).

2.7.4 People and the Kuiseb River

The Lower Kuiseb River from Homeb to Rooibank is home to the Topnaar community, part of the Nama group, whose association with the river extends back over two thousand years, according to archaeological evidence (Botelle et al., 1995). Traditionally this community depended on the river for water obtained from shallow hand-dug boreholes and obtained their food from the sea and the river, including plants and wildlife. The Topnaar diversified to livestock herding somewhere in the last one thousand years (Botelle et al., 1995). The Topnaar's traditional way of life changed with the industrialisation and growth of the ports in the area, especially Walvis Bay (Jenkins et al., 1967). The main activity on the river that generates an income for the Topnaar communities is the herding of livestock, predominantly goats, cattle and donkeys. Some families harvest !Nara fruit and sell the pips to companies in Walvis Bay that produce consumables from the oil (Willie Korumeb, personal communication, 14 September 2012, http://www.nara.com.na/). Most of the !Nara fields are situated in the delta region and harvesters camp out in the delta when harvesting season starts. The Topnaar is no longer a community of small-scale subsistence farmers as many community members rely on

wages from Walvis Bay and sell their goats and !Nara fruit to buyers from Walvis Bay (ERM, 2011).

Walvis Bay is situated in the Erongo region, which has the second highest per capita income after Khomas (MME, 2010). The main industries within the region are fishing, mining and tourism. Mining operations include uranium, gold, dimension stone (marble and granite quarrying), salt, stone and sand quarrying, and gemstones (MME, 2010). The population of Walvis Bay grew from approximately 44,000 in 2001 to 60,000 in 2007 (urban and rural), with a large percentage of this growth comprising people who migrated to the region in search of employment (ERM, 2011). Uranium mining in the area has seen significant growth over the last few years, with it set to continue depending on the uranium price. The mining of uranium is an integral part of Namibia's economic-growth planning, especially in light of the high unemployment levels (±50%) (Wassenaar et al., 2013). Currently there are two established mines (Rössing Uranium and Langer Heinrich), with two further mines under construction (Trekkopje and Husab mines) and a fifth pending development (Valencia). Furthermore, in excess of 39 Exclusive Prospecting Licences (EPLs) have been issued, spanning an area of about 18,000 km^2 (Wassenaar et al., 2013).

Tourism in the region is also undergoing tremendous growth, with an increase in tourist numbers of 57%, from 777,890 travellers in 2005 to 1,218,234 in 2011 (Namibia, 2011). Namibia as a tourism destination relies heavily on nature- and adventure-based tourism (Heinze, 2009). The Namib Desert was the second most visited attraction after Etosha National Park (Heinze, 2009). Large parts of the Namib Desert are contained within protected areas, including the Namib Naukluft Park, of which most of the middle and lower Kuiseb River forms a part.

The Kuiseb River aquifer has played an important part in the industrialisation and development of the area. Water from the aquifer supplies water to Walvis Bay and Swakopmund (in conjunction with the Omaruru aquifer). In addition, water is supplied to several mines in the area from a central pump station in Swakopmund (GCS, 2011). The supply network is summarised in Figure 16.

Figure 16 Abstraction areas, reservoirs and pipelines for the Kuiseb River aquifer (GCS, 2011). Town in red, reservoir in blue, existing pipelines in black, proposed pipelines in orange and abstraction area cross-hatched.

The groundwater level of the Kuiseb aquifer has been on the decline for the past several decades. Ross (1971) reported that each Topnaar village, consisting of a few huts and a kraal or two, was able to obtain water with buckets from shallow wells less than 3 m deep in the late 1960s. Since then the water table has dropped considerably and the Topnaar communities have been reliant on boreholes sunk to a depth of 15-17 m provided by Namwater (Henschel, 2006). The large quantities of water abstracted from the aquifer could be a contributing factor to the drop in the groundwater level (Jacobson et al., 2012).

2.8 Preliminary synopsis

Vickery et al. (2013) identified the Kuiseb River as the dustiest river in Southern Africa with the delta, river and to a lesser extent the gravel plain as potential source areas for the period from 2005 to 2008. A ground-based study to investigate the different surface features of the geomorphological units associated with dust emission will confirm the potential source areas and possible mechanisms associated with dust deflation. In addition, it would be beneficial to determine whether the dust activity from the Kuiseb is due to natural processes or is possibly also altered by anthropogenic influences.

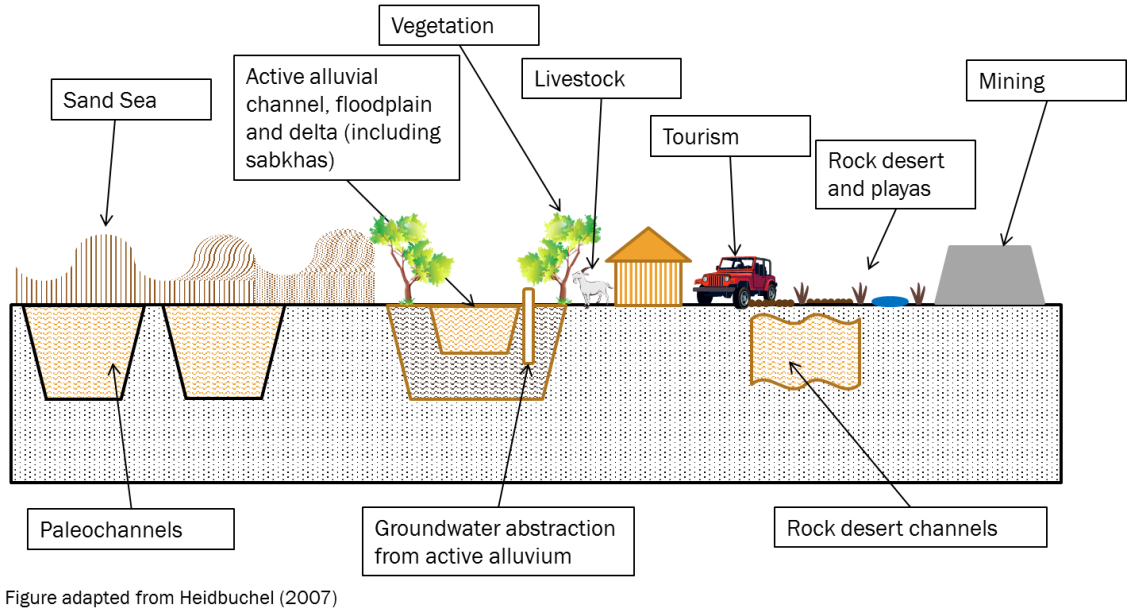

Figure 17 Geomorphological units and human influences within the Kuiseb River basin that could play a role in dust emission (Figure adapted from Heidbuchel, 2007).

2.9 Aim

The aim of this study is to develop an understanding of the surface factors, in particular the sediment, that make the Kuiseb one of the dustiest rivers in Southern Africa and to determine the potential source areas of dust. This could further our understanding of the mechanisms and drivers of dust emission for this region.

2.10 Objectives

This study will identify potential source areas within the catchment based on sediment suitability, as well as availability for wind deflation. This will entail investigating the material characteristics of the sediment as one of the controlling variables of dust emission. The analysis will mainly look at the sediment characteristics, but it will also to a lesser extent consider variables such as surface roughness. In addition, this study will examine whether the anthropogenic activities within the basin have the potential to influence the dust emission activity of the area.

The study will explore the following specific objectives:

- Determine geomorphological units associated with dust emission within lower Kuiseb River basin. This will be based on a desk top study using various data products, including MODIS satellite imagery and Google Earth.
- Conduct field work which will entail sampling of surface sediments of the geomorphological units identified above and record surface roughness elements at the sample sites.
- Determine particle size distributions of surface samples to determine the location of appropriately sized sediment for deflation, i.e. where are the supply areas of appropriate sediment.
- Determine appropriate sediment characteristics to consider the availability of the supply sediments for deflation, i.e. how wind erodible are the surface features.
- Consider the surface roughness at the sample sites identified as potential source areas based on the presence of appropriate sediment for dust emission.
- Examine the extent of anthropogenic modification and possible contribution to dustiness of study area,
- Identify potential source areas of dust emission based on analysis of sediment, surface roughness, dust plumes identified with MODIS imagery and possible anthropogenic influences.

3 Methodology

3.1 Sampling strategy

To assess the dust emission potential and sediment characteristics of the study area, samples were taken in all of the major geomorphological surface units of the lower Kuiseb catchment area. This is similar to the approach followed by Wang et al. (2005) in their study of the surface characteristics of the Badain Jaran Desert in North-western China. The sampling areas for the present study of the Kuiseb basin included the river, consisting of both the floodplain and channel; the delta; the gravel plain and also limited samples from the Sand Sea dune fields and interdune areas.

The choice of sampling sites were guided by the source points identified with the aid of MODIS true colour images by Vickery (2010) (Figure 18). However, in some instances sampling locations were dictated by ease of access. The accessibility was influenced by issues such as transport (motorised versus non-motorised all-terrain vehicles), restricted areas and the road network. MODIS source points were not considered as definitive origin points of the dust plumes due to the uncertainty associated with identifying the source points. The MODIS sensors on board the Terra and Aqua satellites provide two true colour images per day. Terra crosses the equator at 10h30 GMT and the Aqua satellite at 13h30 GMT. As a result, there exists a reasonable amount of temporal and spatial uncertainty with regards to the plume activity and pathways. In addition, plumes are clearly visible over the ocean, but not so clearly discernible over land. To pinpoint the exact location of the origin of a plume from a MODIS image over land is problematic. Given the above considerations it was decided to ensure samples were taken from the majority of the components within the lower catchment with which plumes were associated according to the MODIS imagery.

Figure 18 shows all the sites at which samples were taken during field work in September 2012 and March 2013. Samples from the main river channel were taken along 9 transects (labelled RT1-RT9) starting from Homeb (RT9) to Rooibank at the start of the delta (RT1). Table 5 gives an indication of their location on the lower Kuiseb River and in which segment of the river they fall as classified by Theron et al. (1985).

Table 5 River sampling transects and their locations.

River segment	Transect	Location
Lower riverine woodland	RT1	Rooibank
	RT2	
	RT3	
Middle riverine woodland	RT4	Swartbank
	RT5	
	RT6	
Upper riverine woodland	RT7	Soutrivier
	RT8	
	RT9	Canyon end

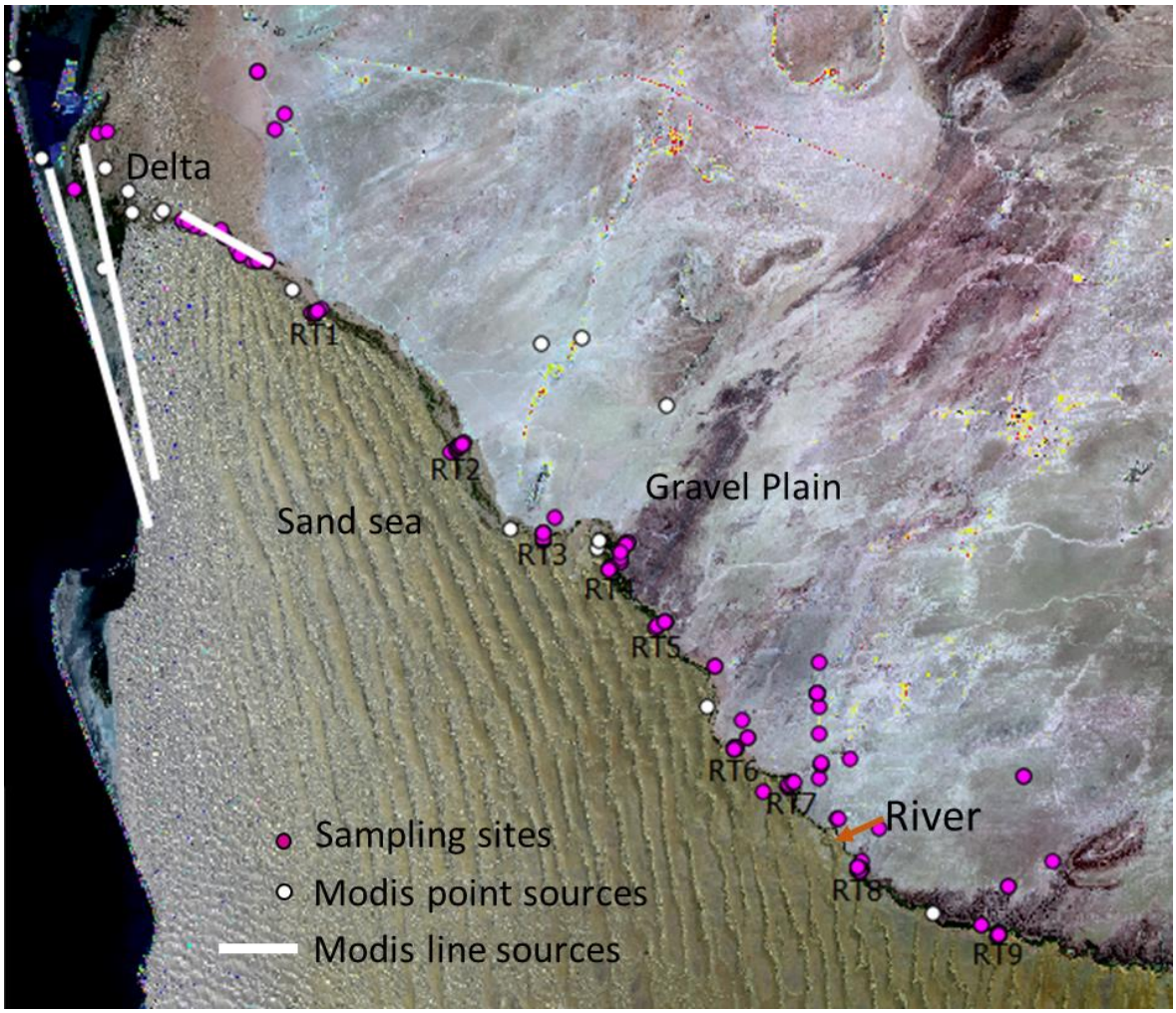

Figure 18 MODIS identified point and line sources from 2005 to 2008 as per Vickery (2010) and sampling sites situated in the major geomorphological units of the basin. RT1-9 indicate the location of the nine river transect samples.

Samples were taken with the aim of establishing where the fines are that can be entrained by the wind for medium to long term (or long distance) suspension. For the river transects this involved sampling across the river from the gravel plain to Sand Sea at a selected site (RT1-9). Samples were predominantly taken where fines were present, but to obtain a complete picture of material characteristics, some samples were also taken where only coarse (sand and gravel) were present. Sampling the delta involved covering greater distances and a donkey car was employed to conduct sampling in September 2012 (Figure 19). The donkeys struggled in the loose sand and did not get as far into the delta as was hoped for. The sampling conducted with the donkey car started at the flood wall in the delta (Figure 10) and covered almost the entire delta channel to the start of the fan.

The delta fan field work was conducted from the Walvis Bay side in March 2013 with a 4×4 vehicle. Unfortunately it turned out that the day chosen to sample the delta was the second wettest day in 50 years, which again did not allow us to penetrate as far into the delta as wished (Figure 20). However, the sampling that was conducted covers a large enough area of the delta to give a good indication of the sediment characteristics.

Figure 19 Transport into the delta. Donkey car courtesy of Oom Willie Korumeb from Armstraat.

Figure 20 Rain in the desert – Kuiseb River delta 30 March 2013.

The gravel plain source points identified by MODIS seem to be mainly associated with springs and playas. The MODIS source points were not easily accessible and through consultation with staff at the Gobabeb Research Station it was decided to visit an alternative salt spring (Hosabes Springs) in the vicinity of Gobabeb which was easier to access. It is reasonable to assume that the springs at Hosabes can be regarded as an appropriate analogue for the salt springs within the study area. The drainage network was predominantly sampled from the road.

Sample codes were allocated based on the location of the samples (Figure 21). River samples were numbered according to where they were located in the river and transect number followed by a unique sample number, e.g. RF1-1 is the first sample taken within the floodplain of transect 1. The individual sample numbers were allocated as samples were taken across the transect and the order have no particular significance. The delta samples were labelled as follows:

- DAC: samples located in the Delta Active Channel other than depositional crusts. These samples were taken before the fan area, where a distinguishable channel area is still visible.

- DCC: samples of depositional crusts located within the active channel were labelled as Delta Channel Crusts.
- DFP: samples not taken within the channel area were labelled as Delta Flood Plain samples.

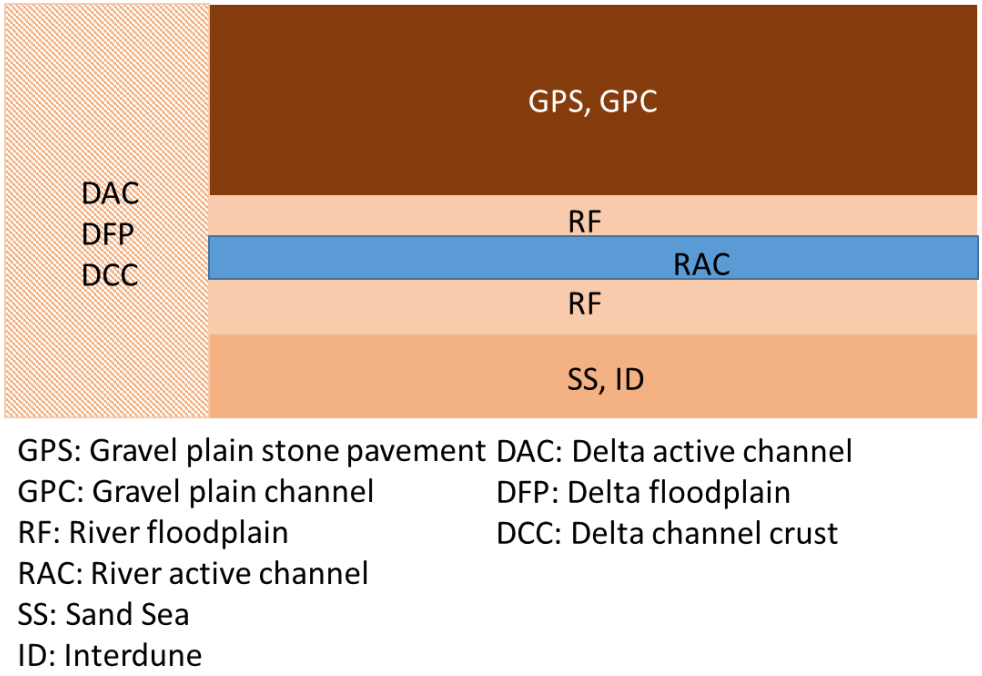

Figure 21 Sample code used to label samples

Samples were taken with a small shovel, scooping the top 1 centimetre from the surface in the case of loose sediment (unconsolidated). Crust samples were taken as whole pieces and every effort was made to keep the crusts intact on route to Cape Town. Figure 22 shows a sample site of typical unconsolidated sediment and a sample site of crusted material. The sampling and removal of sediment might not reflect the surface conditions exactly as it is in the field and therefore may not accurately represent the soil erodibility (Webb et al., 2011), but it provides a good indication of the potential erodibility of the surface.

Figure 22 Sampling of unconsolidated sediment and crust samples

3.2 Particle size analysis

Laboratory analysis consisted primarily of particle size analysis (PSA) with the aid of a laser diffractometer of all the samples. The particle size distributions would provide an indication of the location of fine material within the study area, i.e. the supply of entrainable sediment.

3.2.1 Laser diffraction

The particle size analysis (PSA) was done by means of laser diffraction on a Malvern Mastersizer 2000 attached to a Hydro 2000G wet sample dispersion unit. Laser diffraction involves measuring the scattering pattern produced by a laser beam passing through a sample cell containing the dispersed sample. The sample is pumped from the dispersion unit through a sample cell located in the optical bench. The light scattering pattern is captured by a range of detectors situated in the optical bench (Figure 23). The instrument software then back calculates from the diffraction pattern using appropriate models (Mie or Fraunhofer) to infer the particle size distribution.

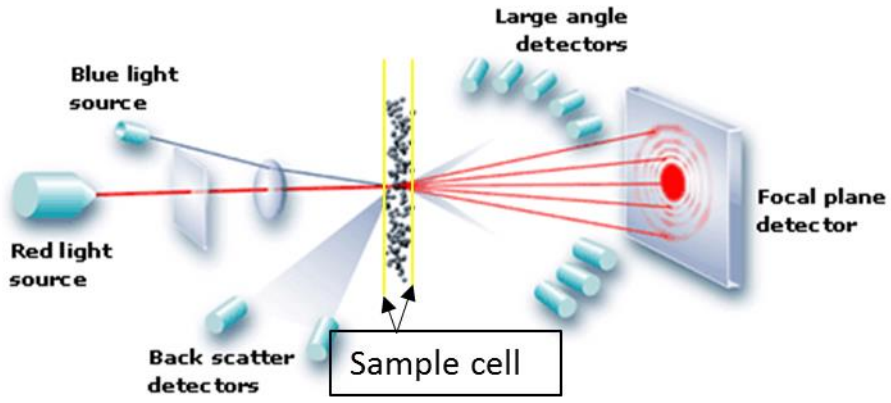

Figure 23 Laser diffraction system used for particle size distribution. Adapted from http://www.malvern.com/labeng/technology/images/laser_diffraction_system.gif

In reality it is not just a diffraction pattern which is created, but a complex pattern involving reflection, refraction, absorption and re-radiation. This complex pattern is called a scattering pattern and this is what makes laser diffraction complicated as there is no detector that can differentiate between the different scattering phenomena listed above. Mie theory was developed in an attempt to account for all the light scattering phenomena occurring if light hits a spherical particle (Keck et al., 2008). The model formula consists of three influencing parameters:

1. Particle radius
2. Angle of scatter
3. Optical parameters (refractive and absorption index), R

The particle radius can be calculated if the angle of scatter and optical parameters are known. In order to obtain accurate results from this theory it is important that the optical parameters of the sample be known. However, for large particles where the angle of scatter becomes very small, the optical parameter contribution to the result becomes negligent. This then becomes equivalent to the Fraunhofer model where no consideration is given to how the light interacts with the particle. In practice the Fraunhofer model can be used if the sample consists of particle sizes that are 5 or 6 times larger than the incident wavelength (Keck et al., 2008). For the Malvern Mastersizer 2000 the blue light source has a wavelength of 470 nm, the cut off for accurate results without optical properties, i.e. Fraunhofer analysis, is therefore 2.8 µm. It is for this reason that Mie theory is thought to be better suited to describe the scattering mode of very fine particles (Wen et al., 2013).

Using laser diffraction to obtain particle size distributions of soil is complicated by the heterogeneous nature of the material. One of the assumptions of Mie theory is that the particles

are spherical and results are reported on a percentage volume basis. Soil or mineral particles are rarely spherical. Furthermore, as the theory describes the way the laser light and particles interact with each other, the optical parameters such as the refractive index (RI) and absorption index (AI) of the sample has to be established. The RI and AI combined are often referred to as the complex refractive index (R). The RI represents the change in velocity of light through the sample compared to the velocity of light in a vacuum and the AI represents the transparency and absorptivity of the tested material (di Stefano et al., 2010). Therefore, R influences the diffraction of light as it passes through a particle and is a function of both the size of the particles and the composition of the material (Wen et al., 2013). As a result of the heterogeneous nature of soil mineral matter, samples will be made up of a number of different minerals (and potentially organic matter if not removed during pre-treatment) and different sizes, with different optical properties. The optical properties chosen for analysis could potentially have a significant influence on the particle size distribution of the finer fraction of a sample.

For this study the influence of different optical properties were assessed using a sample of Homeb silt from the study area in an effort to ascertain appropriate measurement parameters for analysis. The sample of Homeb silt is very consistent and uniformly graded and was therefore also particularly suited for use as a quality control sample for this study. The Malvern software allows for the recalculation of results based on different refractive and absorption indices, which eliminates the need for multiple analyses to test the optical parameters. Absorption values range from 0 for perfectly clear grains to 1 for perfectly opaque grains (Sperazza et al., 2000). The accuracy required for AI is normally an order of magnitude, e.g. 0.01, 0.1, 1 (Malvern, 2012a). It is evident from Figure 24 that variations in the absorption index (AI) has a significant effect on the results. These results also confirm the influence of Mie theory and its dependence on the optical properties of the sample on the fractions smaller than about 3 µm. This can be seen clearly from the differences in the fine tail from about 3 µm for the different absorption indices.

Similarly, the effect of variation in Refractive Index (RI) was also investigated by recalculation of the results at absorption indices of 0.1 and 1 (Figure 26 and Figure 25). For an AI of 1, the influence of the RI becomes less significant. There is virtually no difference in the results obtained for an RI of 1.45, 1.55 and 1.65 as the AI is kept constant at 1 (Figure 25). This is to be expected as an AI of 1 (for perfectly opaque grains) will not account for the interaction between the laser light and the particle to the same extent as for lower values of AI (where

grains become clearer). For an AI of 0.1, the influence of variation in the RI becomes significant (Figure 26).

For this study the RI was set at 1.55 based on the comparison with the results of the Homeb silt and the RIs of the most common minerals in the samples: quartz (RI of 1.544-1.553) and mica (Muscovite: 1.522-1.616, Biotite: 1.565-1.696) (Malvern, 2012b). The AI was set at 0.1 as the default for all analysis. The optical parameters chosen can be evaluated by assessing the data fit and the residuals. Results were recalculated with an AI of 1 where a poor data fit or residuals were produced, but this did not produce significantly different results for the purposes of this study (Figure 27). The <2.8 µm results again demonstrate the influence of the AI on the result.

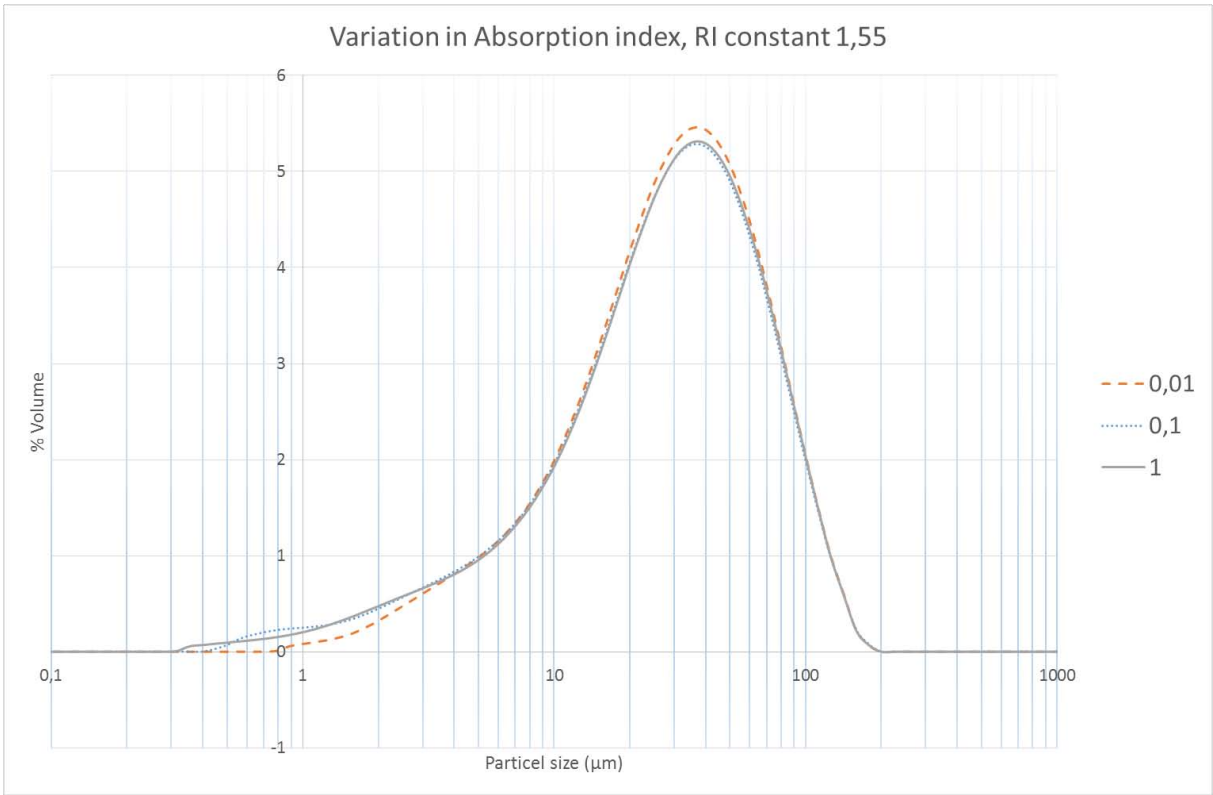

Figure 24 Influence of variation of absorption index on results. Refractive index constant at 1.55 and Absorption index set at 0.01, 0.1 and 1.0.

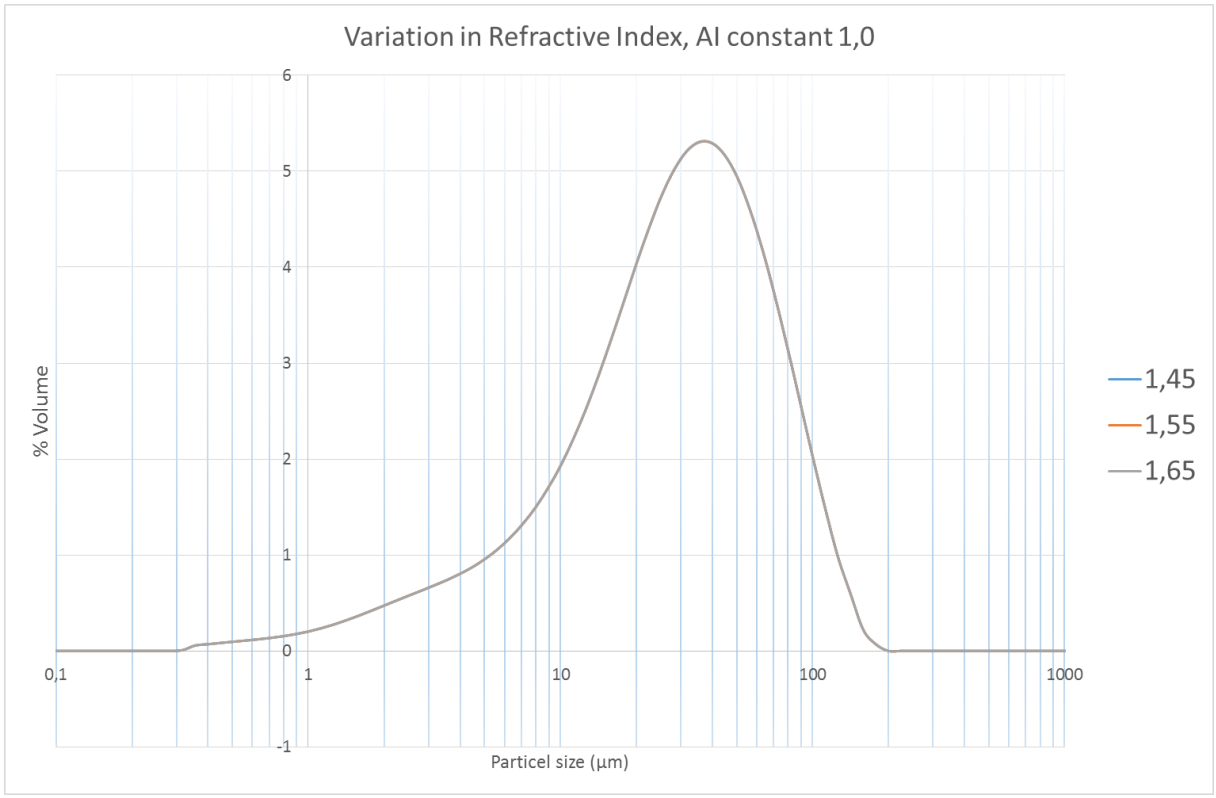

Figure 25 Variation of Refractive index at an Absorption Index of 1

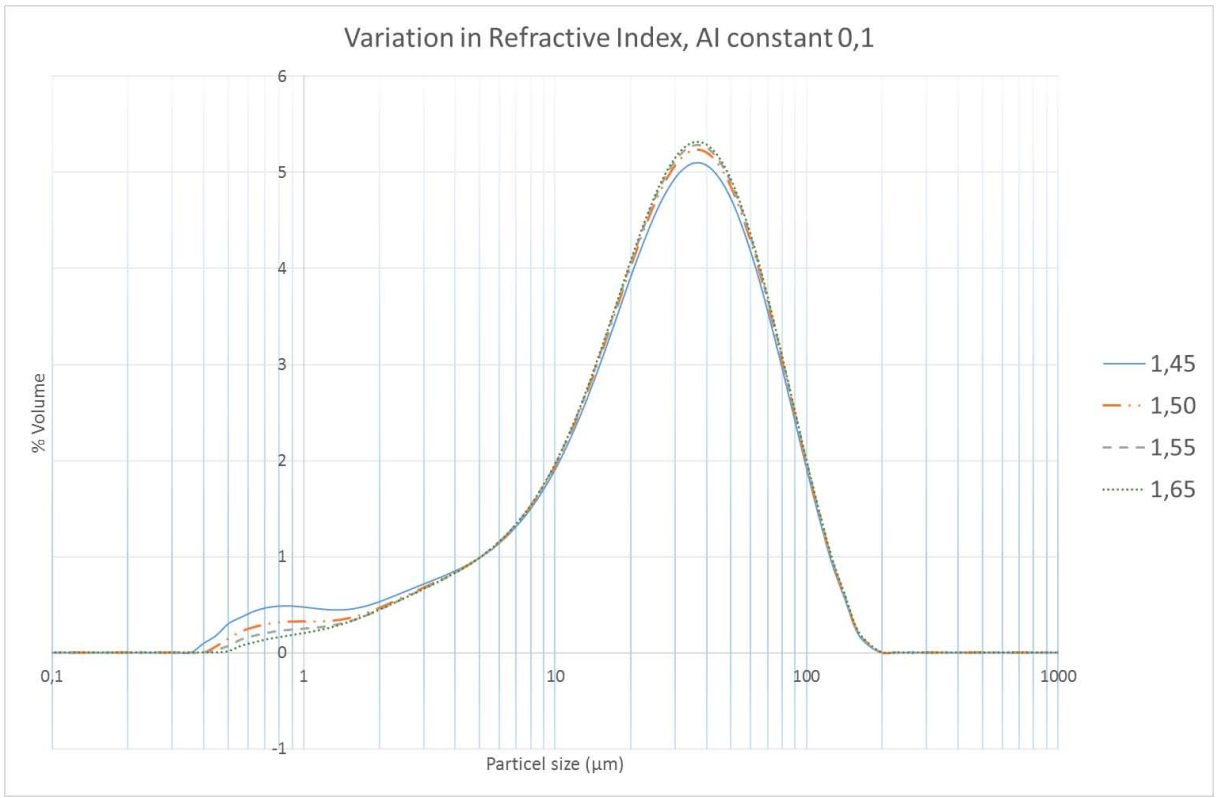

Figure 26 Influence of variation in refractive index at an Absorption Index of 0.1

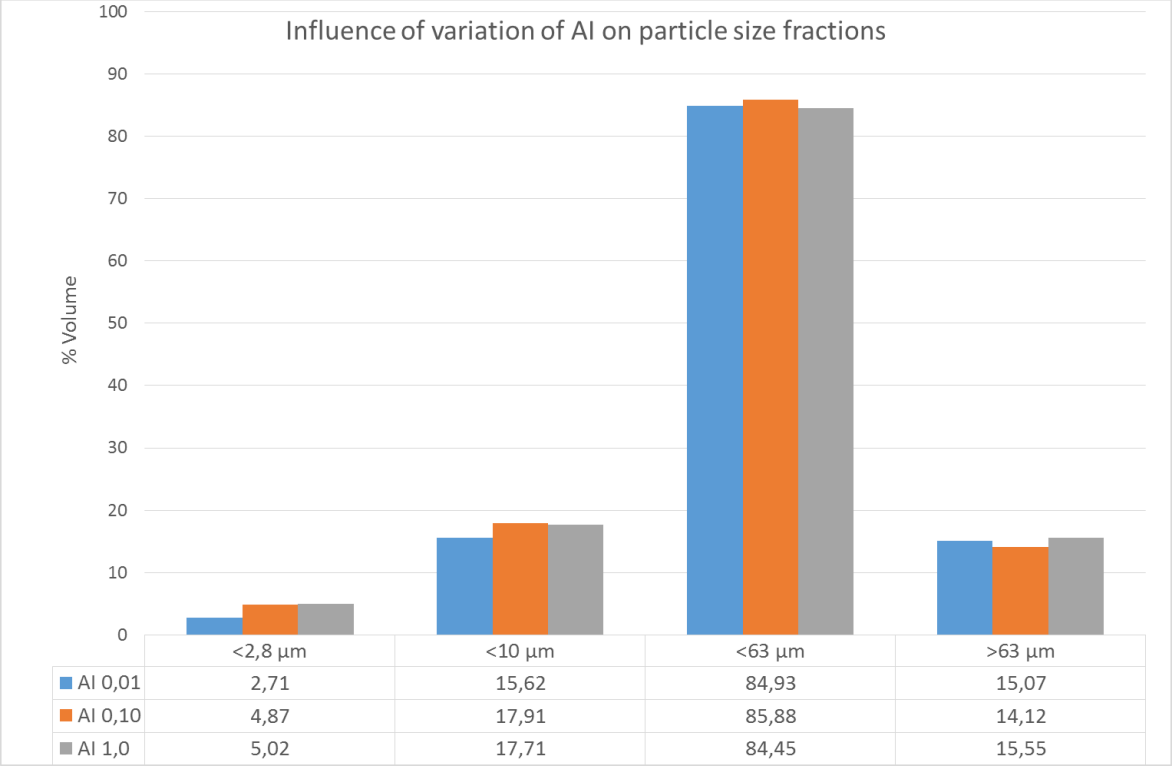

Figure 27 Variation in PM2.8, PM10, and PM63 for Homeb silt with a constant RI of 1.55

Numerous studies have been done with the aim of comparing the different grain size analysis methods available at present and there is wide disparity in the results. A number of studies concluded that laser diffraction significantly underestimates the clay and fine silt fractions and has a tendency to shift the distribution towards the larger sizes (McCave et al., 1986; Beuselinck et al., 1998; Campbell, 2003; Scott-Jackson et al., 2005; Ryzak et al., 2007; di Stefano et al., 2010; Vdovic et al., 2010; Miller et al., 2011; Wen et al., 2013). The two main methods against which laser diffraction have been compared is the Sieve-Hydrometer and pipette method. The main reason given for this underestimation is the fact that the laser technique interprets the mostly platy clay particles as spheres (Vdovic et al., 2010). An irregular shaped soil particle will reflect a cross-sectional area greater than that of an equal volume sphere and as such will be assigned to a larger size fraction (di Stefano et al., 2010). This will then result in an underestimation of the clay fraction. Figure 28 illustrates a cylinder and sphere of equal volumes. The greater cross-sectional area of the cylinder would place it in a larger size fraction.

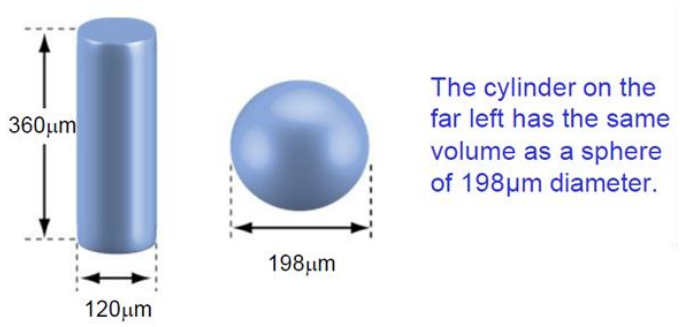

Figure 28 Equal volume cylinder vs sphere (Malvern, 2012c)

It should be noted that the assumption of sphericity affects both laser diffraction and sedimentation methods such as the hydrometer method. The hydrometer method is based on Stokes' law which differentiates particles based on the velocity with which they settle in suspension and include the following two assumptions: soil particles are rigid, spherical and smooth; and they have similar densities. The assumption of uniform density is another major source of error in sedimentation methods (di Stefano et al., 2010).

Goossens (2008) did a comprehensive study comparing ten different instruments for wet analysis of particle size distribution. The instruments covered the four main principles on which techniques for particle size analysis are based: laser diffraction (four instruments from different manufacturers), sedimentation, impedance measurement and optical measurement. The study assessed each instrument based on a set of predetermined criteria, which included reproducibility, analysis time, analytical range, resolution (in terms of number of grain size classes) and data processing. The laser diffraction (LD) instruments generally scored best for all the criteria. In the study done by Goossens (2008) it was noted that the laser diffractometers generally measured higher clay contents than the Atterberg method, but less than the Sedigraph (both of which uses sedimentation). However, the LD instruments also measured slightly higher amounts of sand. Wen et al. (2013) on the other hand obtained good comparisons between the Sieve-hydrometer and LD method for the sand fraction. The authors contend that this could be explained by fairly simple mineralogy of the sand fraction where quartz dominates and other minerals such as feldspar, biotite, hornblend and others are minor.

The present study did not include a comprehensive comparison between laser diffraction and any other method. However, a sample of the Homeb silt was dry sieved over a 38 µm sieve and the passing fraction was analysed with LD. The results obtained with LD showed that 90% of the sample analysed was smaller than 41.6 µm.

Another focus of research on laser diffraction has been on the appropriate settings for the various measurement parameters. Several researchers commented on the importance of reporting the optical and measurement parameters as they are important for comparison of results between different studies (Ryzak et al., 2011). The dispersant used was tap water which were free of impurities which could potentially interact with the particles (See Appendix 8.1 for analysis of tap water used as dispersant). The dispersion unit includes a pump/stirrer with a speed range of 0 to 4000 rpm. The pump/stirrer ensure that the sample is homogeneously dispersed in the tank and pumped through the sample flow cell for measurement and the speed needs to be sufficient for coarser particles to remain in suspension. Some studies have attempted to determine an optimum pump speed – Ryzak et al. (2011) maintain that a pump speed of <2000 rpm produce results with large uncertainties, Sperazza et al. (2004) concluded that optimal results were achieved with pump speeds between 1600-2300 rpm. It is important to note that due to the heterogeneous nature of soils, a uniform pump speed to be utilised across the board for all soil types cannot be determined. For this study a pump/stirrer speed of 2000 rpm was employed.

The dispersion unit also has a built in ultrasonic probe with variable tip displacement (ultrasonic energy) to aid dispersion of the sample. Chappel (1998) studied methods for dispersing sandy soils and concluded that a combination of Calgon and ultrasonic action was the most efficient dispersion technique, but added that the slight advantage provided by the combination of chemical and physical dispersion methods were outweighed by the extra preparation time. The author also cautioned against using lengthy periods of ultrasonic action (longer than 6 minutes) as this could result in particle breakdown. The standard adopted at the conclusion of the research study by Chappel (1998) was tap water as the dispersant with 3 minutes of ultrasonic action, which he concluded was the optimum duration from their results. The dispersion method for the present study consisted of ultrasonic action set at 50% tip displacement for 3 minutes prior to measurement. The use of sodium hexa-metaphosphate was tested, but made no significant difference in the dispersion of the samples. Ryzak et al. (2011) caution against the use of chemical and physical dispersion methods together as this can lead to aggregation of soil particles.

In addition, the measuring time must be set and will determine the number of “snaps” that are taken of the diffraction pattern as the sample is pumped through the flow cell. A measurement time of 30 seconds will produce 30,000 snaps (one snap taken every millisecond) for both the blue light and the red light measurement, with a total measurement time of 60 s and 60,000

snaps. The coarser the sample, the more beneficial a larger amount of snaps become. The obscuration is an indication of the number of particles visible by the laser and can be used as an indication of the most appropriate method of sample dispersion (Chappel, 1998).

According to the manufacturer, the Malvern Mastersizer 2000 has a measurement range of 0.02 – 2000 µm "dependent on the sample and sample preparation" (Malvern, 2013). The measurement cell has a width of 2400 µm and this dictates the upper limit. However, analysing samples with a particle size >1200 µm could potentially scratch the lenses and reduce their lifespan (Mr Philip Verwey, personal communication, 29 January, 2013). In addition, samples that contained a larger fraction of coarse sand caused the dispersion unit to make grinding noises. It was therefore decided to maintain an upper limit of 1000 µm and all samples were screened over a 1000 µm sieve before splitting and analysis. Maintaining an upper limit of 1000 µm was not problematic as the focus is on dust sized particles with a particle size of much less than 1000 µm.

Table 6 Summary of optical and measurement parameters used for the particle size analysis in this study

RI	1.55
AI	0.1
Dispersant	Tap water*
Pump/stirrer speed	2000rpm
Ultrasonics	50% tip displacement for 3min
Measuring time	60 seconds (30s red light, 30s blue light)

*see analysis in the Appendix 8.1.

A further complication in terms of using laser diffraction in the present study was the possible influence of mica on the analysis. Hayton et al. (2001) did a study on the affect that mica particles have on particle size distributions by adding small amounts (by weight %) of mica, consisting of a mixture of biotite and muscovite between 63-250 µm, to fine to medium grained quartzofeldspathic beach sand (125-500 µm). The study concluded that the addition of mica shifted the particle size distribution primarily to the mica based particle size distribution rather

than the total sediment distribution. The authors contend that this is because of the larger number of particles per unit weight of mica compared to the same unit weight of the sand. In addition, the shape of the mica particles have a similar effect to that of the platy clay particles. Therefore the number of particles and their cross sectional area play a proportionally greater role to the total scattered light. For the present study the effect of mica on the analysis was not investigated. This was due to two reasons. Firstly, the samples Hayton et al. (2001) analysed consisted of predominantly sand fractions, whereas this study focuses on the finer fractions (<63 µm). Secondly, the mica in the study by Hayton et al. (2001) contained smaller particles than the sand and it would therefore be expected that the samples that contain mica show distributions slightly finer than the pure sand samples. For the natural sediment samples from the Kuiseb catchment it is more likely that the <63 µm fraction particle size distributions will be shifted to a slightly coarser distribution due to the presence of mica, as a result of the flat shape of the particle similar to the influence of that of clay particles. The SEM images of material in the floodplain attest to the predominance of mica in this size fraction.

From the multitude of studies done on particle size analysis it is clear that the optimum grain size analysis technique will depend of the objective of the study (Goossens, 2008). Di Stefano et al. (2010) also make the distinction between the ultimate and effective grain size distributions. An ultimate distribution, where particles are fully dispersed might be important when evaluating certain soil chemical and physical properties, whereas effective grain size distributions would be important when considering other processes such as erosion and sediment transport.

It is also clear that there is not a one size fits all formula for the measurement settings due to the heterogeneous nature of soil and these parameters would have to be determined for different materials. The laser diffraction method was the optimum technique to use for this study, based on the number of samples, the speed of measurement and ease of analysis. Moreover, there is no method of particle size determination without limitations.

3.2.2 Sample preparation

With the exception of the samples taken in March in the delta, all of the samples were already air dry at the time of sampling. The wet samples were air dried before analysis took place. An important consideration in terms of sample preparation for PSA was how to obtain a

representative sample to analyse with the laser diffractometer. Samples taken in the field were generally in the order of 200 – 300 g each. For analysis, approximately 0.3-1 g of sample was needed per replicate. The appropriate amount of sample is largely determined by the obscuration of the laser beam. The obscuration is simply the amount of light lost due to either scattering or absorption of the laser beam and is determined by the concentration of the sample added to the dispersant.

The most accurate splitting technique for obtaining a representative sample is a rotary splitter, but this proved too time consuming and expensive. A method of cone and quartering was developed and tested, which gave reproducible results (Figure 29 and Figure 30). Samples were split in half using this technique, each half was then split further until the desired amount of sample was achieved. Two replicates were taken from each half, giving a total of four replicates. At least two of the four replicates were analysed, with the additional replicates only analysed if the results were not reproducible. The working surface was thoroughly cleaned to avoid cross-contamination before a new sample was split.

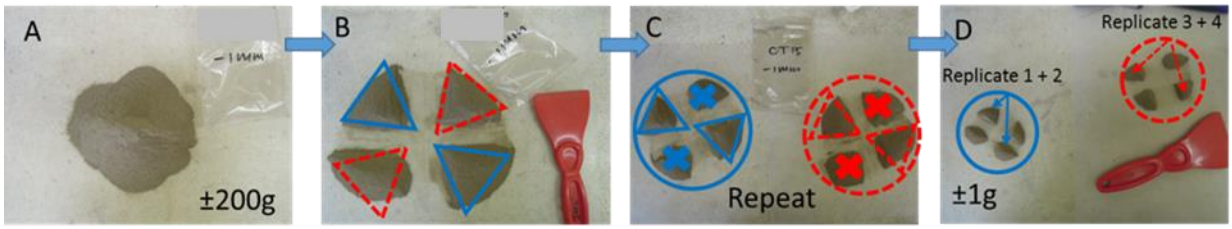

Figure 29 Cone and quartering procedure. A: total sample coned. B: quartering of the whole sample. Opposing quarters mixed together to obtain two halves. C: Quartering of the halves. Remove opposing quarters, join remaining quarters and repeat until required amount of sample obtained. D: Replicates from each half for analysis.

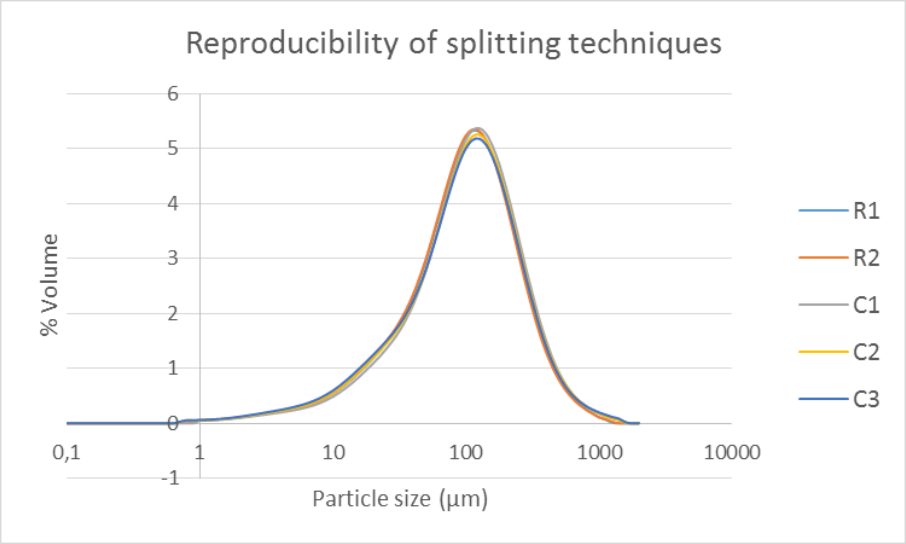

Figure 30 Reproducibility of splitting techniques. R1-2: split to required amount of sample with rotary splitter. C1-3: split to required amount by using cone and quartering technique described in Figure 29.

For this study the samples were not subjected to any pre-treatments such as organic matter or carbonate removal. The objective of this investigation was to look at the material as it would occur naturally. Therefore the size distributions obtained with this analysis cannot be seen as optimum or ultimate grain size distributions, but effective distributions with a focus on availability for wind deflation. In terms of an effective grain size distribution it would have probably been better to use a dry dispersion unit coupled to the laser diffractometer, but this was not available. The presence of organic matter in the finer fractions is confirmed by the SEM images of the sample material and this material is small enough to form part of the supply of wind deflated particles. The removal of organic matter does however have an effect on the particle size distributions of the samples (see the Appendix 8.2).

3.2.3 Cluster analysis

As this investigation involved a large number of samples (±170 analysed), a cluster analysis was conducted based on the percentage of <10 µm and <63 µm to explore possible source areas and trends present. The clustering was done using Ward's method of hierarchical tree clustering, using the Euclidean distance as the measure of distance. The tree plot is included in the Appendix (section 8.3). Clusters were determined using Statistica statistical software.

3.3 Other sediment characteristics

Based on the PSA, selected samples were then chosen to obtain images with a Scanning electron microprobe (SEM) with EDS, as well as analysis of soluble salts and organic content. This would provide further information on the small-scale material characteristics, which have an effect on the availability of the sediment for deflation.

3.3.1 Mineralogy and morphology: Scanning Electron Microscopy (SEM)

The <63 µm fraction of five samples representing the four finest cluster groups were selected for investigation with the SEM/EDS. The five samples chosen were also representative of various geomorphological units within the basin. Sample characteristics are given in Table 7. SEM yields images of the surface of the samples to determine particle morphology and structure, whereas EDS provides information on the elemental composition of the samples (Amonette, 2002). The samples were air dried, sieved and then mounted on a stub with water based glue mixed with colloidal graphite. They were carbon coated once dry and then analysed with a Nova Nanosem 230 with both VCD and ETD detectors.

Table 7 Samples selected for further investigation of small scale surface characteristics

Sample ID	Cluster type	Location	State
GPC47	1	Gravel Plain: drainage network silt accumulation	Depositional crust
DFP19	1	Delta fan: silt deposit in fan close to Walvis Bay	Depositional crust
RF9-15	2	River: Canyon end on floodplain within vegetation	Depositional crust
RF1-12	3	River/Delta channel: Rooibank, start of delta channel silt accumulation in between nebkhas	Depositional crust
RF8-5	4	River: sample taken in goat path on floodplain within vegetation	Unconsolidated material

3.3.2 Moisture content

Moisture content was determined for the samples in Table 7. This was done using an oven at 105°C for 24 hours. Samples were weighed as soon as a stable reading could be achieved.

3.3.3 Organic matter content

Estimates of organic content of the five representative samples were determined gravimetrically with the Loss on ignition method by placing samples in a furnace set at 400°C for 24 hours.

3.3.4 Soluble salts

The same five representative samples were analysed for selected soluble salts with AAS (Atomic Absorption Spectroscopy). 5 g equivalent of dry soil was added to 50 ml distilled water and shaken once a day for five days prior to analysis. The samples were filtered and centrifuged to remove all particulate matter.

3.4 Remote sensing

Several images were obtained from Google Earth to gauge the surface roughness elements (mainly vegetation) present at the various sample locations at the transect scale. This would provide additional information to consider the availability of the supply sediments for deflation. Google Earth was also utilised to assess the degree of anthropogenic modification within the study area. This was used in conjunction with observations taken during the fieldwork conducted. Google Earth is available at http://www.google.com/earth/.

Moderate Resolution Imaging Spectroradiameter (MODIS) true colour imagery was used to identify dust plumes (see Vickery (2010) for a more in depth handling of this data type). Images used in this study were downloaded from the NASA Rapid Response website:

http://lance-modis.eosdis.nasa.gov/imagery/subsets/?subset=Namibia.

In addition, QGIS software was used to create several of the figures. A Landsat 8 image taken on 24 May 2013 was used as backdrop in GIS for most of images displaying sample results. This image was obtained from the USGS Earth Explorer website:

http://earthexplorer.usgs.gov/

A list of images used from MODIS is provided in the Appendix 8.4.

4 Results

The particle size analysis done with laser diffraction will be discussed first. This will involve primarily the results from the cluster analysis. Individual sample results, their locations and cluster types will be included in the discussion where appropriate. A list of all the samples analysed with laser diffraction used for the cluster analysis and their average particle size fractions are given in the Appendix (section 8.5). Following this will be the results of selected small-scale sediment characteristics. These will be considered in the discussion according to the relevant geomorphological unit.

4.1 Particle size analysis

A cluster analysis was conducted for all the particle size results based on the <10 µm and <63 µm size fraction for each sample. The cluster analysis produced six clusters, which will be referred to from here on as Type 1 to 6. The cluster types vary from Type 1, containing the largest quantity of fines to Type 6, which contain virtually no fines. The average particle size distributions of each cluster type are given in Figure 31 and summary statistics is given in the Appendix (section 8.6). In addition, the average particle size fractions for each cluster are given in Figure 32. The natural sediments of the study area will lie somewhere on the continuum between Type 1 and 6, but for purposes of this analysis the six discrete types were employed as a means to group the large number of samples into representative clusters. The location of all the samples per cluster type is given in Figure 33 to Figure 38.

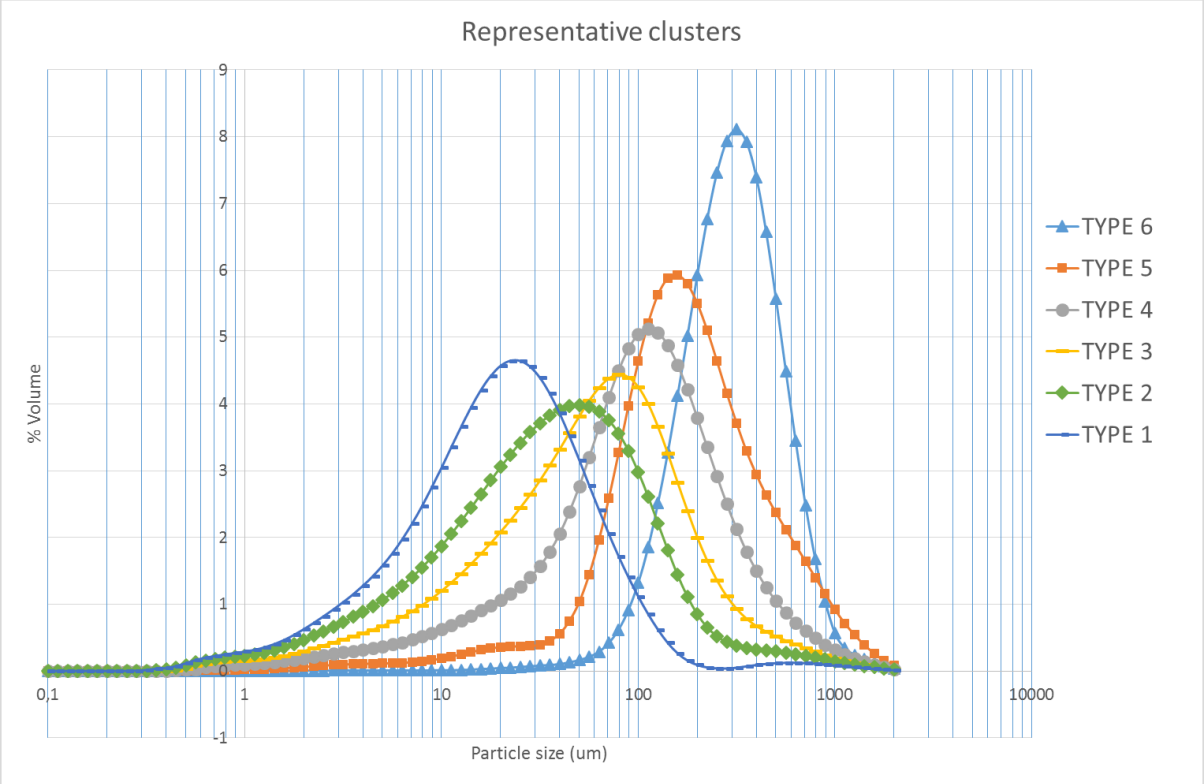

Figure 31 Average particle size distributions for cluster Type 1-6

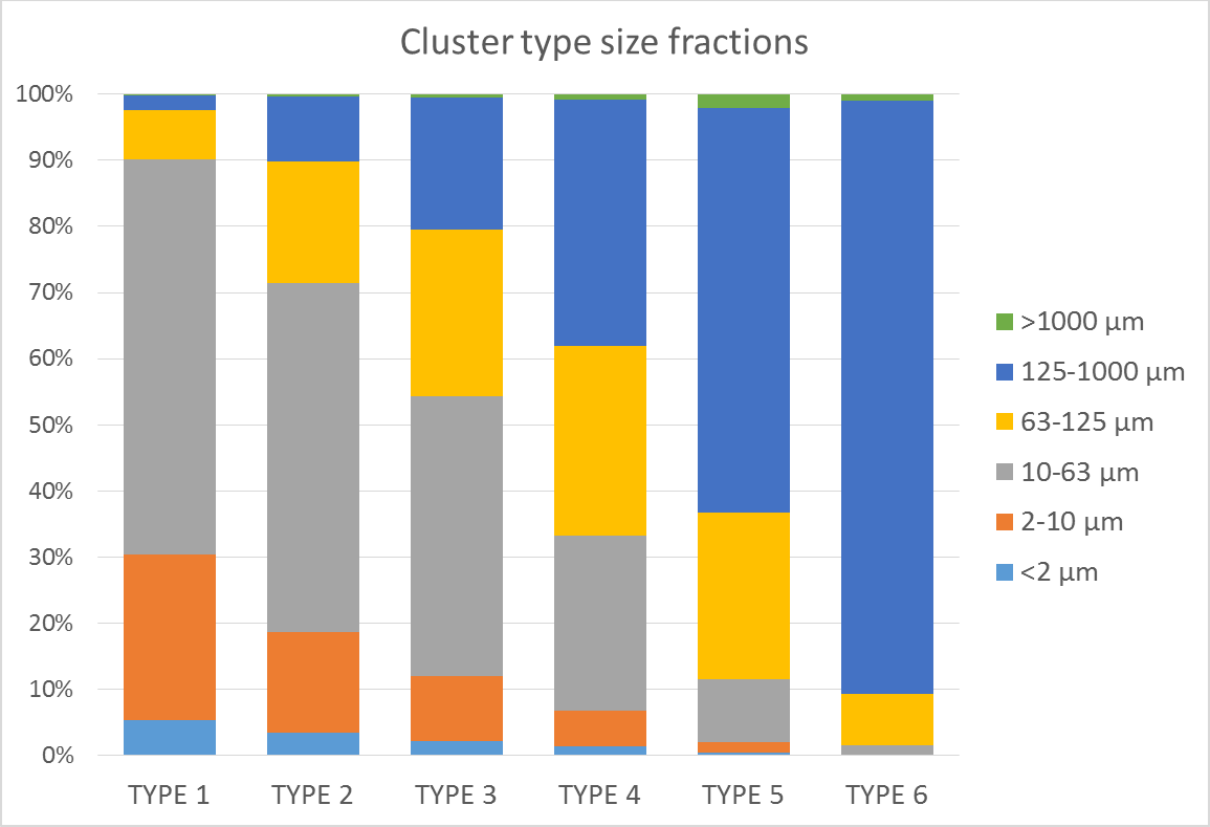

Figure 32 Average particle size fractions for cluster Type 1-6

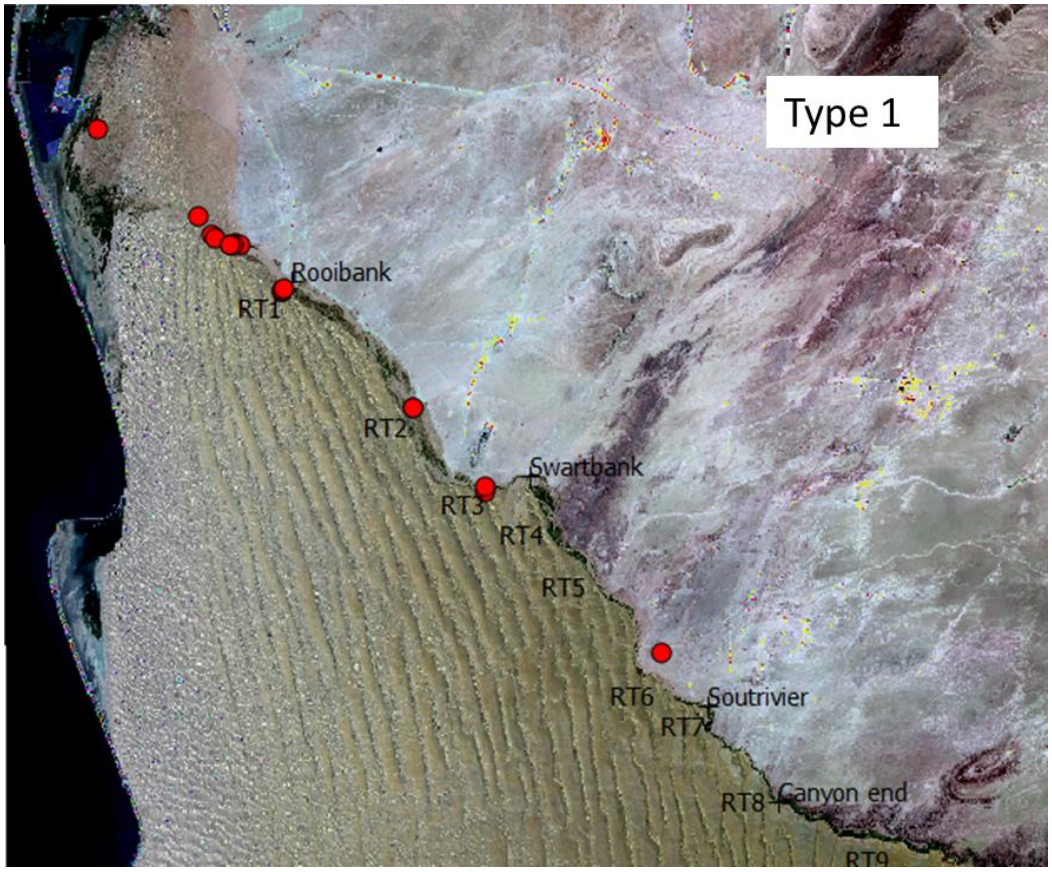

Figure 33 Cluster Type 1 sample locations

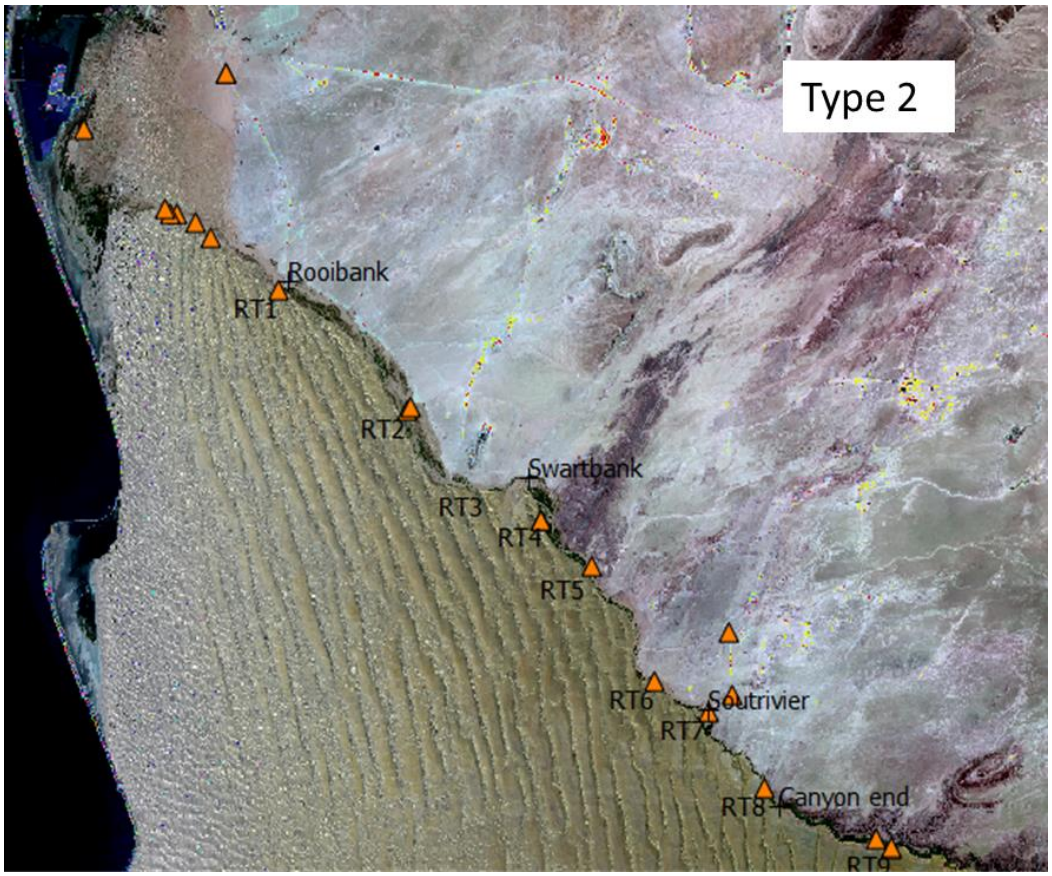

Figure 34 Cluster Type 2 sample locations

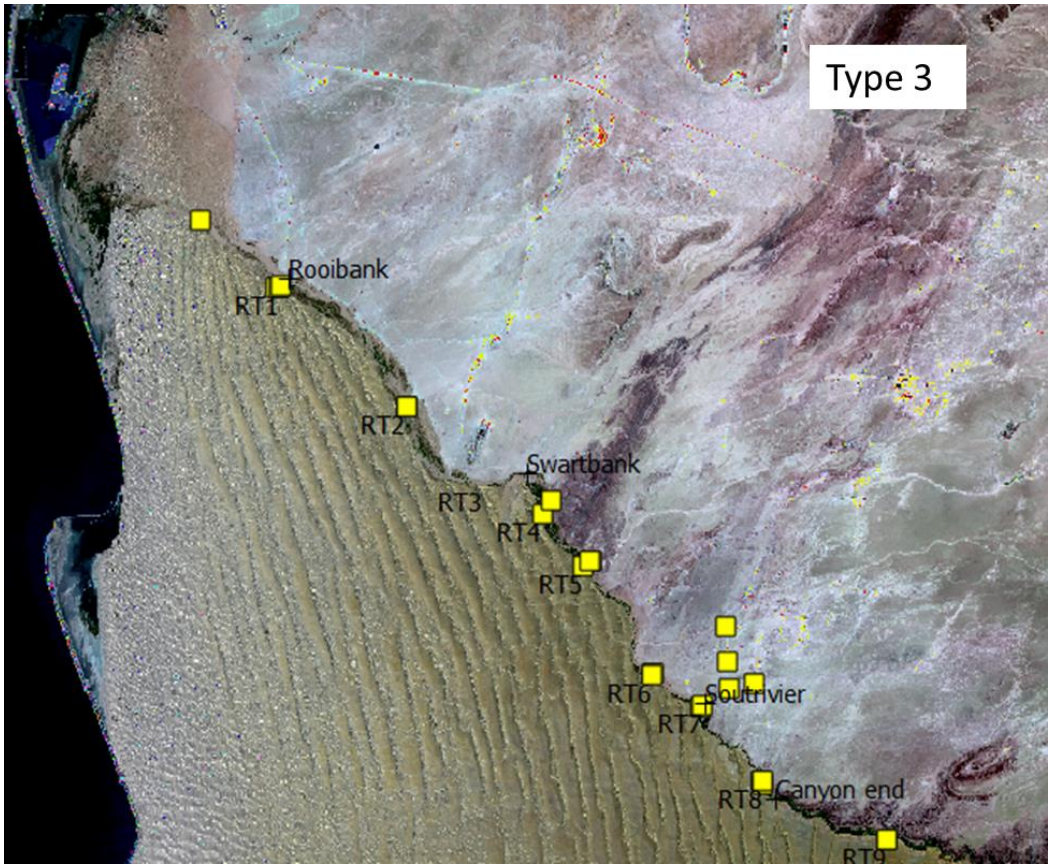

Figure 35 Cluster Type 3 sample locations

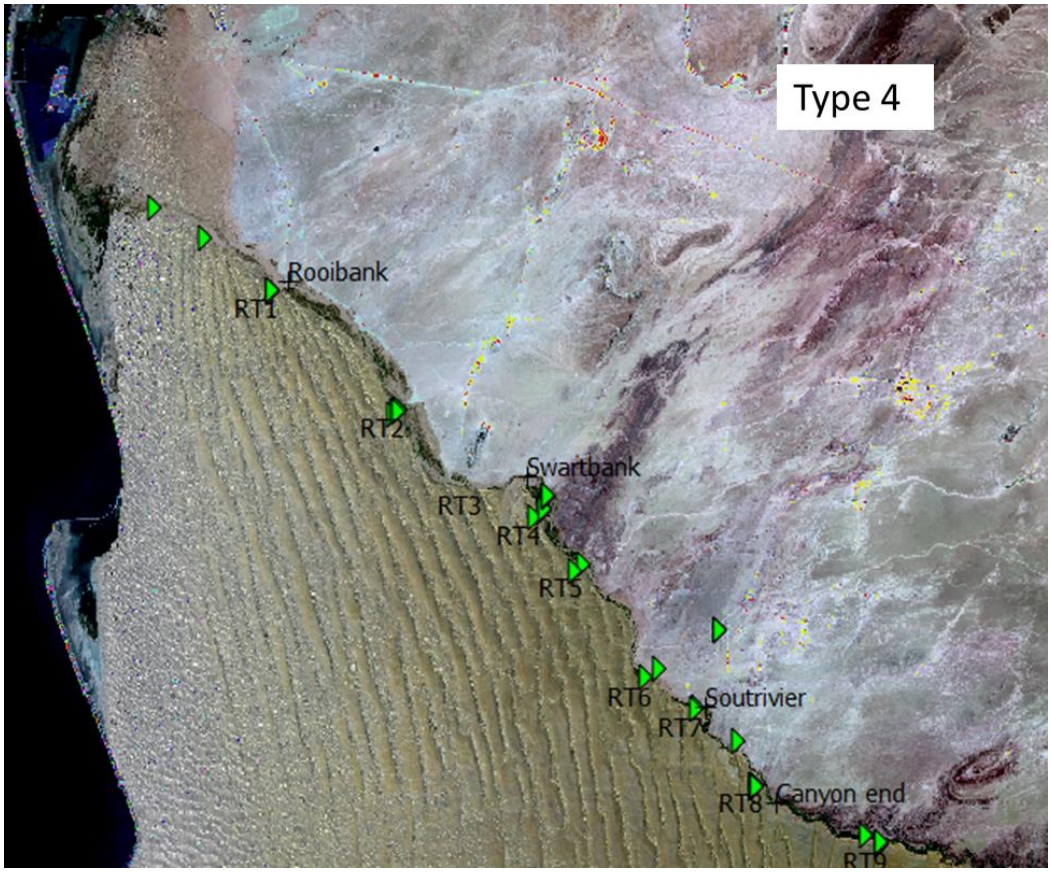

Figure 36 Cluster Type 4 sample locations

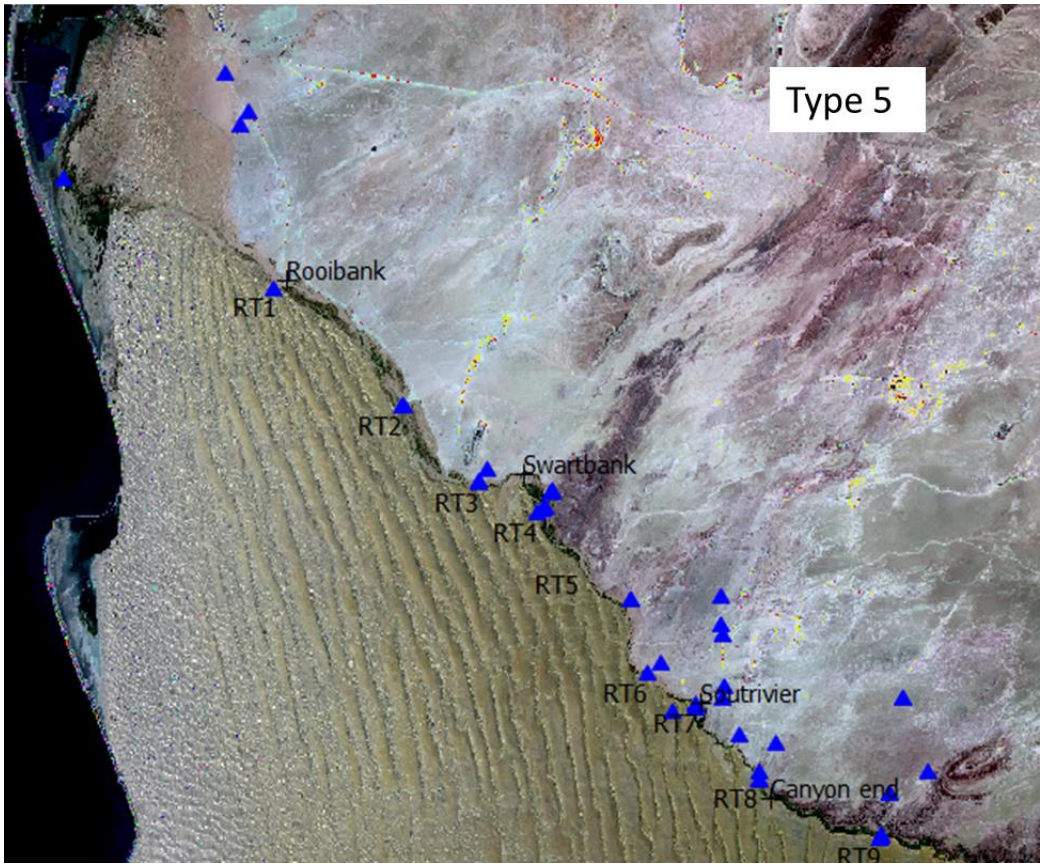

Figure 37 Cluster Type 5 sample locations

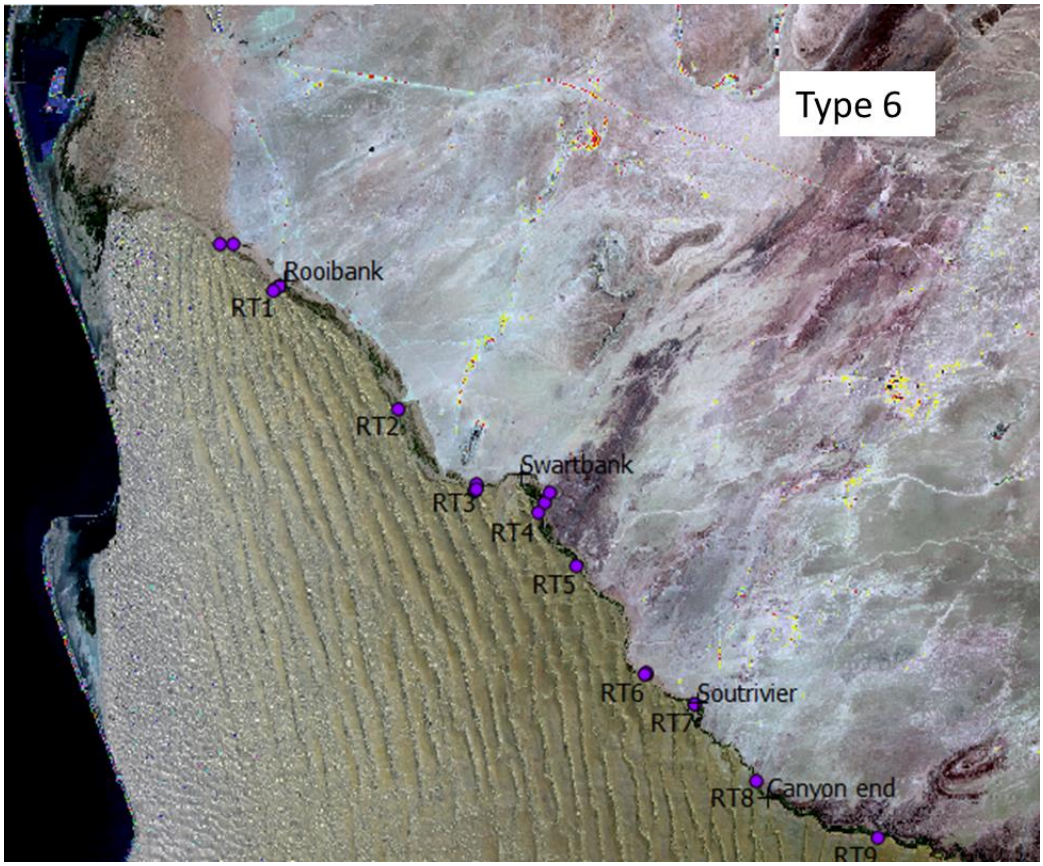

Figure 38 Cluster Type 6 sample locations

4.2 Other sediment characteristics

The mineralogy and morphology of the five selected samples were investigated with SEM/EDS. The locations of the samples selected for further analysis are provided in Figure 39, with their particle size distributions (Figure 40) and summary of selected size fractions (Figure 41). These samples were selected based on their cluster type (Type 1 to 4 samples selected) and their location within the most likely dust producing geomorphological units (river, delta and gravel plain). Four of the five samples consisted of depositional crust, with one consisting of unconsolidated material (RF8-5).

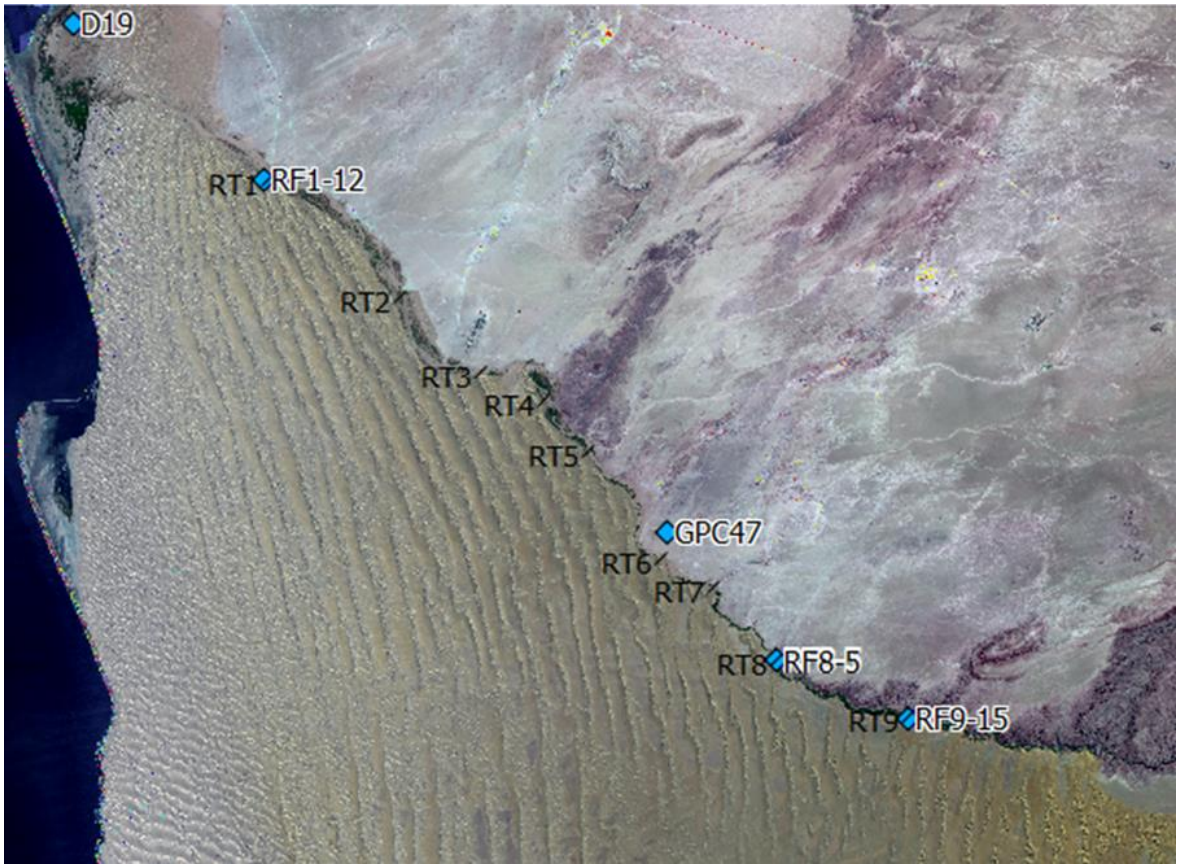

Figure 39 Location of samples selected for further analysis

Sample GPC47 was taken from the drainage network of the gravel plain close to where the channel flows into the Kuiseb River and consisted of dried out crust. This sample consisted of the finest material sampled in this study, with approximately 50% <10 µm (Figure 41).

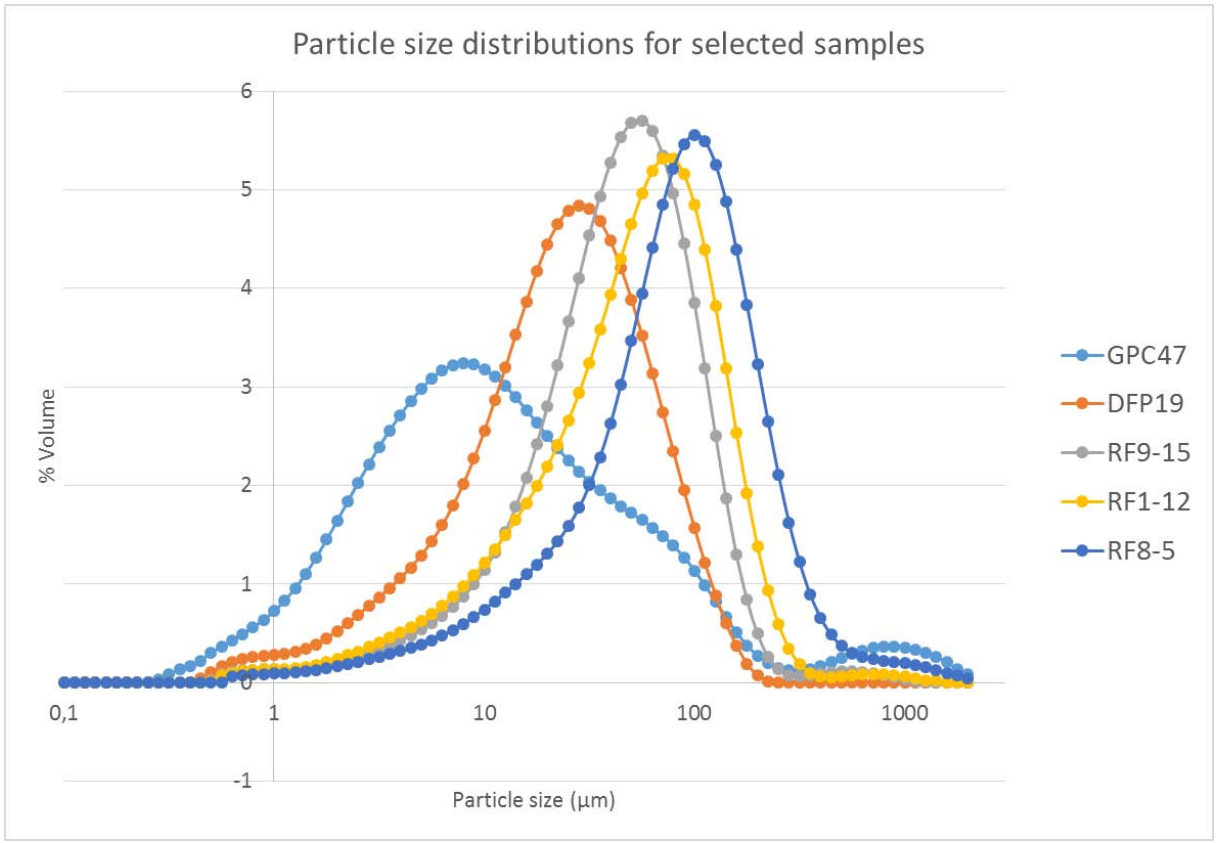

Figure 40 Particle size distribution of samples selected for further analysis

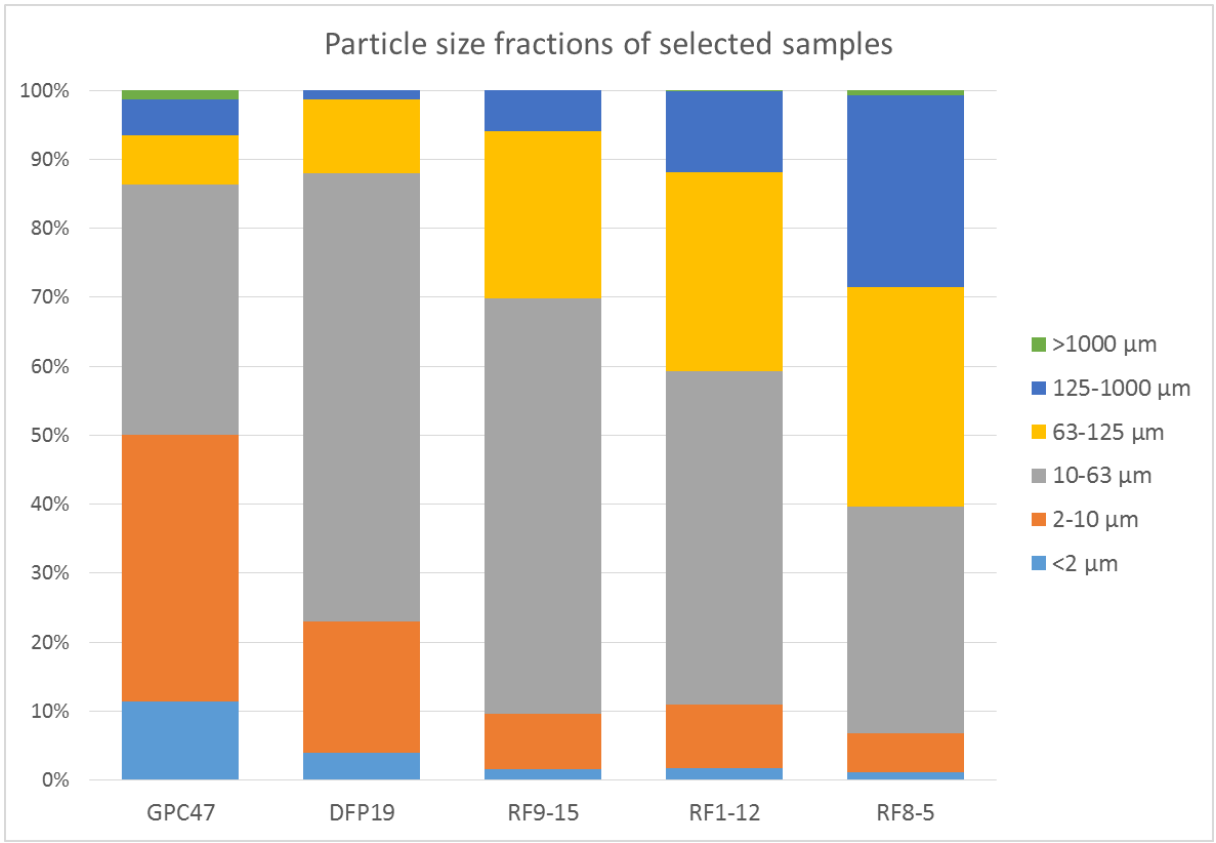

Figure 41 Size fractions summaries for samples selected for further analysis.

4.2.1 Moisture content

The moisture content of the samples are given in Table 8. The moisture contents were determined as a precursor to the organic content determined gravimetrically with Loss on Ignition. The surface moisture content during winter in the Namib Desert is low enough not to have an influence on the availability of sediment. The sample from the delta (DFP19) was taken in summer on the second wettest day on record for the area and will therefore have a high moisture content. The three samples from the river (RF1-12, RF8-5, RF9-15) have moisture contents that one would expect of the dry conditions in the desert. The moisture content of the crust sample from the gravel plain (GPC47) is surprisingly high.

The moisture contents were determined on a after the particle size analysis was conducted (on a new sample fraction from the same bag) and the samples were exposed to the wet winter conditions of Cape Town. Even though the samples were sealed in plastic bags for most of the time (samples were split and analysed with laser diffraction prior to moisture content determination), they could have taken on some moisture from the ambient conditions in Cape Town. The results here could therefore be slightly elevated compared to what they were at the time of sampling. The higher clay content and mineralogy of sample GPC47 would mean that it has a higher water holding capacity than the other samples (Schulze, 2002) and would therefore also be affected to a greater extent by the conditions in Cape Town.

Table 8 Moisture content of selected samples

Sample ID	Moisture content, %
GPC47	5.3
DFP19	7.9
RF9-15	0.9
RF1-12	0.9
RF8-5	0.9

4.2.2 Organic matter

The organic matter results determined by LOI are given in Figure 42. The content of GPC47 on the gravel plain at first seemed unrealistically high. On further investigation it would seem that LOI method to determine organic matter content is not the best option, especially where

carbonates are present. The LOI method has a number of shortcomings, for example: incomplete combustion of organic residues, the overestimation of organic matter due to hydrous clays and the inability of the method to distinguish between organic and inorganic carbon (Bisutti et al., 2006; Dr AG Hardie, personal communication, 19 August 2013). Sample GPC47 has a large percentage of calcite and this could lead to an inflation of the gravimetric determination of organic carbon. However, partially treating this sample with hydrogen peroxide revealed the presence of particulate organic matter, which could also account for the high result to a certain extent (Figure 43).

A better method of organic carbon determination for samples that contain carbonates would be to use either the Walkley-Black method or to a use acid fumigation-dry combustion method (Dr AG Hardie, personal communication, 19 August 2013). The latter method is preferred in a laboratory situation that does not specialise in Walkley-Black as the method uses dichromate which is highly toxic. The acid-fumigation method is described in more detail in Appendix section 8.7.

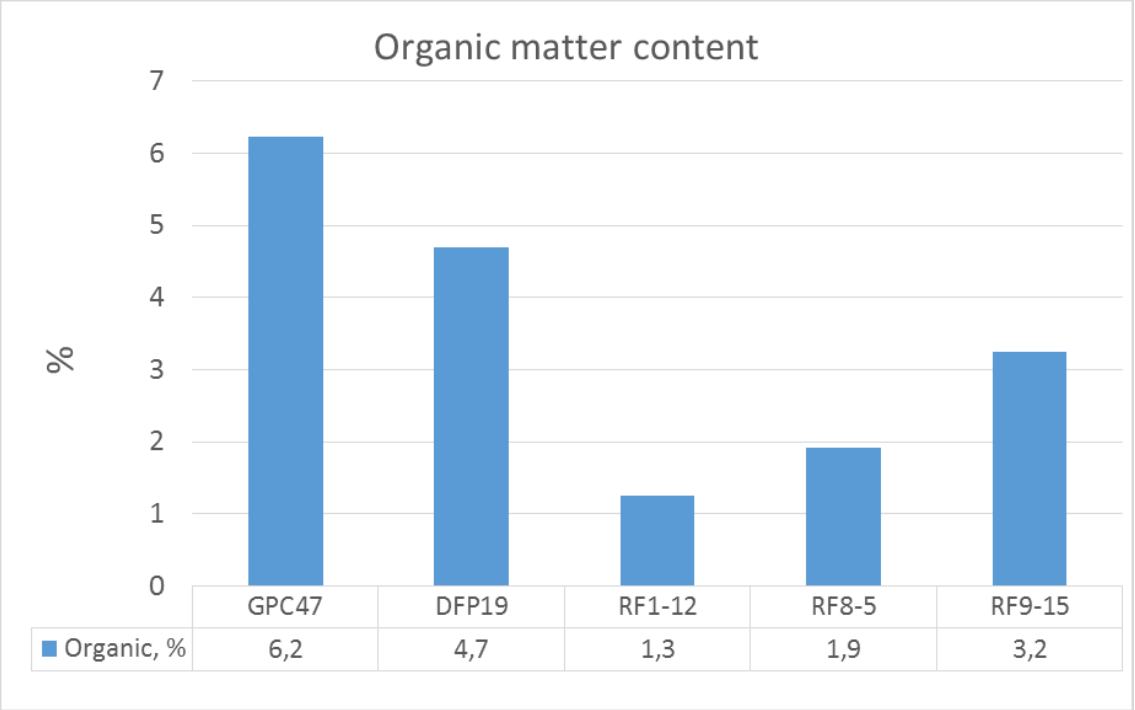

Figure 42 Organic content determined gravimetrically by Loss on Ignition.

Figure 43 Particulate organic matter in sample GPC47 after partial treatment with hydrogen peroxide.

4.2.3 Soluble salts

The analysis for soluble salts revealed significant concentrations of Ca and Na and lesser concentrations of K and Fe.

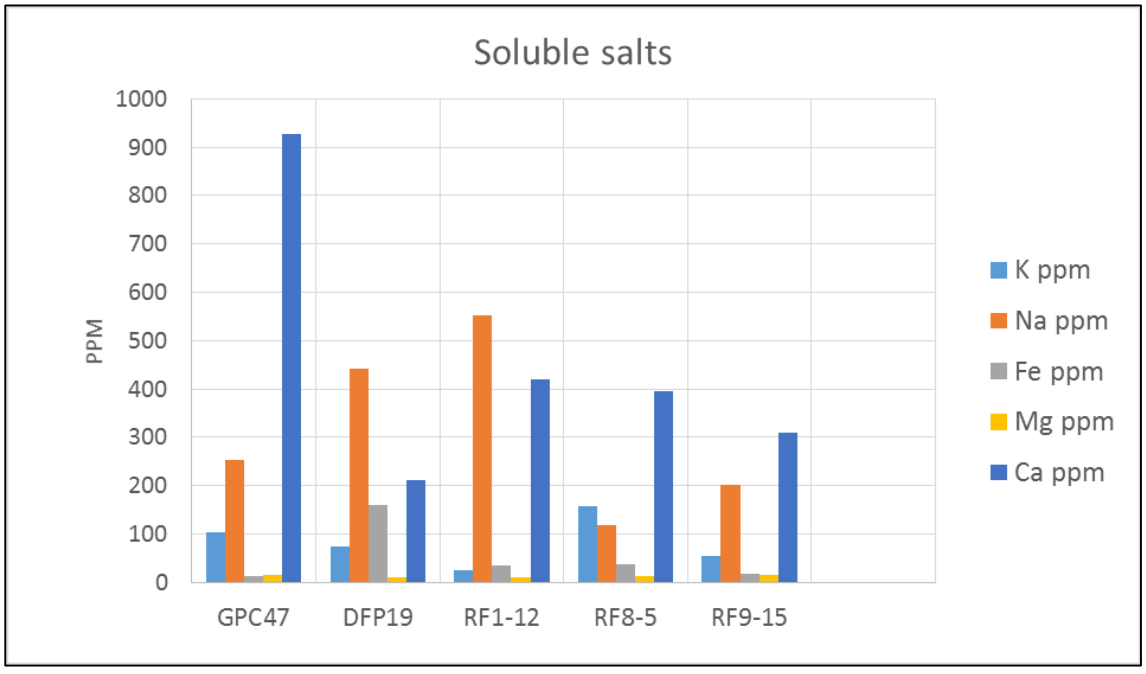

Figure 44 Soluble salt content (ppm) of each of the five representative type samples

The supernatants used for soluble salt determination for all samples except GPC47 remained discoloured despite numerous centrifuge attempts (Figure 45). This is possibly due to the higher dissolved organic matter contents within the samples that remained discoloured, especially in the case of the sample from the delta fan (DFP19) (Dr L Khomo, personal communication, 18 October 2013).

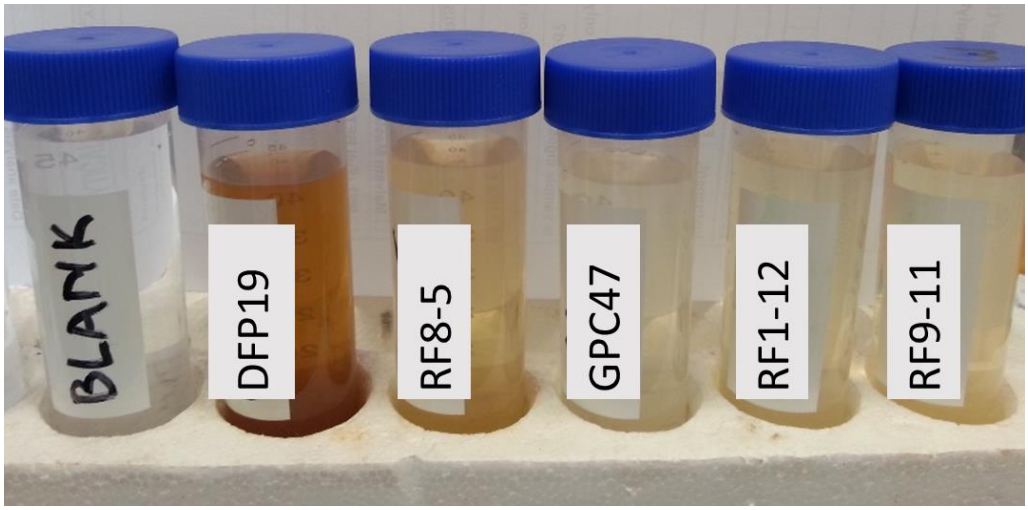

Figure 45 Discolouration of supernatant following preparation of samples for soluble salt content

4.2.4 SEM with EDS

The SEM images in combination with EDS confirms the difference in mineralogy between material from the gravel plain and river (Figure 47 to Figure 51). Although it is not possible to accurately identify the minerals present without XRD, it does give an idea of the mineralogy. As expected, there are mica flakes present in all the samples as a result of the dominant schist geology of the basin.

Sample GPC47 from the gravel plain is made of up of aggregates of different minerals. It is difficult to identify which minerals are present as the EDS analyses is based on mixtures. The mixture of minerals seem to be fairly homogeneous as shown by EDS. This sample contains considerable calcite/aragonite (Figure 47, image b), which was confirmed with vigorous bubbling upon addition of HCl. In addition, there also appears to be very fine particulate organic matter in the same sample (Figure 47, image a and d). The presence of fine particulate organic matter could also explain the raised organic content in this sample measured by LOI (Figure 42). The predominance of calcite in the sample is partly as a result of the wide spread

calcrete duricrust deposits found on the gravel plain to the east of the sample location (Figure 46). The drainage channel from which the sample was taken flows from the playa situated within the calcrete duricrust area into the main channel of the Kuiseb River.

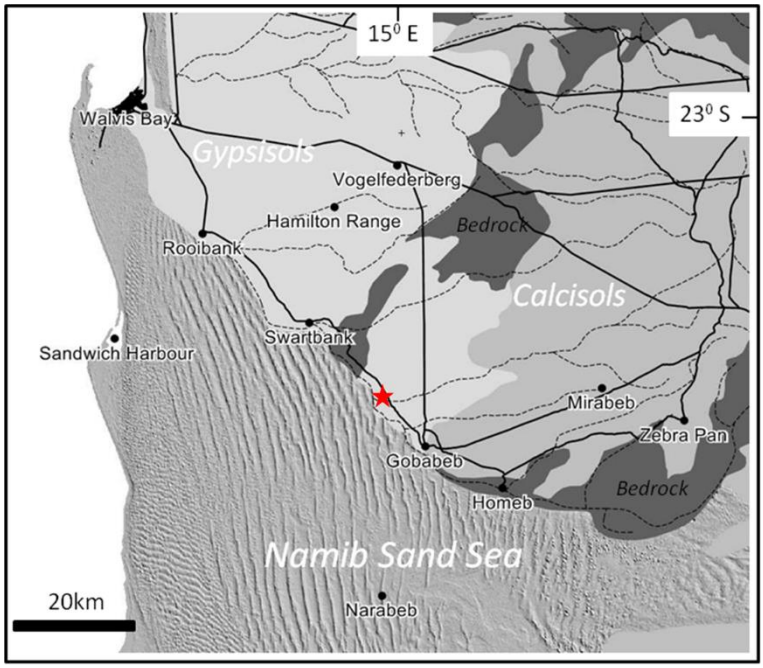

Figure 46 Distribution of duricrust and bedrock on the gravel plain within the study area. Map taken from Eckardt et al. (2013). Note the predominance of Calcisols to the east and Gypsisols to the west. Sample I1 location marked with a ★.

The micas found within the river consist of various possible biotite and muscovite end members. The general formula for the mica group minerals are: $X\ Y_{2-3}\ Z_4\ O_{10}\ (OH)_2$, where X represents the interlayer sites, Y the octahedral sites and Z the tetrahedral sites (Practical aspects of mineral Thermobarometry, 2004). The most common site preferences and substitutions for biotite and muscovite are as follows:

Tetrahedral: Si, Al

Octahedral: Al, Cr, Fe, Ti, Mg, Mn

Interlayer site: K, Na, Ca

There is an abundance of cations present for substitution within the octahedral sites, for example: Fe, Ti, Mg and Mn. Similarly, cations such as K, Na and Ca are present for substitution within the interlayer site.

Sample DFP19 (Figure 48) taken in the delta fan area close to Walvis Bay confirms the presence of fine material as shown by the grain size analysis. There are no particles greater than 100 μm, which is in agreement with the particle size distribution obtained with laser diffraction (Figure 40). The botryoidal material present in many of the samples appears to be soluble salts cementing other grains together (Dr Pat Harris, personal communication, 11 November 2013), see sample DFP19 (image c).

What is also evident from the SEM images is the amount of fine dust particles adhering to the larger particles which could be released during entrainment as the particles undergo abrasion (Bullard et al., 2007). Sample RF8-5 (Figure 51) illustrates this very well and several EDS measurements were attempted on what seemed to be smaller particles adhering to larger particles. The pinpoint EDS analysis (image a and c) probably receives a lot of contribution from the background and is therefore not accurate (Dr Pat Harris, personal communication, 11 November 2013).

Even though there is evidence of organic matter within the samples, the Carbon picked up by EDS is most probably from the carbon coating during sample preparation.

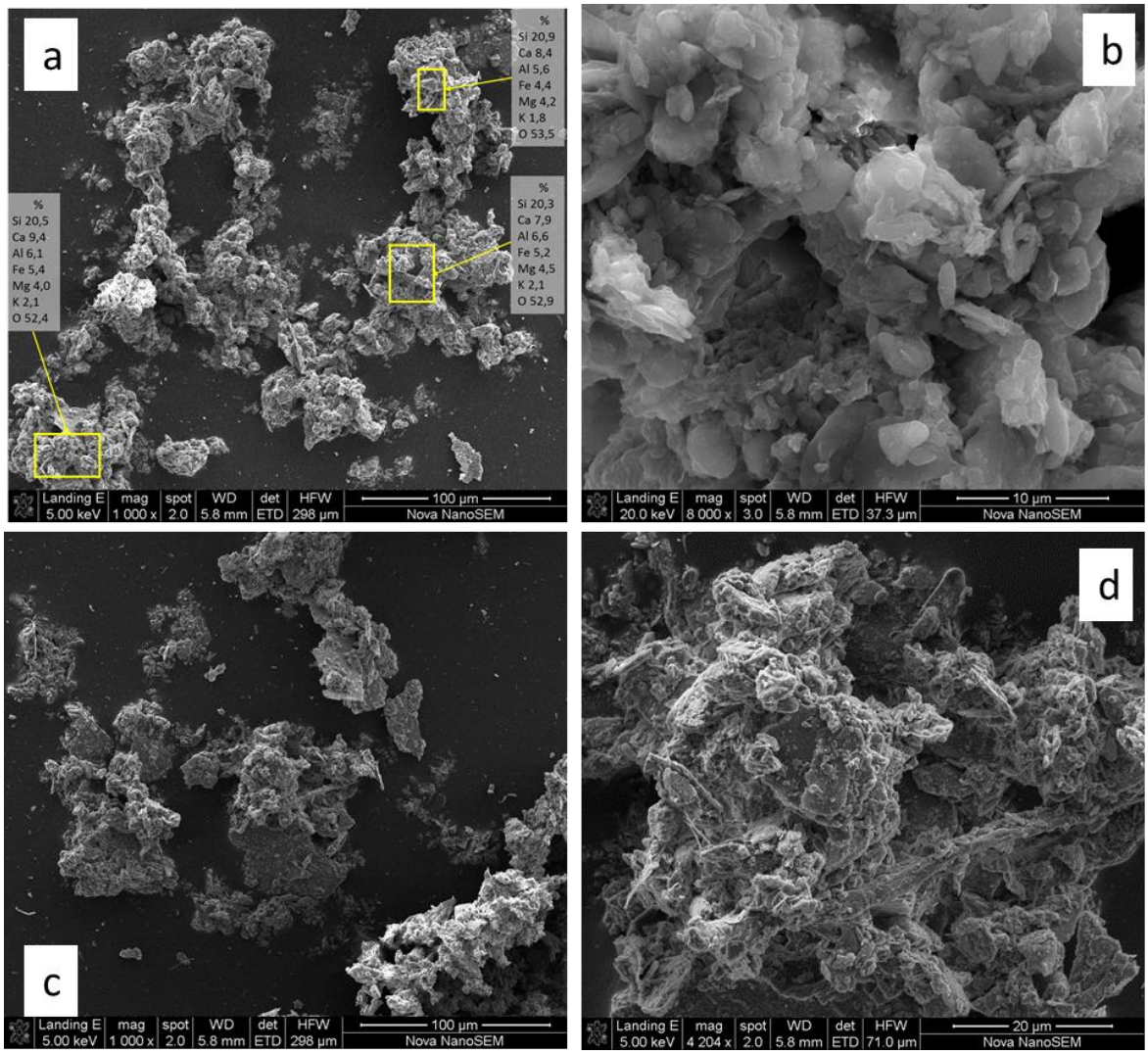

Figure 47 SEM images of sample GPC47 (Type 1)

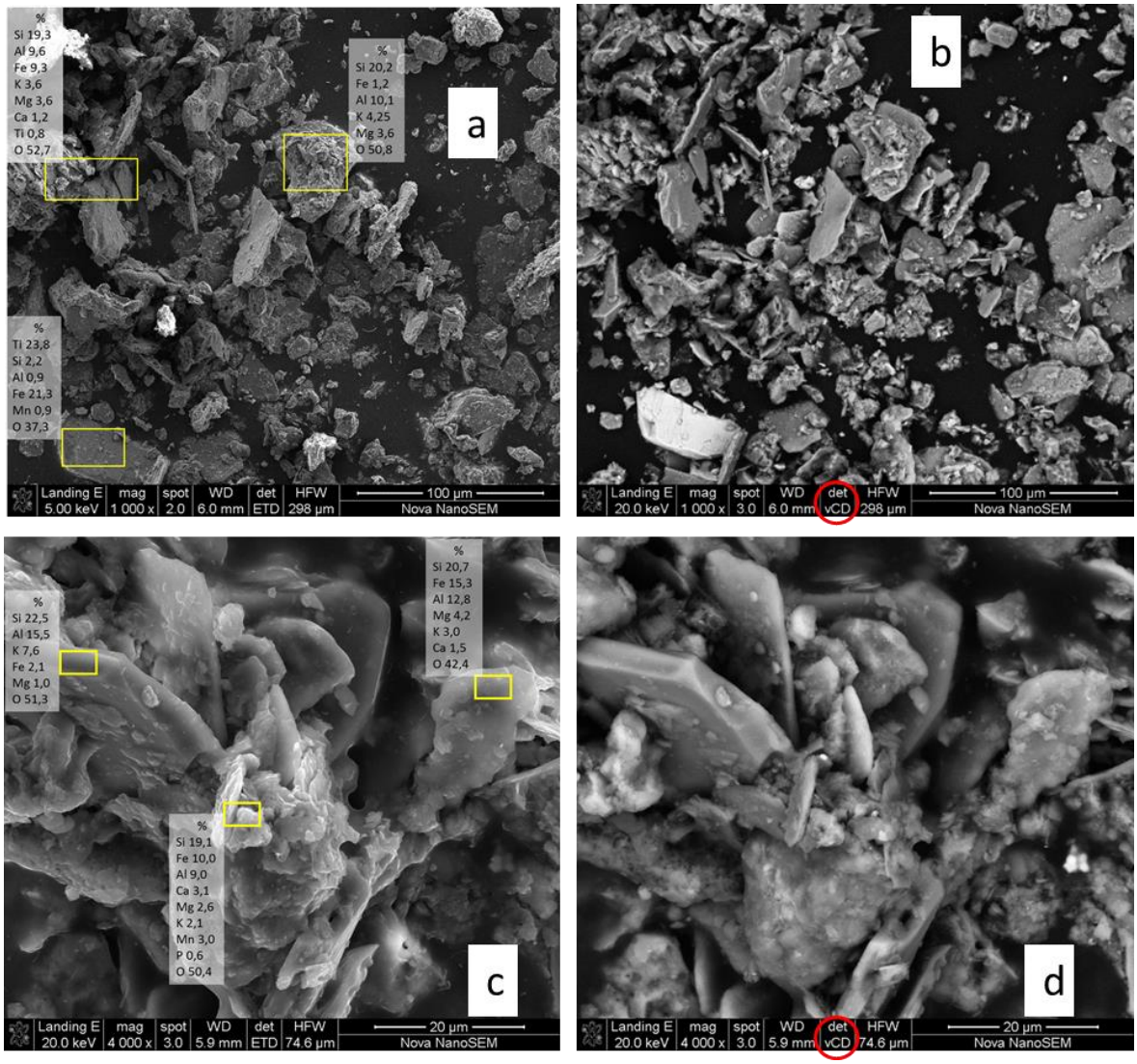

Figure 48 SEM images of sample DFP19 (Type 1)

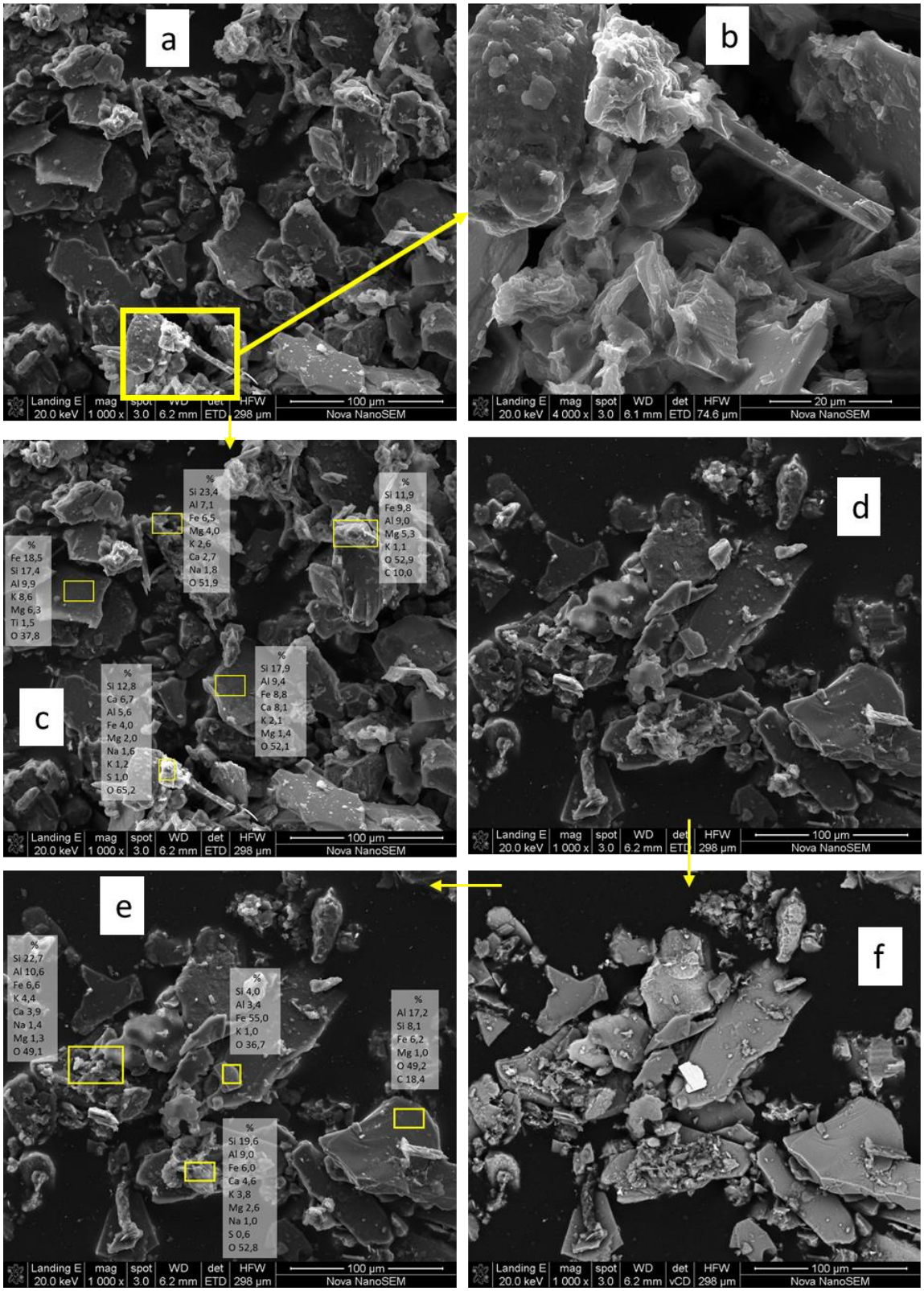

Figure 49 SEM images of sample RF9-15 (Type 2)

RF1-12 again show aggregation of different minerals. The high carbon content is most likely from the carbon coating.

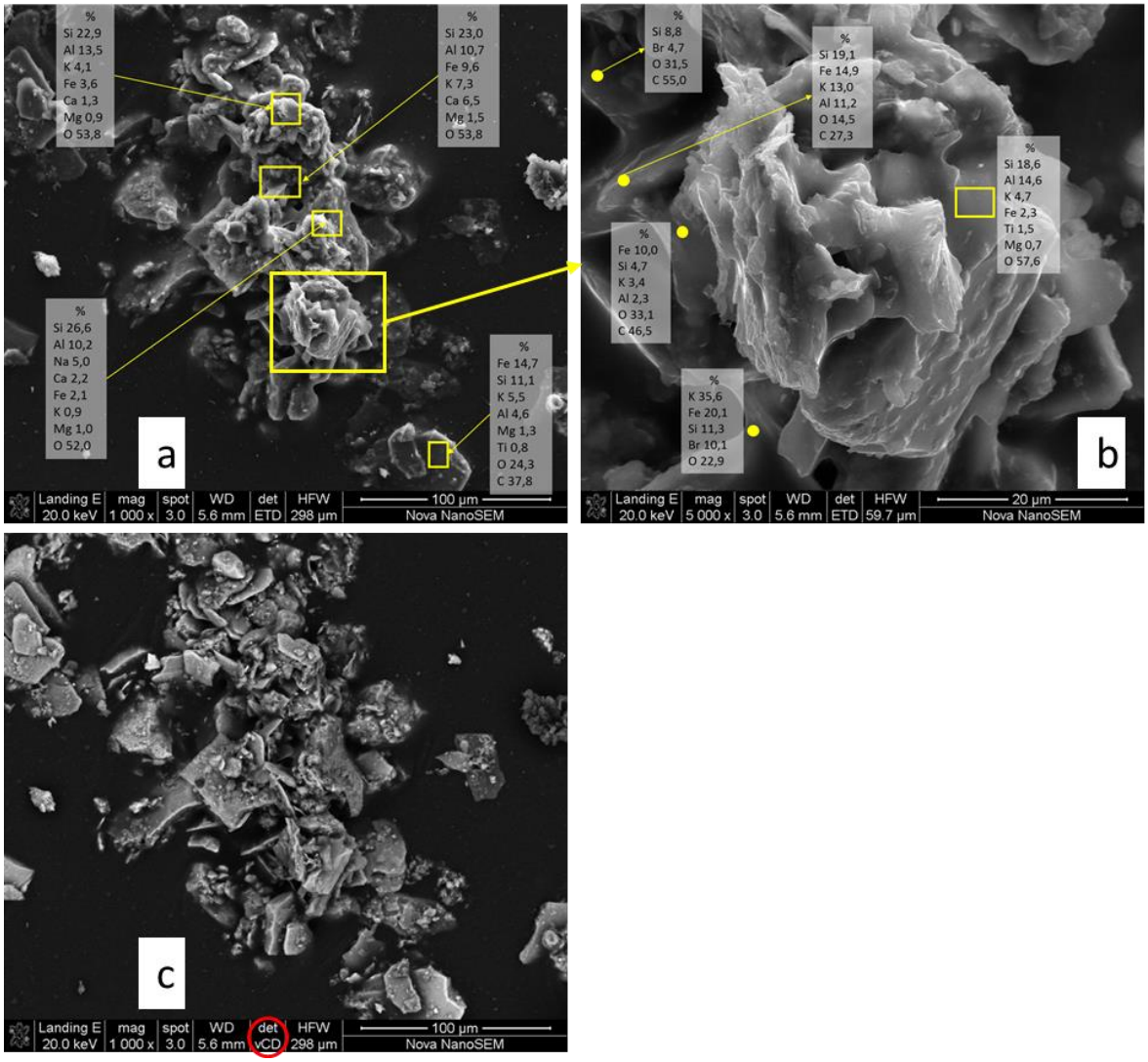

Figure 50 SEM images of sample RF1-12 (Type 3)

Samples RF8-5 show contain mica and quartz, with abundant Fe. The rounded particle in the top right corner of image c and d could possibly be organic matter.

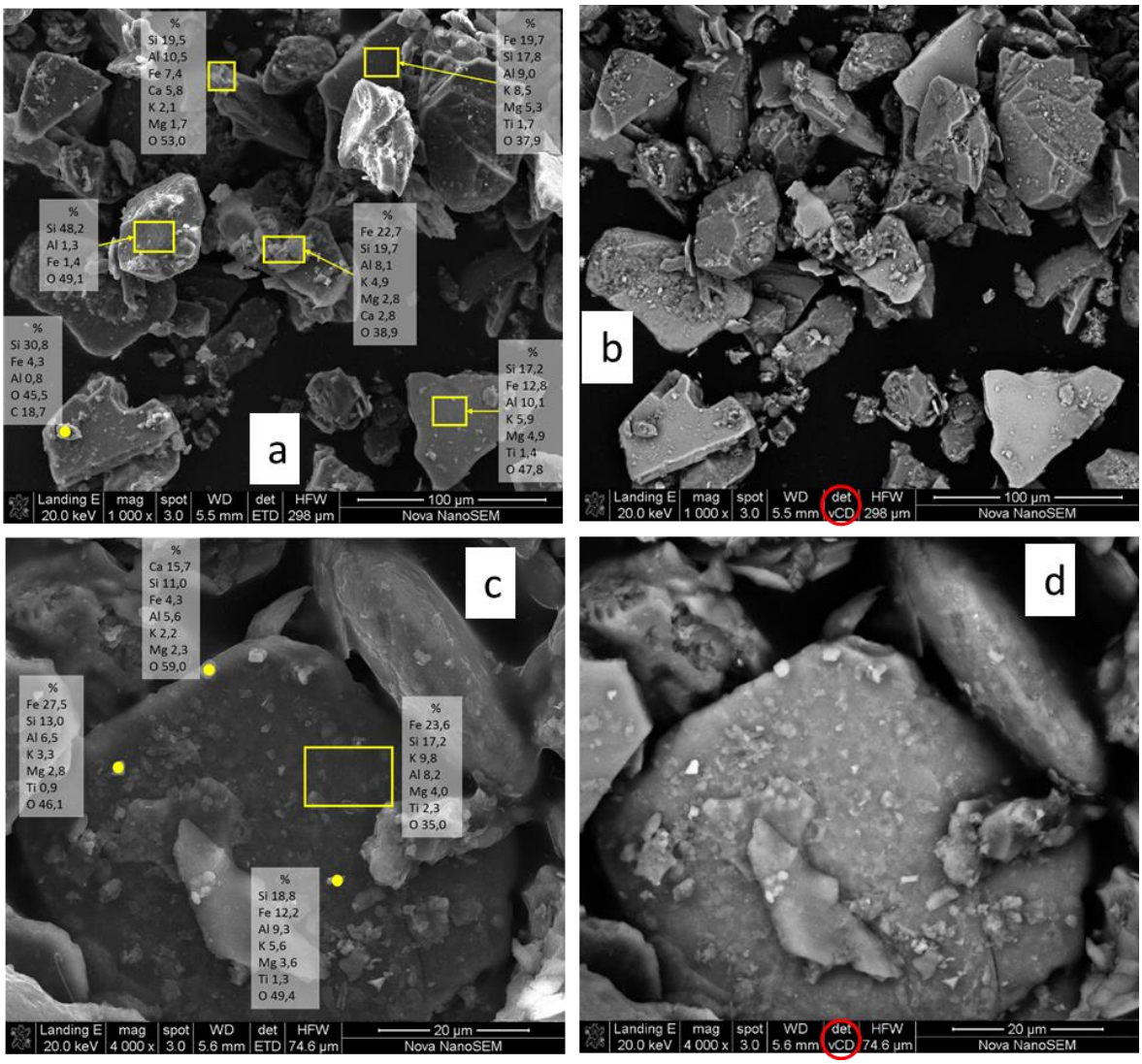

Figure 51 SEM images of sample RF8-5 (Type 4).

4.3 Remote sensing

Even though the MODIS imagery does not lend itself to accurately identifying source points over land, it was used in this analysis to get an idea of the relative contribution to dust plumes by the various geomorphological units. This is similar to the investigation done by Vickery (2010), but extends the study period to 2013. For the period from 2005 to 2013 a total of 73 dust days were identified (Figure 52). The identification of the source areas of the plumes for the same period was attempted (Figure 22). The number of dust days for 2005 to 2008 corresponds to that identified by Vickery (2010).

The MODIS images that were used are listed in Appendix section 8.4.

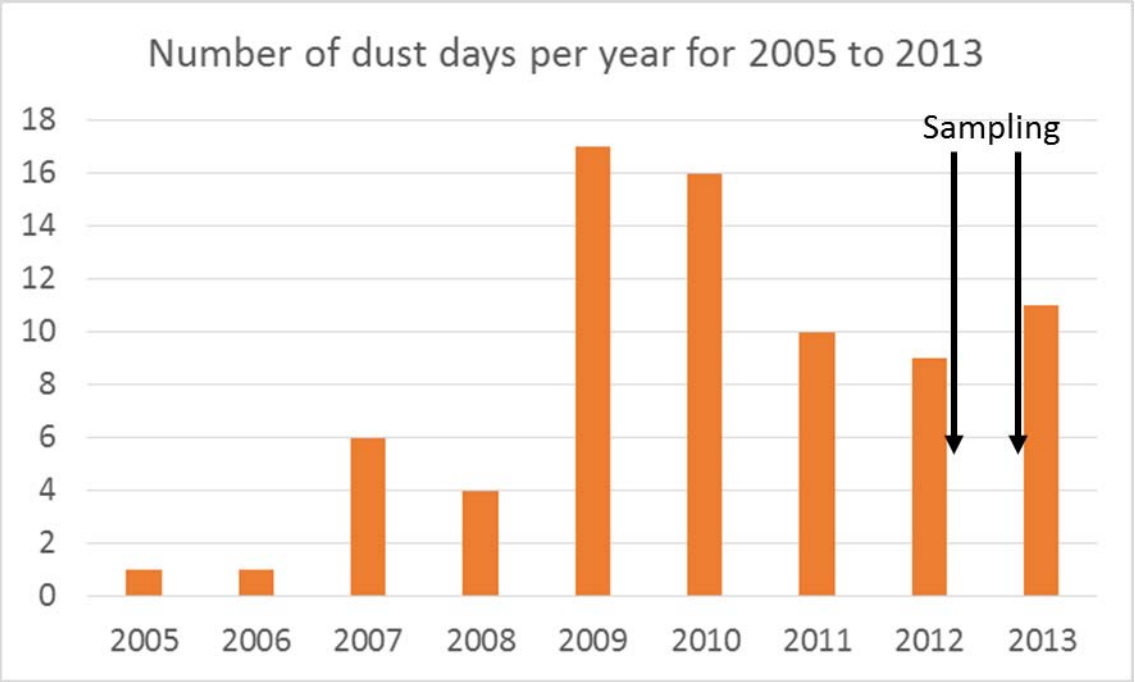

Figure 52 Number of dust days per annum from 2005 to 2013 identified with MODIS imagery. Timing of sampling conducted for this study indicated.

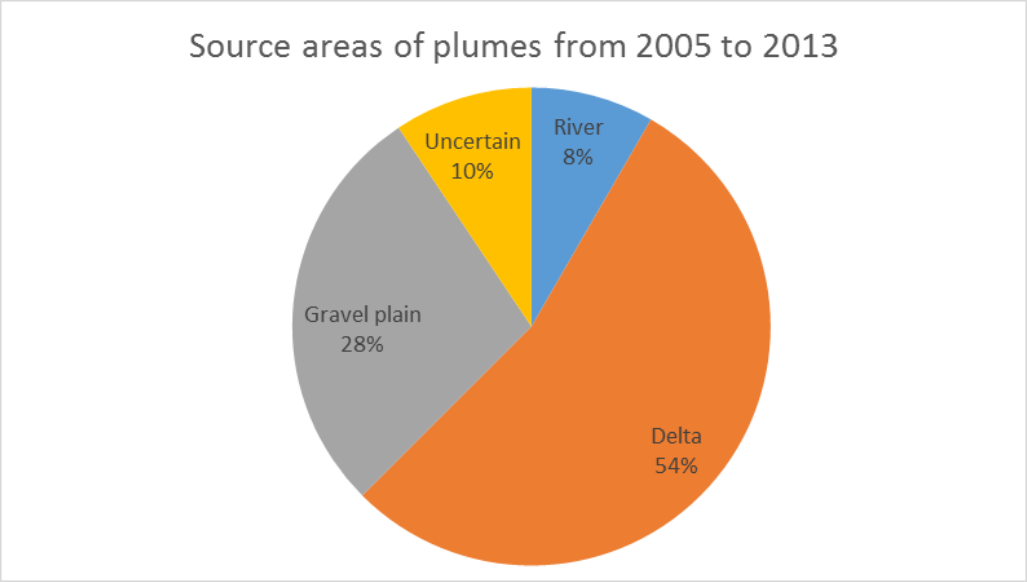

Figure 53 Source areas of plumes identified with MODIS for 2005 to 2013. Uncertain category could not be identified.

This analysis only gives an idea of the source points as it is not possible to identify the exact source area in most instances. For 10% of the images no source area could be identified with reasonable certainty. This was often due to the clarity of the images (see Figure 54). The plumes originating in the gravel plain to the north-east of the delta were assigned to the gravel plain and the delta. The dust activity from the sabkhas (including the Kuiseb delta sabkha, Sandwich harbour and Conception Bay) were also recorded and 18% of the plumes from the Kuiseb delta seem to involve the sabkha. The contribution to plumes by different geomorphological units differs somewhat to that of Vickery (2010). This can be attributed to:

a. The difficulty in identifying the plumes with MODIS imagery over land and, as a consequence, the subjective nature of the selection of the source areas.
b. Some plumes were attributed to more than one unit where it is uncertain from which geomorphological unit they originate.
c. The inclusion of an uncertain category for plumes that cannot be pinpointed with reasonable certainty, mainly due to the poor quality of the images.
d. Lastly, the relatively small study area for this study compared to that of Vickery (2010) enabled a more focused analysis.

The plume source areas identified are given in Appendix section 8.4.

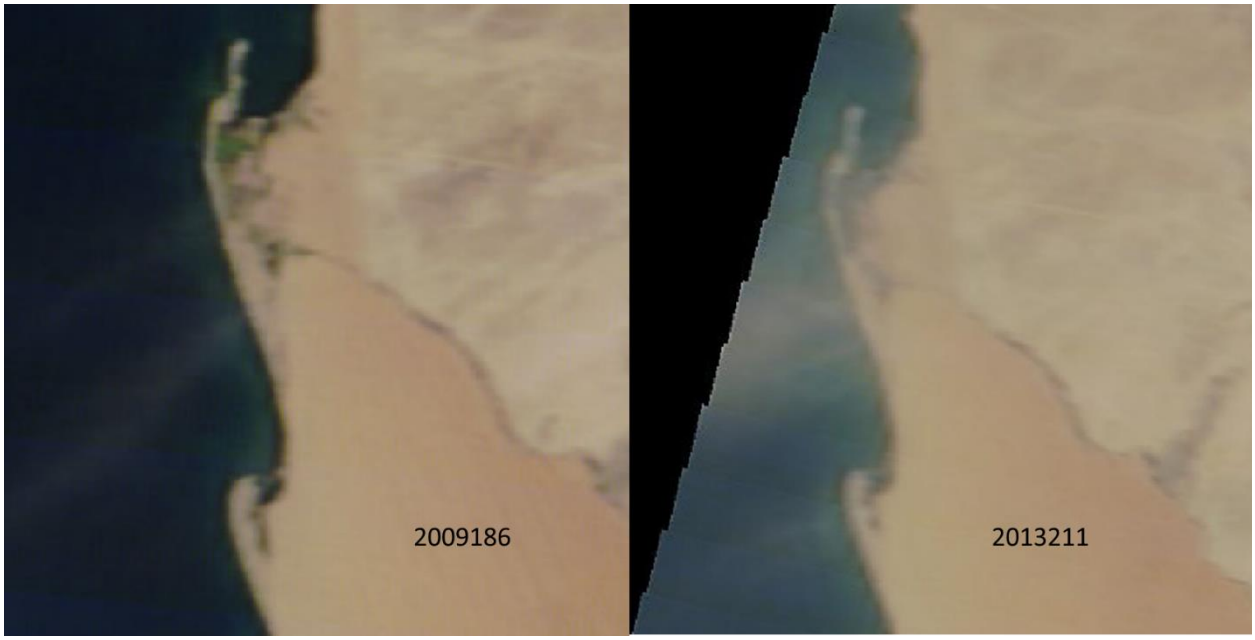

Figure 54 Unclear images to which no source point was assigned

5 Discussion

For the purposes of this discussion the Kuiseb study area will be divided into the segments listed in Table 9. The likelihood of a geomorphological unit acting as a dust source can first be evaluated by looking at the particle size distribution for the sediment sampled in each unit. Following an evaluation of the sediment size characteristics, the segments that are identified to house appropriately sized sediment, will undergo further consideration by, examining the potential for sediment deflation taking into account the surface roughness, such as vegetation cover. In addition, the degree to which human influence plays a role in the dust activity of each unit identified as a likely source area will be assessed.

Table 9 Segments of the various geomorphological units found in the Kuiseb basin.

Unit	Code	Segment
River	RU	Upper river floodplain: comprising the most upstream section of the Lower Kuiseb River. From the Canyon to Soutrivier.
	RM	Middle river floodplain: from Soutrivier to Swartbank
	RL	Lower river floodplain: comprising the most downstream section of the river before it opens up into the delta. From Swartbank to Rooibank.
	RAC	River active channel
Delta	DAC	Delta active channel sand
	DCC	Delta channel depositional crust
	DFP	Delta floodplain
Gravel plain	GPC	Depositional crust in the drainage network channels of the gravel plain
	GPS	Stone pavement with gravel overlay
Sand Sea	SS	Sand Sea sand
	ID	Interdune sediment

5.1 Potential source areas: a supply of sediment

The average particle size fractions for each segment gives a good preliminary indication of which units are likely to act as source areas of dust, specifically the <63 µm fraction (Figure 55). These results indicate that the potential primary sources of dust are the delta channel crusts and delta floodplain, the floodplains of the entire Lower Kuiseb River, and the gravel plain

crusts. Potential secondary sources of dust include the gravel plain stone pavement and the interdune surfaces. Segments not considered as dust producing are the delta active channel (sands other than depositional crusts), the river active channel and the Sand Sea sand. These non-dust producing areas are, however, important sources of sand for saltation, and their proximity to the sources of dust plays an important role in the dust activity of the Lower Kuiseb River as a whole. Cahill et al. (1996) found that a source of sand situated several kilometres away from crusted fines can still act as saltators with sufficiently high-magnitude winds. Furthermore, even though dust emission is possible from these depositional crusts as a consequence of aerodynamic forces alone, it is more likely that the emission of dust from the crusts, as elsewhere, is predominantly a consequence of saltation (Baddock et al., 2011).

Looking at the percentage of samples in each cluster type for the different locations provides a summary of the cluster data (Figure 56). This confirms the delta (in the form of depositional crusts in the channel and floodplain), the lower river and the gravel plain drainage channels as containing the finest material by the presence of Type 1 samples. These are most likely the predominant sources of dust which remain in long term suspension (refer Figure 2) for this region, provided that they are available for entrainment. The predominance of Type 1 samples in the delta and lower river is to be expected. The downstream fining occurs as the finest suspended sediments are carried by the floodwater to the furthest reaches of the flood (Jacobson et al., 2000). Sampling in September 2012 took place almost 16 months after the largest flood event in decades. The 2011 flood, which reached the Atlantic Ocean, would have carried large quantities of fine sediment into the delta area, including fines deposited in the upstream section of the river in previous floods. There are also a significant number of Type 2, 3 and 4 samples in the middle and upper river segments that could act as additional medium to long distance dust sources.

A supply of appropriately sized sediment is, however, not sufficient to confirm a potential source area of dust. Dust emission is also dependent on the availability of these sediments for deflation by the wind. This availability is partly dictated by small-scale surface characteristics such as particle size distribution, moisture content, mineralogy (for example, soluble salt and clay content) and organic matter content. These characteristics of the sediment will affect the strength of the inter-particle bonds. This is especially pertinent given the wide distribution of depositional crusts within the Kuiseb basin. In addition, the availability of the fines for entrainment is also dependent on the surface roughness. The dense riparian woodlands found

along the Lower Kuiseb River could have a significant influence on hampering the dust emission potential of some of the segments.

Each preliminary potential source area identified above will be evaluated for the availability of the sediment in each segment. This will involve analysis of the small-scale surface characteristics listed above for selected segments, as well as consideration of the surface roughness at the location of the fines for each segment. Source areas will be reclassified as primary or secondary based on this evaluation. Primary sources can be regarded as areas with the largest dust emission capacity and are confirmed dust producing areas. Secondary sources are areas with a less significant dust emission capacity. These areas show the possibility of dust emission, but still need further investigation to confirm.

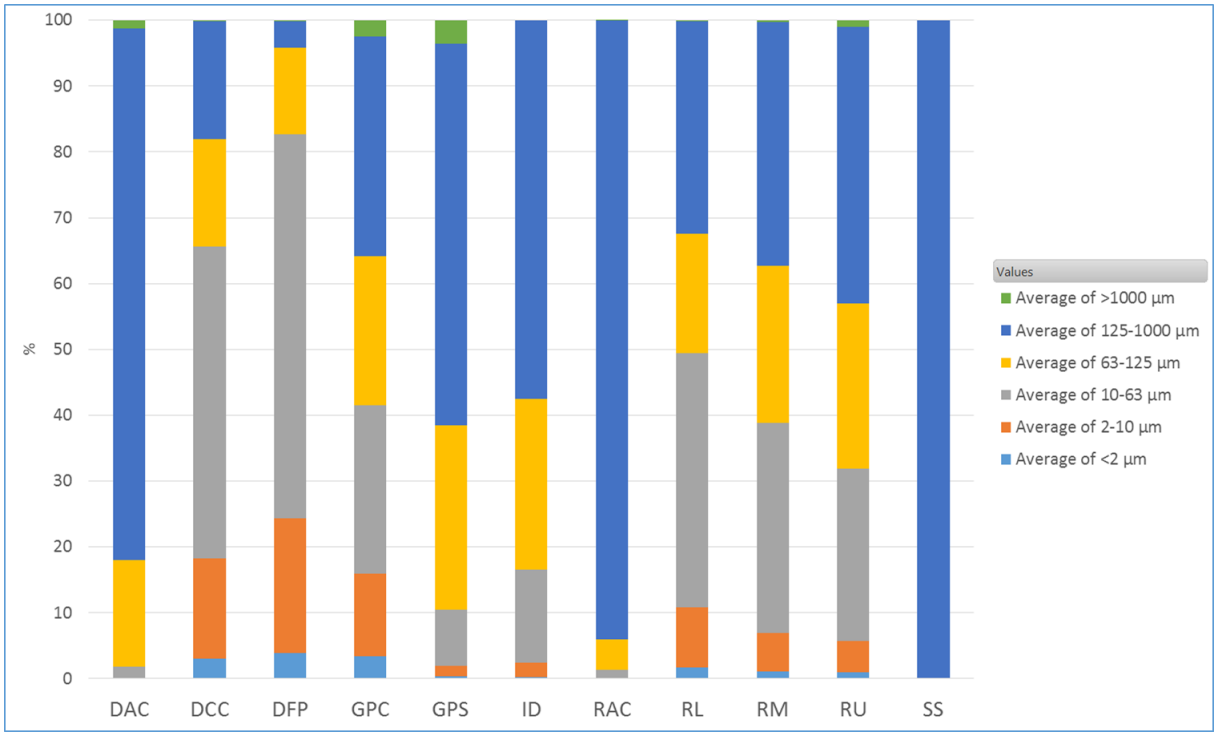

Figure 55 Particle size fractions for various segments (refer to Table 9 for explanation of codes).

Figure 56 Percentage of cluster type samples in various segments of the river. The delta samples (Delta Floodplain (DFP) and Delta Channel depositional Crusts (DCC)) have been grouped together.

5.2 Evaluation of source areas

Each source area will be discussed with the aid of the following graphic elements:

- Transect profile showing the surface features and topography of the segment
- Location and cluster type of samples taken in the segment
- Particle size fractions of the samples
- Photographs of surface features for each segment
- MODIS images of dust plumes if relevant
- Other graphics will be included where relevant.

These images can be found after the discussion of each potential source area. This discussion will refer to the different cluster types and Figure 57 provides a recap of the six cluster types: Figure 58 gives an indication of the river segments.

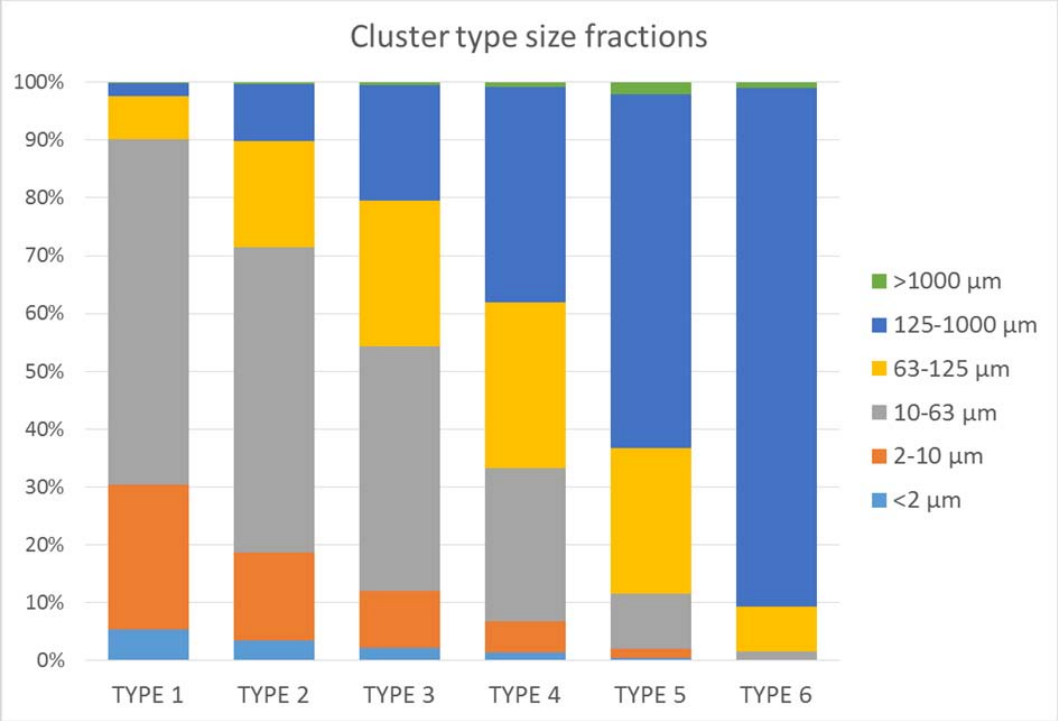

Figure 57 Average particle size fractions for cluster Type 1-6

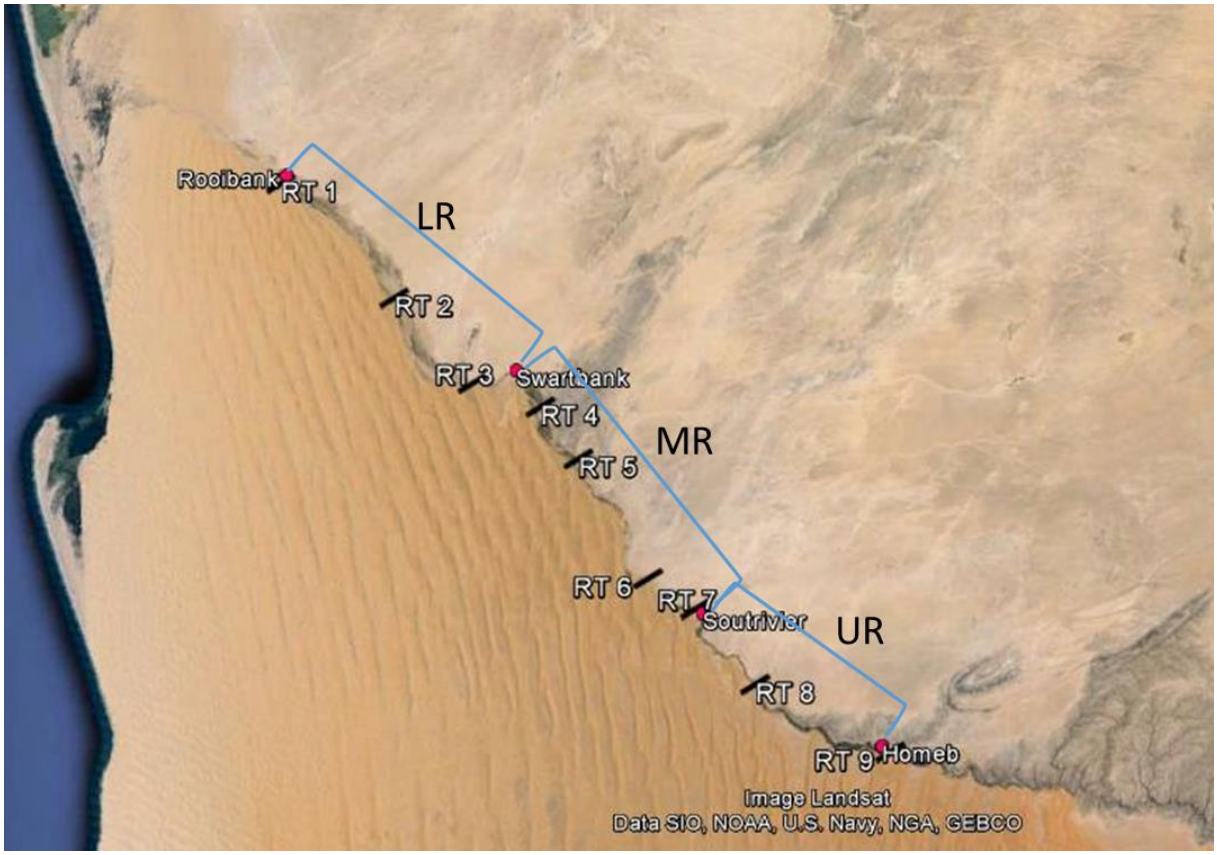

Figure 58 River segments LR, MR, UR

5.2.1 Primary source areas

5.2.1.1 RU (Upper river: 80-100 km from the coast)

The upper river segment starts at the end of the canyon where the river is still confined to bedrock, but is already bordered by the Sand Sea to the south and ends at Soutrivier. This segment of the river falls in the Upper Riverine Woodland section, as described by Theron et al. (1985).

The most upstream transect (RT9) is situated just upstream of Homeb. At this transect, the river floodplain and channel sit in a valley with an approximate bottom width of 600 m and depth of about 20 m. At transect RT8 the river is no longer deeply incised into bedrock canyon. The elevation difference between the river and the gravel plain/rock boundary to the north becomes fairly low and in most places becomes less than 3 m. The channel morphology is consistently one of a meandering active channel with floodplain sections formed as point bars along the river course (Huggett, R., 2007). The vegetation on the floodplain remains dense in most places and consists of large trees– especially *F. Albida* and *A. Erioloba*– shrubs and grasses. The floodplain takes on a width of approximately 100-300 m and appears to narrow when compared to the upstream segment at the canyon end. The active channel widens slightly in places with a width of about 50-100 m. This segment has no Type 1 samples but has several Type 2 and 3 samples. These fines take the form of both depositional crusts and unconsolidated material due to trampling by livestock. In fact, the area around Homeb and Natab has the highest density of livestock along the Lower Kuiseb River (covered later in discussion, 5.3.1).

In the period from 2005 to 2013, only one clearly observable dust plume has been identified from this segment of the river with the aid of MODIS imagery (Figure 70). It is also not clear whether this plume originates from the river or from the gravel plain.

Despite the presence of fines in this section of the river, it is unlikely that the river itself will be a significant source of sediment for wind deflation. Based on the lack of Type 1 samples, the topography and the density of the vegetation, it is more likely that this section of the river will act as a deposition site for any dust entrained from the gravel plain with the north-easterly quadrant winds. Wiggs et al. (2002) evaluated the influence of valley topography on airflow characteristics and developed a conceptual model identifying potential areas of deposition and erosion (Figure 59). According to their study, the wind accelerated as it travelled towards the valley edge, resulting in an increase in erosion. This was followed by a deceleration of the wind

as it descended into the valley, which results in an area of deposition. The deposition of sediment will then be further enhanced by the dense vegetation within the floodplain. The area of erosion identified at the downwind valley slope as a result of wind acceleration will not occur in this section of the Kuiseb, as a result of the presence of the vegetation in this transect.

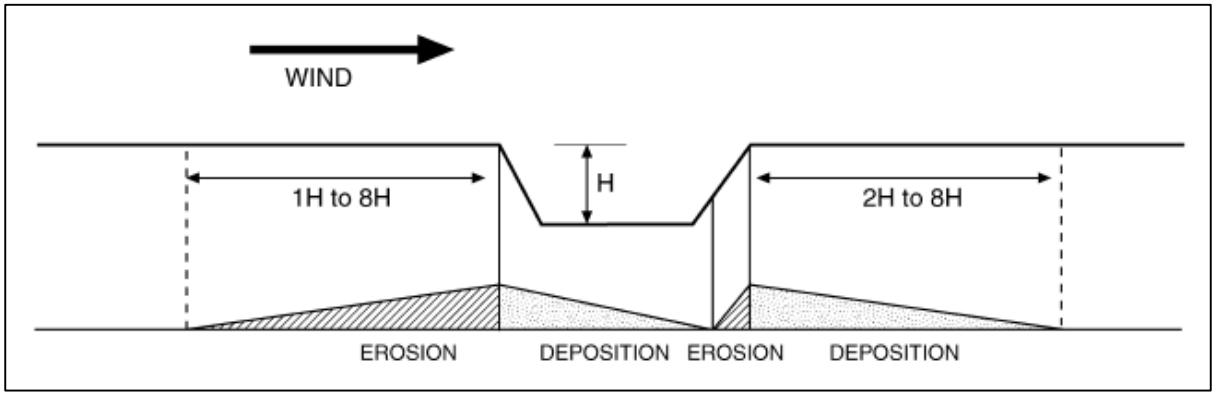

Figure 59 Areas associated with deposition and erosion according to the model developed by Wiggs et al. (2002). H is the depth of the canyon. Diagram taken from Wiggs et al. (2002) p376.

A further indication of deposition within the valley comes from the bimodal nature of RF9-17 (Figure 66). This bimodality has been attributed to the mixing of sediments from different sources or deposition processes (McTainsh et al., 1997). Within this system, sediment is deposited by wind from the gravel plain, as well as by the Sand Sea, and fluvially by the river floods and from the gravel plain drainage during sporadic rain events. River floods that reach the location of RF9-17 will rarely occur. This sampling point is located beyond the Oswater Garden Project and close to Tatamutsis village. Sample RF9-17 consists entirely of unconsolidated material with no signs of any depositional crust.

The meandering nature of the river and the consistently dense vegetation would result in very little sediment being available for deflation, regardless of the direction of the wind (see Figure 69, b). In addition, the rough terrain between the gravel plain and the river valley would further aid the deceleration of the wind (Figure 69, a). The unconsolidated material created by the trampling of the goats occur predominantly on the floodplain terraces, where the vegetation is at its densest and the sediment is generally unavailable for the wind to entrain.

The plume detected on 9 July 2005 was the only plume identified in that year. Prior to 2005 the area experienced a dry period. The eight years preceding 2005 were characterised by less than average rainfall (±13mm/yr.), with no rainfall in 2003 (Figure 11 gives rainfall at

Gobabeb). In addition, the river experienced very little flow during the four years preceding 2005 (Figure 13). Water input into the system potentially play an important role in the dust activity of the area, both in terms of supplying sediment with flow in the river and gravel plain channels and in terms of recharging the various groundwater systems of the basin. The mechanism and influence of water input and flow in the system on dust activity has yet to be determined.

This segment of the river is considered a secondary dust source area. This is based on the lack of Type 1 samples, the density of the vegetation, the topography at the canyon side of the segment and the fact that only one plume has been detected for this stretch of the river.

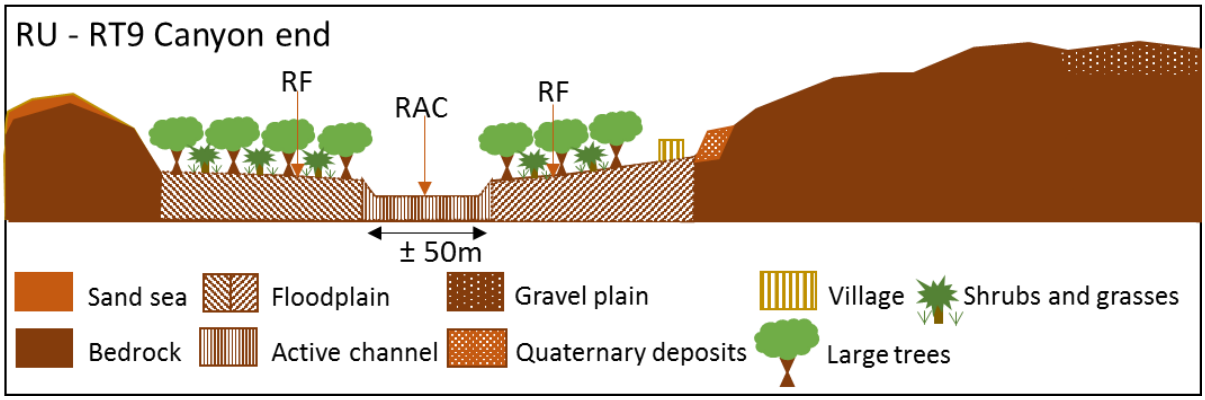

Figure 60 Transect profile of RT 9: canyon end.

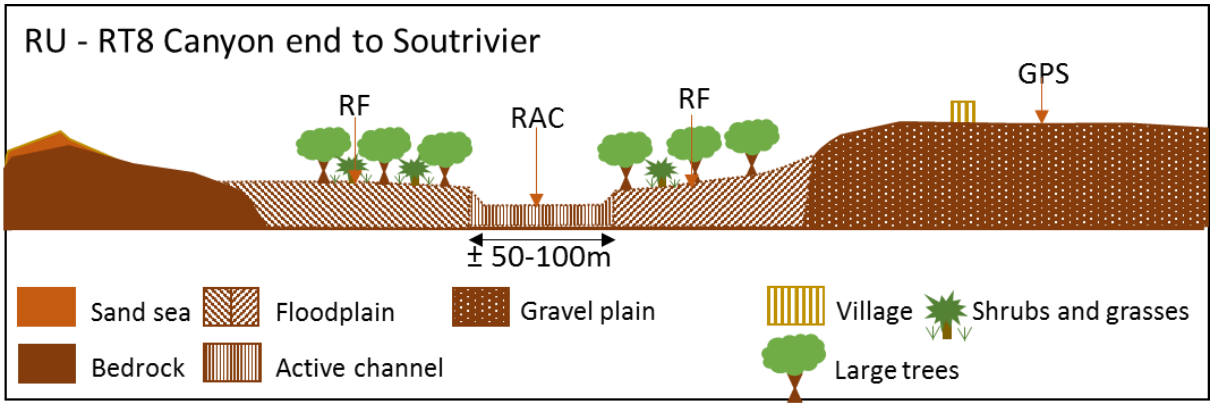

Figure 61 Profile for canyon end to Soutrivier segment (RT8).

Figure 62 Sample location and cluster types for RT9.

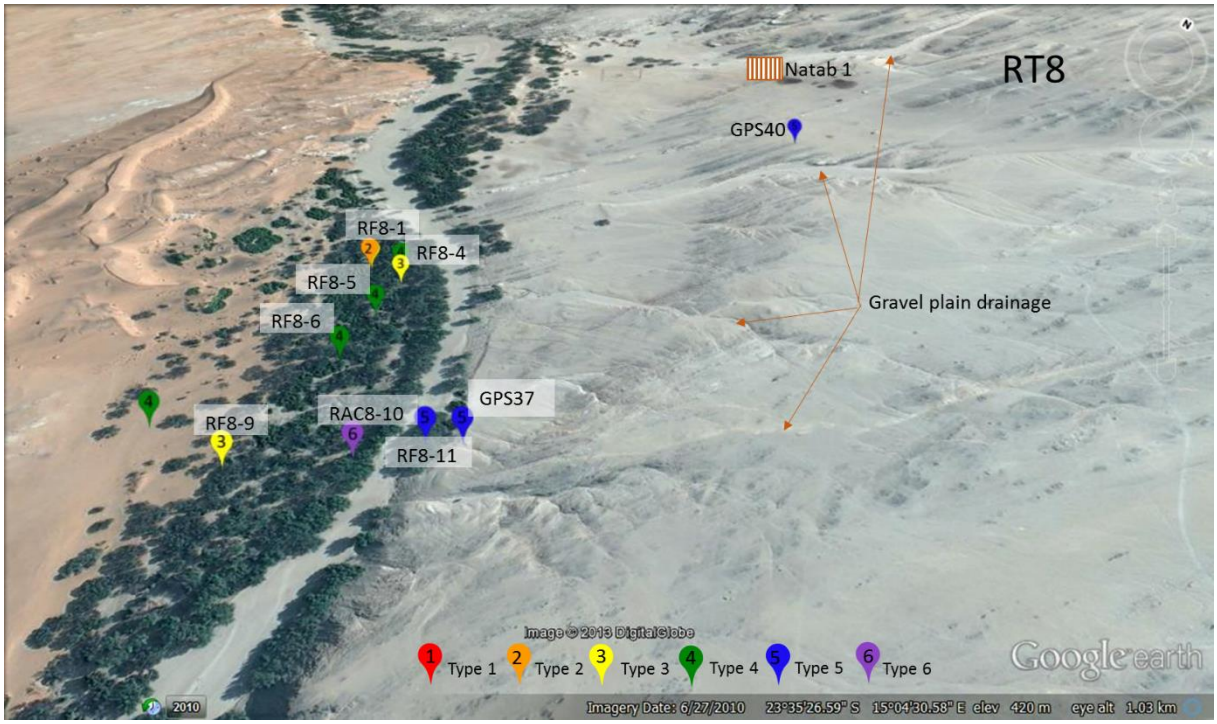

Figure 63 Sample location and cluster types for RT8.

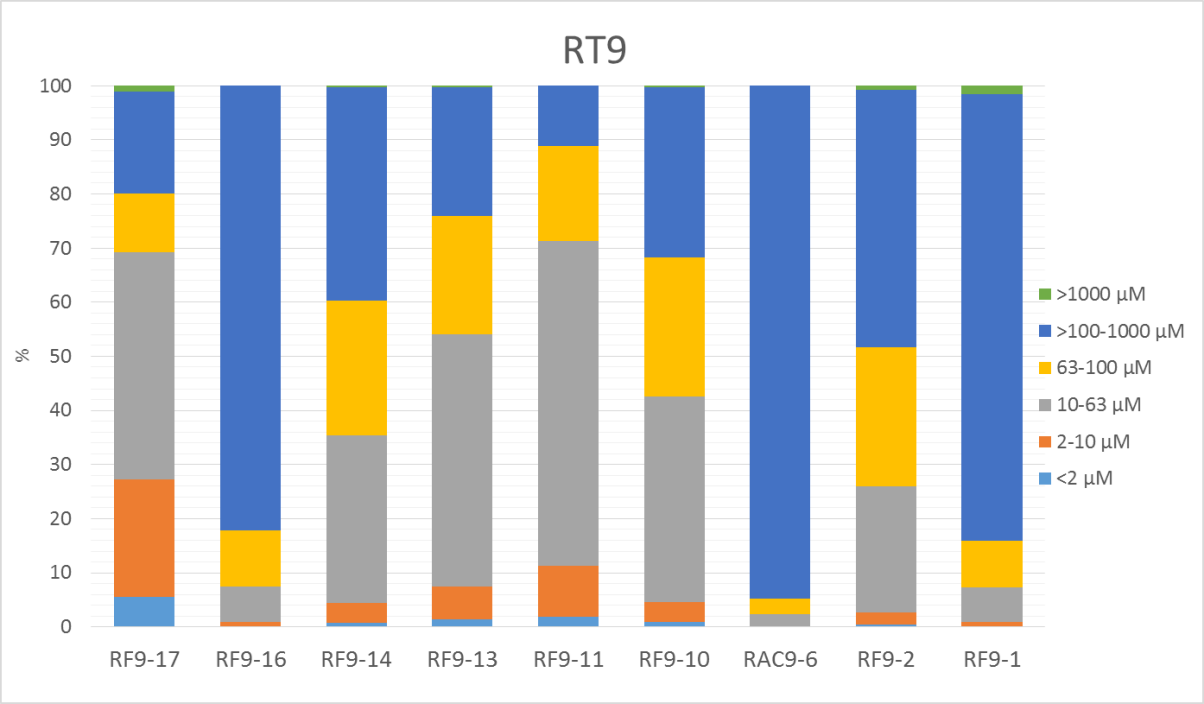

Figure 64 Particle size fractions for selected samples from transect RT9.

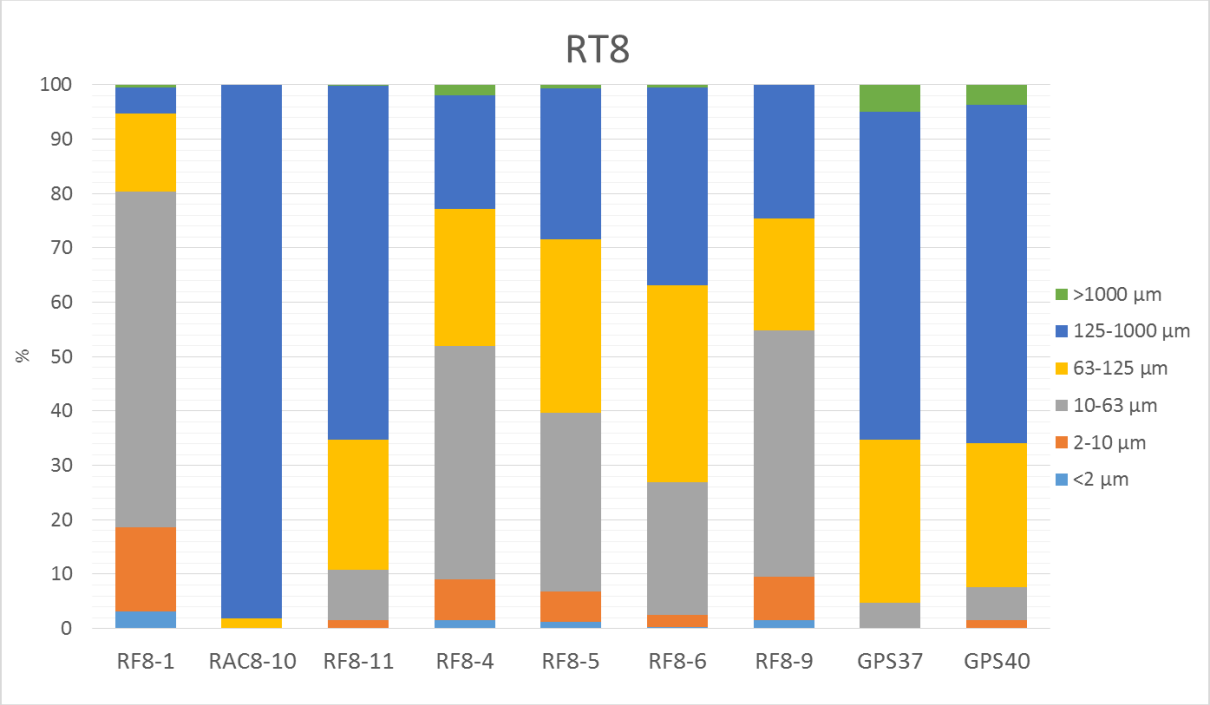

Figure 65 Particle size fractions for selected samples from transect RT8.

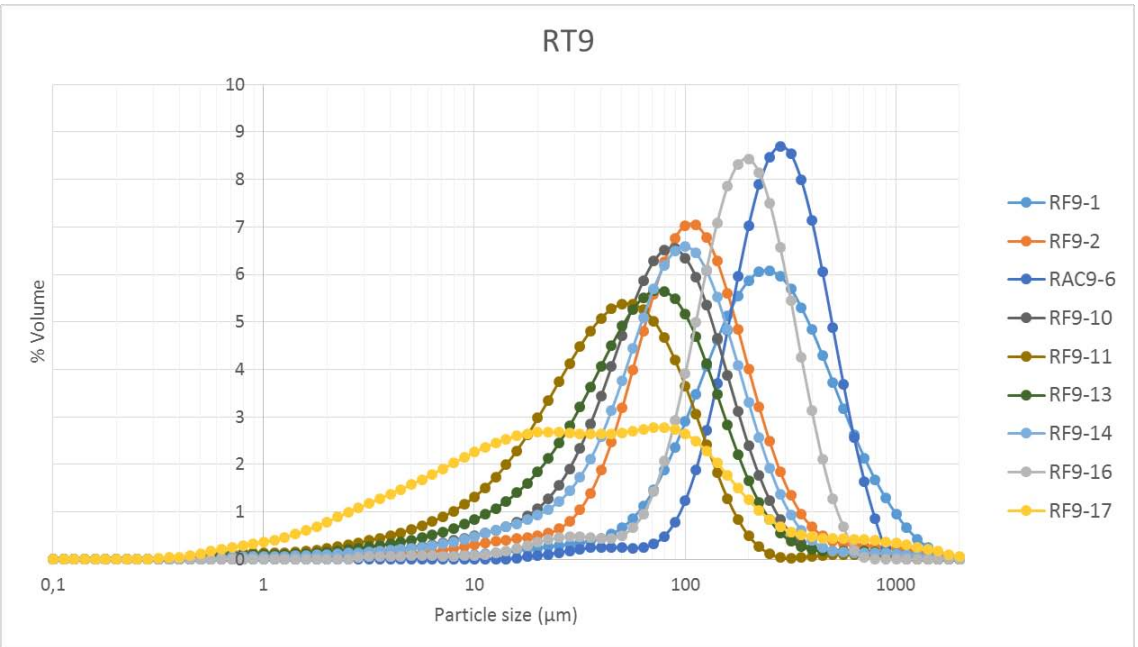

Figure 66 Particle size distributions of selected samples from RT9. Note the bimodal nature of RF9-17.

Figure 67 Surface features at transect RT9.

Figure 68 Surface features at transect RT8.

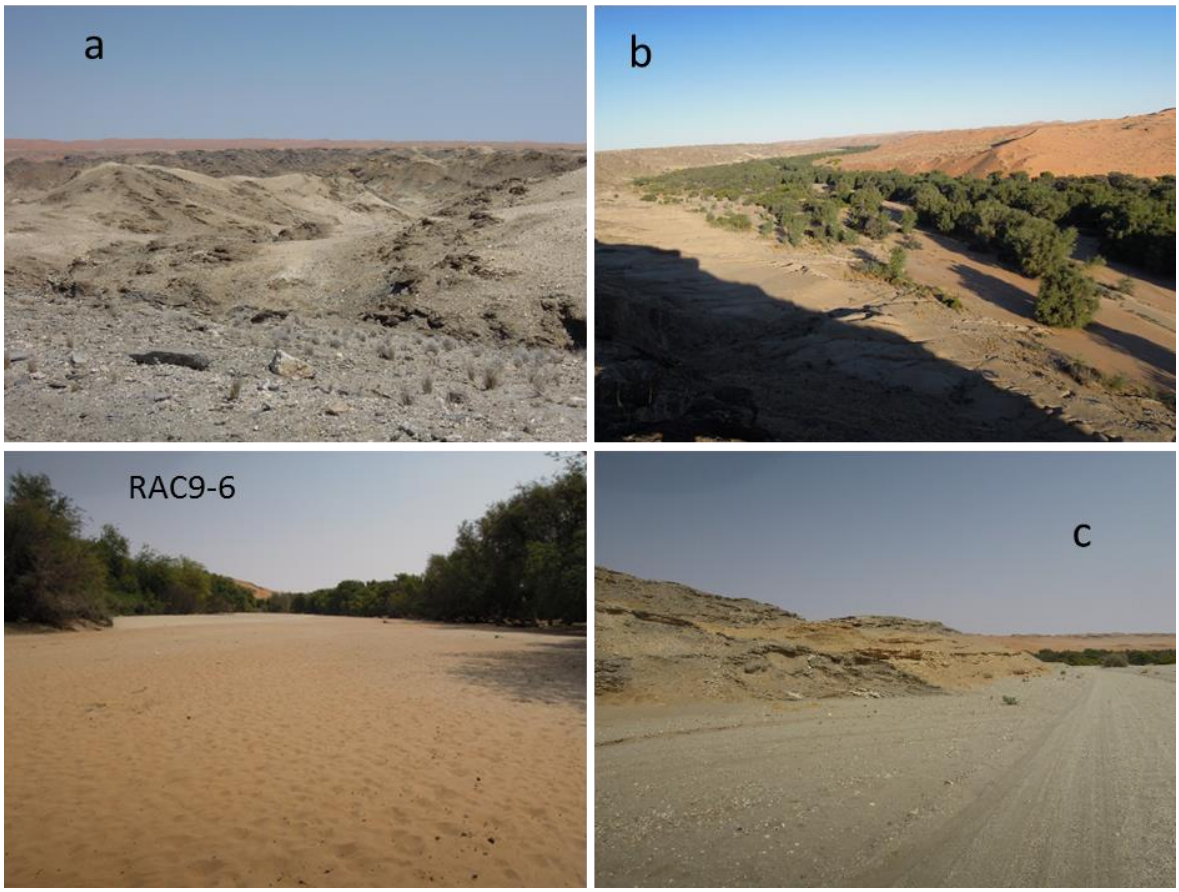

Figure 69 Dense vegetation, topography and morphology all play a role in limiting availability and transport. Image a: rough topography between the start of the true gravel plain pavement and the river, with the Sand Sea in the background. Image b: meandering of the river and incised valley between the bedrock and Sand Sea. Image RAC9-6: active channel of the river with large Ana trees on either side: sample site RAC9-6. Image d: road leading to the river from the gravel plain past the Quaternary Homeb deposits (on left). Tops of large F. Albida trees in river visible.

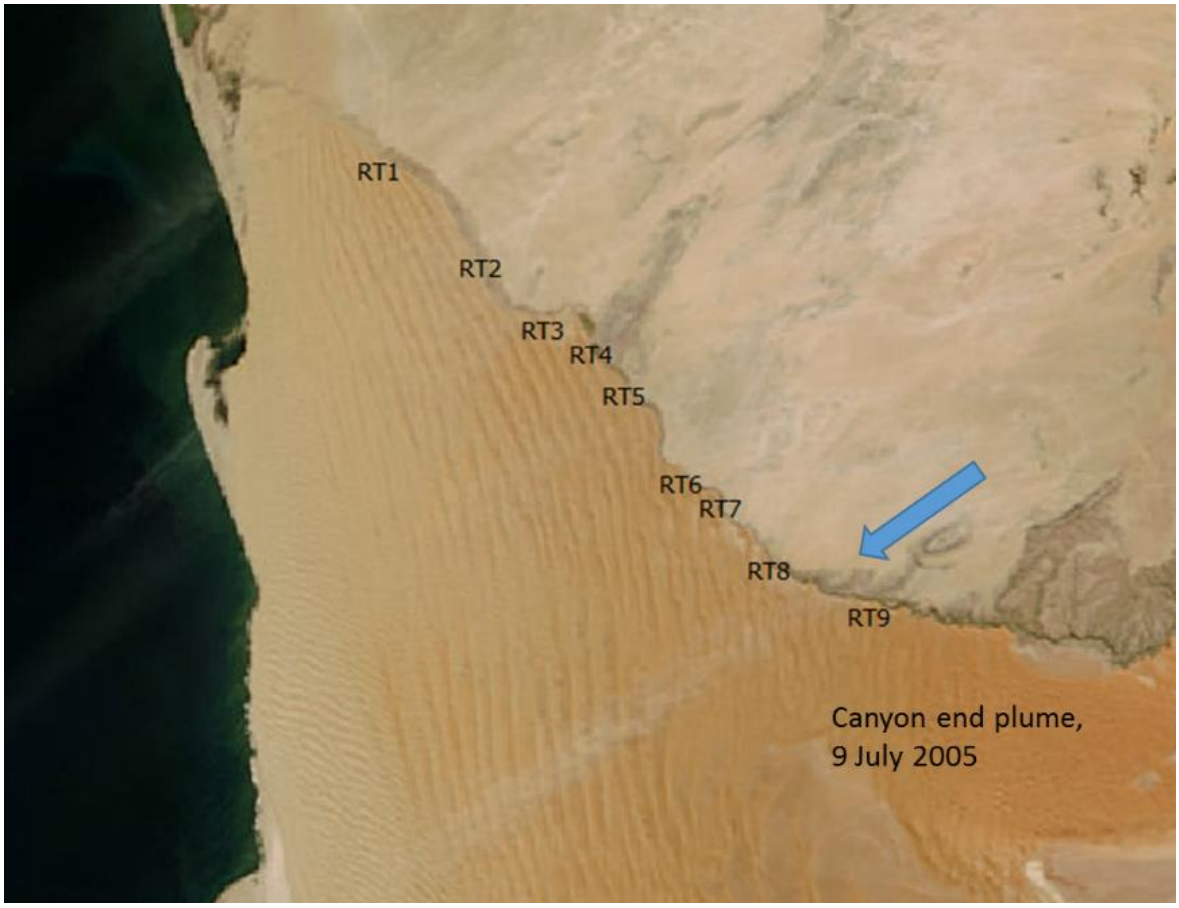

Figure 70 Dust plumes detected on 9 July 2005.

5.2.1.2 RM (Middle river: 50-80 km from the coast)

In this segment of the river the channel and floodplain is anything from 100 m to 500 m wide and is braided, with islands of vegetation. The vegetation is less dense than in the upper river, and there are areas on the segment that have no large trees, especially on the gravel plain side of the river (for example transect RT6). This segment covers the same area as the Middle Riverine Woodland as described by Theron et al. (1985). Four transects were done on this stretch of the river: RT7 at Soutrivier to RT4 before Swartbank. There are no Type 1 samples along this segment, but there are several that clustered as Type 2 and 3. There is also trampling by livestock visible on the transects located close to villages (RT7 and RT5).

The finest material along the middle river section was found in the drainage network of the gravel plain (sample GPC49), sampled as part of transect RT7. This sample was taken from a gravel plain channel about a 100 m before it joins the Kuiseb River (Figure 72). The particle size fraction results are included in Figure 76 for comparison with the main river sediments.

This segment of the river could still be considered a potential source area; however, the MODIS images reveal that the plumes associated with the middle river segment seem to originate from the playa situated on the gravel plain, rather than from the river itself. This playa area seem to be an active dust source area in combination with the easterly wind, rather than the north-easterly wind (Figure 82). Therefore, considering the lack of Type 1 samples and the plumes on the MODIS images almost certainly originating in the gravel plain drainage network, this segment of the river will be re-categorised as a secondary source area.

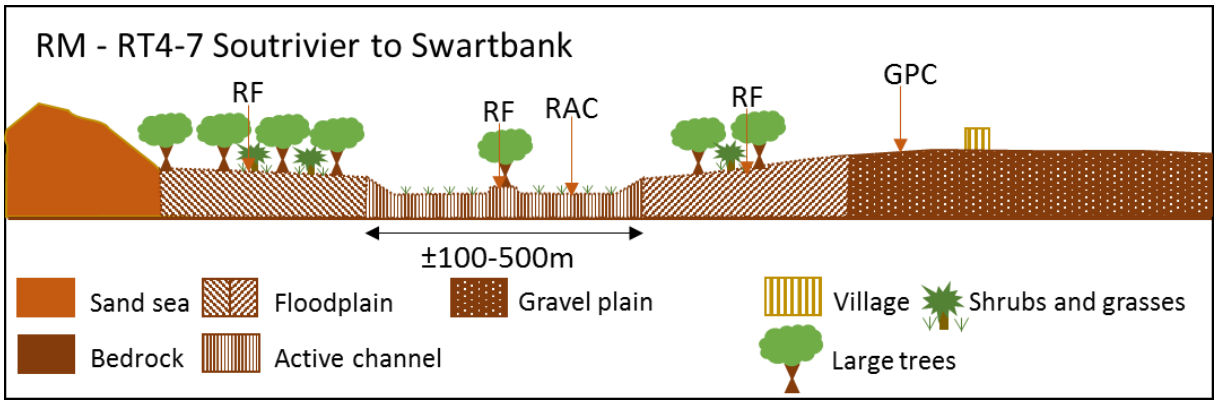

Figure 71 Transect profile of RT 4-7: Soutrivier to Swartbank.

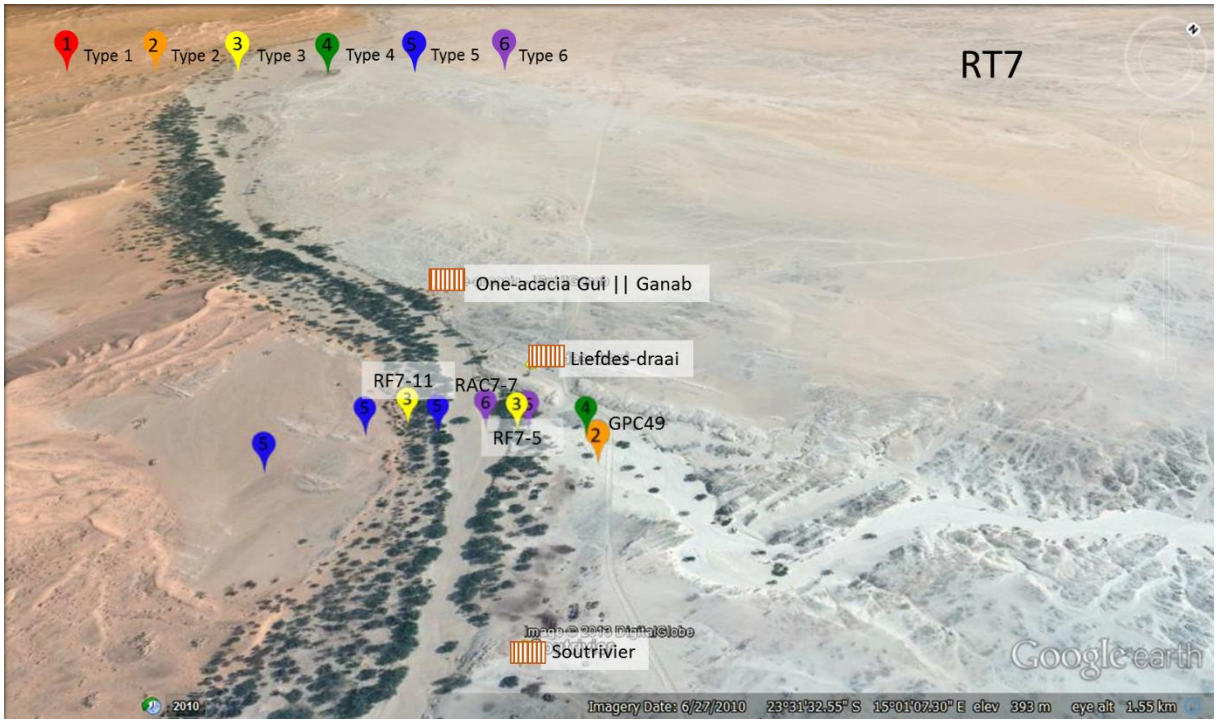

Figure 72 Sample location and cluster types for RT7.

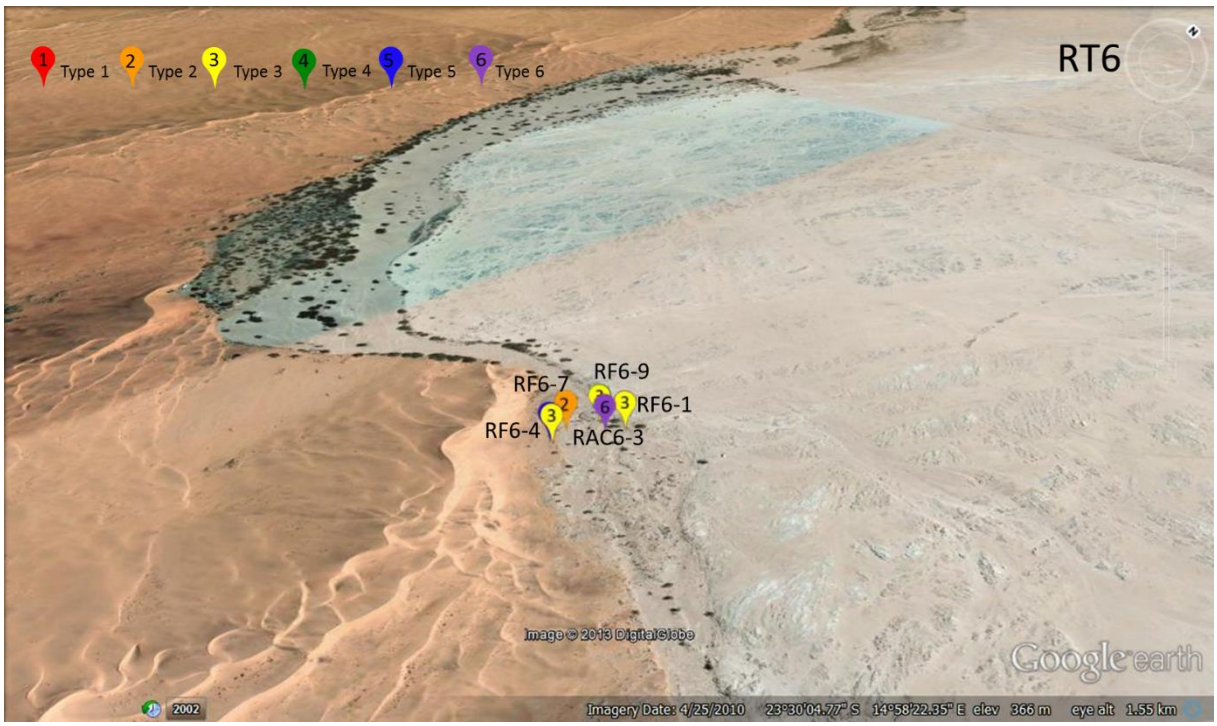

Figure 73 Sample location and cluster types for RT6.

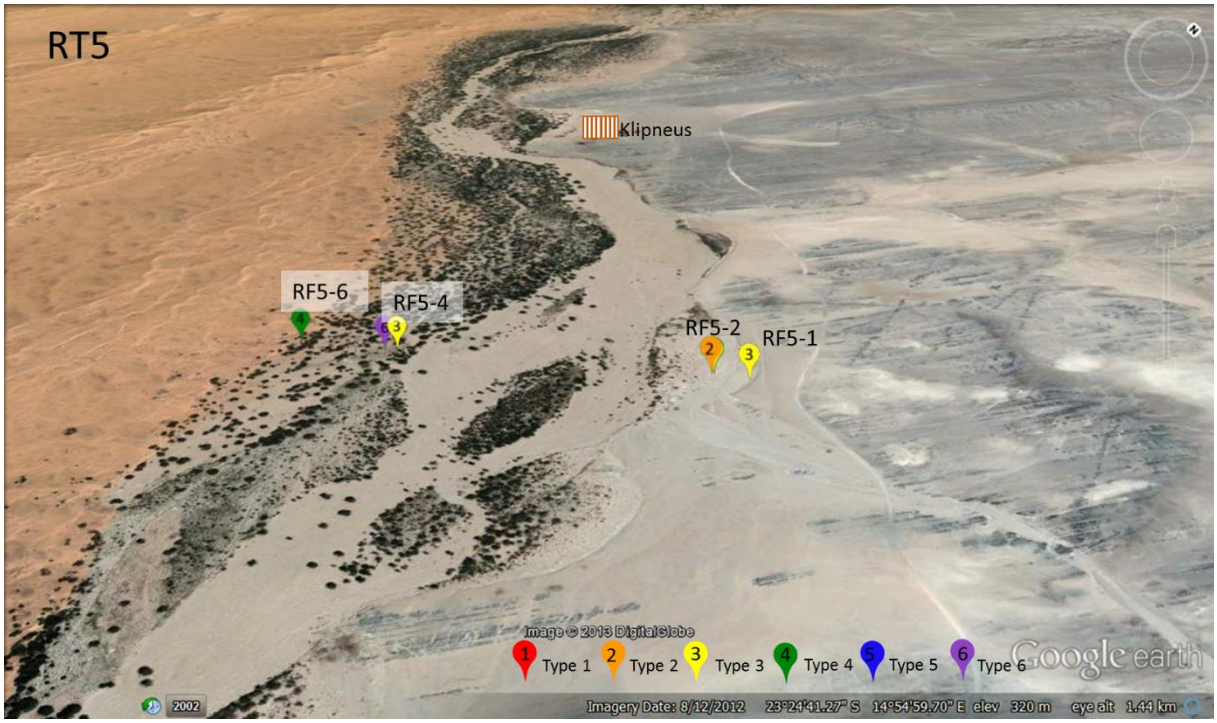

Figure 74 Sample location and cluster types for RT5.

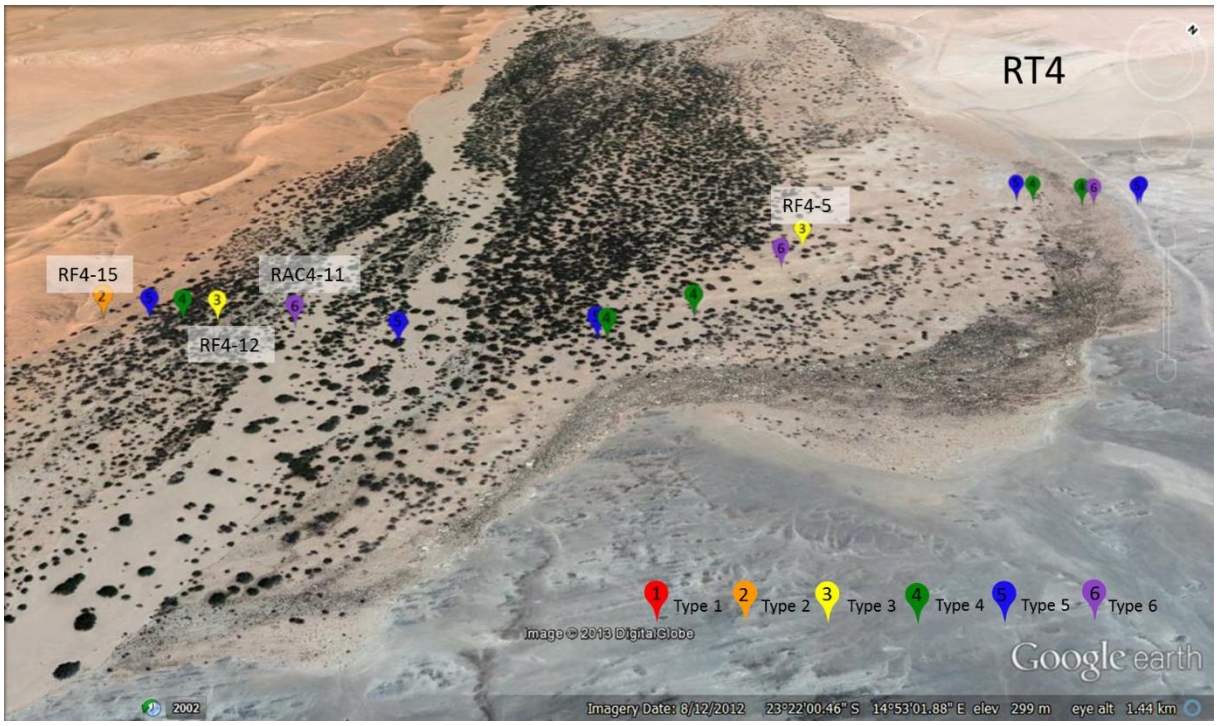

Figure 75 Sample location and cluster types for RT4.

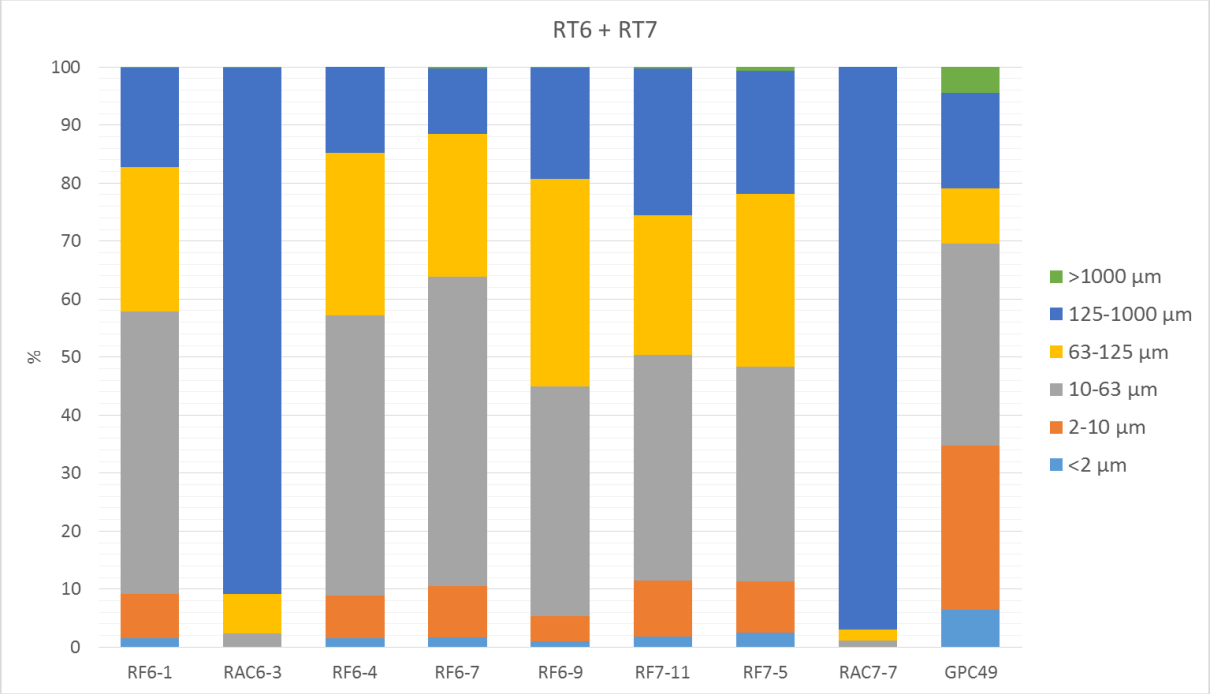

Figure 76 Particle size fractions for selected samples from transect RT6 and RT7.

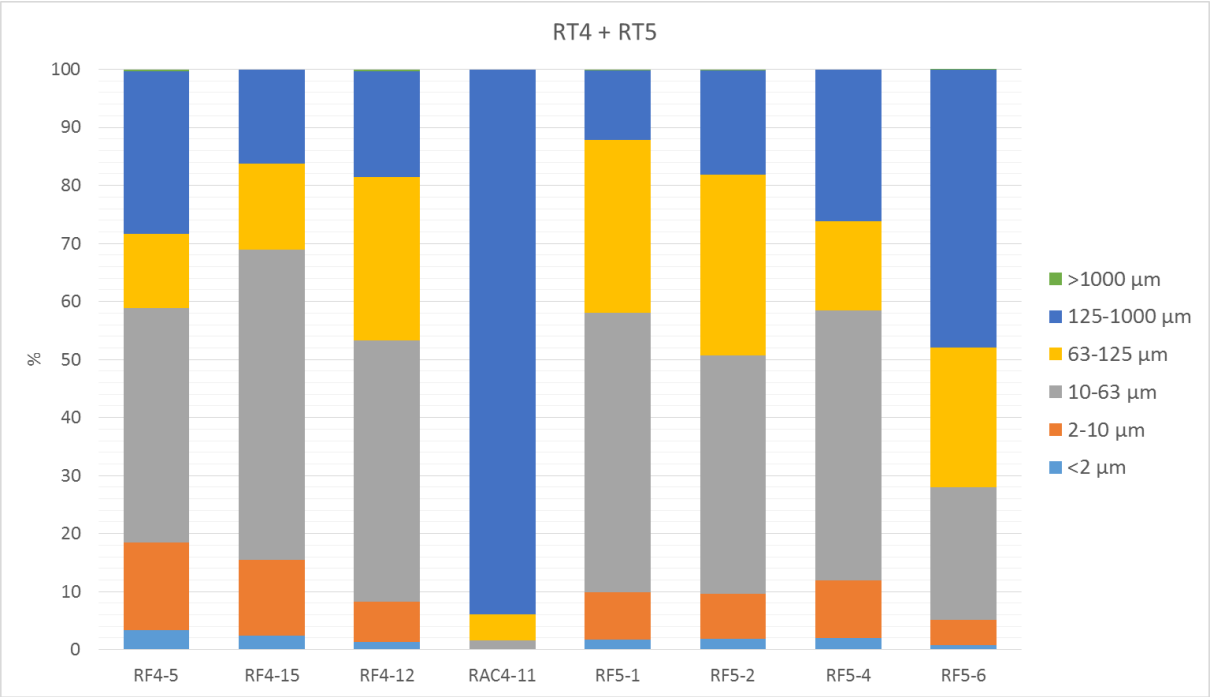

Figure 77 Particle size fractions for selected samples from transect RT4 and RT5.

Figure 78 Surface features at transect RT7. GPC47 shows the broken-up depositional crust within the gravel plain drainage network. RF7-5 and RF7-11 are situated within the river floodplain. The floodplain of this transect shows significant livestock activity (bottom right image).

Figure 79 Surface features at transect RT6. The images on the right show vegetation and rocky outcrops at this location. RF6-7 is depositional crust found within the active channel of the river.

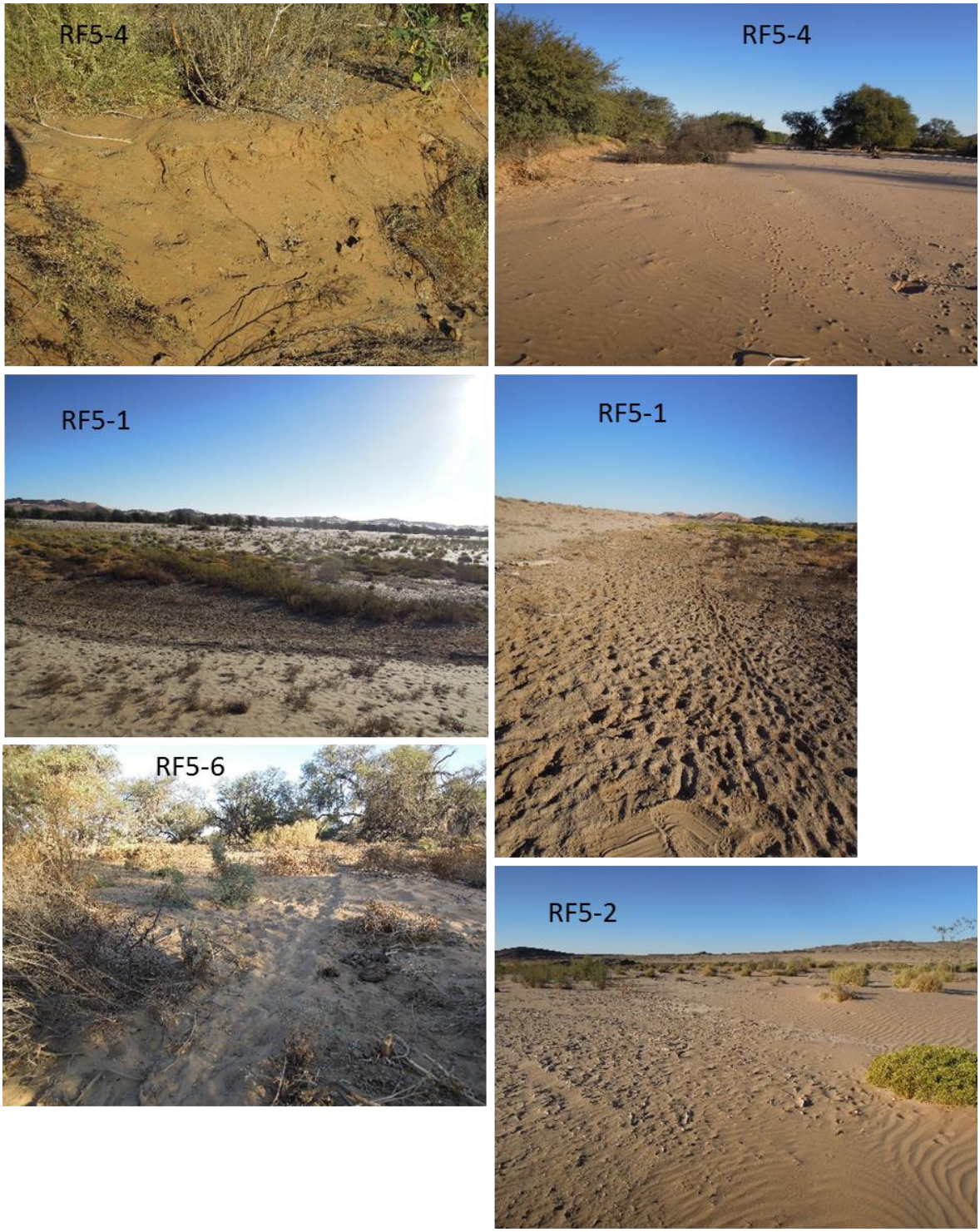

Figure 80 Surface features at transect RT5. The area on the gravel plain side of the river has very sparse vegetation and broken up depositional crust present (RF5-1 and RF5-2). A great deal of evidence of livestock is present at this transect.

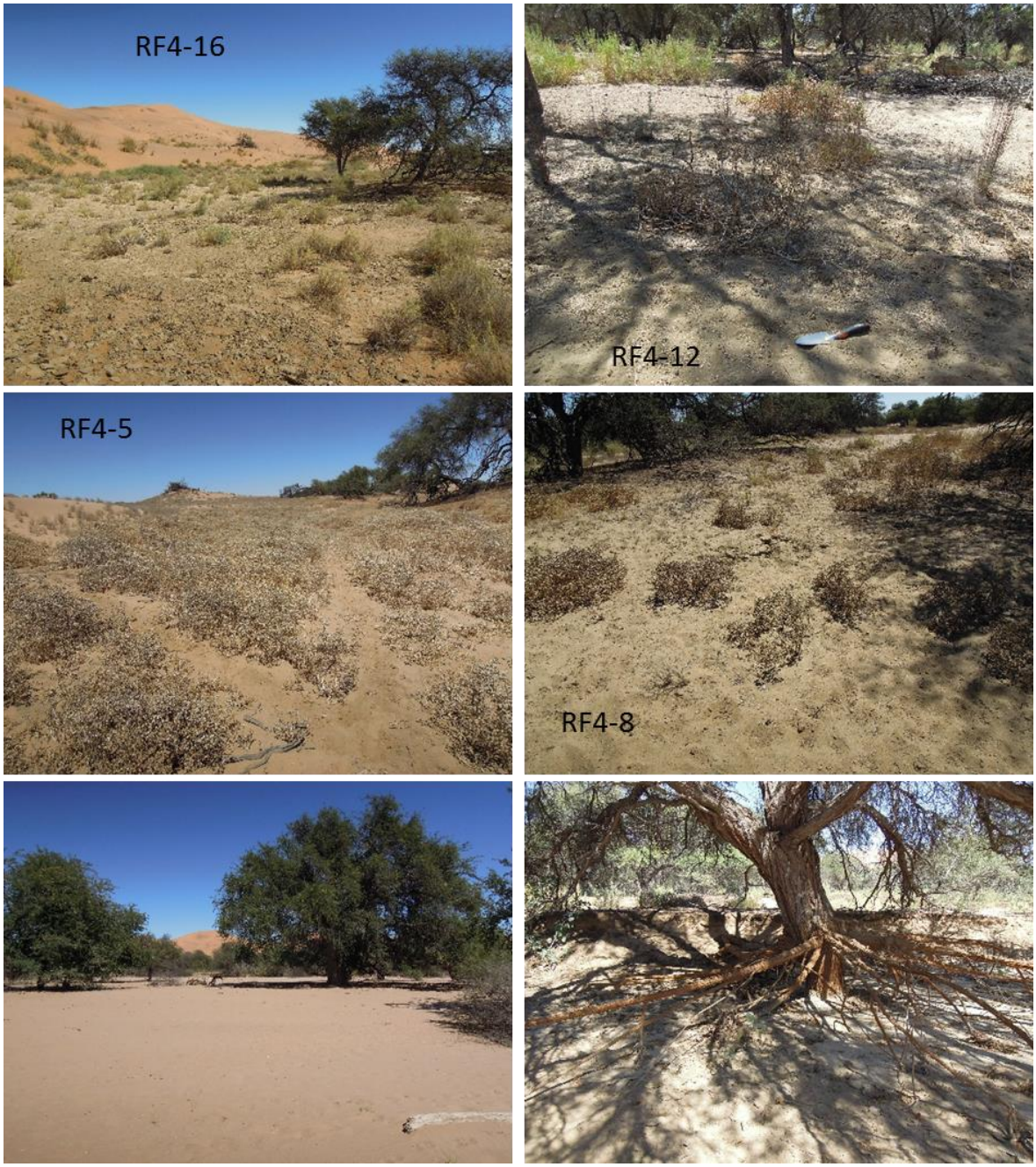

Figure 81 Surface features at transect RT4. The active channel is wide and braided with large trees (bottom left image). Floods not only transport material from the upper river, but also serve to rework sediments deposited in earlier floods. The big floods in 2011 probably washed the sediment under this tree away and deposited it further downstream.

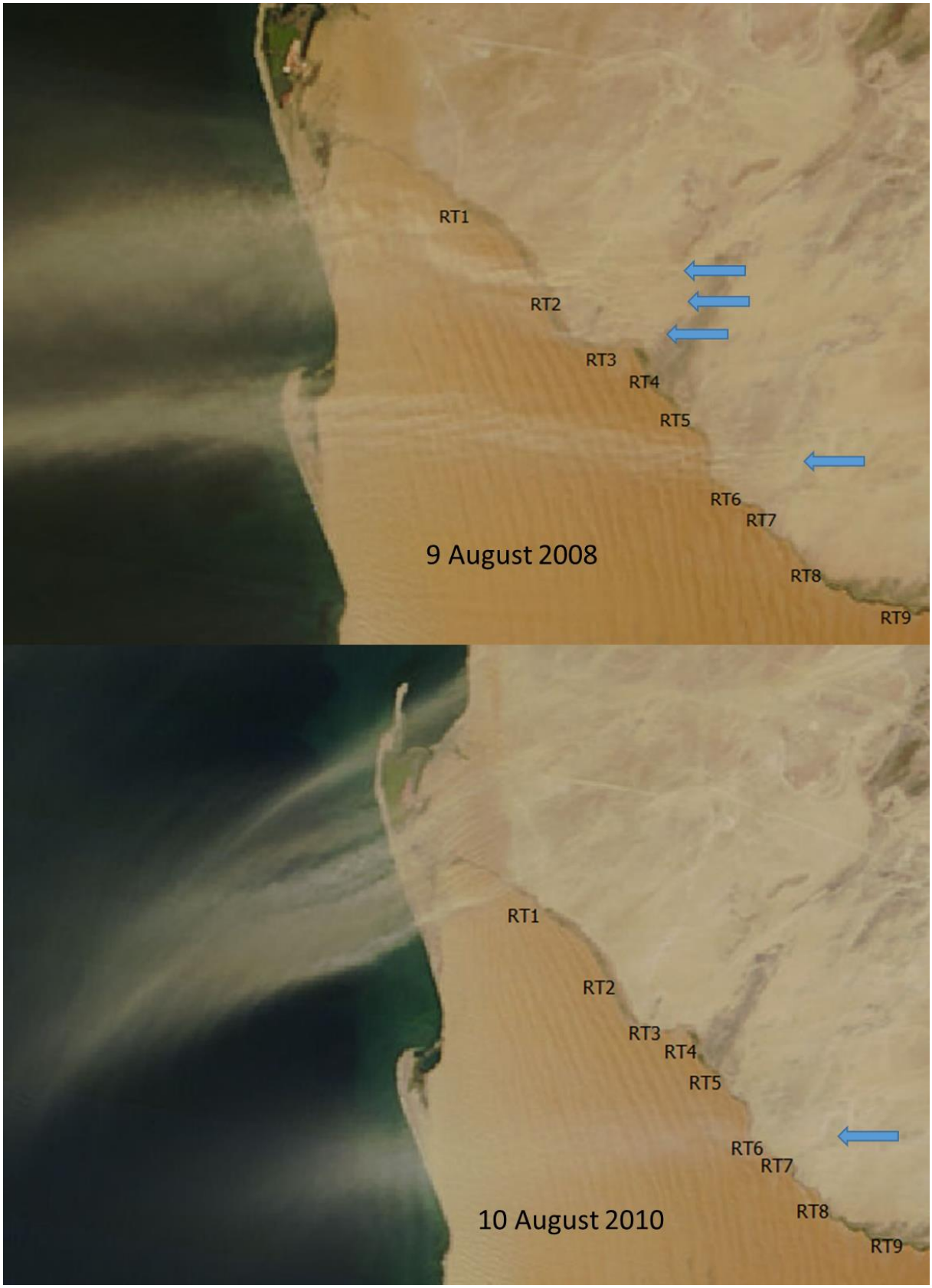

Figure 82 Dust plumes identified for the middle river segment with the aid of MODIS imagery. Plumes seem to originate from playa areas on the gravel plain with the easterly wind. The plume of 10 August 2010 is no longer clearly discernable and this image could be towards the end of the dust activity as a result of the easterly wind. The plume to the north-west over the gravel plain and delta seem to indicate that the wind direction has changed to north-east.

5.2.1.3 RL (Lower river: 20-50 km from the coast)

This segment of the river stretches from Swartbank to Rooibank at the start of the delta channel. Here the floodplain is flat and widens to over 2000m in places. This segment is the least densely vegetated stretch of the river as is evident from the photos (Figure 90 and Figure 89) and the survey done by Theron et al. (1985). The Swartbank and Rooibank A aquifers are situated within this segment and are the start of large-scale water abstraction from the river for bulk water supply (refer to Figure 16 in section 2.7.4). This is also the most populated stretch of the river in terms of people, with approximately 71% of the Kuiseb River Topnaar population believed to be residing along this segment of the river (Botelle et al., 1995). The upper river segment (RU) is the most populated in terms of livestock (see section 5.3.1).

On average there is an 86% reduction in mean annual runoff between Gobabeb and Rooibank (Jacobson et al., 1999), which means many of the floods terminate in the lower and middle segments of the Lower Kuiseb River. The terminal stages of a flood would result in the deposition of Type 1 sediment. The first Type 1 samples are found within this segment of the river (Figure 86 to Figure 84). At RT2 and RT3, the Type 1 fines are in the form of depositional crust found within the channel. At RT1 at Rooibank, the Type 1 samples are mostly confined to the nebkha dunes, similar to those described in the delta section (5.2.1.4). The fines situated between the nebkha dunes are more likely to act as sediment stores, rather than as active dust sources (Figure 86).

It is interesting to note that transect RT3 consisted only of Type 1 and Type 6 samples (this bimodality could possibly be the perfect long term suspension dust source particle size combination). At this transect the vegetation consists mainly of a few large trees and widely dispersed shrubs (Figure 89). The river channel is flat with no distinction between floodplain and active channel. At transect RT2 the river widens considerably and there is widespread trampling by livestock. The vegetation is denser than at RT3, but still dispersed enough to possibly create corridors of deflation, especially where trampling creates unconsolidated fines with a lower threshold friction velocity.

The crust characteristics of sample RF1-12 are similar to the sample tested in the delta (DFP19). The organic content is lower (1.3%), but the Na and Ca content is slightly higher. These small-scale features are not likely to make a substantial difference to the threshold friction velocity. The SEM image and EDS analysis show similar mineralogy to that found in sample DFP19. The sample consists of mica flakes cemented together by an aggregate of minerals (SEM image

reproduced in Figure 88). Sample RF1-12 is a Type 3 sample (compared to Type 1 for DFP19) and it would appear that there is less fine aggregate material cemented onto larger mica flakes in sample RF1-12.

As with the delta, for some MODIS images it is difficult to say with certainty whether the plumes originate from the river or the gravel plain, or possibly from both (Figure 92). Transect RT2 is situated downwind of a salt spring that was also identified as a source point by Vickery et al. (2013). The plume dated 8 August 2010 in Figure 92 seems to originate from the playa area on the gravel plain rather than from the river. This segment of the river will still be considered a primary source of dust based on the presence of Type 1 samples, the reduced density of the vegetation and the dust originating from the vicinity of RT1 and RT3, as evident on the MODIS images.

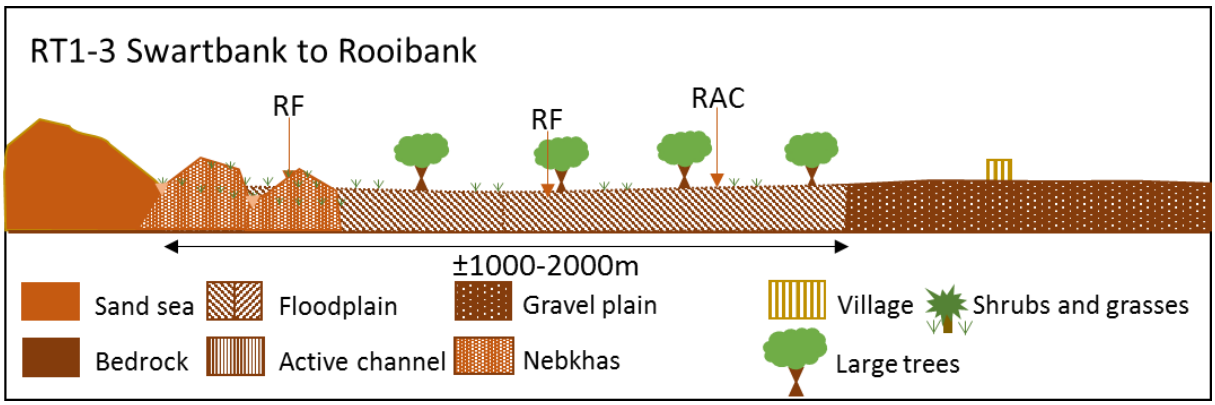

Figure 83 Transect profile of RT 1-3: Swartbank to Rooibank.

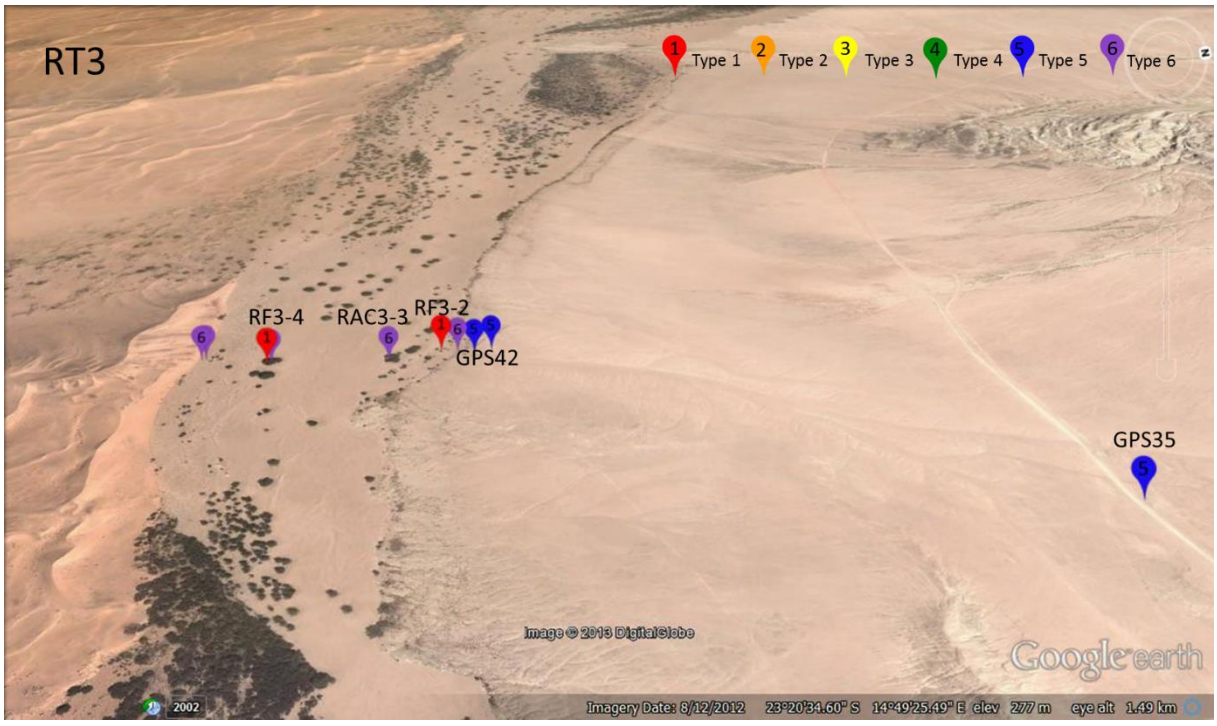

Figure 84 Sample location and cluster types for RT3.

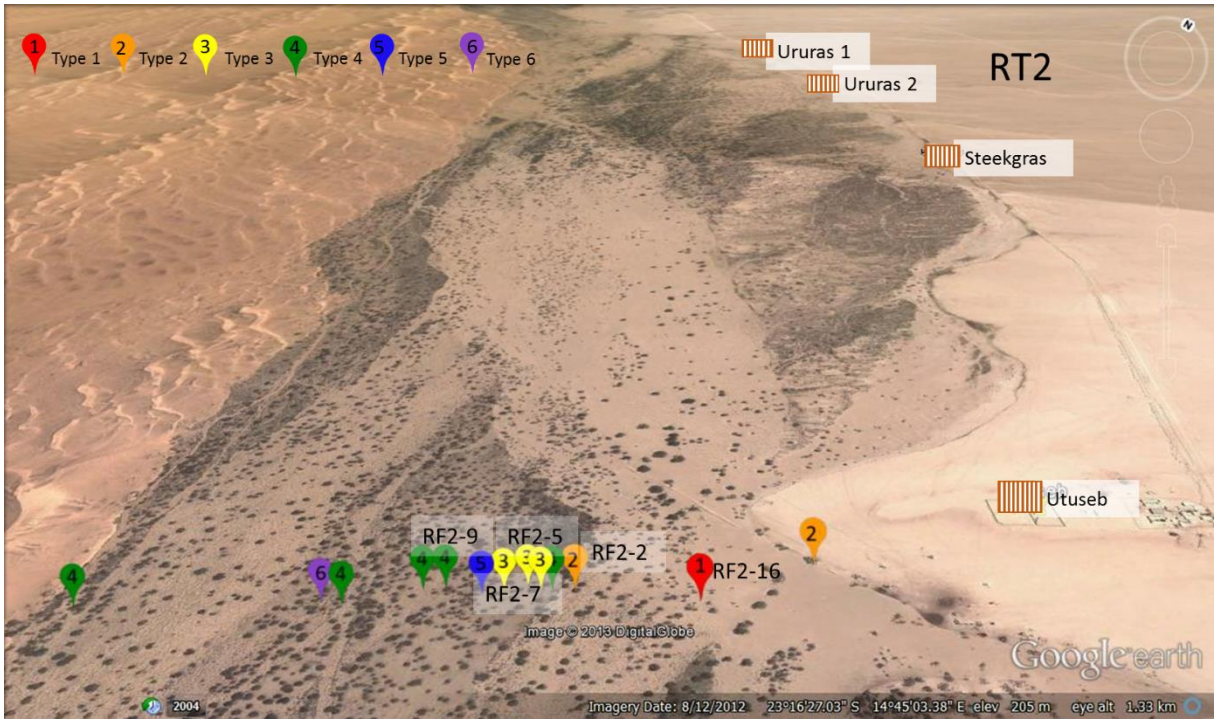

Figure 85 Sample location and cluster types for RT2.

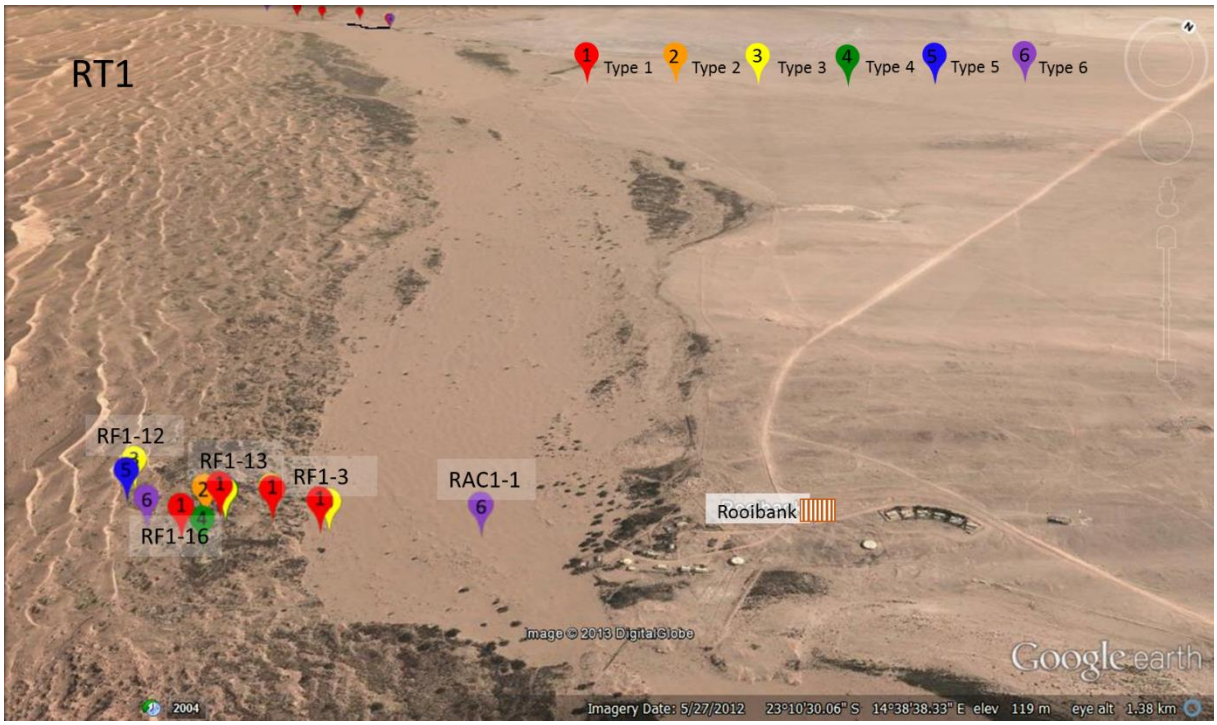

Figure 86 Sample location and cluster types for RT1. Delta samples and the floodwall are visible at the top of the image.

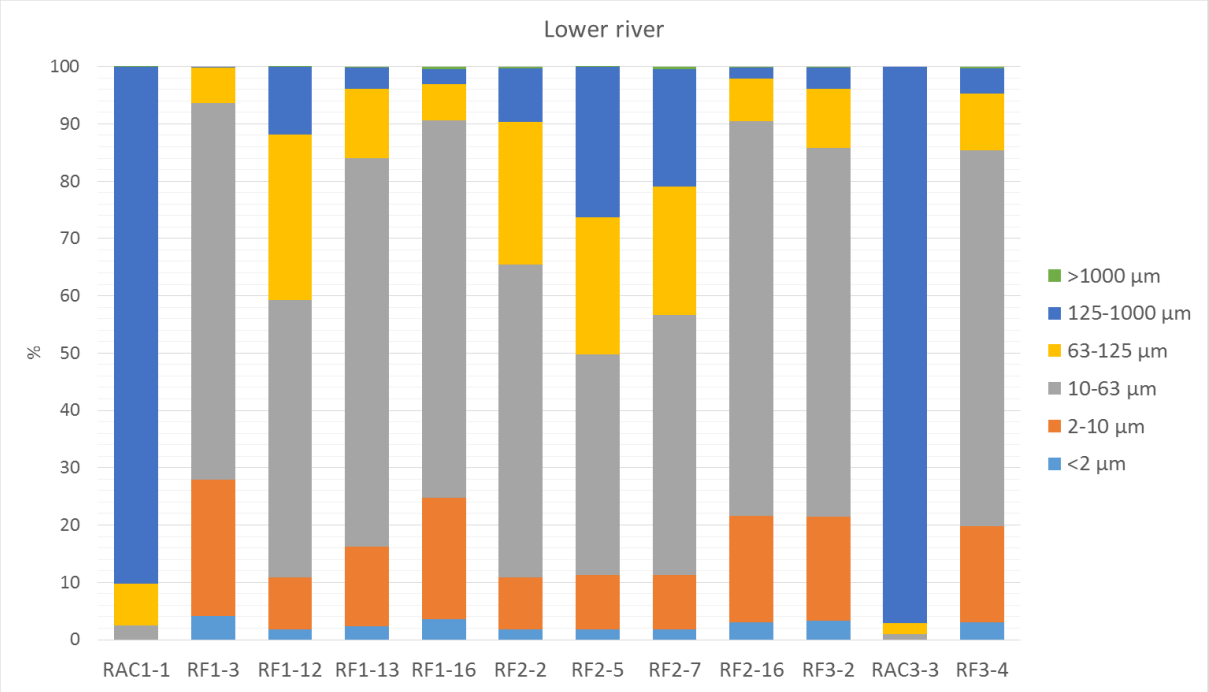

Figure 87 Particle size fractions for selected samples from transect RT1, 2 and 3.

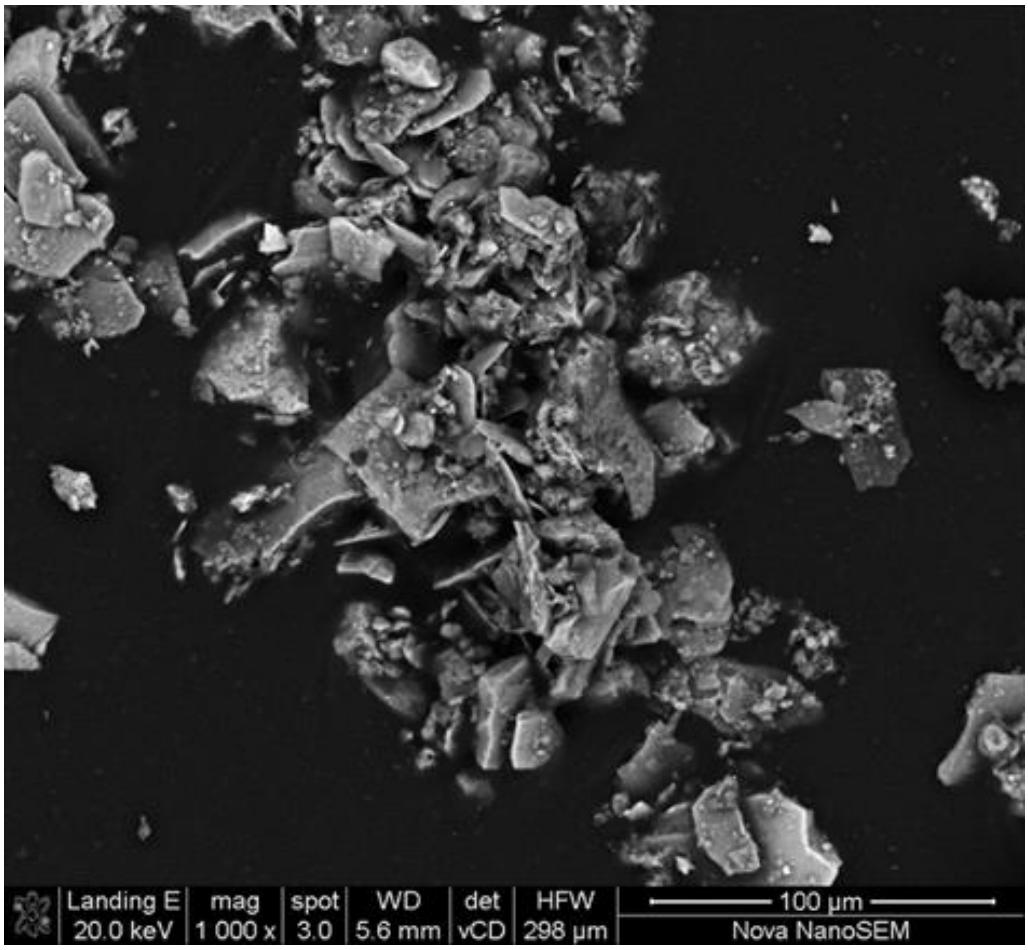

Figure 88 SEM image of sample RF1-12, Type 3.

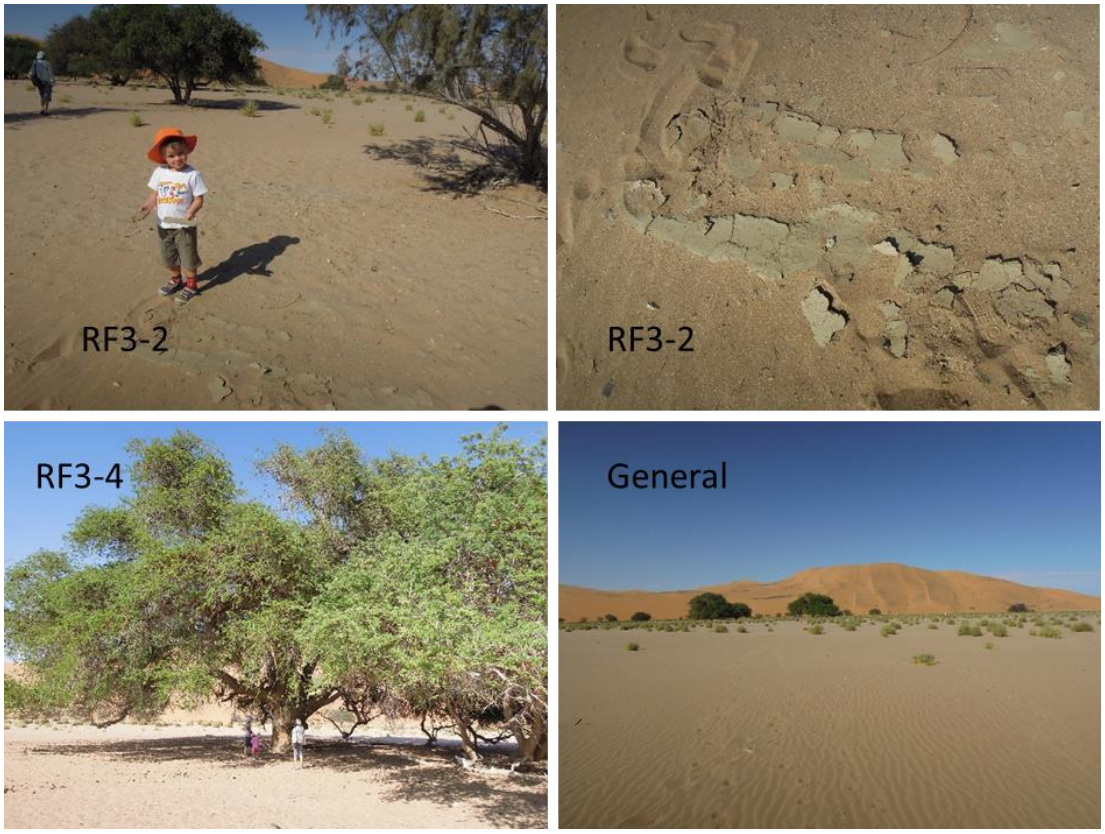

Figure 89 Surface features at transect RT3. Samples consisted of only Type 1 and Type 6. The photo labelled general gives an indication of the surface features at transect RT3. The photo was taken with the gravel plain at the back, facing the Sand Sea, with the river situated at the foot of the dune.

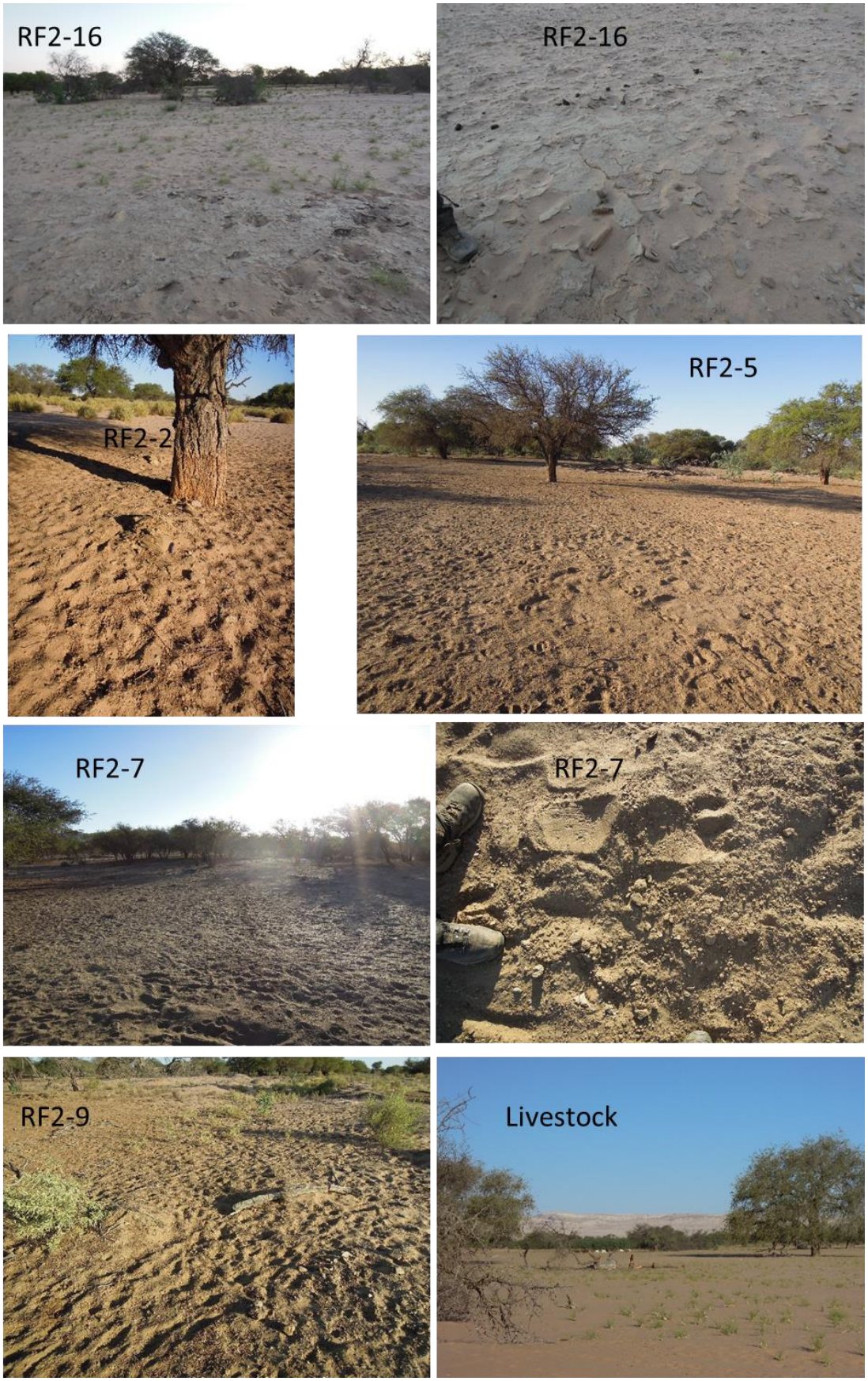

Figure 90 Surface features at transect RT2. Trampling by livestock is widespread at this transect.

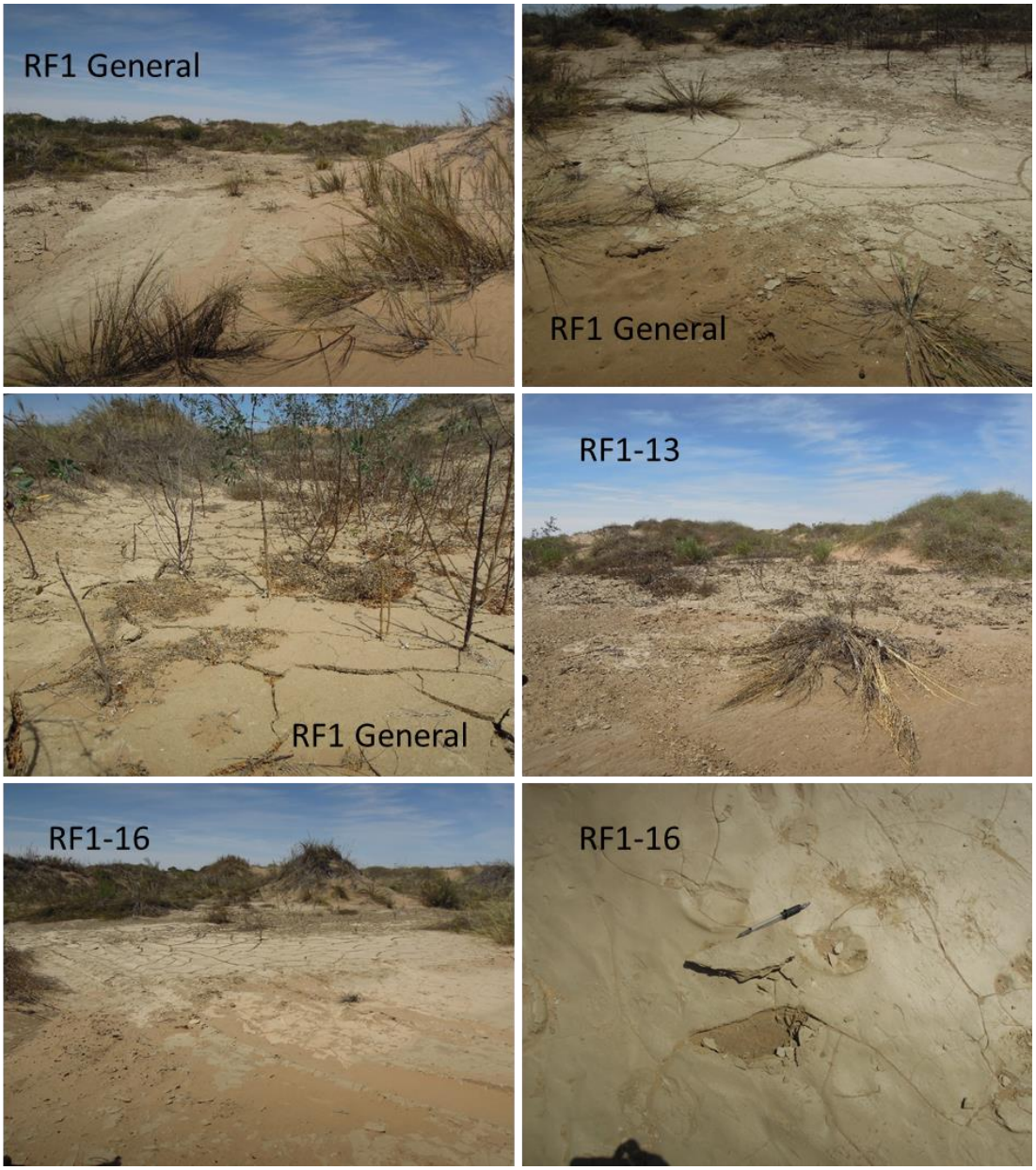

Figure 91 Surface features at transect RT1. The fines are mostly located in the nebkha dunes situated on the Sand Sea side of the river.

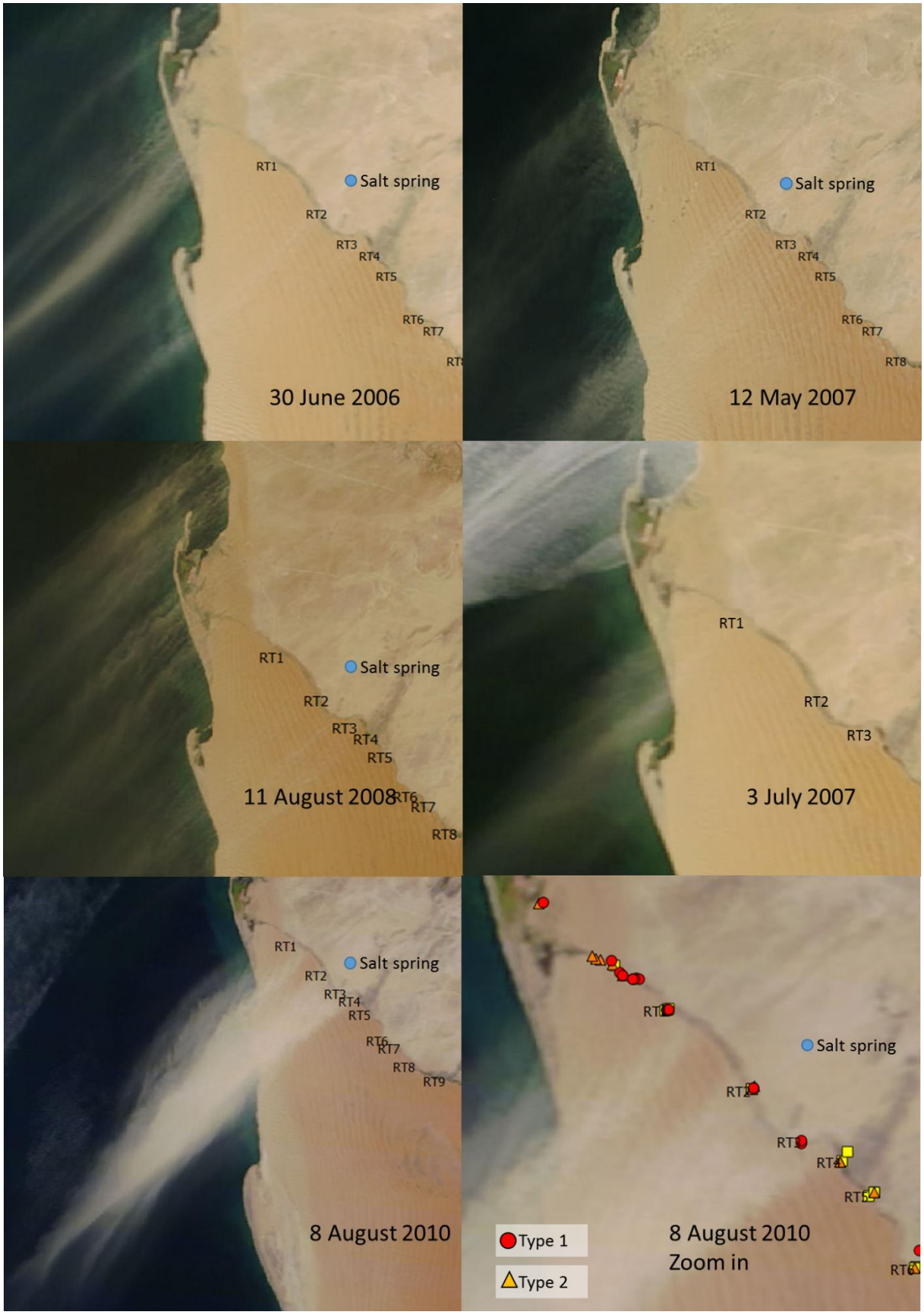

Figure 92 Plumes identified with MODIS imagery for the lower river segment. There are numerous salt springs evident on Google Earth, but the one marked above seems to consistently produce the dust identified on MODIS images.

5.2.1.4 Delta (0-20 km from the coast)

The delta has extensive deposits of fine grained sediment, especially Type 1. These fines are predominantly in the form of depositional crusts lying on the active channel (DCC), within the nebkha dunes bordering the flood channel (DFP) and as large deposits found within the fan area (DFP) (Figure 93). It is interesting to note that most of the fines within the active channel are either Type 2 or 3. The Type 1 samples are mainly located within the nebkha dunes and in the deposits sampled in the fan area on the Walvis Bay side. The crusts found within the active channel show signs of decay (Figure 97). This is most likely as a result of erosion by the wind in combination with bombardment by saltators. The sands of the active channel (DAC) and the Sand Sea to the south provide an abundant supply of saltators. The crusts in the delta channel are sparsely vegetated, have ample saltators and are therefore prone to sandblasting making them a likely source of dust. The absence of Type 1 material is either due to the removal of the top layer, consisting of the finest material, by wind erosion or possibly due to the fact that this was not the terminal stage of the last flood and that the Type 1 material was transported further downstream. Most of the samples in the delta channel were taken after the windy season in 2012, with only a few taken in March 2013 (e.g. DFP19 and 20 in the fan). However, the river did not flow at all during the summer of 2012/2013 and all samples can therefore be said to be in a post windy season state.

The fines within the nebkha dunes do not appear to be available for deflation due to the surface roughness elements consisting of vegetation and dune mounds. The nebkhas are anchored by vegetation and form by the deposition of sand as the wind velocity is lowered by the vegetation (Laity, 2008). The spaces between the nebkhas (which in some cases take the form of depressions) become potential sites of deposition of suspended sediments transported with the floods creating reservoirs of fine material (Figure 98, samples DFP7 and DFP17). This fine material then further enhances the ability of the vegetation to spread, which in turn will affect the nebkha growth. The anchoring vegetation around which these nebkhas form are dependent on groundwater for its survival. The fine sediment will only become available for deflation if the vegetation dies and the nebkha dunes become destabilised.

The delta fan area comprises various landforms: barchan dunes, nebkha dunes and sabkha, as well as areas with dense vegetation consisting of shrubs, reeds and grasses (Figure 98). The depositional crusts sampled in the fan area are surrounded by low-level vegetation consisting of shrubs and grasses (Figure 98, DFP 19 and DFP20). These deposits cover extensive areas of

the delta fan, judging by the flow of the flood water (see Figure 95 for image of river in flood: water is dark in areas within the delta) and by crusts visible on Google Earth images (Figure 99). Even though these crusts are interspersed between low-level shrubs and grasses, it is likely that they could still act as source areas. In their study of the playa crusts at Lake Owen, Cahill et al. (1996) found that even in the presence of a vegetation density of 10-15% between the crusts and sand source, sufficient quantities of sand (25-50%) were able to pass through the vegetation zone to act as saltators. The dunes situated 600 m to the right of the crusts provide the source of sand necessary for saltation and the resultant sandblasting. A determination of the vegetation density was not attempted as part of this study.

The crusts found in the delta are likely to be highly erodible due to their particle size distribution. The percentage of clay-sized sediment has an important influence on the strength of the crusts and therefore on their erodibility. Gillette et al. (1982) found that the clay content was the most important parameter affecting the strength of the crusts. Lopez et al. (2007) similarly found that soil texture was the most important predictor of the soil erodibility fraction for the soils tested in their study – especially the ratio of sand, silt and clay. The highest fraction of <2 μm material found in the delta was 6.6%, with an average content of 3.5%. The clay content has to be substantially higher (>20%) for it to play an important role in crust strength (Gillette, 1979). However, even at a clay content of >20% the crust is likely to undergo degradation due to sandblasting with each successive high-magnitude wind event, which would gradually result in a lowering of the threshold friction velocity and the switching on of a dust source (Baddock et al., 2011). In addition, Gillette et al. (1982) tested soils with four different dominant clay mineralogy groups: smectite, mica-smectite, mica and kaolinite-chlorite (they defined clay as <4μm). The authors found that the mica group had much lower crust strength compared to the other groups and attributed this to the lower specific surface of the mica group. The depositional crusts formed by the river floods consist predominantly of mica (though mostly in the silt-size fraction).

The role played by organic matter in the wind erodibility of the crusts is uncertain. The organic content of the delta fan sample (4.7%) seems to consist predominantly of dissolved organic matter (Result section, Figure 45). Alfaro et al. (2008) tested the susceptibility to sandblasting of four soils with different organic matter contents and different clay contents. In their study it was found that the soil with the highest organic matter content (2.1%) and a high clay content (41% by mass) had a susceptibility to sandblasting at least one order of magnitude greater than the other soils. Lopez et al. (2007) on the other hand found that organic matter decreased the

erodibility of soils due to the aggregation resulting from higher organic contents. Desert soils generally do not have significant quantities of organic matter, but the Kuiseb River flood deposits have been shown to have substantial particulate and dissolved organic contents due to the lush riparian vegetation (Jacobson et al., 2000). The organic content of the Kuiseb deposits might affect the threshold friction velocity of the crusts, but its role in the dust activity of the depositional crusts is unknown and is probably insignificant in relation to the sandblasting power unleashed on the crusts during successive high-magnitude wind events experienced in winter. Furthermore, the test method for organic matter needs to be improved before any conclusions can be drawn. Even though the organic content might not have a significant influence on the resistance to erosion, it could have important consequences for the impact of dust, specifically the delivery of nutrients to the ocean. None of the crusts tested in this study consisted of biological crusts.

Similarly the concentration of soluble salts is most likely not high enough to play a significant role in resisting erosion. The concentration of salts that have shown to affect crust strength has been several orders of magnitude higher than the results for the Kuiseb depositional crusts. Houser et al. (2001) found that crust strength increased as the NaCl concentration increased, but the concentrations were three to four orders of magnitude higher than the salt concentrations for the Kuiseb silt deposits. Langston et al. (2005) tested salt crusts (5% NaCl, two orders of magnitude higher at 50,000 ppm than the salt content of the delta crust) in a wind tunnel and found that they broke down rapidly with bombardment by saltating grains. Such high concentrations of salt are more likely to be found in salt crusts associated with playa and sabkha deposits. The coastal sabkhas were not sampled during this study and the inland gravel plain playa salt crusts will be covered in the relevant discussion (5.2.1.5).

The SEM images of sample DFP19 (reproduced in Figure 100) confirm the particle size distribution results obtained with laser diffraction and the clustering of this sample as a Type 1 sample. The sample is predominantly made up of fine-grained (<100 μm) mica flakes together with aggregate minerals. The EDS analysis provides further information regarding possible impacts of this sediment as a dust source. For example, the EDS analysis identified the presence of Ti in sample DFP19. TiO_2 has recently been identified as playing an important role in certain photo-chemical induced chemical reactions, specifically the uptake of NO_2 and the formation of HONO on the particle surfaces (Ndour et al., 2008). In addition, the presence of Fe in the SEM images for all of the samples provides an input of iron-rich dust to the ocean.

The MODIS imagery reveals that it is likely that the majority of the area covered by flood water in the delta – and, as a result, the deposition of suspended sediment – will act as a potential source area. In some instances it is difficult to distinguish between the delta and the gravel plain as the dominant source area for a specific plume and it is likely that there is some contribution from both. The plumes in Figure 101 seem to originate from the delta and shows that the plume origin correspond with the depositional areas of the floods. In addition, the MODIS image dated 17 June 2010 shows the plumes originating predominantly from the river mouths (Omaruru, Swakop, Kuiseb and Tsauchab Rivers), playas and sabkhas (Sandwich Harbour and Conception Bay, plus possibly the sabkha in the Kuiseb delta). The largest percentage of plumes (54%) was identified as originating from the delta area. This evaluation therefore confirms the delta as a primary source of dust emission.

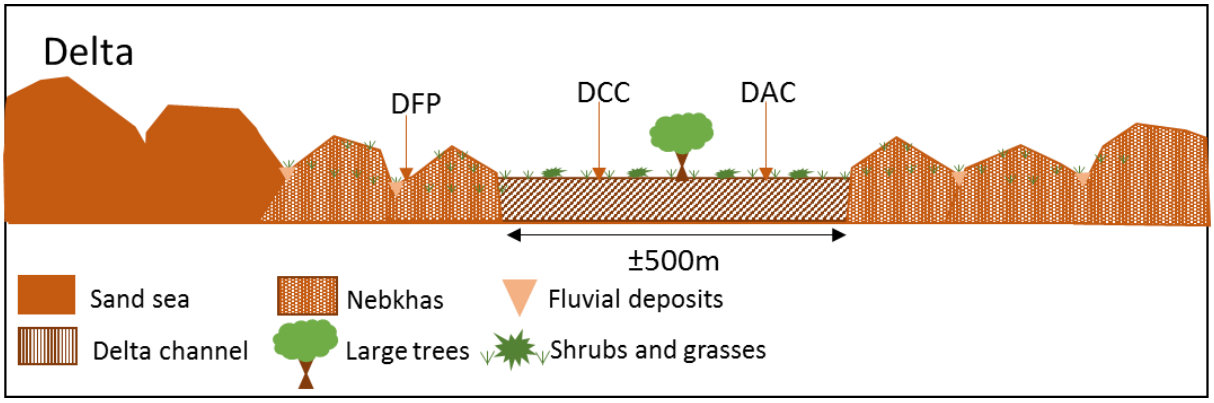

Figure 93 Transect profile for the delta.

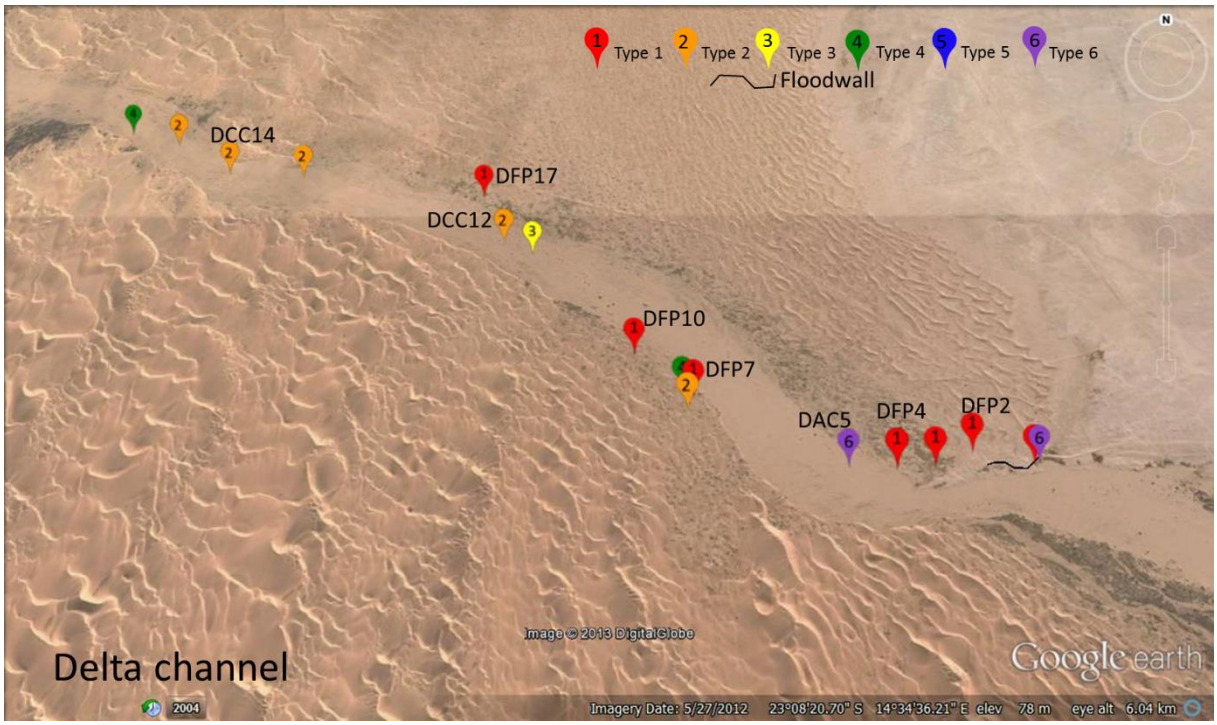

Figure 94 Sample location and cluster types for the delta channel.

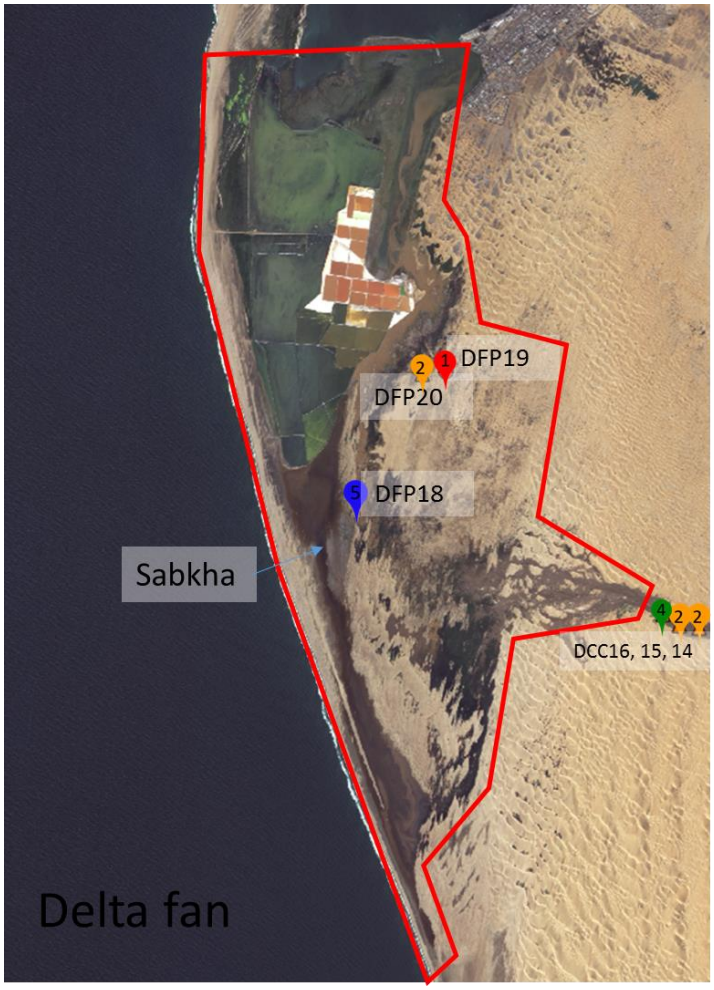

Figure 95 Sample location and cluster types for the delta fan. This image shows the river in flood flowing into the ocean.

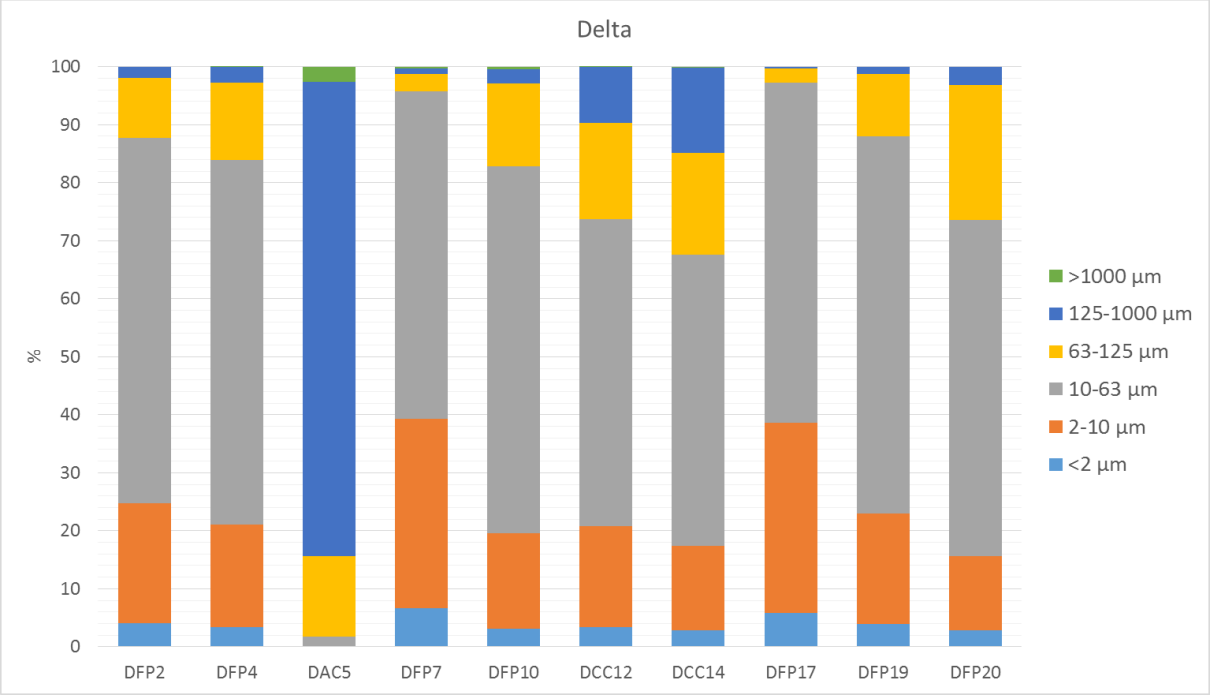

Figure 96 Particle size fractions for selected samples from the delta.

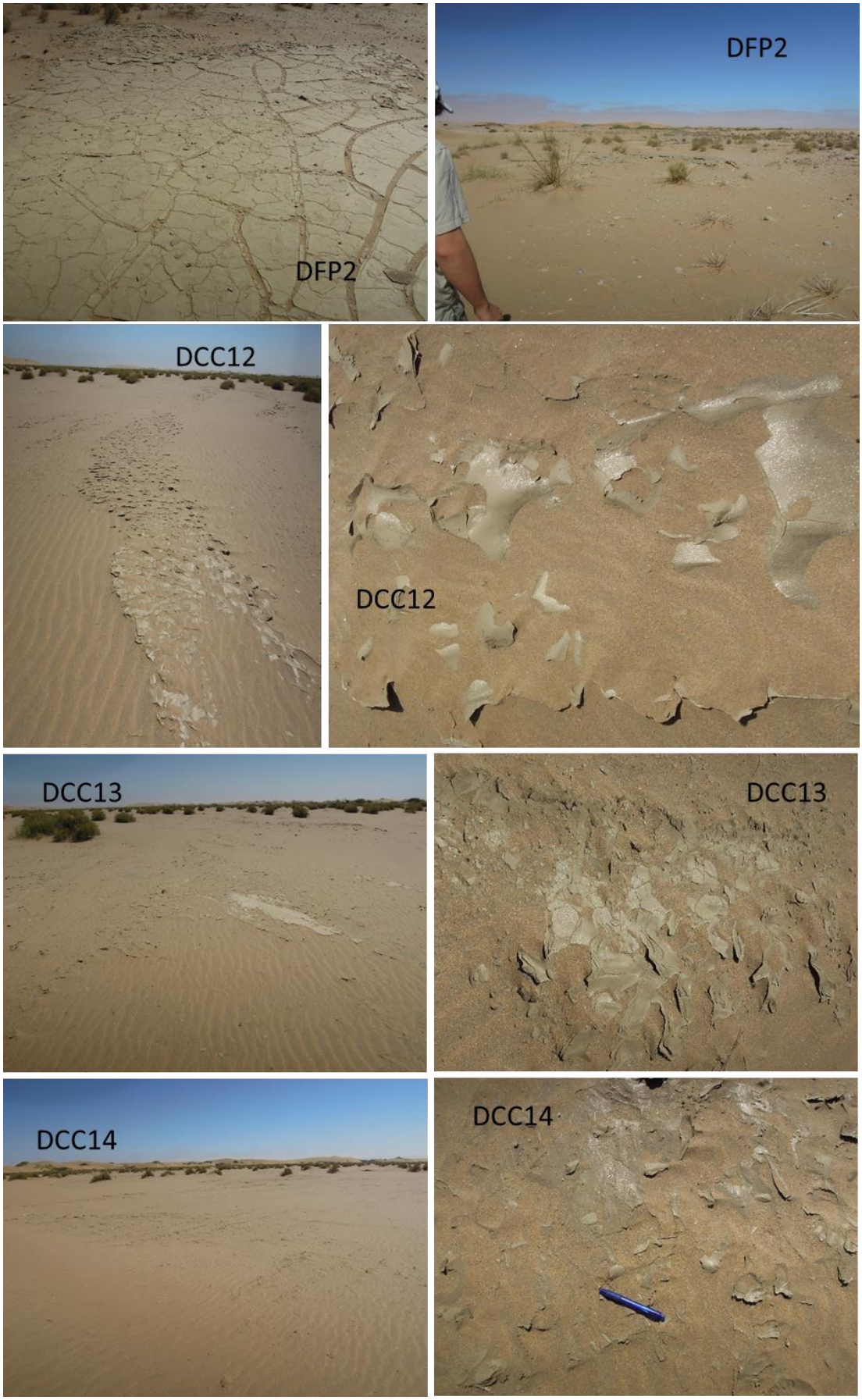

Figure 97 Surface features of the delta.

Figure 98 Surface features of the delta (continued).

Figure 99 Crusts in the delta fan area (light-coloured areas) covering extensive areas in proximity to a sand source for saltation (±600m).

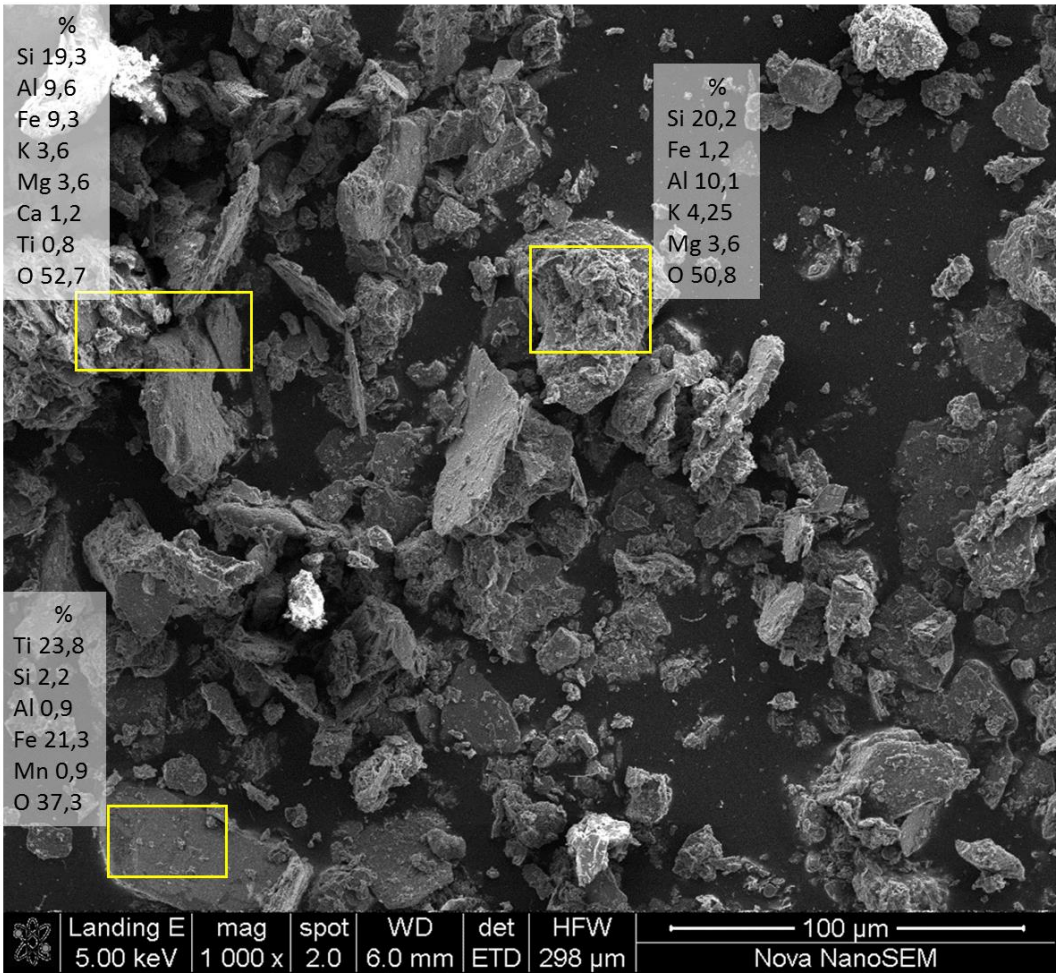

Figure 100 SEM image of DFP19 confirming Type 1 cluster and presence Ti and Fe.

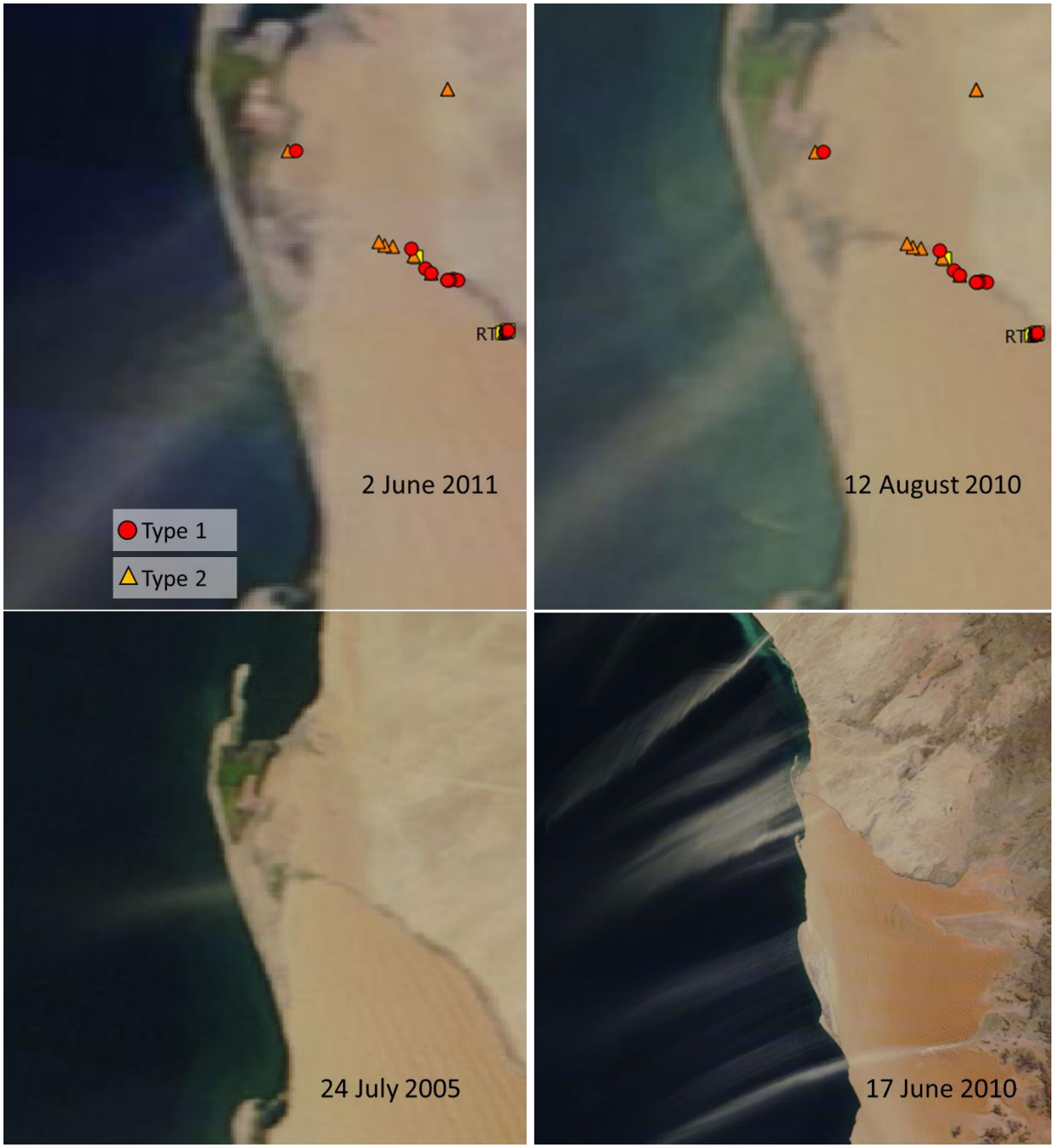

Figure 101 Dust plumes detected with MODIS imagery from the delta. The plumes on 24 July 2005, 2 June 2010 and 12 August 2010 seem to originate from areas of flood water reach (see Figure 95). The plume on 17 June 2010 seems to originate mainly from the rivers, sabkhas and playas.

5.2.1.5 GPC (Gravel plain drainage channels)

The gravel plain drainage channels and playas were identified as primary source areas based on the presence of suitable fine material in the depositional crusts. These drainage channels dissecting the gravel plain originate at the foothills of the escarpment and inselbergs, and flow towards the Atlantic Ocean, with the majority draining into the Kuiseb River. Along the way there are several places within the channels that form pans with permanent standing water fed by salt springs. The salt springs are generally associated with ground water flow that is being obstructed and ponded by linear NE-SW bedrock outcrops (Eckardt et al., 2001).

The water from these salt springs is extremely saline and is associated with aggressive salt weathering, which has been shown to produce silt-sized particles in the short term (Viles et al., 2007). Flow on the surface of the drainage channels is contingent on the occurrence of sporadic, yet significant, rainfall events on the gravel plain. Surface runoff during such rainfall events transport eroded material from the rock outcrops and gravel plain into the pans and drainage channels– and ultimately into the Kuiseb River, for those channels that drain into the river. There are numerous playas or salt springs situated on the gravel plain. Figure 105 shows the playas in the vicinity of Hosabes springs that could be identified with Google Earth.

The finest material found in this study was from the gravel plain drainage channels in the form of depositional silt crusts. Sample GPC47 had the smallest particle sizes and largest quantity of clay-sized material (11.4% <2 μm) of all the samples analysed. Although this is slightly higher than the highest clay content found in the delta, the average clay content of the GPC samples is 3.4%. This is very similar to the delta (DCC and DFP) clay content (3.5%). Similarly to the delta crusts, this is not likely to be a significant factor with the high-magnitude north-easterly wind events. However, it could possibly increase the strength of the crust to the extent that it is not emissive with slightly lower-magnitude wind events.

The organic content result is not regarded as reliable due to the presence of inorganic carbon in sample GPC47. However, the organic material that is visible in the sample after partial treatment with peroxide appears to be predominantly particulate organic matter. It is speculated here that this would not have an effect on the strength of the crust as it would not increase the binding energy between the organic material and the clay and silt particles, i.e. on a small-scale. Fine-grained particulate organic material (<100 μm) is visible on the SEM images and

this would be relevant when considering the impact of the dust from this source area (Figure 107).

Sample GPC47 also had a high Ca content (±900 ppm), which was confirmed by SEM (Figure 107) and treatment with HCl to be from carbonates in the sample. The effect that the carbonates will have on the erodibility of the crust is uncertain. Some studies conclude that $CaCO_3$ will strengthen the crusts as it acts like a binding agent surrounding the larger clasts (Gillette et al., 1982). This binding is evident in the SEM images for all samples, where the aggregate minerals appear to bind the larger particles together. Others contend that the soft Calcite (3 on the Moh's scale of hardness) will have very little resistance to abrasion (Pye et al., 1990, p75). Gillette (1979) also pointed to the increased erodibility of calcareous silt loams versus to non-calcareous silt loams. The depositional crusts in the drainage channels of the gravel plain on the western side of the basin dissect an area dominated by Gypsisols (see Figure 46 in results). These crusts would potentially have a different erodibility response to the calcareous crusts of the eastern side.

Also present in the drainage network of the gravel plain are salt crusts, which are associated with the groundwater present along the channels (Figure 109). As mentioned in the delta discussion (5.2.1.4), these salt crusts potentially break down rapidly when bombarded by saltators (Langston et al., 2005). Samples were taken of the salt crusts found on the gravel plain, but they were not analysed for particle size distribution. The laser diffraction methodology with aqueous dispersion used for this study was not suited to measuring the particle size distribution of the salt crusts. Sample GPC21 (Figure 109) was taken just upstream of an area covered in salt crust. The salt crust surfaces probably give rise to saline dust storms, consisting of a high concentration of saline and alkaline material, e.g. sulphates, NaCl and $CaCO_3$ (Abuduwaili et al., 2010). Reynolds et al. (2009) refer to dust from saline sources as evaporite-mineral dust, as opposed to conventional clastic dust from clay and silt sources. The impacts of the two different dust sources will potentially be very different. Figure 106 shows the different particle size distributions for selected samples, including sample GPC21. Some samples have a tri-modal particle size distribution attributed to different processes and sources.

One of the proposed mechanisms for wind erosion of salt crusts involves the formation of a soft, fluffy salt layer at the surface produced by efflorescence after a rainfall event (Reynolds et al., 2007). This is not likely to be the case for the crusts in the sabkhas and playas of the Kuiseb basin, as these surfaces deflate predominantly during winter when there is no rainfall.

The influence of the frequent fog events in the Namib Desert on the salt crusts and their dust activity is unknown. A mechanism involving saltation is more likely for this area. The channels also consist of ample sand, which could act as a source of saltators (Figure 111 shows what happens if you tackle the gravel plain drainage channels without a 4X4). The crusts found in the channels also showed evidence of degradation due to wind erosion (GPC27 in Figure 108).

The binding media present in the crusts will vary in composition and distribution and the erodibility of the crusts could therefore show considerable spatial variation. This physical and chemical heterogeneity of the crusts could be part of the reason for the intermittent nature of the dust activity of the area, in terms of both space and time.

The vegetation in the gravel plain channels and playas is minimal consisting mostly of low-level shrubs and grasses (Figure 108). Where vegetation is present it will play only a localised role in minimising dust emission and is therefore not considered a significant force of resistance to dust activity from these areas.

Lastly, the playa areas are also frequented by wildlife (e.g. Springbok and Oryx) as is evident from the trampled crusts found at Hosabes spring (GPC46 in Figure 108). This would also influence the dust activity from the playa, possibly increasing it (by creating unconsolidated material) or decreasing it (due to the increase in surface roughness). Baddock et al. (2011) tested playa crusts in a portable wind tunnel in the field after one and ten passes of a cow. The results indicated that the dust flux increased significantly between one and ten cow passes and highlights the level of disturbance needed for a surface to become an active dust source.

Some of the dust plumes originating from the gravel plain can be linked to the playa areas with reasonable certainty (see Figure 82 in RM section 5.2.1.2). Other plumes clearly originate from the gravel plain but cover large areas, and it is uncertain which surfaces are acting as the dust sources (Figure 110). There are numerous playas spread all over the gravel plain (Figure 105 gives an indication of the springs in the vicinity of Hosabes Spring) and it is fairly certain that they play an important role (either directly or indirectly) in the dust activity from the gravel plain. The extensive areas of depositional crusts, the presence of Type 1 samples, and the lack of vegetation and plumes identified by MODIS all confirm the playas as a primary source areas of dust. However, the mechanism involved still has to be confirmed.

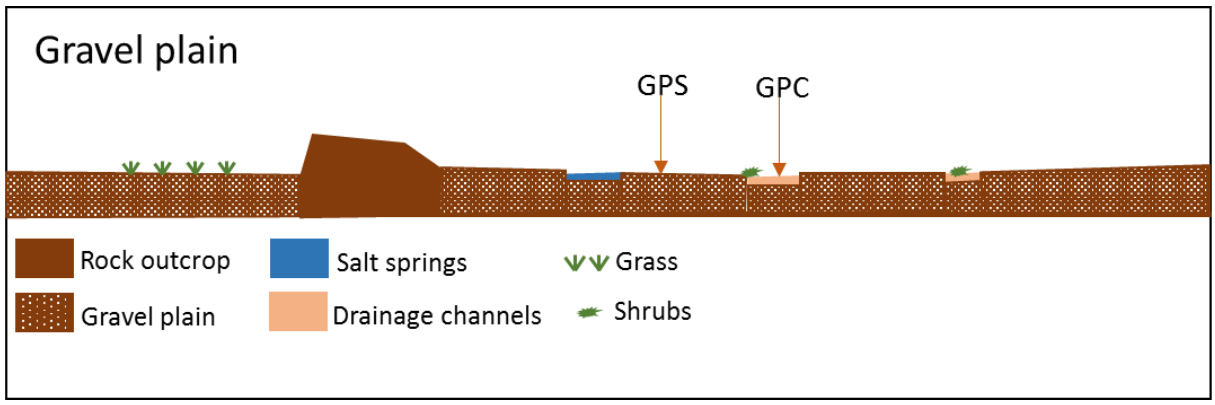

Figure 102 Profile of the gravel plain.

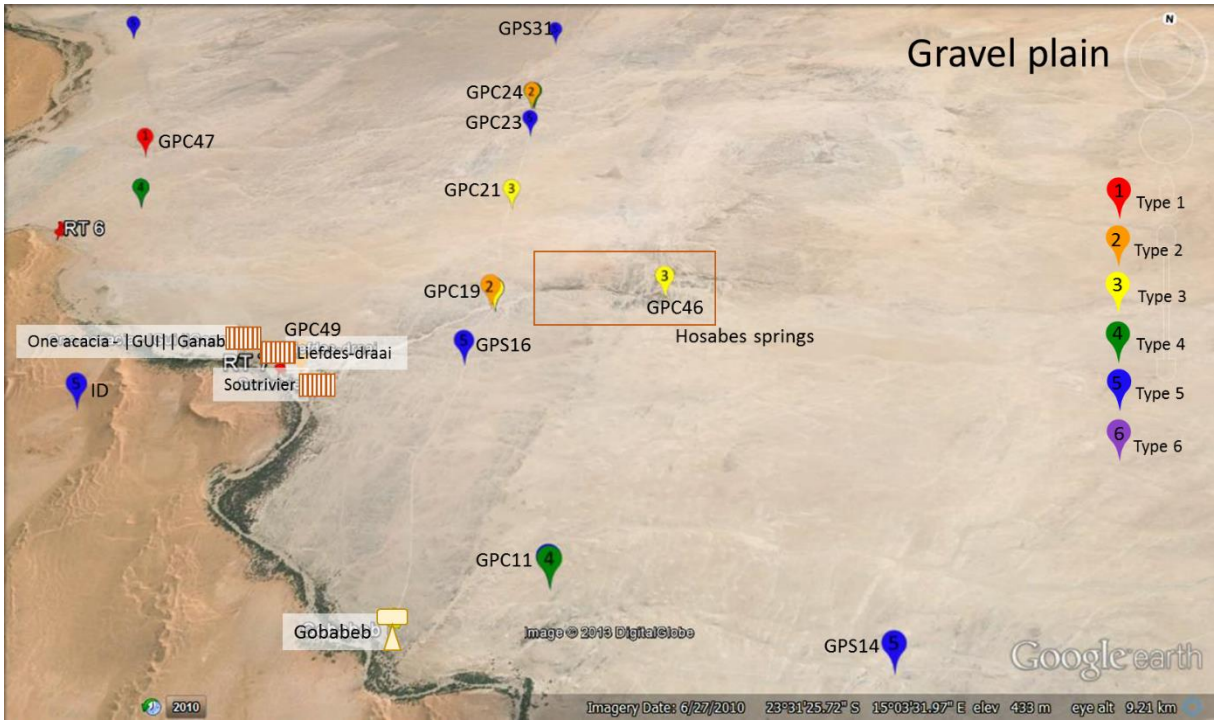

Figure 103 Sample location and cluster types for a part of the gravel plain.

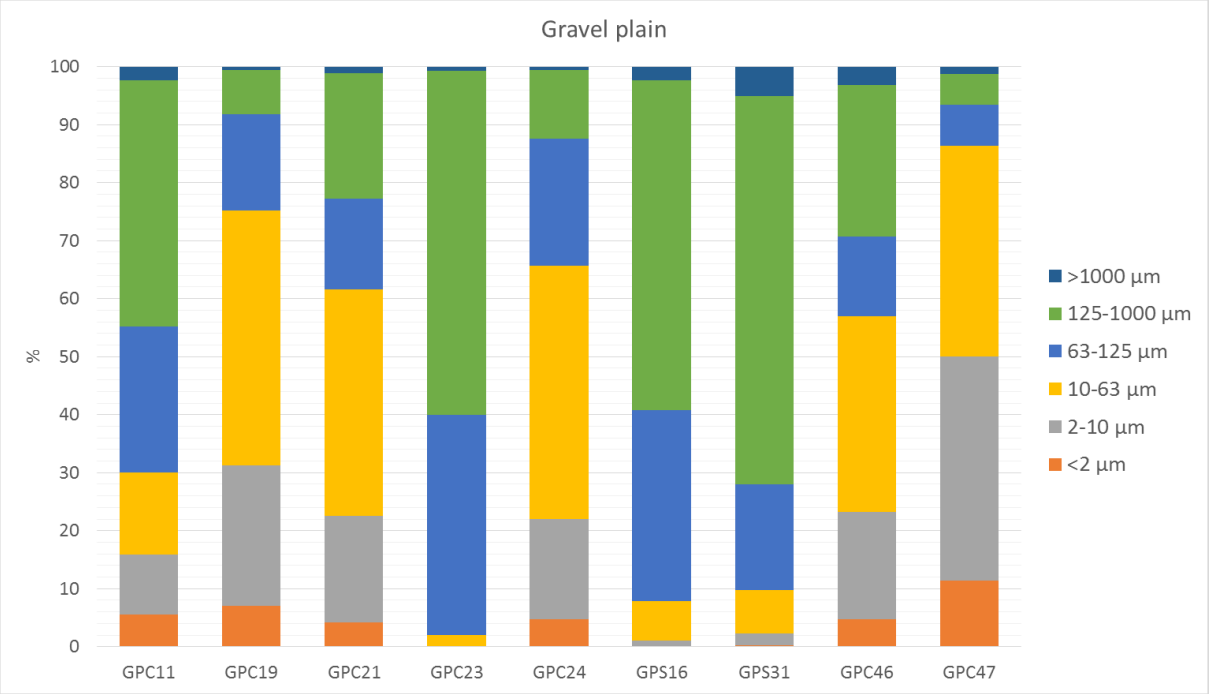

Figure 104 Particle size fractions for selected samples from the gravel plain.

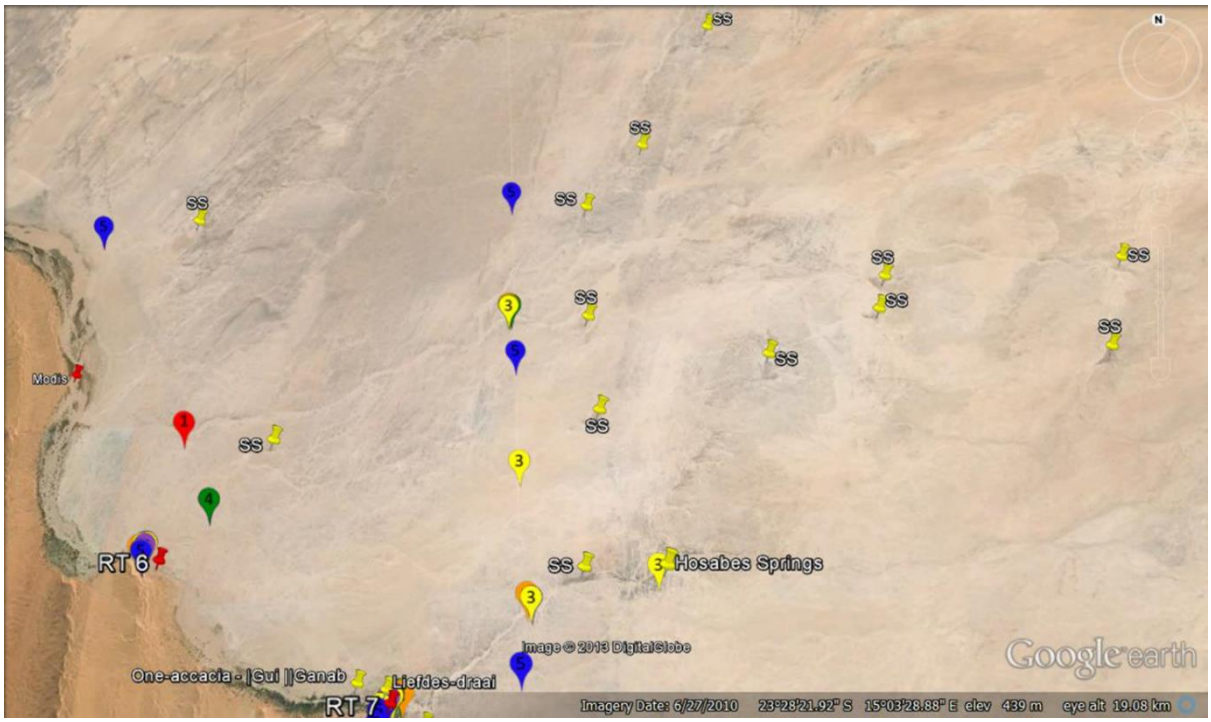

Figure 105 The distribution of playas in the vicinity of Hosabes Springs, as identified on Google Earth. Salt springs marked as SS.

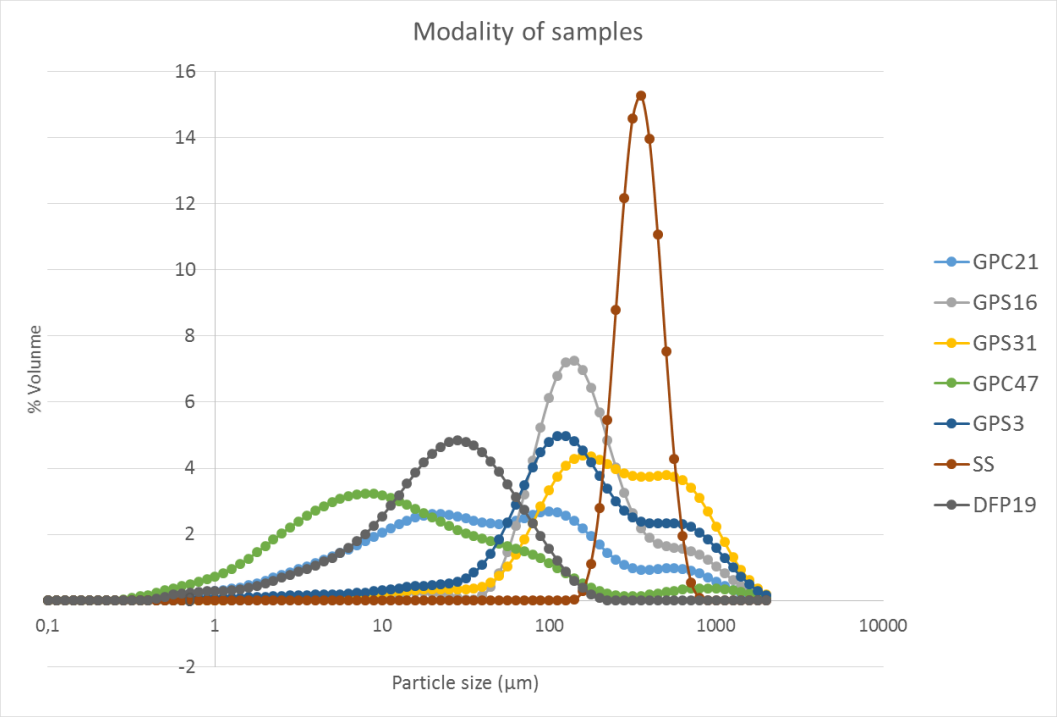

Figure 106 Particle size distributions of selected samples showing bi- and tri-modality due to different sources and processes. Sand Sea sample (SS) and delta fan sample (DFP19) for comparison.

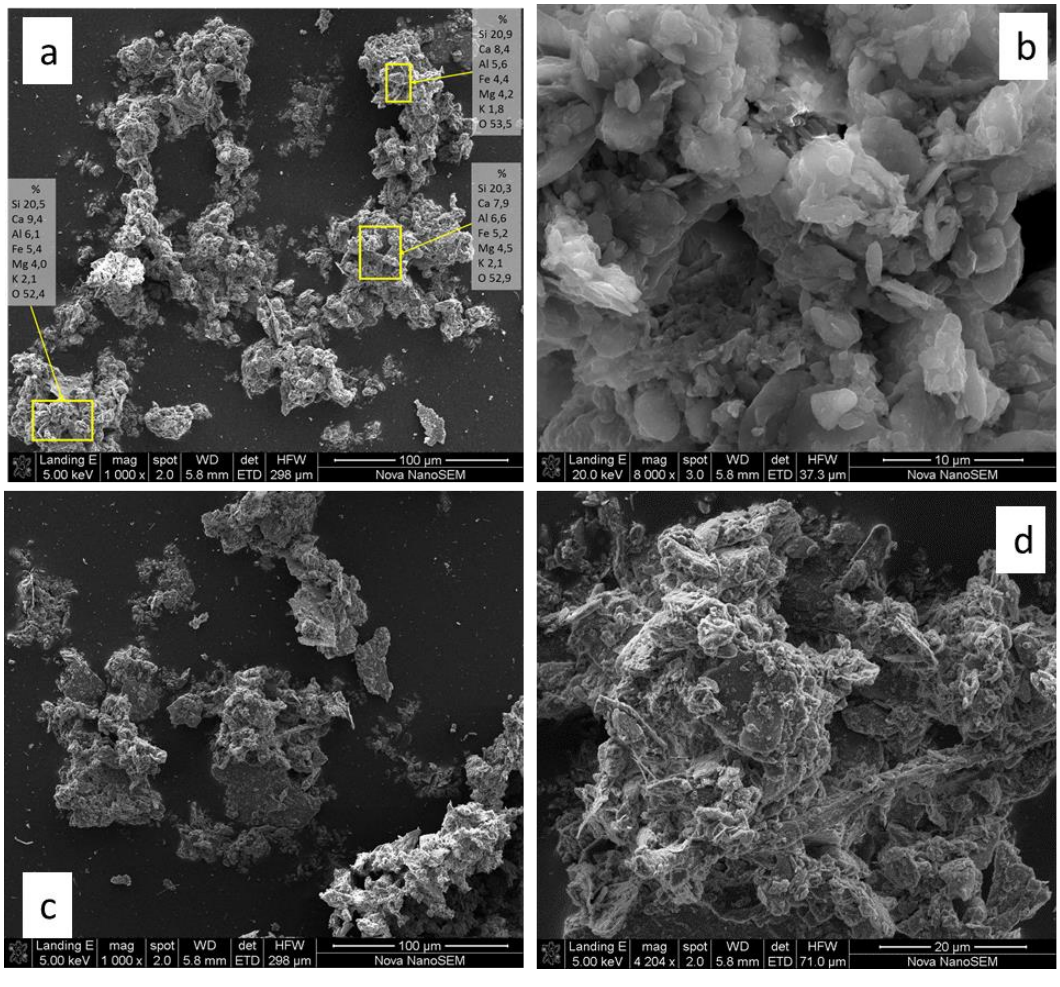

Figure 107 SEM image of GPC47, Type 1.

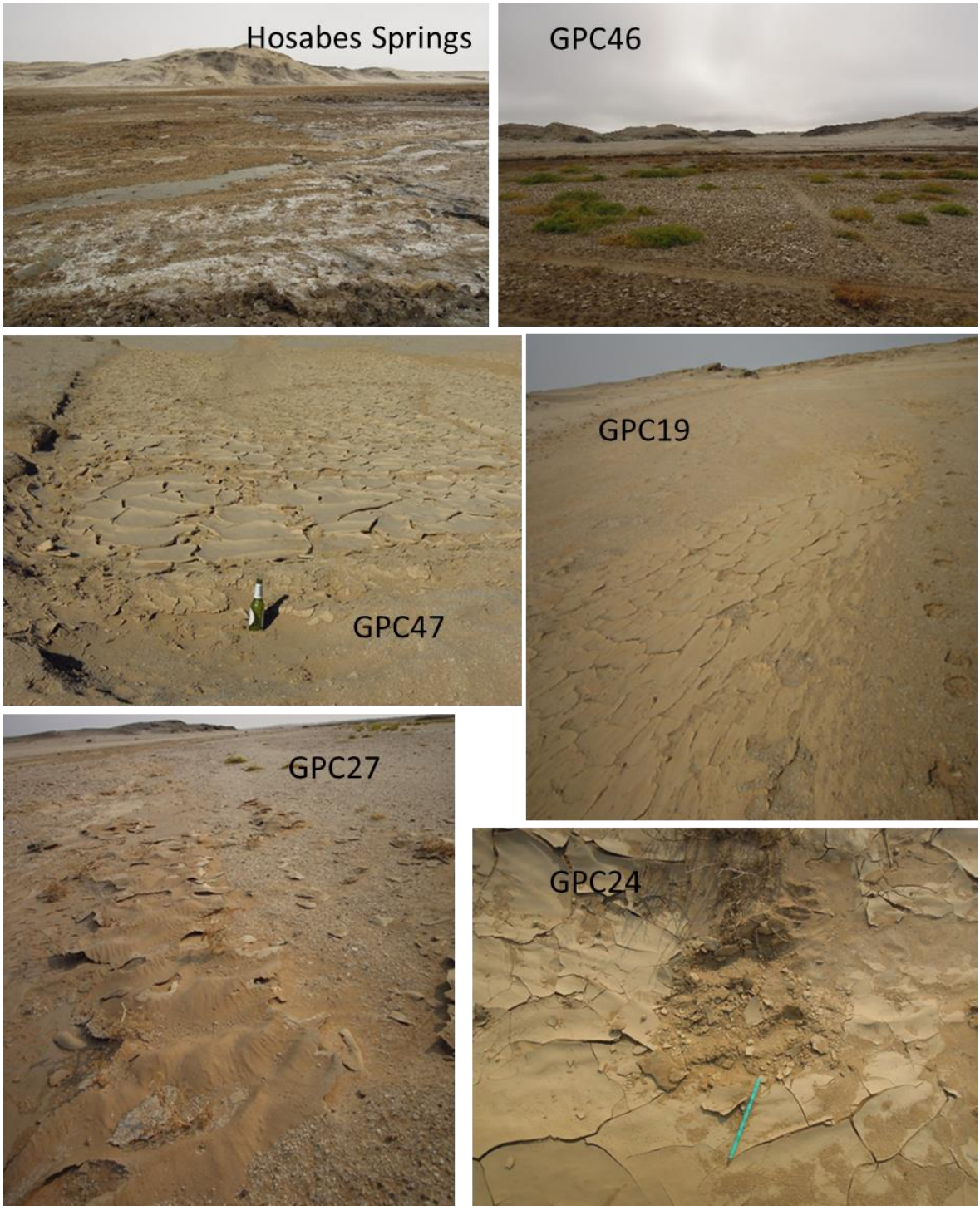

Figure 108 Depositional crusts of the gravel plain drainage channels.

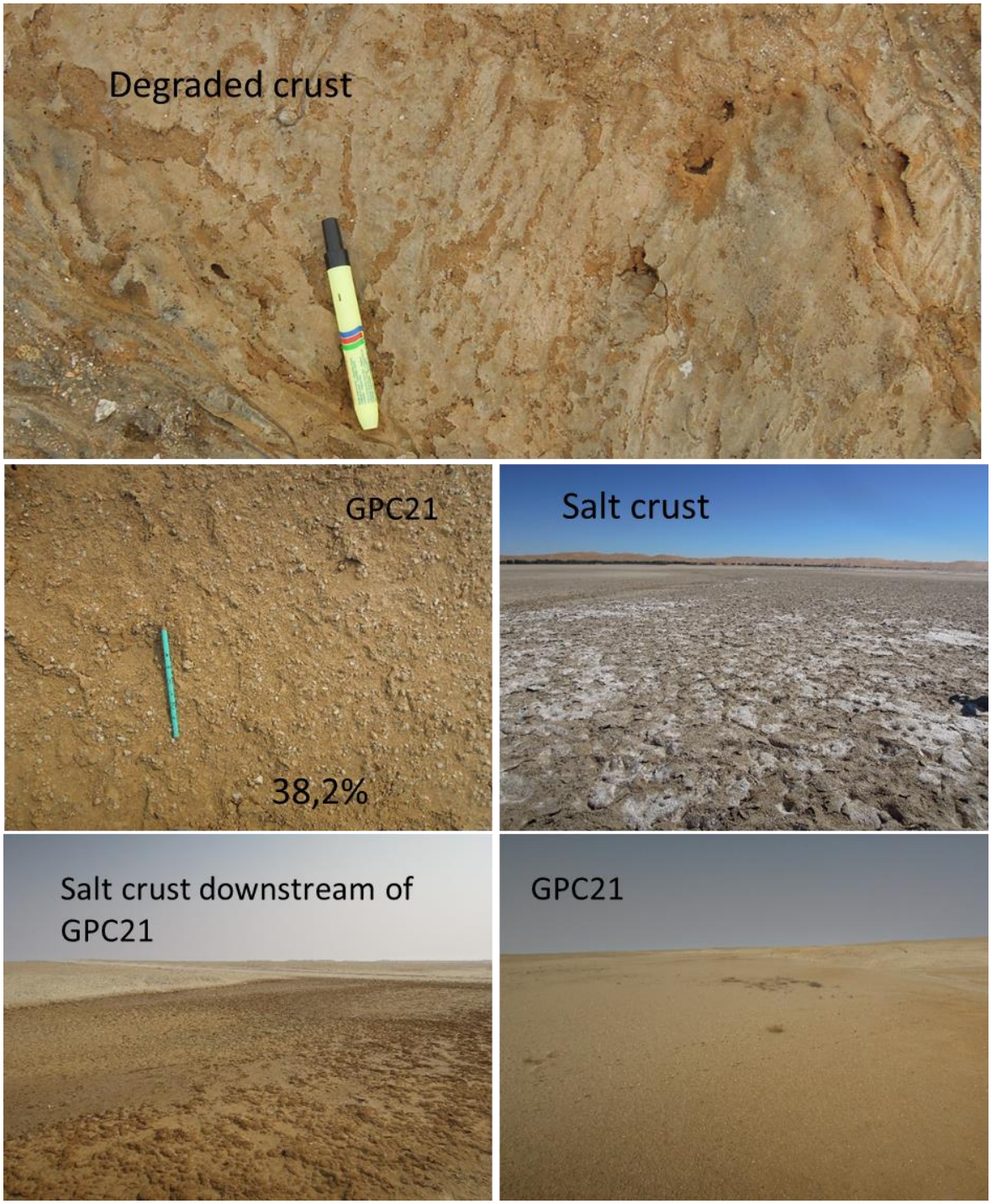

Figure 109 Degradation of crust at Hosabes Springs (top). Sample GPC21 taken just upstream of salt/silt crusted area. Middle right is an example of salt crust found in the vicinity of Soutrivier.

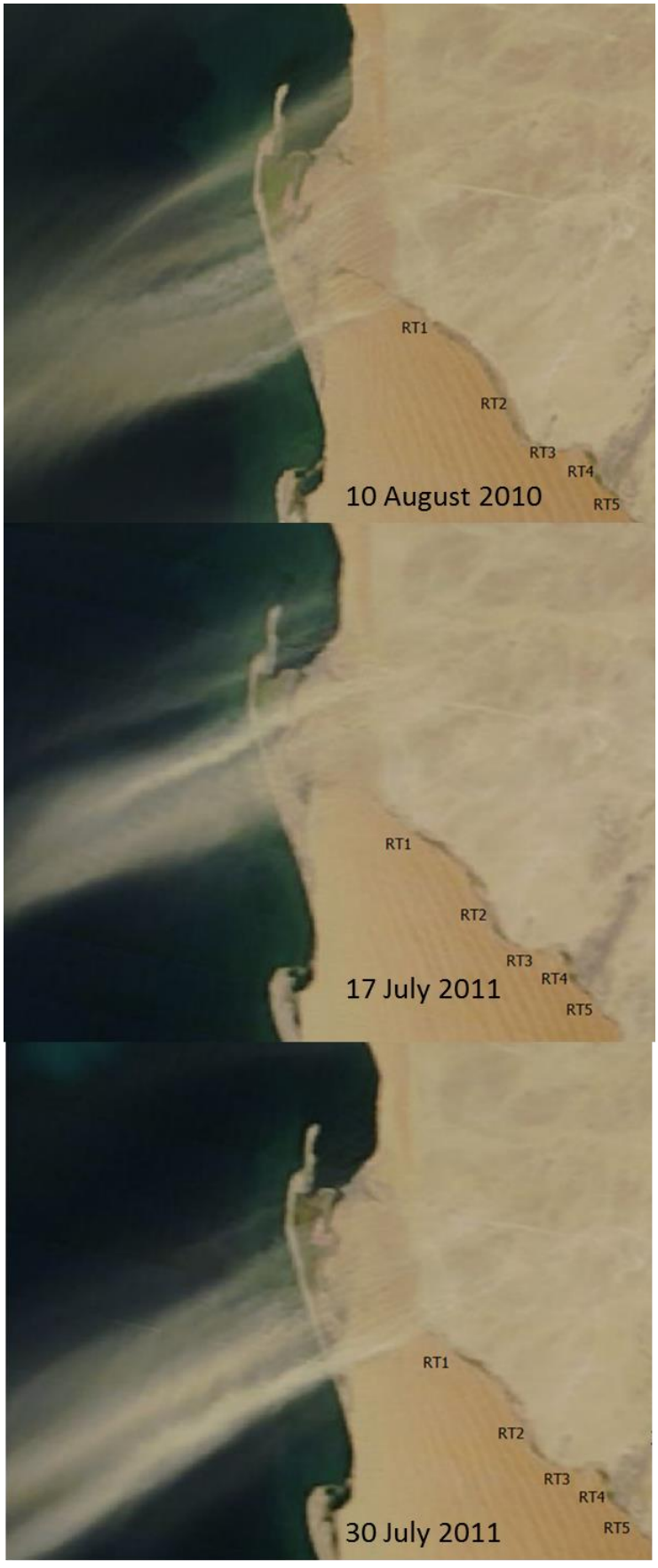

Figure 110 Dust plumes originating from the gravel plain.

Figure 111 Sand in the drainage channels. A likely source of saltators.

5.2.2 Secondary source areas

5.2.2.1 GPS (Gravel plain stone pavement)

The stone pavement surface consists of a sand and silt substrate covered with a layer of coarse gravel. Most of the samples from this surface clustered as Type 5 samples, with only one Type 4 sample (GPS11). In addition to the reduced amount of fines present on this surface, the protection afforded by the gravel layer to the sand and silt substrate would appear to make any fine sediment less available for wind deflation. The stone pavement of the gravel plain would seem an unlikely source of dust emission. Some studies have found that these surfaces are very low emitters of dust due to the gravel cover, for example Sweeney et al. (2011) in the Mojave Desert in California. In contrast, other studies have found that similar surfaces are large emitters of dust. Xuan et al. (2002) found that the gobi surface was the second largest source of dust in Northern China after the Takliman Desert. Note that the term gobi refers to a surface type paved with gravel or rock debris found in the Asian Desert areas as used by Xuan et al. (2002), whereas the same authors use the term gobi-desert to refer to an area of alternating sandy desert, gobis and grassland. The authors point out that the ability of the stony desert to emit dust was unexpected due to the gravel armouring. Wang et al. (2012) found that 75% of the dust emission activity in Western China and Southern Mongolia emanated from gobi-desert. The results from the wind tunnel experiments showed that dust emission from gobi surfaces were low at low velocities (8-10 ms^{-1}), but that these surfaces can emit large quantities of dust at high wind velocities (12-22 ms^{-1}). Wind speeds over 12 ms^{-1} occur within the Kuiseb River area with the north-easterly Bergwinds in winter (Vickery, 2010).

Wang et al., (2012) maintain that the effect the gravel cover has on dust emission from these surfaces is complicated and that the gravel overlay may not be the most important control on the emissivity of the surface. With gravel covers of less than approximately 30%, sediment transport increased with increasing gravel cover. Beyond the 30% threshold dust emission decreased with increasing gravel cover. There was also a tendency to overestimate gravel cover with visual estimates in the field (60-80%), whereas photographic analyses revealed substantially less cover (18–43%) (Wang et al., 2012). A photograph of the stone pavement tested by Wang et al. (2012) is included in Figure 116. The mass percentage of gravel (>2000 μm) from the Kuiseb basin gravel plain is included in Figure 116 on the image for each sample. These figures give an idea of the gravel content of the surface sediments, but does not equate

to percentage cover. No photographic analysis or quantification of the gravel cover was attempted for the Kuiseb stone pavements.

The study by Wang et al. (2012) did not investigate the influence of surface characteristics, although they speculate that sediment transport from these surfaces is controlled by the interaction between air flow and a complicated combination of surface characteristics, such as particle size distribution, cohesion as a result of silt and clay content, and the nature of the gravel overlay. Xuan et al. (2004) agree that the gravel cover can both enhance and reduce the dust activity of the surface. A complete cover of gravel can act to reduce dust emission, whereas reduced gravel armouring can affect the wind flow in various ways to enhance dust emission (Xuan et al., 2004). It is therefore possible that the gravel pavement of the gravel plain within the Namib Desert is a larger source of dust emission than previously thought. Aeolian sediment reworking from the river, delta and gravel plain silt and salt crusts within the drainage channels could deposit sediments onto the gravel surface during low-magnitude, high-frequency winds (predominantly consisting of south-west winds in summer), which could undergo medium- to long-term suspension with appropriate transport conditions (high-magnitude winds) in the future. This sediment reworking – and, to a lesser extent, in-situ weathering– is probably the reason for the dominance of the Type 5 cluster on the gravel plain. These surfaces therefore serve as silt- and clay-holding areas, rather than being dominant producers of fine fractions for deflation (Sun, 2002). The percentages of <63 μm on the stone pavements of the Kuiseb River basin are in many instances more than reported by Wang et al. (2005) for similar gobi desert surfaces (5-7%).

The dust activity in the basin also potentially has important consequences for the development of soil underneath the gravel overlay of the stone pavement. The “accretionary-inflationary” mechanism of soil profile development (AIP) proposed by McFadden (2013) relies almost exclusively on inputs of dust for the development of a soil profile underneath the stone pavement (Figure 115). The dust provides important materials for soil formation, including clay-sized sediments, Fe oxides and soluble salts. The rate of dust influx and migration to below the surface is such that the stone pavement does not become buried and result in the accumulation of loess (McFadden, 2013). This does not preclude the stone pavement from being a store of sediment for future dust emission. On the contrary, the balance of deposition and deflation of dust from this surface could be important components in the development of a soil profile corresponding to the AIP model.

In addition to the dust plumes identified with MODIS imagery as originating from the gravel plain in winter (section GPC, Figure 110), there are also dust storms originating in the gravel plain during summer that cannot be identified with MODIS images due to cloud cover (Figure 117). These dust storms occur with the turbulent flow of downdrafts in summer. The summer dust storms are mobile dust storms and the mechanisms involved are different to the winter stationary dust storms for which the source remains fixed (Xuan et al., 2004). It is possible that the stone pavement silt and clay holding areas act as the dominant source for these mobile dust storms. What is also evident from Figure 116 is the variable nature of the stone pavement within the area. Even though all the samples clustered as Type 5 based on silt-sized particles, the gravel content and type of overlay appears to be quite different (see different stone pavements in Figure 116). The dust potential of this surface would need to be investigated further to gain a proper understanding of its role in the dust activity of the basin.

The gravel plain stone pavement of the Namib Desert will remain a secondary source until further investigation can determine the potential of this source area to produce (or not produce) dust. Evidence from other parts of the world suggests that this surface might have the potential to be a significant source of dust.

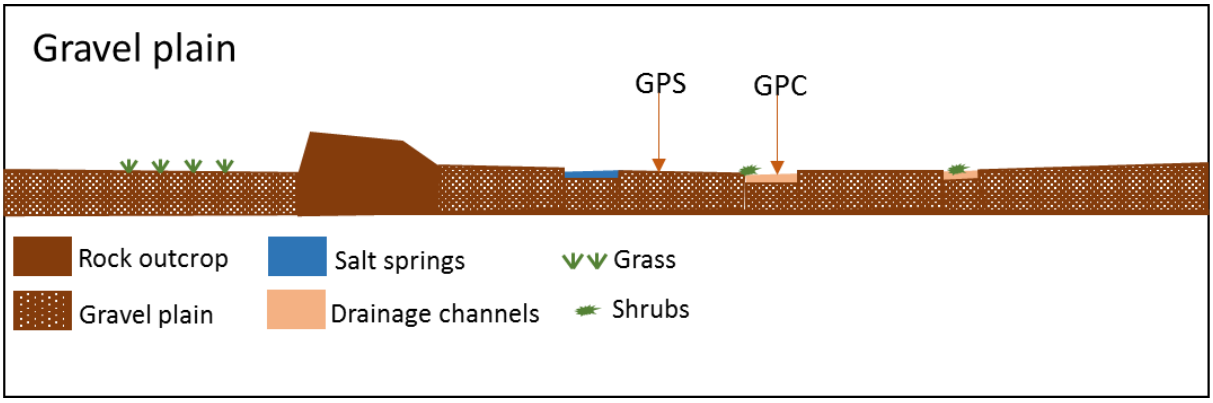

Figure 112 Profile of the gravel plain.

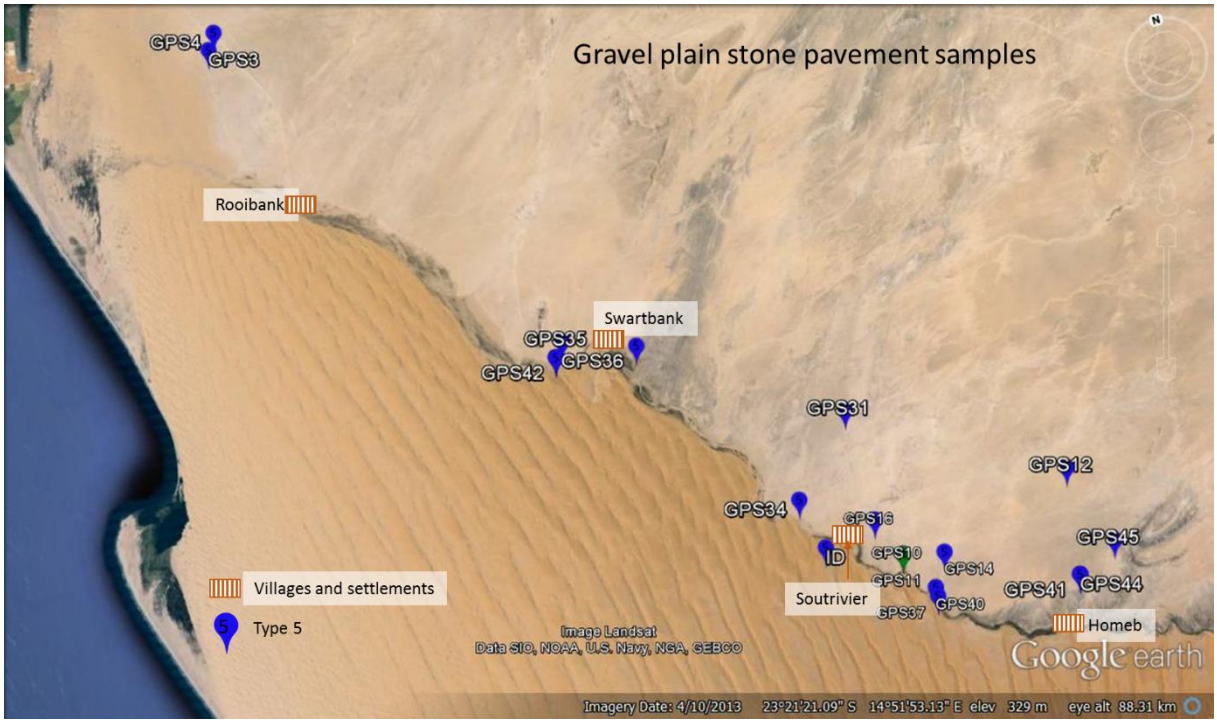

Figure 113 Sample location and cluster types for a part of the gravel plain stone pavement.

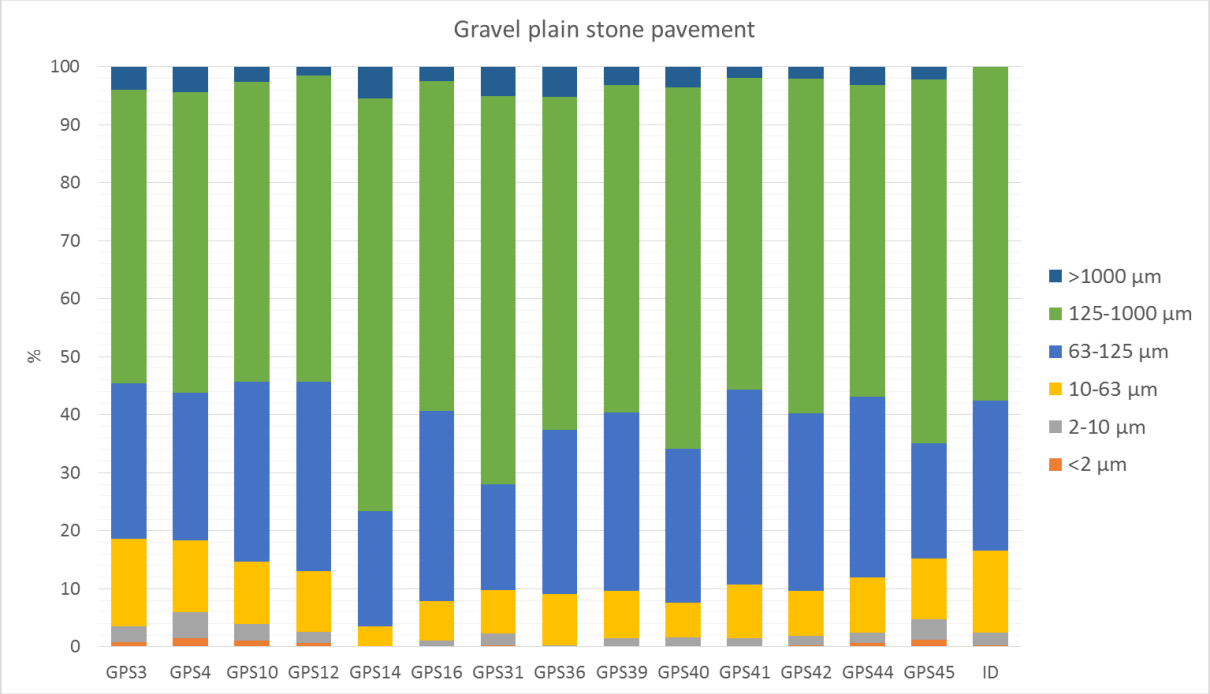

Figure 114 Particle size fractions for selected samples from the gravel plain stone pavement and interdune area (section 4.2.2.2).

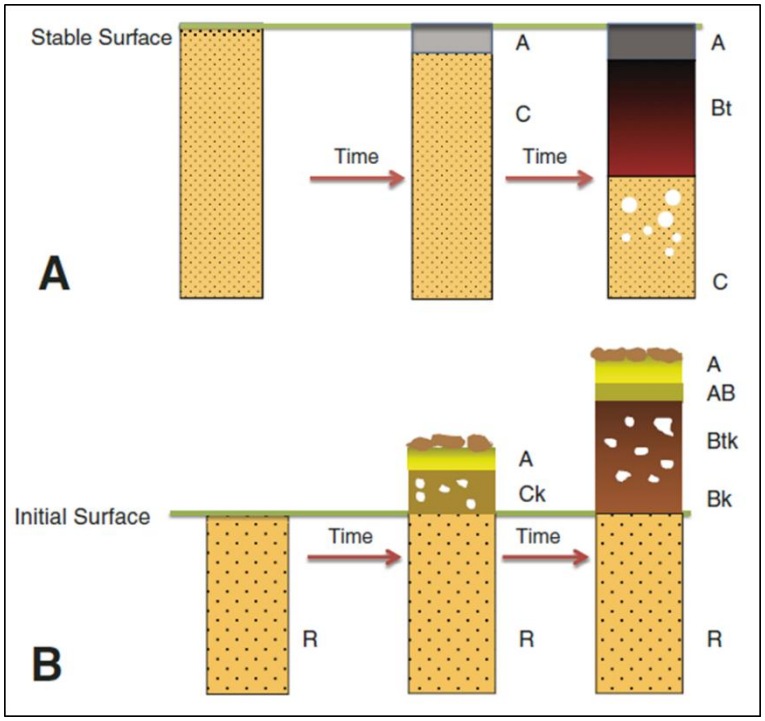

Figure 115 Two models of soil profile development. Diagram A: a representation of the classic A/B/C model of soil profile development. Diagram B: the "accretionary-inflationary" model of upward soil profile development as proposed by McFadden (2013). Diagram from McFadden (2013).

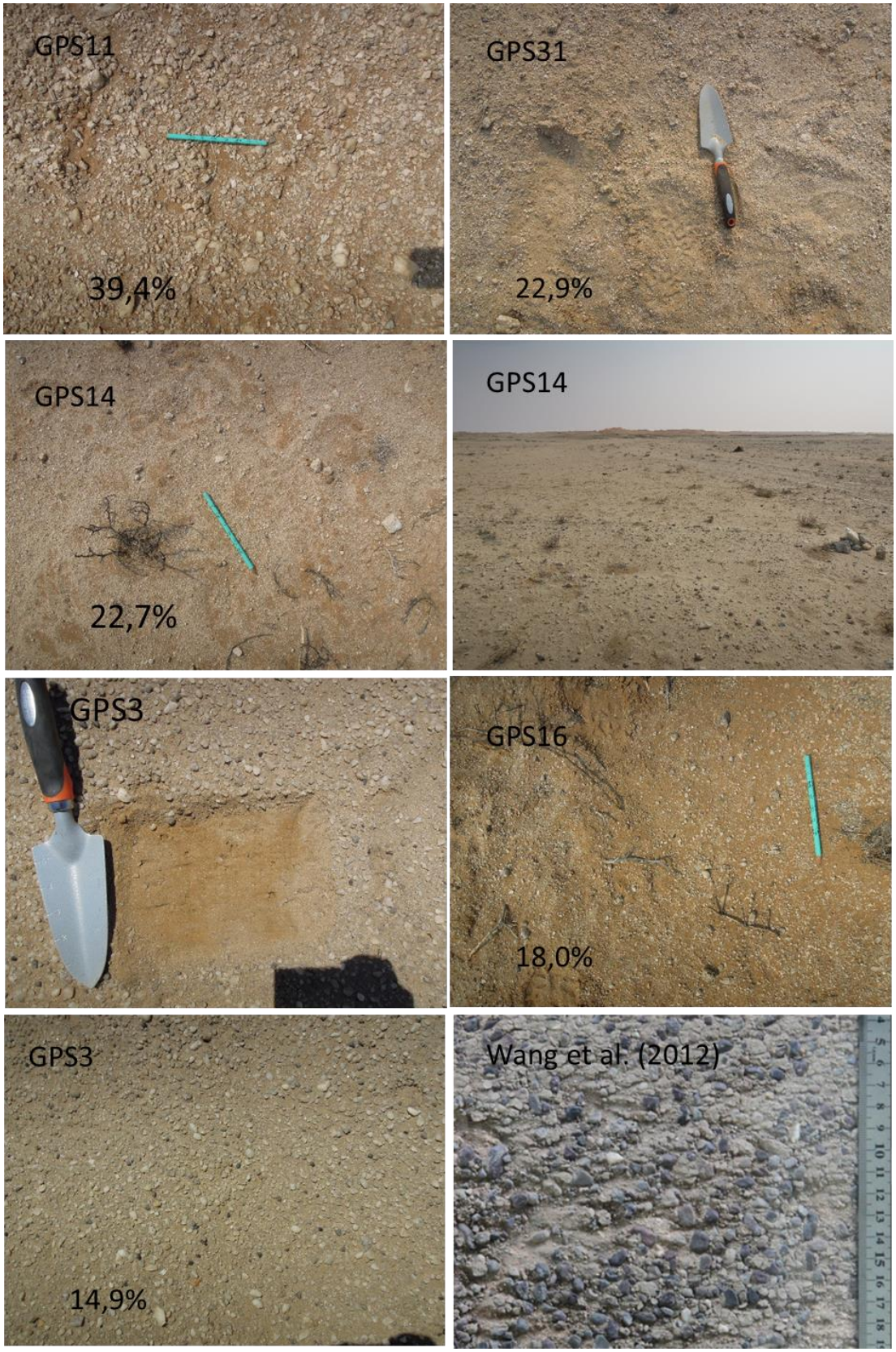

Figure 116 Surface features of the gravel plain stone pavement. Percentages given are percentage gravel in sample (by mass). The bottom right image is one of the stone pavements tested by Wang et al. (2012).

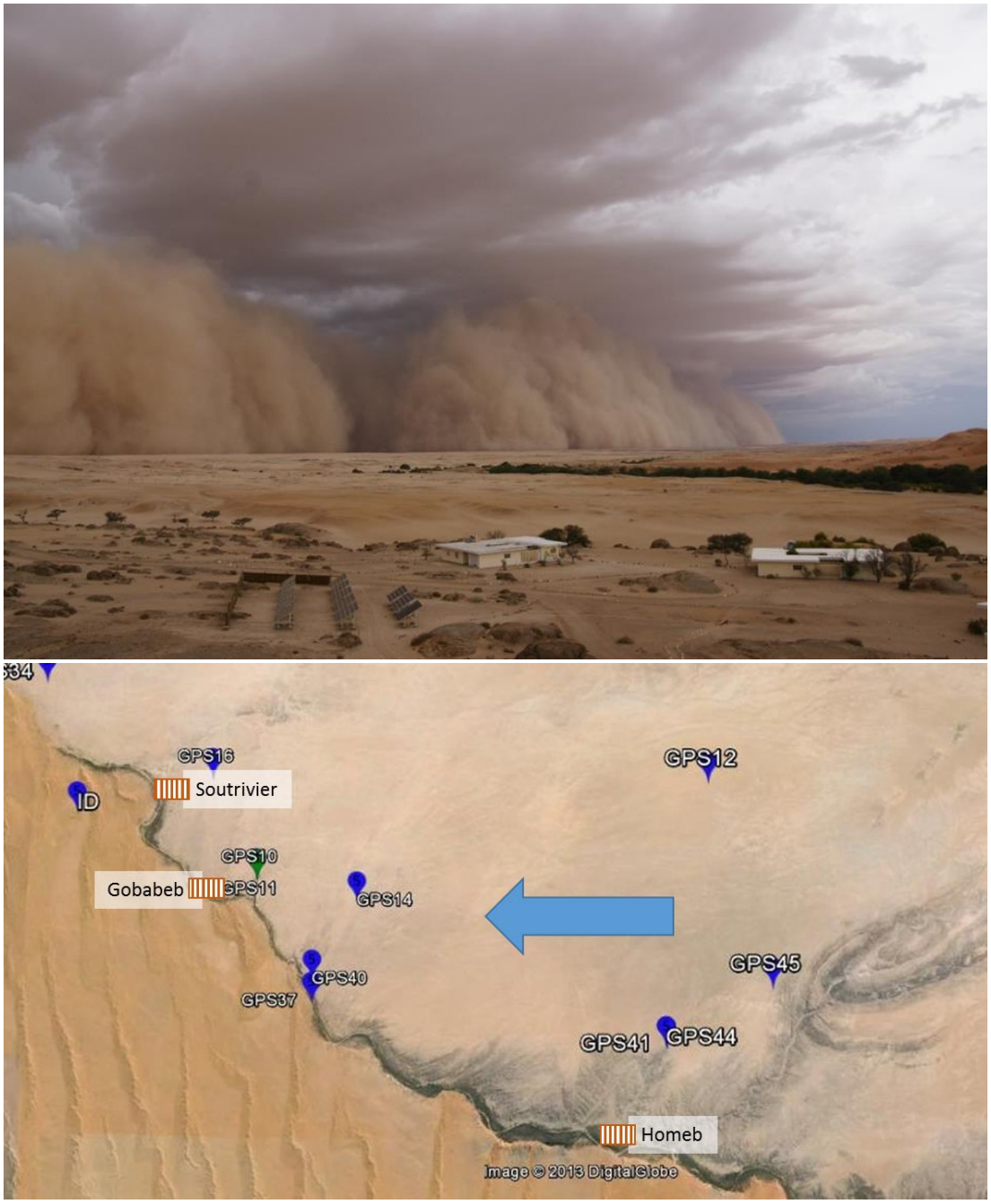

Figure 117 Mobile dust storm associated with summer downdrafts. Top image taken from Gobabeb and bottom image shows approximate pathway and direction. Photo courtesy of Joh Henschel taken on 4 January 2011.

5.2.2.2 ID (Interdune areas)

The interdune sample also clustered as a Type 5 sample and therefore is very similar to the gravel plain stone pavement samples. Most of the interdune areas are situated within the linear dunes of the Namib Sand Sea, which are oriented perpendicular to the direction of the winter north-easterly winds with which dust emission is associated. These areas will therefore remain a secondary source of dust emission.

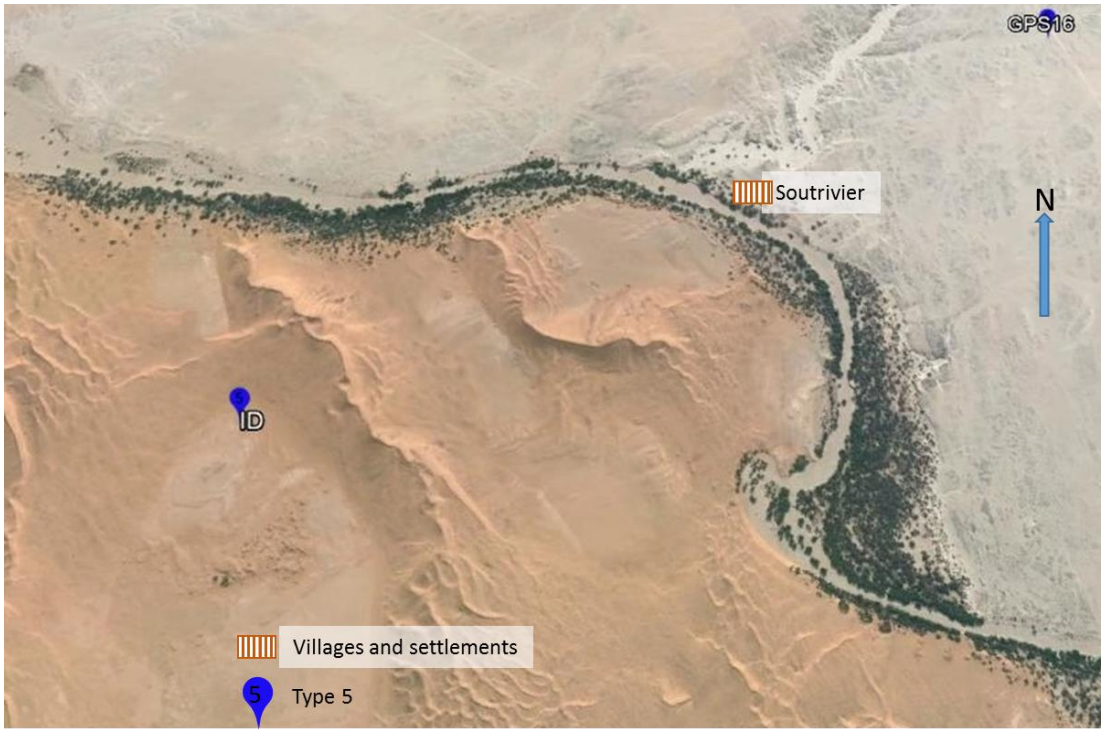

Figure 118 Sample location of the interdune sample.

Figure 119 Surface features of the interdune area identified in Figure 118. Photo courtesy of Frank Eckardt.

5.3 Anthropogenic influences

During the course of the fieldwork and the desk-top study it became evident that the Kuiseb River area has been altered by human activities to a large extent. The gravel plain has been subjected to a significant number of infrastructure and mining activities (Figure 120).

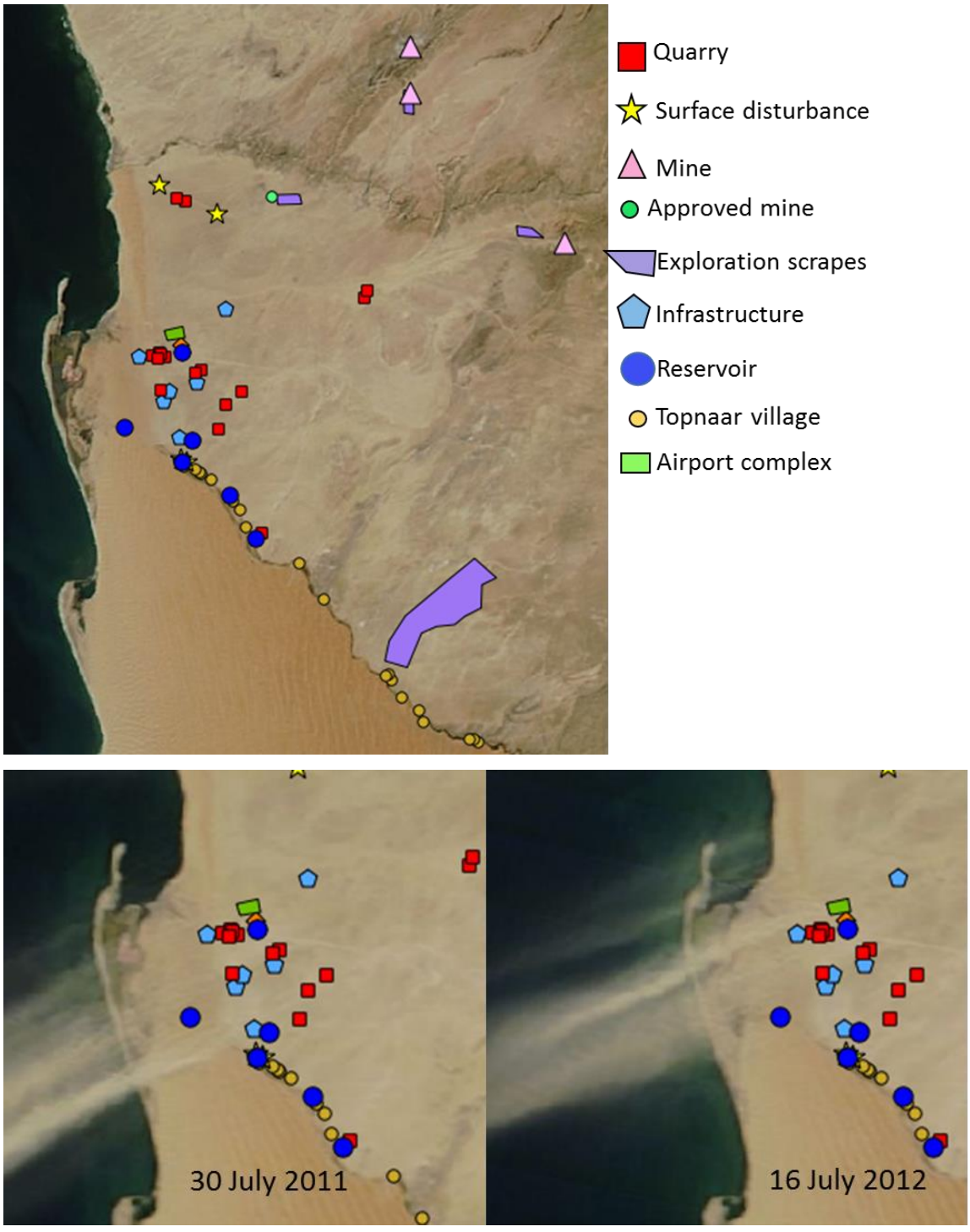

Figure 120 Human alterations to the region as identified with Google Earth. Bottom images show identified activities compared to two plumes visible on MODIS images for 2011 and 2012.

5.3.1 Livestock

Livestock kept by the Topnaar people on the river can potentially affect dust emission in two ways. Firstly, it could affect dust emission by trampling the silt crusts deposited with the river floods and thereby creating large amounts of unconsolidated material. Unconsolidated material has a lower threshold for entrainment. Secondly, the goats could affect the vegetation on the river, thereby changing the roughness of the surface. Reduced vegetation could increase dust activity. Trampling was widespread along most of the river transects conducted for this study. Table 10 from Henschel et al. (2010) provides the type and numbers of livestock per village along the river from a 2002 survey conducted by the Directory of Engineering and Extension Services, Ministry of Agriculture, Water and Forestry.

Table 10 Number and type of livestock on the Kuiseb River according to villages. Table from Henschel et al (2010). Data from a 2002 survey conducted by the Directory of Engineering and Extension Services, Ministry of Agriculture, Water and Forestry.

Name	Cattle	Goats	Sheep	Donkeys	Horses	Total
Armstraat	0	50	0	19	0	69
Goadanab	0	132	0	4	0	136
Ururas	11	467	0	20	0	498
Utuseb	83	256	0	35	0	374
Swartbank	33	353	0	92	0	478
Klipneus	10	156	0	28	0	194
Soutrivier	0	258	8	25	0	291
Natab	2	525	0	21	0	548
Homeb	17	826	102	29	12	983
Total	156	3023	110	273	12	3571

Henschel et al. (2010) estimate that one animal makes about 10,000 hoof changes per day outside of its kraal and water point, for a distance of 1.2-2.5 km walked (which is a conservative distance: most goats probably walk much farther). This would result in 36 million trampling actions per day by the total livestock population (Henschel et al., 2010). The trampling would be concentrated around the settlements. Moser-Norgaard et al. (2011) estimate that goats can walk up to 5 km and cattle up to 15 km from their home kraals. The same authors found that livestock has a negative influence on the regeneration of *F. Albida* and *A. Erioloba* due to juvenile plants being eaten and trampled. This could result in fewer trees reaching maturity,

which would mean not only reduced fodder for livestock, but also a possible increase in dust emission. In addition, Dausab et al. (1994) refer to a clearly visible browse line in areas with large numbers of livestock present on the Kuiseb River. This could further reduce roughness density within a height of 1.5 m from the surface.

Donkeys could also play a role in enhancing the dust emissions in the vicinity of the river. The donkeys spend the day on the gravel plains and cause disruption to the stone pavement, thereby making more fines available for entrainment (Figure 121).

Figure 121 Donkeys on the gravel plain disrupting the gravel overlay.

5.3.2 Water diversion and abstraction

Within the Namib Desert the abstraction of groundwater from the aquifers for towns and mining has resulted in a drop of the groundwater level. A further drop in the groundwater level would affect the vegetation that relies on the groundwater as its primary source of water, such as *F. Albida* and *A. Erioloba* (Schachtchneider et al., 2010). This could potentially enhance dust emission along the river.

In addition, the anchoring vegetation on the nebkha dunes in the delta is also dependent on groundwater. Extensive water abstraction could potentially affect the ability of the vegetation on these dunes to use this source of water, if the groundwater level were to drop significantly. This would result in the destabilisation of these dunes and therefore in the availability of large quantities of fine material for deflation. This has been the case in the Mojave Desert in California, where groundwater pumping caused the death of vegetation, the destabilisation of

the nebkha dunes along the Mojave River and the subsequent release of large quantities of sediment (Laity, 2008).

Furthermore, the establishment of large quantities of dams within the upper catchment will have an influence on the flow of water reaching the middle and lower sections of the river. The Friedenhau Dam constructed in 1972 is the largest dam on the river. According to Ito (2005), the number of farm dams has increased from 152 in 1972 to 362 in 1997. Reduced flow will result in a reduction of groundwater recharge in the aquifers of the lower Kuiseb. A reduction in flow could, however, result in reduced dust activity by decreasing the supply of sediments from the upper Kuiseb. The groundwater (both playa and sabkha source) and active alluvium from the river are all connected and the relationship between groundwater flow and dust emission could prove to be more significant than it at first appears.

The survey done by Theron et al. (1985) was done in 1978 and again in 1981 (Table 11). The river experienced no flooding from 1977 to 1983 and the difference in the vegetation is mainly attributed to the lack of river flow. Periods of drought compounded by water diversion and abstraction will have an influence on the surface roughness and consequently on the dust activity of the area.

Table 11 The average density (individuals per ha) of vegetation in different height classes.

Height class	Upper Riverine Woodland		Middle Riverine Woodland		Lower Riverine Woodland	
	1978	1981	1978	1981	1978	1981
5 m	91	41	16	8	1	2
4-5 m	119	53	101	25	82	19
3 m	71	200	194	169	221	174
2 m	22	37	51	33	16	45
1 m	26	18	50	10	23	10
0,5 m	91	15	55	12	12	10
TOTAL	420	364	467	257	355	260

5.3.3 Mining

Mining is a major activity in the area and is set to increase in the future. Large parts of the area are covered by exploration licences, many of which fall within protected areas (Figure 122). In addition to the open pit mines like Rössing Uranium and Langer Heinrich, there is also the possibility of surficial uranium mining in the area. The surficial deposits are generally situated in a layer between 5 and 30 m from the surface and consist predominantly of lower grade ore

(Simonsen et al., 1984). The large area of exploration scrapes in the vicinity of Hosabes springs (Figure 123) is made up of deposits of surficial uranium. This form of mining will result in much larger areas of surface disturbance than traditional open pit mining, potentially increasing the dust emission from these areas.

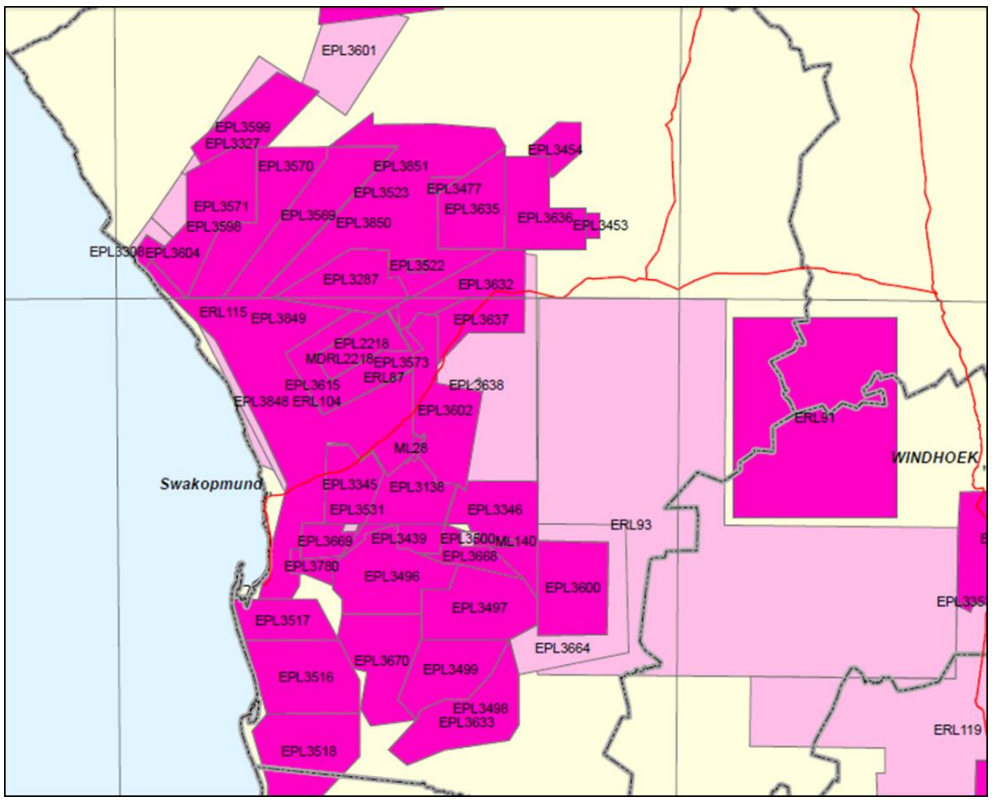

Figure 122 Exploration licences for nuclear fuels within the Erongo region for 2007.

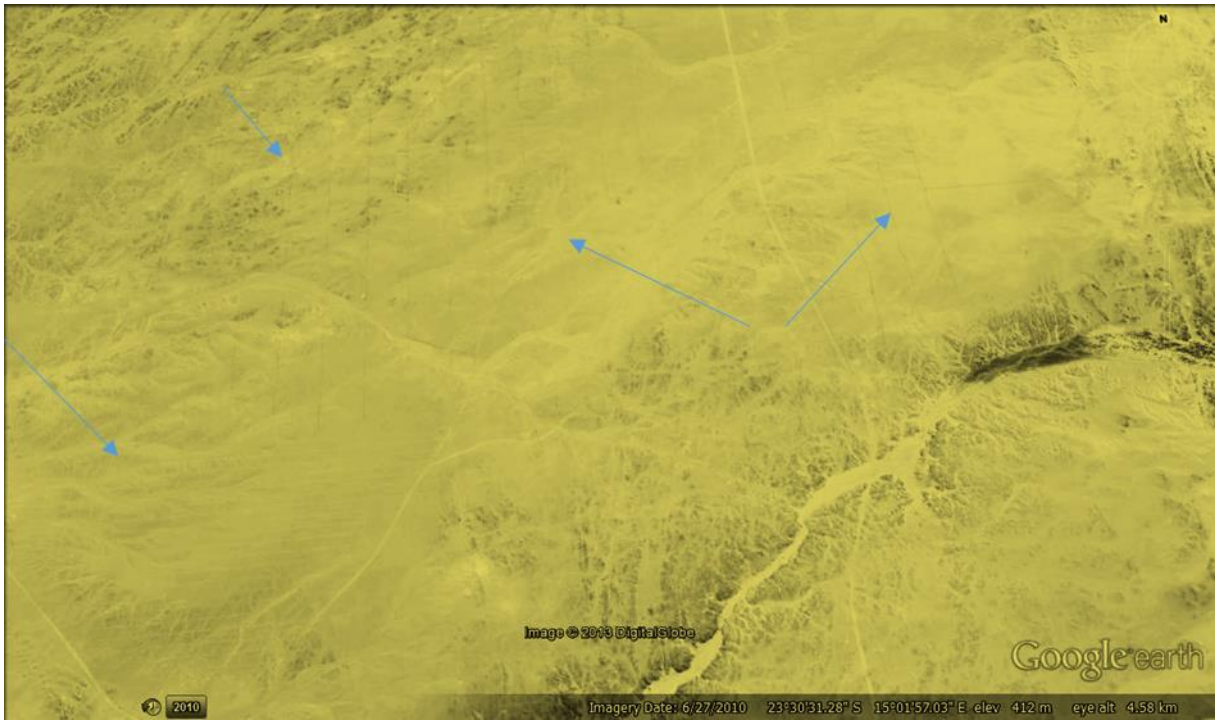

Figure 123 Exploration scrapes near Hosabes spring. The exploration scrapes are also marked in Figure 120. Colour altered to show scrapes. Blue arrows indicate large areas of scrapes.

5.3.4 Off-road vehicles

Lastly, the proliferation of roads to access the infrastructure within the area, as well as off-road vehicle activity, has also caused severe disturbance to the landscape. Heinze (2009) lists leisure activities, such as sand-boarding and fishing; tourism activities, including quad biking and 4×4 routes; mining and exploration; and movie production as some of the sources of off-road vehicle activities. Looking at the area with Google Earth, there appears to be little control over off-road vehicle activity and the establishment of vehicle tracks (Figure 124). Disturbance due to off-road vehicles is not a recent phenomenon. Eckardt et al. (1997) noted the widespread disruption to the stone pavement as a result of off-road vehicles that took place around the former South African Rooikop Airbase (now Walvis Bay Airport). Recent activity around the airport seems to be associated with quarrying and airport expansion, rather than off-road vehicle tracks (Figure 125). Disturbance to the surface of the gravel plain stone pavement disrupts the gravel overlay, degrades the drainage channel crusts and could enhance dust activity.

Figure 124 Tracks on the gravel plain causing disturbance of the stone pavement.

Figure 125 Quarrying operations just north of the Walvis Bay Airport.

The widespread disturbance that is evident on the gravel plain will increase the dust activity from this geomorphological unit. It would seem as if the dust activity from the gravel plain has increased for the period from 2009 to 2013, compared to the period from 2005-2008. Whether this is the case, and whether this is due to anthropogenic alteration of the surfaces, would need to be investigated further.

5.4 Discussion conclusion

The source areas can be reclassified as follows, based on the evaluation above:

Primary source areas	Secondary source areas	Non-dust producing areas
Delta (DCC and DFP)	Middle river (RM)	Interdune areas (ID)
Lower river (RL)	Upper river (RU)	Sand Sea (SS)
Gravel plain drainage channels (GPC)	Gravel plain stone pavement (GPS)	Active channels (RAC and DAC)

The gravel plain stone pavement (**GPS**) will remain a secondary source until its potential as a significant source observed in other parts of the world can be confirmed, especially given the evidence of widespread anthropogenic modification.

The interdune areas (**ID**) will not be regarded as potential source areas.

6 Conclusion

Particle size distributions of the 153 surface samples analysed with laser diffraction suggest that appropriately sized fines for dust deflation are present within the entire length of the Lower Kuiseb River, between Natab and the coast. Due to a number of factors, most likely vegetation cover and topography, not all the fines are equally available for dust deflation. The relatively open and vegetation free flood plains in the downstream section (RL: lower river) from Swartbank to Rooibank and delta (DFP and DCC) host the finest (Type 1) and most available material for entrainment. The intermittent river floods, supply the majority of fine silty sediment that is available for deflation. These are temporarily stored in depositional crusts, formed shortly after the floods and are probably not very resistant to wind erosion, due to the ratio of sand, silt and clay of the sediments making up the crusts.

The supply of fine material to the lower river and delta is dependent on the reach of the floods and periods of little flow could potentially see reduced dust activity from these segments. However, longer periods during which floods are absent, could result in the desiccation and subsequent reduction of vegetation, increasing the availability of sediment for deflation. This will be the case particularly for a reduction in vegetation and resultant destabilisation of the nebkhas, which would make large quantities of sediment available for deflation. The influence of surface roughness on the dust activity of the area would need further investigation to be conclusive.

The gravel plain is a more significant source of dust than previously considered, based on the presence of clay- and silt-sized sediment and the number of plumes detected with MODIS imagery. The playas appear to play an important role in the dust emission from this unit. However, the MODIS images show gravel plain emitting dust beyond the playa margin and could also include the gravel plain drainage network which along with the playas is also a store for fines. Dust sources from the gravel plain could either be saline dust from salt crusts and/or silt and clay deposits from the playa drainage network. Silt and clay deposits are potentially produced as a result of aggressive weathering within the saline environment of the playas. The depositional crusts from the playas have a higher clay content than the crusts formed within the river, but are in most instances not likely to be high enough to prevent deflation.

Sediment reworking from different geomorphological units within the basin could potentially play an important role in making sediment available for deflation. For example, high frequency,

low magnitude winds in summer could displace sediment from river and playas onto the gravel plain stone pavement where this could also become a source area. Dust input is an important component of stone pavements according to the Accretionary Inflationary Profile (AIP) model of soil development proposed by McFadden (2013). Similar stone pavements in China and Mongolia have been shown to be significant sources of dust. The ability of the Kuiseb stone pavement to act as a source of dust still has to be confirmed.

Small-scale sediment characteristics, such as clay content, organic matter and mineralogy, could play a role in the switching on and off of a dust source. The composition and distribution of these characteristics vary and could be an important control on the erodibility of the crusts. Crust fatigue brought about by bombardment of the surface with successive storms and proximity to a sand supply, could result in the switching on of a potential source areas. Bombardment of the crusts by saltating grains is an important additional process within the system and sand sized particles that fulfil this role are in ample supply in and around the Lower Kuiseb catchment. The ultimate and precise mechanisms and conditions for dust emission, such as the role of saltation, moisture and crust strength still have to be examined.

The SEM analysis revealed that the morphology and mineralogy of the sediment from the river and playas seem to be substantially different. The fines located in the river consist predominantly of mica, whereas the playa drainage network crusts are mainly made up of aggregates of different minerals. The finest material were found within the gravel plain drainage network. Dust activity from each of these geomorphological units will have different impacts. For example, dust from the silt-clay deposits within the playas are rich in calcite in certain areas of the basin which could be significant cloud condensation nuclei. Dust activity from the river on the other hand could potentially have a greater impact on solar radiation, due to the light scattering ability of the mica. Dust from the salt crusts and sabkhas are most likely predominantly saline and have different characteristics and impacts than conventional or clastic dust storms.

MODIS imagery successfully identifies the dust plumes created with the north-east wind during winter, but there may also be dust activity not associated with the north-east wind within the basin which is not picked up by satellite imagery due to various factors, such as cloud cover. The winter dust activity appears to be mostly from stationary dust storms and the summer plumes appear to be mobile in nature. It was found that the origin points of the stationary dust plumes are difficult to pinpoint with an accuracy of a few kilometres with MODIS true colour

images which rely on the light colour of the dust over the dark blue ocean for identification. Distinguishing the origin points accurately over land is therefore problematic. For some of the plumes it is difficult to identify whether the origin is from the gravel plain or whether it originates from the river and delta.

Finally, the influence that people have on the dust activity of the area still needs to be determined and quantified. Livestock were found to be present in most of the areas sampled and the effects of trampling of crusts were clearly evident. This could potentially have a significant impact on dust deflation from the river – both in the lower and middle river segments. Livestock increase the erodibility of the fine material by creating large areas of unconsolidated material due to the trampling of the depositional crusts. In addition, the livestock could have the ability to change the surface roughness along the river as they affect the vegetation. The precise role of aquifer pumping on dust production also requires further examination.

According to recent MODIS imagery we seem to have seen a potential increase in dust plumes originating from the gravel plain, when compared to the period from 2005 to 2008 (Vickery, 2010). These more recent plumes appear to originate from much larger areas, both from within and outside the playa and drainage margins. This may correspond to a period of increased rainfall and flooding as well as a notable increase in human activities, which are now widespread and extend well beyond the Walvis Bay, Rooibank and Rooikop areas into the park itself. A preliminary evaluation, using Google Earth, shows a distinct and relatively recent human footprint caused by exploration, mining and quarrying, as well as other surface activities such as off-road driving. All of these activities are leaving their mark on the ancient surfaces of the gravel plain which expose additional fines for deflation.

It is clear that sediment size is not the only control in making the Lower Kuiseb one of the dustiest areas in Namibia. Stores of fines are clearly widespread and, in light of recent trends such as frequent flooding and disturbance, prone to increased availability. The varied nature of source points, require multiple modes for supply and entrainment and are likely to have varied impacts in the downwind environment including the river valley itself, Walvis Bay, the lagoons and the ocean.

7 References

Abuduwaili, J., Liu, D. and Wu, G., 2010. Saline dust storms and their ecological impacts in arid regions. *Journal of Arid Land*, 2(2), pp. 144–150. Available at: http://pub.chinasciencejournal.com/article/getArticleRedirect.action?doiCode=10.3724/SP.J.1227.2010.00144

Alfaro, S.C., 2008. Influence of soil texture on the binding energies of fine mineral dust particles potentially released by wind erosion. *Geomorphology*, 93(3-4), pp.157–167. Available at: http://linkinghub.elsevier.com/retrieve/pii/S0169555X07000748

Amonette, J., 2002. Methods for Determination of Mineralogy and Environmental Availability. (In Dixon J.B. and Schulze, D.G. (eds), Soil Mineralogy with Environmental Applications, Soil Science Society of America Book Series No. 7), pp.153-197.

Baddock, M.C., Zobeck, T. M., Van Pelt, R.S. and Fredrickson, E.L., 2011. Dust emissions from undisturbed and disturbed, crusted playa surfaces: Cattle trampling effects. *Aeolian Research*, 3(1), pp. 31–41. Available at: http://linkinghub.elsevier.com/retrieve/pii/S1875963711000267

Bagnold, R.A., 1941. The Physics of blown sand and desert dunes. Chapman and Hall, London, 265pp.

Belnap, J. and Gillette, D.A., 1997. Disturbance of biological soil crusts: impacts on potential wind erodibility of sandy desert soils in southeastern Utah. *Land Degradation & Development*, 8(4), pp 355–362. Available at: http://doi.wiley.com/10.1002/%28SICI%291099-145X%28199712%298%3A4%3C355%3A%3AAID-LDR266%3E3.0.CO%3B2-H.

Beuselinck, L. Govers, G., Poesen, J., Degraer, G. and Froyen, L., 1998. Grain-size analysis by laser diffractometry: comparison with the sieve-pipette method. *Catena*, 32(3-4), pp.193–208. Available at: http://linkinghub.elsevier.com/retrieve/pii/S0341816298000514.

Bisutti, I., Hilke, I., Schumacher, J. and Raessler, M., 2007. A novel single-run dual temperature combustion (SRDTC) method for the determination of organic, in-organic and total carbon in soil samples. *Talanta*, 71(2), pp.521–8. Available at: http://www.ncbi.nlm.nih.gov/pubmed/19071336

Botelle, A. and Kowalski, K., 1995. Changing resource use in Namibia's lower Kuiseb valley: Preceptions from the Topnaar community. *Institute of South African Studies at the University of Lesotho and the Social Sciences Division at the University of Namibia, Windhoek*, p.145.

Bristow, C.S., Drake, N. and Armitage, S., 2009. Deflation in the dustiest place on Earth: The Bodélé Depression, Chad. *Geomorphology*, 105(1-2), pp. 50–58. Available at: http://linkinghub.elsevier.com/retrieve/pii/S0169555X08002742

Bryant, R.G., 2003. Monitoring hydrological controls on dust emissions: preliminary observations from Etosha Pan, Namibia. *The Geographical Journal*, 169(2), pp.131–141.

Bullard, J.E. and McTainsh, G.H., 2003. Aeolian–fluvial interactions in dryland environments: examples, concepts and Australia case study. *Progress in Physical Geography*, 27(4), pp.471–501. Available at: http://ppg.sagepub.com/cgi/doi/10.1191/0309133303pp386ra

Bullard, J.E., Mctainsh, G.H. and Pudmenzky, C., 2007. Factors affecting the nature and rate of dust production from natural dune sands. *Sedimentology*, 54(1), pp.169–182. Available at: http://doi.wiley.com/10.1111/j.1365-3091.2006.00827.x

Bullard, J., Baddock, M., McTainsh, G. and Leys, J., 2008. Sub-basin scale dust source geomorphology detected using MODIS. *Geophysical Research Letters*, 35(15): L15404. Available at: http://doi.wiley.com/10.1029/2008GL033928

Bullard, J.E., Harrison, S.P., Baddock, M.C., Drake, N., Gill, T.E., McTainsh, G. and Sun, Y., 2011. Preferential dust sources: A geomorphological classification designed for use in global dust-cycle models. *Journal of Geophysical Research*, 116(F4): F04034. Available at: http://doi.wiley.com/10.1029/2011JF002061

Cahill, T.A., Gearhart, E.A. and Gillette, D.A., 1996. Saltating particles, playa crusts and dust aerosols at Owens (Dry) Lake, California. *Earth Surface Processes and Landforms*, 21, pp. 621–639.

Campbell, J.R., 2003. *Advances in Regolith (In* I.C. Roach (ed) *LIMITATIONS IN THE LASER PARTICLE SIZING OF SOILS)*, CRC LEME.

Chappell, A., 1998. Dispersing sandy soil for the measurement of particle size distributions using optical laser diffraction. *Catena*, 31(4), pp.271–281. Available at: http://linkinghub.elsevier.com/retrieve/pii/S0341816297000490.

Chen, P.-S. Tsai, F.T., Lin, C.K., Yang, C., Chan, C., Young, C. and Lee, C., 2010. Ambient influenza and avian influenza virus during dust storm days and background days. *Environmental health perspectives*, 118(9), pp. 1211–6. Available at: http://www.pubmedcentral.nih.gov/articlerender.fcgi?artid=2944079&tool=pmcentrez&rendertype=abstract

Dausab, F., Francis, G., Johr, J.R., Kambatuku, M., Molapo, S.E., Shanyengana, S E. and Swartz, S., 1994. *Water usage patterns in the Kuiseb Catchment Area (with emphasis on sustainable use)*, DRFN Occasional paper no.1, Windhoek.

Di Stefano, C., Ferro, V. and Mirabile, S., 2010. Comparison between grain-size analyses using laser diffraction and sedimentation methods. *Biosystems Engineering*, 106(2), pp.205–215. Available at: http://linkinghub.elsevier.com/retrieve/pii/S1537511010000656

Eckardt, F. and White, K., 1997. Human induced disruption of stone pavement surfaces in the Central Namib Desert , Namibia : Observations from Landsat Thematic Mapper. *International Journal of Remote Sensing*, 18(16), pp.3305–3310.

Eckardt, F.D. and Spiro, B., 1999. The origin of sulphur in gypsum and dissolved sulphate in the Central Namib Desert, Namibia. *Sedimentary Geology*, 123(3-4), pp. 255–273. Available at: http://linkinghub.elsevier.com/retrieve/pii/S0037073898001377.

Eckardt, F.D., Drake, N., Goudie, A.S., White, K. and Viles, H., 2001. The role of playas in pedogenic gypsum crust formation in the Central Namib Desert: a theoretical model. *Earth Surface Processes and Landforms*, 26(11), pp. 1177–1193. Available at: http://doi.wiley.com/10.1002/esp.264

Eckardt, F.D. and Kuring, N., 2005. SeaWiFS identifies dust sources in the Namib Desert. *International Journal of Remote Sensing*, 26(19), pp. 4159–4167. Available at: http://www.tandfonline.com/doi/abs/10.1080/01431160500113112

Eckardt, F.D., Soderberg, K., Coop, L.J., Muller, A.A., Vickery, K.J., Grandin, R.D., Jack, C., Kapalanga, T.S. and Henschel, J., 2012. The nature of moisture at Gobabeb, in the central Namib Desert. *Journal of Arid Environments*, 93, pp. 7–19. Available at: http://linkinghub.elsevier.com/retrieve/pii/S0140196312000432

Eckardt, F. D., Livingstone, I., Seely, M. and Von Holdt, J. (2013), The Surface Geology and Geomorphology Around Gobabeb, Namib Desert, Namibia. Geografiska Annaler: Series A, Physical Geography, 95, pp. 271–284. doi: 10.1111/geoa.12028

ERM, 2011, Etango Project Environmental and Social Impact Assessment, Bannerman Mining Resources, Namibia. Available at www.erm.com.

Formenti, P., Schütz, L., Balkanski, Y., Desboeufs, K., Ebert, M., Kandler, K., Petzold, A., Scheuvens, D., Weinbruch, S. and Zhang, D., 2011. Recent progress in understanding physical and chemical properties of African and Asian mineral dust. *Atmospheric Chemistry and Physics*, 11(16), pp. 8231–8256. Available at: http://www.atmos-chem-phys.net/11/8231/2011/

GCS, 2011. Nampower coal-fired power station baseline report. Hydrogeological, geotechnical, soils and water supply. Namibian Power Corporation (Pty) Ltd, Windhoek, Namibia. Available on: www.gcs-sa.biz.

Gillette, D.A., 1979: Environmental factors affecting dust emission by wind erosion. (In Morales, C (ed) Saharan Dust, SCOPE 14, John Wiley and Sons, 71–91)

Gillette, D.A. Adams, J., Muhs, D. and Kihl, R., 1982. Threshold friction velocities and rupture moduli for crusted desert soils for the input of soil particles into the air. *Journal of Geophysical Research*, 87(C11), p 9003. Available at: http://doi.wiley.com/10.1029/JC087iC11p09003.

Gillette, D.A., 1999. A Quantitative Geophysical Explanation for "Hot Spot" Dust Emitting Source Regions. *Contr. Atmos. Phys.*, 72(1), pp. 67–77.

Gillette, D.A., Herrick, J.E. and Herbert, G.A., 2006. Wind Characteristics of Mesquite Streets in the Northern Chihuahuan Desert, New Mexico, USA. *Environmental Fluid Mechanics*, 6(3), pp. 241–275. Available at: http://link.springer.com/10.1007/s10652-005-6022-7

Gillies, J.A., 2013. 11.4. Fundamentals of Aeolian Sediment Transport : Dust Emissions and Transport – Near Surface in *Treatise on Geomorphology* J. F. Shroder, ed., San Diego: Academic Press. Available at: http://dx.doi.org/10.1016/B978-0-12-374739-6.00297-9.

Goossens, D. and Gross, J., 2002. Similarities and dissimilarities between the dynamics of sand and dust during wind erosion of loamy sandy soil. *Catena*, 47(4), pp. 269–289. Available at: http://linkinghub.elsevier.com/retrieve/pii/S0341816201001886.

Goossens, D., 2004. Effect of soil crusting on the emission and transport of wind-eroded sediment: field measurements on loamy sandy soil. *Geomorphology*, 58(1-4), pp. 145–160. Available at: http://linkinghub.elsevier.com/retrieve/pii/S0169555X03002290

Goossens, D., 2008. Techniques to measure grain-size distributions of loamy sediments: a comparative study of ten instruments for wet analysis. *Sedimentology*, 25, pp.65–96. Available at: http://doi.wiley.com/10.1111/j.1365-3091.2007.00893.x

Griffin, D. and Kellogg, C., 2004. Dust Storms and Their Impact on Ocean and Human Health: Dust in Earth?s Atmosphere. *EcoHealth*, 1(3), pp. 284–295. Available at: http://www.springerlink.com/index/10.1007/s10393-004-0120-8

Hayton, S., Nelson, C., Ricketts, B., Cooke, S., Wedd, M., 2001. Effect of mica on particle size analysis using laser diffraction technique. *Journal of Sedimentary Research*, 71(3), pp.507–509.

Heidbuechel, I. 2007. Recharge Processes in Ephemeral Streams Derived from a Coupled Stream Flow Routing / Groundwater Model - Application to the Lower Kuiseb (Namibia). Freiburg: University of Freiburg (Diplomarbeit Thesis)

Heinze, C., 2009. Spatial planning for off-road driving areas – Pros and cons of environmental regulations A case study in a semi-arid environment, Namibia, Enschede, The Netherlands: International Institute for Geo-Information Science and Earth Observation (MSC Thesis)

Henschel, J.R., 2006. Sustaining life and livelihood along an Ephemeral River. *Geographische Rundshau International Edition*, 2(3), pp.28–33.

Henschel, J.R. and Parr, T., 2010. Population changes of alien invasive plants in the Lower Kuiseb River. *Dinteria*, 31, pp.5–17

Houser, C. A., and Nickling, W.G., 2001. The factors influencing the abrasion efficiency of saltating grains on a clay-crusted playa. *Earth Surface Processes and Landforms*, 26(5), pp. 491–505. Available at: http://doi.wiley.com/10.1002/esp.193.

Hugget, R.J., 2007. Fundamentals of Geomorphology, 2nd Edition. London: Routledge, 458p.

Huntley, B. J., 1985, The Kuiseb Environment. (*In* Huntley, B.J. (ed), *The Kuiseb Environment: the development of a monitoring baseline*. SA National Science Programme Report #106, CSIR, p7-20)

Ito, M. 2005. Changes in the distribution of the !Nara plant that affect the life of the Topnaar people in the Lower Kuiseb River, Namib Desert. *African Study Monographs*, *30*(March), pp. 65-75.

Jacobsen, P.J., Jacobsen, K.M. and M.K. Seely, (1995) Ephemeral Rivers and their Catchment, Windhoek, Namibia: Desert Research Foundation of Nambia

Jacobson, P.J., Jacobson, K.M., Angermeier, P.L. and Cherry, D.S., 1999. River Transport, retention , and ecological significance of woody debris within a large ephemeral river. *Journal of the North American Benthological Society*, 18(4), pp.429–444.

Jacobson, P.J., Jacobson, K.M., Angermeier, P.L. and Cherry, D.S., 2000. Variation in material transport and water chemistry along a large ephemeral river in the Namib Desert. *Freshwater Biology*, 44(3), pp. 481–491. Available at: http://doi.wiley.com/10.1046/j.1365-2427.2000.00604.x

Jacobson, P.J. and Jacobson, K.M., 2012. Hydrologic controls of physical and ecological processes in Namib Desert ephemeral rivers: Implications for conservation and management. *Journal of Arid Environments*, 93, pp.1–14. Available at: http://linkinghub.elsevier.com/retrieve/pii/S0140196312000420

Jenkins, T. and Brain, C.K., 1967. THE PEOPLES OF THE LOWER KUISEB VALLEY. *Scientific Papers of the Namib Desert Research Station*, 35, 24p.

Kanatani, K.T., Ito, I., Al-Delaimy, W.K., Adachi, Y., Mathews, W.C. and Ramsdell, J.W., 2010. Desert dust exposure is associated with increased risk of asthma hospitalization in children. *American journal of respiratory and critical care medicine*, 182(12), pp. 1475–81. Available at: http://www.pubmedcentral.nih.gov/articlerender.fcgi?artid=3159090&tool=pmcentrez&rendertype=abstract

Keck, C.M. and Müller, R.H., 2008. Size analysis of submicron particles by laser diffractometry--90% of the published measurements are false. *International journal of pharmaceutics*, 355(1-2), pp.150–63. Available at: http://www.ncbi.nlm.nih.gov/pubmed/18201848

Kjelgaard, J.F., Chandler, D.G. and Saxton, K.E., 2004. Evidence for direct suspension of loessial soils on the Columbia Plateau. *Earth Surface Processes and Landforms*, 29(2), pp. 221–236. Available at: http://doi.wiley.com/10.1002/esp.1028

Klaus, J., Külls, C. and Dahan, O., 2008. Evaluating the recharge mechanism of the Lower Kuiseb Dune area using mixing cell modeling and residence time data. *Journal of Hydrology*, 358(3-4), pp. 304–316. Available at: http://linkinghub.elsevier.com/retrieve/pii/S002216940800293X

Koven, C.D. and Fung, I., 2008. Identifying global dust source areas using high-resolution land surface form. *Journal of Geophysical Research*, 113(D22), p.D22204. Available at: http://doi.wiley.com/10.1029/2008JD010195 [Accessed September 16, 2013].

Laity, J. E**.,** 2008**.** *Deserts and Desert Environments*, Wiley-Blackwell, Chichester**,** 342 p

Langston, G. and McKenna Neuman, C., 2005. An experimental study on the susceptibility of crusted surfaces to wind erosion: A comparison of the strength properties of biotic and salt crusts. *Geomorphology*, 72(1-4), pp.40–53. Available at: http://linkinghub.elsevier.com/retrieve/pii/S0169555X05001613

Lawrence, C.R. and Neff, J.C., 2009. The contemporary physical and chemical flux of aeolian dust: A synthesis of direct measurements of dust deposition. *Chemical Geology*, 267(1-2), pp. 46–63. Available at: http://linkinghub.elsevier.com/retrieve/pii/S0009254109000655

Livingstone, I. and Warren, A. (1996) *Aeolian Geomorphology: an Introduction.* Harlow: Longman. 058208704X

López, M.V., de Dios Herrero, J.M., Hevia, G.G., Gracia, R. and Buschiazzo, D.E., 2007. Determination of the wind-erodible fraction of soils using different methodologies. Geoderma, 139(3-4), pp.407–411. Available at: http://linkinghub.elsevier.com/retrieve/pii/S0016706107000717

Malvern, 2012a. Optical property selection made easy, Malvern Instruments.

Malvern, 2012b. Sample dispersion and Refractive index guide, Malvern Instruments.

Malvern, 2012c. Demystifying laser diffraction, Malvern Instruments.

Malvern, 2013. Mastersizer 2000 product overview. Available at URL: (http://www.malvern.com/labeng/products/mastersizer/ms2000/mastersizer2000.htm?specification

McCave, I.N., Bryant, Robert.G., Cook, H.F., Coughanowr, C.A., 1986. Evaluation of a laser-diffraction-size Analyzer for use with Natural Sediments. *Research Method Papers*, (November 1985), pp.561–564.

McFadden, L.D., 2013. Strongly dust-influenced soils and what they tell us about landscape dynamics in vegetated aridlands of the southwestern United States. *Geological Society of America Special Papers*, 500, pp. 501–532, doi:10.1130/2013.2500(15)

McTainsh, G.H., Nickling, W.G. and Lynch, A.W., 1997. Dust deposition and particle size in Mali, West Africa. *Catena*, 29(3-4), pp.307–322. Available at: http://linkinghub.elsevier.com/retrieve/pii/S0341816296000756.

McTainsh, G. and Strong, C., 2007. The role of aeolian dust in ecosystems. *Geomorphology*, 89(1-2), pp. 39–54. Available at: http://linkinghub.elsevier.com/retrieve/pii/S0169555X06003564

McTainsh, G., Livingstone, I. and Strong, C., 2013. 11.3 Fundamentals of Aeolian Sediment Transport : Aeolian Sediments in *Treatise on Geomorphology* J. F. Shroder, ed., San Diego: Academic Press. Available at: http://dx.doi.org/10.1016/B978-0-12-374739-6.00296-7.

Miller, B.A. and Schaetzl, R.J., 2011. Precision of Soil Particle Size Analysis using laser Diffractometry. *Soil Science Society of America Journal*, 76, pp.1719–1727.

MME (2010). Strategic Environmental Assessment for the central Namib Uranium Rush. Ministry of Mines and Energy, Windhoek, Republic of Namibia.

Morin, E. Grodek, T., Dahan, O., Benito, G., Kulls, C., Jacoby, Y., Langenhove, G.V., Seely, M. and Enzel, Y., 2009. Flood routing and alluvial aquifer recharge along the

ephemeral arid Kuiseb River, Namibia. *Journal of Hydrology*, 368(1-4), pp. 262–275. Available at: http://linkinghub.elsevier.com/retrieve/pii/S0022169409000882

Moser-Nørgaard, P.M. and Denich, M., 2011. Influence of livestock on the regeneration of fodder trees along ephemeral rivers of Namibia. *Journal of Arid Environments*, 75(4), pp.371–376. Available at: http://linkinghub.elsevier.com/retrieve/pii/S0140196310003186

Namibia, 2007. Ministry of Mines and Energy. Exploration for nuclear fuel licence map. Windhoek, Namibia. Available at URL: http://www.mme.gov.na/pdf/licences-nuclear-fuel-1207.pdf

Namibia, 2011. Namibia Tourism Board: Statistical Report 2011. Ministry of Environment and Tourism, Windhoek, Namibia. Available on URL: http://www.namibiatourism.com.na/uploadedFiles/NamibiaTourism/Global/Downloads_Modules/Research_Center/MET-%202011%20Tourist%20Arrival%20Statistics%20Report.pdf

Ndour, M., D'Anna, B., George, C., Ka, O., Balkanski, Y., Kleffmann, J., Stemmler, K. and Ammann, M., 2008. Photoenhanced uptake of NO 2 on mineral dust: Laboratory experiments and model simulations. *Geophysical Research Letters*, 35(5), p.L05812. Available at: http://doi.wiley.com/10.1029/2007GL032006

Okin, G.S., Gillette, D.A. and Herrick, J.E., 2006. Multi-scale controls on and consequences of aeolian processes in landscape change in arid and semi-arid environments. *Journal of Arid Environments*, 65(2), pp. 253–275. Available at: http://linkinghub.elsevier.com/retrieve/pii/S014019630500162X

Okin, G.S., 2008. A new model of wind erosion in the presence of vegetation. *Journal of Geophysical Research*, 113(F2): F02S10. Available at: http://doi.wiley.com/10.1029/2007JF000758

Practical Aspects of Mineral Barometry. Micas: biotite and muscovite. 2004. Available at: http://www.earth.ox.ac.uk/research/groups/metamorphic_petrology/thermobarometry/chemical_mineralogy_of_common_mineral_groups/mica [10 September 2013]

Prospero, J.M., Ginoux, P., Torres, O., Nicholson, S.E. and Gill, T.E., 2002. Environmental characterization of global sources of atmospheric soil dust identified with the NIMBUS 7 Total Ozone Mapping Spectrometer (TOMS) absorbing aerosol product. *Reviews of Geophysics*, 40(1), pp. 1-31. Available at: http://doi.wiley.com/10.1029/2000RG000095

Pye, K. 1987. Aeolian Dust and Dust Deposits. Academic Press, London. 334pp.

Pye, K. and Tsoar, H., 1990. Aeolian Sand and Sand Dunes. Unwin Hyman, London. 396p.

Reynolds, R.L., Yount, J.C., Reheis, M., Goldstein, H., Chavez, P., Fulton, R., Whitney, J., Fuller, C. and Forester, R.M., 2007. Dust Emission from Wet and Dry Playas in the Mojave Desert, USA †. *Earth Surface Processes and Landforms*, 32, pp.1811–1827.

Reynolds, R.L., Bogle, R., Vogel, J., Goldstein, H., and Yount, J., 2009, Dust emission at Franklin Lake Playa, Mojave Desert (USA): Response to meteorological and hydrologic changes 2005-2008, *Natural Resources and Environmental Issues*: Vol. 15, Article 18. Available at: http://digitalcommons.usu.edu/nrei/vol15/iss1/18

Ross, E.S., 1971. Tbe Kuiseb's Topnaar Hottentots. *S.W.A. Annual*, pp.170–175.

Ryżak, M., Bieganowski, A. and Walczak, R.T., 2007. Application of laser diffraction method for determination of particle size distribution of grey-brown podzolic soil. *Research in Agricultural Engineering*, 53(1), pp.34–38.

Ryżak, M. and Bieganowski, A., 2011. Methodological aspects of determining soil particle-size distribution using the laser diffraction method. *Journal of Plant Nutrition and Soil Science*, 174(4), pp.624–633. Available at: http://doi.wiley.com/10.1002/jpln.201000255

Sankey, J.B. Glenn, N.F., Germino, M.J., Gironella, A.N. and Thackray, G.D., 2010. Relationships of aeolian erosion and deposition with LiDAR-derived landscape surface roughness following wildfire. *Geomorphology*, 119(1-2), pp. 135–145. Available at: http://linkinghub.elsevier.com/retrieve/pii/S0169555X10001194

Sankey, J.B., Eitel, J.U.H., Glenn, N.F., Germino, M.J. and Vierling, L.A., 2011. Quantifying relationships of burning, roughness, and potential dust emission with laser altimetry of soil surfaces at submeter scales. *Geomorphology*, 135(1-2), pp 181–190. Available at: http://linkinghub.elsevier.com/retrieve/pii/S0169555X11004144

Schachtschneider, K. & February, E.C., 2010. The relationship between fog, floods, groundwater and tree growth along the lower Kuiseb River in the hyperarid Namib. *Journal of Arid Environments*, 74(12), pp.1632–1637. Available at: http://linkinghub.elsevier.com/retrieve/pii/S0140196310001692

Schulze, D.G., 2002. An introduction to soil mineralogy. (In Dixon J.B. and Schulze, D.G. (eds), Soil Mineralogy with Environmental Applications, Soil Science Society of America Book Series No. 7), pp.1-35.

Scott-Jackson, J.E. and Walkington, H., 2005. Methodological issues raised by laser particle size analysis of deposits mapped as Clay-with-flints from the Palaeolithic site of Dickett's Field, Yarnhams Farm, Hampshire, UK. *Journal of Archaeological Science*, 32(7), pp.969–980. Available at: http://linkinghub.elsevier.com/retrieve/pii/S030544030500035X

Sengpiel, K.P., Maus, S., Röttger, B., 2000, Calculated configuration and relative magnetisation of the basement rocks in the Kuiseb Dunes helicopter survey area. Bundesanstalt fur Geowissenschaften und Rohstoffe (BGR), GNGEP Follow up report vol 3, Technical cooperation project number: 89.2034.0, Hannover.

Shao, Y., Raupach, M.R. and Findlater, P.A., 1993. Effect of Saltation Bombardment on the Entrainment of Dust by Wind. *Journal of Geophysical Research*, 98(D7), pp. 719–726.

Simonsen, H.A. and Floeter, W., 1984. Beneficiation of surficial uranium deposits. In Surficial uranium deposits, Report of the working group on uranium geology organised

by the IAEA. Vienna, Austria. Available on URL: http://www-pub.iaea.org/MTCD/publications/PDF/te_322_web.pdf.

Soderberg, K. and Compton, J.S., 2007. Dust as a Nutrient Source for Fynbos Ecosystems, South Africa. *Ecosystems*, 10(4), pp. 550–561. Available at: http://www.springerlink.com/index/10.1007/s10021-007-9032-0

Sperazza, M., Moore, J.N. and Hendrix, M.S., 2004. High-resolution particel size analysis of naturally occurring very fine-grained sediment through laser diffractometry. *Journal of Sedimentary Research*, 74(5), pp.736–743.

Strong, C., Leys, J.F. and McTainsh, G.H., 2004. Dust from crusts: who are the high achievers? Poster, International Soil Conservation Organisation (ISCO) Conference, Brisbane, Australia, July, 2004-08-25.

Sun, J., 2002. Provenance of loess material and formation of loess deposits on the Chinese Loess Plateau. *Earth and Planetary Science Letters*, 203, pp.845–859.

Sweeney, M.R., McDonald, E. V. and Etyemezian, V., 2011. Quantifying dust emissions from desert landforms, eastern Mojave Desert, USA. *Geomorphology*, 135(1-2), pp. 21–34. Available at: http://linkinghub.elsevier.com/retrieve/pii/S0169555X1100376X

Theron, G.K., van Rooyen, N., van Rooyen, M.W., Jankowitz, W.J., 1985, Vegetation structure and vitality in the lower Kuiseb. (*In* Huntley, B.J. (ed), *The Kuiseb Environment: the development of a monitoring baseline*. SA National Science Programme Report #106, CSIR, pp. 81-91)

Vdović, N., Obhođaš, J. and Pikelj, K., 2010. Revisiting the particle-size distribution of soils: comparison of different methods and sample pre-treatments. *European Journal of Soil Science*, 61(6), pp.854–864. Available at: http://doi.wiley.com/10.1111/j.1365-2389.2010.01298.x

Vickery, K. 2010. Southern African dust sources as identified by multiple space borne sensors. Cape Town: University of Cape Town (MSc Thesis)

Vickery, K.J. and Eckardt, F.D., 2013. Dust emission controls on the lower Kuiseb River valley, Central Namib. *Aeolian Research*, 10, pp. 125–133. Available at: http://linkinghub.elsevier.com/retrieve/pii/S1875963713000219

Viles, H. A. and Goudie, A. S., 2013. Weathering in the central Namib Desert, Namibia: Controls, processes and implications. *Journal of Arid Environments*, 93, pp. 20–29. Available at: http://linkinghub.elsevier.com/retrieve/pii/S0140196311002862

Wang, G., Wanquan, T. and Mingyuan, D., 2004. Flux and composition of wind-eroded dust from different landscapes of an arid inland river basin in north-western China. *Journal of Arid Environments*, 58(3), pp.373–385. Available at: http://linkinghub.elsevier.com/retrieve/pii/S0140196303001691

Wang, X. Dong, Z., Yan, P., Yang, Z. and Hu, Z., 2005. Surface sample collection and dust source analysis in northwestern China. *Catena*, 59(1), pp. 35–53. Available at: http://linkinghub.elsevier.com/retrieve/pii/S0341816204000773

Wang, X., Lang, L., Hua, T., Wang, H., Zhang, C .and Wang, Z., 2012. Characteristics of the Gobi desert and their significance for dust emissions in the Ala Shan Plateau (Central Asia): An experimental study. *Journal of Arid Environments*, 81, pp.35–46. Available at: http://linkinghub.elsevier.com/retrieve/pii/S0140196312000468.

Ward, J.D. 1987. The Cenozoic succession in the Kuiseb Valley, central Namib Desert. Geological Survey SWA/Namibia, Memoir, vol 9. Geological Survey, Windhoek, pp 1-124

Wassenaar, T.D., Henschel, J.R., Pfaffenthaler, M.M., Mutota, E.N., Seely, M.K. and Pallett, J., 2013, Ensuring the future of the Namib's biodiversity: Ecological restoration as a key management response to a mining boom. *Journal of Arid Environments*, 93, pp. 126–135. Available at: http://linkinghub.elsevier.com/retrieve/pii/S0140196312001681

Washington, R., Todd, M., Middleton, N.J. and Goudie, A.S., 2003. Dust-Storm Source Areas Determined by the Total Ozone Monitoring Spectrometer and Surface Observations. *Annals of the Association of American Geographers*, 93(2), pp. 297–313. Available at: http://www.tandfonline.com/doi/abs/10.1111/1467-8306.9302003.

Washington, R., Todd, M. C., Lizcano, G., Tegen, I., Flamant, C., Koren, I., Ginoux, P., Engelstaedter, S., Bristow, C. S., Zender, C. S., Goudie, A. S.,Warren, A. and Prospero, J. M., 2006. Links between topography, wind, deflation, lakes and dust: The case of the Bodélé Depression, Chad. *Geophysical Research Letters*, 33(9), pp. L09401. Available at: http://www.agu.org/pubs/crossref/2006/2006GL025827.shtml

Webb, N.P. and Strong, C.L., 2011. Soil erodibility dynamics and its representation for wind erosion and dust emission models. *Aeolian Research*, 3(2), pp. 165–179. Available at: http://linkinghub.elsevier.com/retrieve/pii/S1875963711000139

Wen, B., Aydin, A. and Duzgoren-aydin, N., 2013. A Comparative Study of Particle Size Analyses by Sieve-Hydrometer and Laser Diffraction Methods. *Geotechnical Testing Journal*, 25(4), pp.1–9.

Wiggs, G.F.S., Bullard, J.E., Garvey, B., Castro, I., 2002. Interactions between airflow and valley topography with implications for aeolian sediment transport. *Physical Geography*, 23(5), pp.366–380.

Xuan, J. and Sokolik, I.N., 2002. Characterization of sources and emission rates of mineral dust in Northern China. *Atmospheric Environment*, 36(31), pp. 4863–4876. Available at: http://linkinghub.elsevier.com/retrieve/pii/S135223100200585X.

Xuan, J., Sokolik, I.N., Hao, J., Guo, F., Mao, H. and Yang, G., 2004. Identification and characterization of sources of atmospheric mineral dust in East Asia. *Atmospheric Environment*, 38(36), pp.6239–6252. Available at: http://linkinghub.elsevier.com/retrieve/pii/S1352231004007150

Zhang, Y., 2005. The microstructure and for-mation of biological soil crusts in their early developmental stage. *Chinese Science Bulletin*, 50(2), pp. 117-121. Available at: http://219.238.6.200/article?code=982004-559&jccode=98

8 Appendix

8.1 Analysis of tap water

The analysis of the tap water used as dispersant in the particle size analysis reveal low concentrations of selected cations. It should therefore not have any significant effect on the results.

Table 12 Analysis of tap water used as dispersant in particle size analysis.

Sample ID	K (ppm)	Na (ppm)	Fe (ppm)	Mg (ppm)	Ca (ppm)
Distilled water	0,0	2,2	0,0	0,0	0,6
Tap water	0,0	8,7	0,0	0,8	11,9

Distilled water made in the laboratory included for comparison.

8.2 Effect of organic matter removal on particle size distribution

The removal of organic matter from selected samples does have an effect on the particle size distribution for all but one sample (Figure 126 and Figure 127). Sample RF8-5 maintains the same particle size distribution after removal of organic matter. This could be due to the fact that this is a coarser sample (Type 4), with fewer aggregate minerals present compared to the other samples (See comparison of SEM between Type 4 and Type 1 samples, Figure 128). The rest of the samples obtain a slightly coarser distribution after removal of the organic matter. Sample GPC47 appears to have a peak at around a 1000µm that is not there when the organic matter has been removed. This would further provide support for the presence of particulate organic matter.

The differences in the particle size distributions before and after organic matter removal are not substantial enough to influence the conclusions drawn in this study. This was therefore not investigated further.

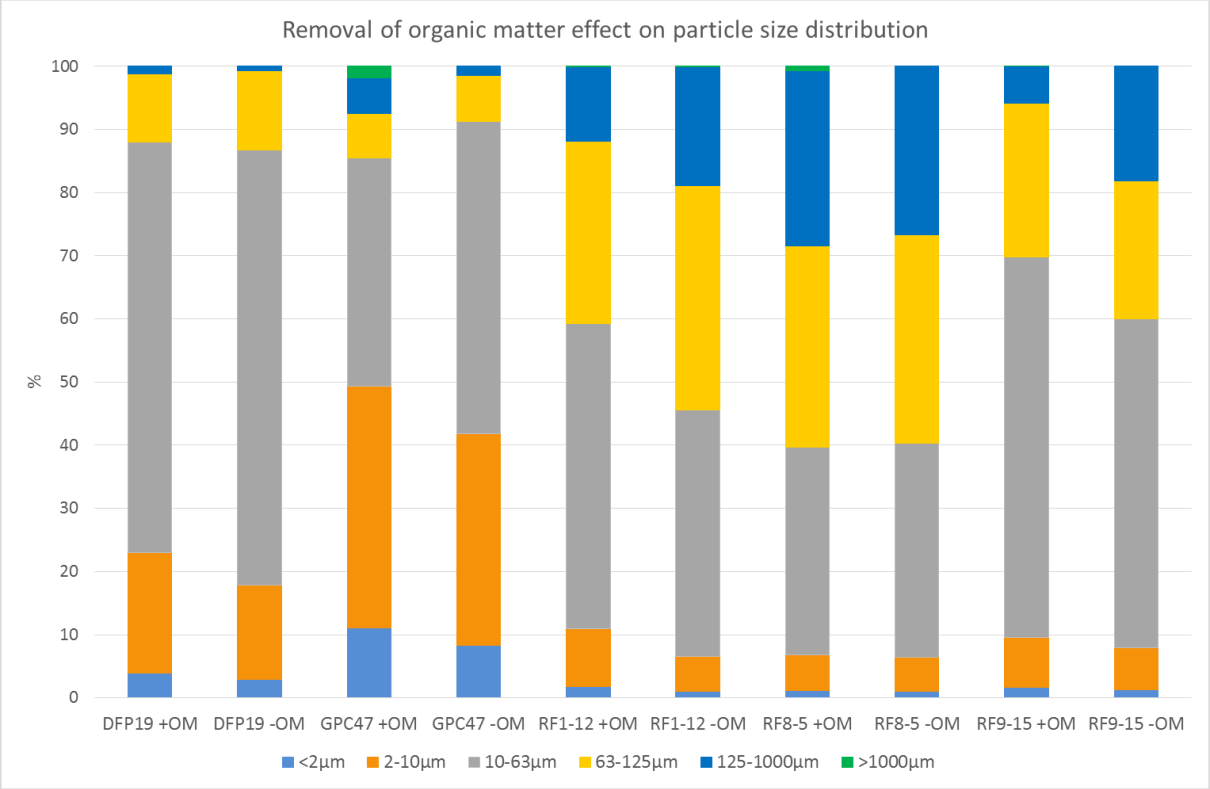

Figure 126 Particle size fractions of selected samples before removal of organic matter (+OM) and after removal of organic matter (-OM).

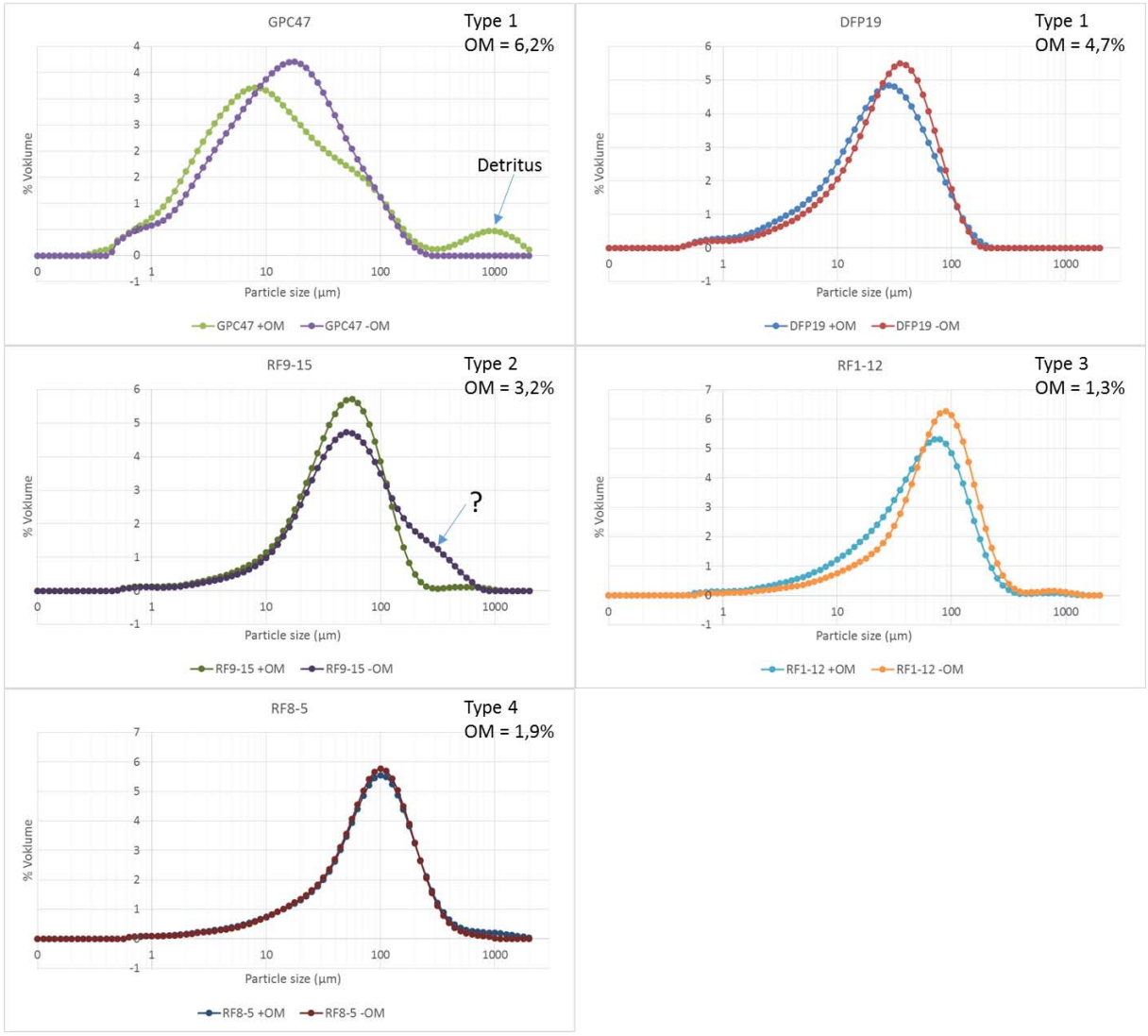

Figure 127 Particle size distributions of selected samples before organic removal (+OM) and after removal of organic matter via LOI (-OM).

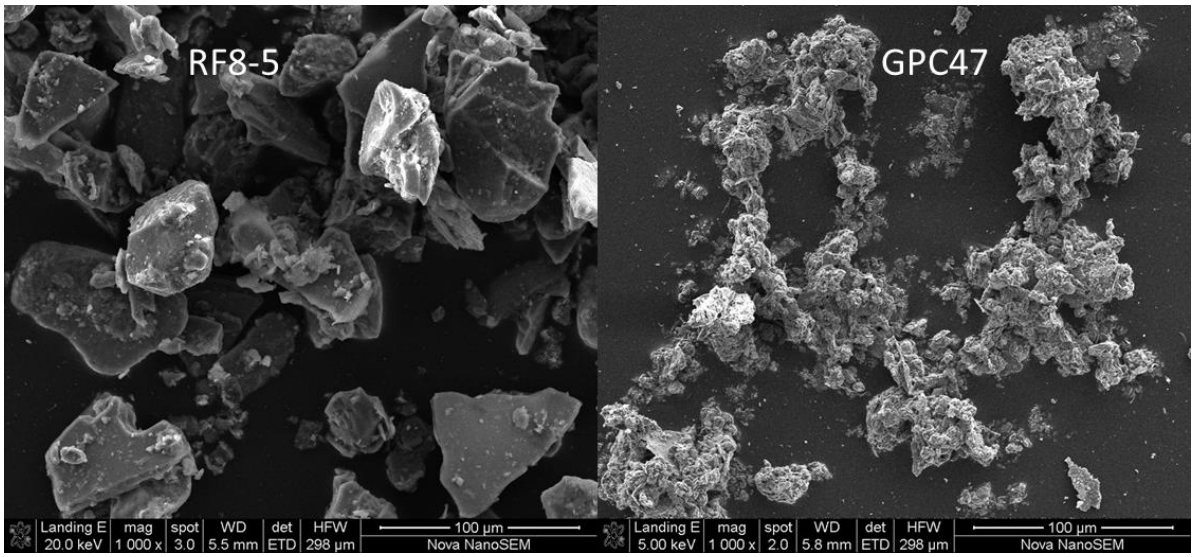

Figure 128 SEM of Type 4 sample RF8-5 compared to Type 1 sample GPC47.

8.3 Tree plot of cluster analysis

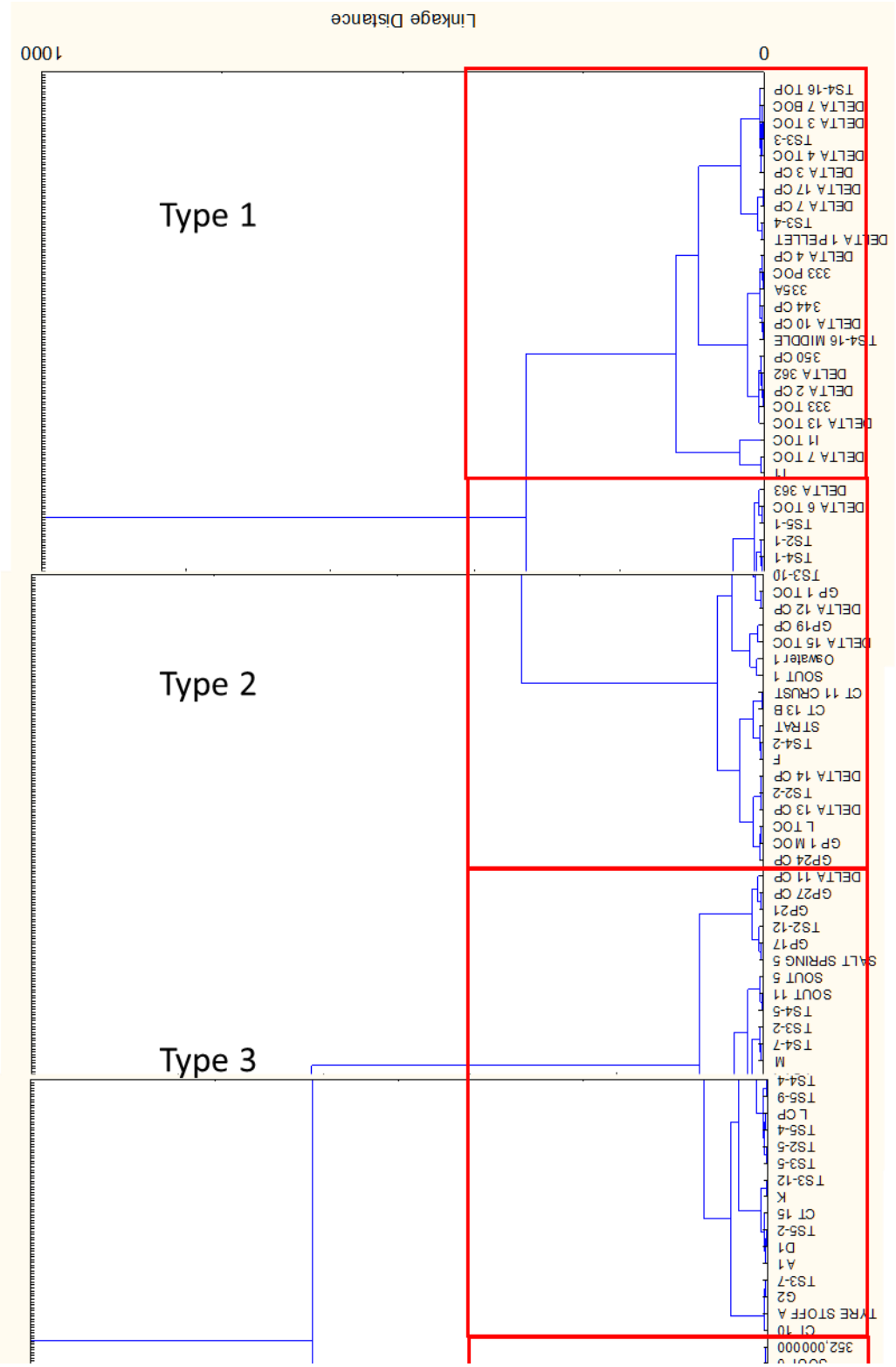

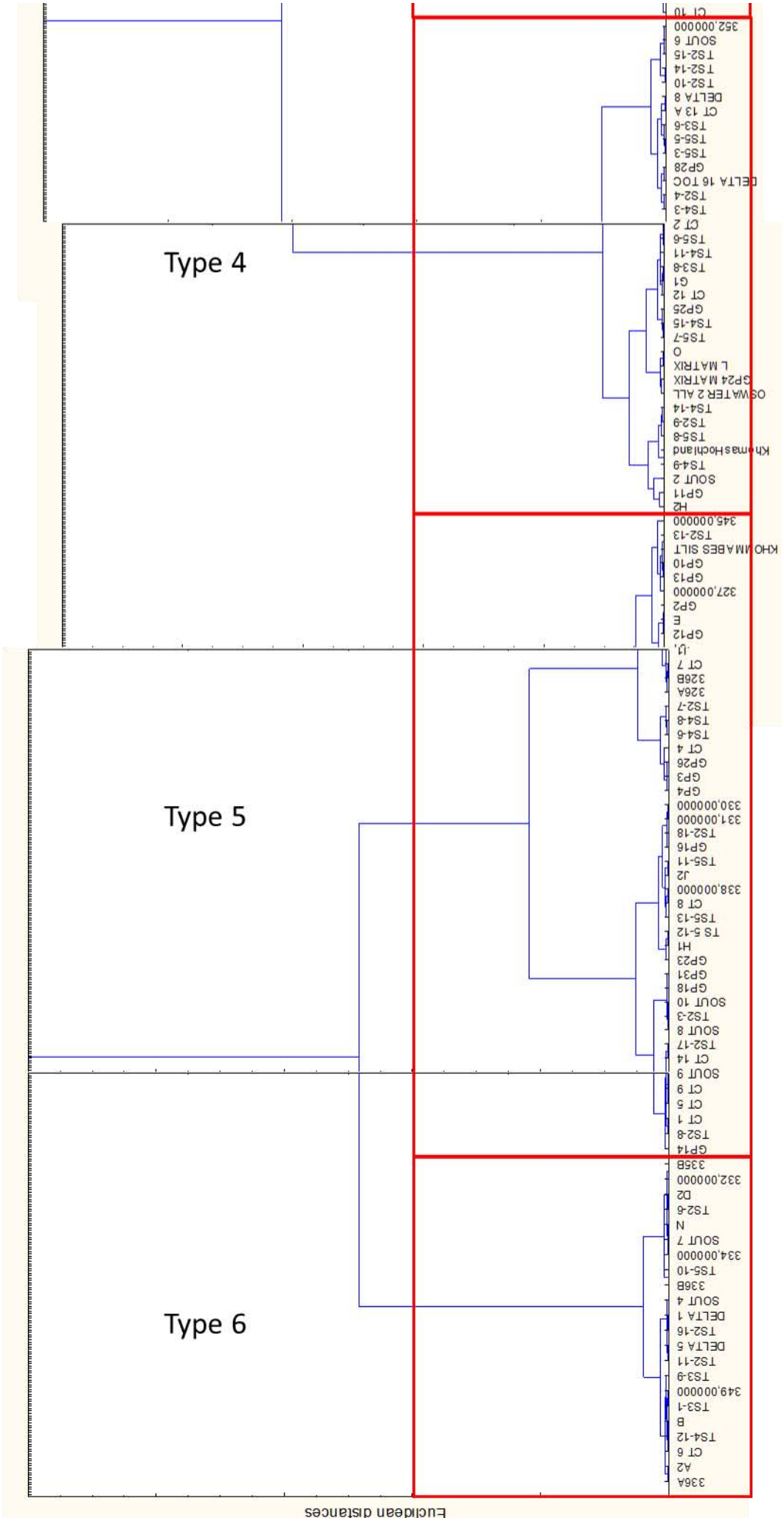
Type 4
Type 5
Type 6

8.4 List of MODIS satellite images used

Image	Day	River	Delta	GP	Sabkhas	Rivers	Unclear	Uncertain	Comments
2005190	09-Jul	1		1	1				
2006181	29-Jun	1	1	1	1	1			
2006182	30-Jun				1				
2007127	06-May		1						Swakop only + delta
2007132	11-May	1		1					
2007168	16-Jun		1						
2007183	01-Jul		1		1				
2007184	02-Jul	1		1					
2007196	14-Jul		1		1				
2008112	21-Apr		1						
2008113	22-Apr		1				1		
2008222	09-Aug			1					
2008224	11-Aug	1	1	1	1				
2009178	26-Jun						1	1	
2009179	27-Jun	1							
2009182	30-Jun			1					
2009185	03-Jul		1		1				
2009186	04-Jul						1	1	
2009187	05-Jul						1	1	
2009188	06-Jul				1		1		
2009189	07-Jul		1				1		
2009190	08-Jul		1		1		1		
2009197	15-Jul		1			1			
2009198	16-Jul		1			1			
2009199	17-Jul		1	1			1		
2009200	18-Jul		1				1		
2009205	23-Jul		1						
2009206	24-Jul		1	1	1				
2009207	25-Jul		1	1	1				
2009208	26-Jul				1				
2010136	15-May						1	1	
2010141	20-May						1	1	
2010142	21-May			1					
2010153	01-Jun						1	1	
2010168	16-Jun		1	1	1				
2010169	17-Jun		1	1			1		
2010175	23-Jun		1				1		
2010177	25-Jun		1						
2010183	01-Jul		1						
2010184	02-Jul						1	1	
2010189	07-Jul		1				1		
2010198	16-Jul		1				1		
2010222	09-Aug			1					
2010223	10-Aug	1		1					
2010224	11-Aug		1	1			1		
2010225	12-Aug		1						
2011153	01-Jun		1				1		
2011177	25-Jun		1						
2011187	05-Jul			1					
2011188	06-Jul		1				1		
2011192	10-Jul		1	1			1		
2011193	11-Jul		1				1		

Image	Day	River	Delta	GP	Sabkhas	Rivers	Unclear	Uncertain	Comments
2011196	14-Jul		1	1					
2011197	15-Jul		1				1		
2011199	17-Jul		1						
2011211	29-Jul			1					
2012094	03-Apr		1						
2012154	02-Jun		1	1			1		
2012156	04-Jun		1						
2012163	11-Jun		1	1					
2012164	12-Jun		1						
2012165	13-Jun		1						
2012198	16-Jul		1	1					
2012199	17-Jul		1						
2012210	28-Jul		1						
2013121	30-Apr		1						
2013124	03-May						1	1	
2013125	04-May		1	1					
2013126	05-May		1	1			1		
2013161	09-Jun		1		1				
2013162	10-Jun		1						
2013168	16-Jun	1	1	1			1		
2013202	20-Jul			1	1				
2013207	25-Jul		1						
2013211	29-Jul						1	1	
2013212	30-Jul		1		1				
		8	52	27	16	3	28	9	

8.5 List of samples

New ID	Sample Name	TYPE	Transect	LOCATION	Way point	Sampling date	Latitude	Longitude	<2 µm	2-10 µm	10-63 µm	63-125 µm	125-1000 µm	>1000 µm
D1	DELTA 1	6	DELTA	DAC		14-09-2012	-23,14606	14,6044167	0,0	0,0	1,9	18,4	79,7	0,0
D1 PELLET	DELTA 1 PELLET	1	DELTA	DFP		14-09-2012	-23,14606	14,6044167	5,2	30,3	58,6	3,9	1,7	0,3
D10	DELTA 10 CP	1	DELTA	DFP	168	14-SEP-12 12:34:30P	-23,13776	14,57878	3,1	16,5	63,2	14,2	2,6	0,4
D11	DELTA 11 CP	3	DELTA	DCC	170	14-SEP-12 1:21:41PM	-23,12912	14,57104	3,6	16,9	45,6	9,7	23,9	0,3
D12	DELTA 12 CP	2	DELTA	DCC	173	14-SEP-12 1:30:35PM	-23,12802	14,56898	3,4	17,4	52,9	16,6	9,7	0,1
D13	DELTA 13 CP	2	DELTA	DCC	181	14-SEP-12 2:22:41PM	-23,1214	14,55259	2,5	12,7	50,4	20,0	14,1	0,3
D14	DELTA 14 CP	2	DELTA	DCC	187	14-SEP-12 2:41:02PM	-23,12095	14,54662	2,9	14,5	50,2	17,5	14,8	0,1
D15	DELTA 15 TOC	2	DELTA	DCC	192	14-SEP-12 2:58:56PM	-23,11788	14,54176	4,3	22,0	53,4	8,5	11,5	0,2
D16	DELTA 16 TOC	4	DELTA	DCC	193	14-SEP-12 3:08:31PM	-23,11659	14,53745	1,4	7,7	31,5	25,7	33,6	0,0
D17	DELTA 17 CP	1	DELTA	DFP	196	14-SEP-12 4:16:12PM	-23,12359	14,5673	5,9	32,8	58,6	2,4	0,3	0,0
D2	DELTA 2 CP	1	DELTA	DFP	157	14-SEP-12 11:14:35A	-23,14519	14,60061	4,0	20,7	63,0	10,4	1,9	0,0
D3	DELTA 3 CP	1	DELTA	DFP	159	14-SEP-12 11:21:03A	-23,14616	14,59802	4,2	24,0	63,8	6,3	1,4	0,2
D4	DELTA 4 CP	1	DELTA	DFP	161	14-SEP-12 11:29:08A	-23,14624	14,59553	3,3	17,7	62,9	13,4	2,7	0,0
D5	DELTA 5	6	DELTA	DAC	164	14-SEP-12 11:37:46A	-23,14624	14,59212	0,0	0,0	1,8	13,9	81,7	2,6
D6	DELTA 6 TOC	2	DELTA	DFP	165	14-SEP-12 11:59:18A	-23,1411	14,58271	2,9	14,3	60,5	19,4	2,9	0,0
D7	DELTA 7 CP	1	DELTA	DFP	165	14-SEP-12 11:59:18A	-23,1411	14,58271	6,6	32,7	56,4	3,0	0,9	0,3
D8	DELTA 8	4	DELTA	DFP	165	14-SEP-12 11:59:18A	-23,1411	14,58271	0,7	4,0	31,2	39,0	25,2	0,0
D19	DELTA 362	1	DELTA	DFP	363	2013-03-30 11:11	-23,0513	14,47705	3,9	19,1	65,1	10,7	1,3	0,0
D20	DELTA 363	2	DELTA	DFP	362	2013-03-30 11:04	-23,05191	14,47027	2,9	12,7	58,0	23,2	3,2	0,0
D18	D359		DELTA	FAN SAND	359				2,3	4,7	4,3	0,5	87,9	0,3
GPBL13	GP13	5	GP	GPBL	249	16-SEP-12 12:07:41P	-23,5240	15,2040	1,2	3,0	11,5	25,2	57,5	1,7
GPBL18	GP18	5	GP	GPBL	256	16-SEP-12 3:35:06PM	-23,5149	15,0428	0,3	1,8	6,1	21,0	66,5	4,4
GPBL2	GP2	5	GP	GPBL	103	12-SEP-12 12:15:33P	-23,0067	14,5964	0,3	1,6	12,1	32,0	50,9	3,1
GPC1	GP1	2	GP	GPC	103	12-SEP-12 12:15:33P	-23,0067	14,59637	3,8	16,9	49,4	21,4	8,3	0,3
GPS11	GP11	4	GP	GPC	246	16-SEP-12 11:36:58A	-23,5554	15,0559	5,6	10,3	14,2	25,2	42,4	2,3
GPC17	GP17	3	GP	GPC	256	16-SEP-12 3:35:06PM	-23,5149	15,0428	4,5	17,4	34,2	20,1	21,2	2,6
GPC19	GP19 CP	2	GP	GPC	?	16-Sep	0,0000		7,1	24,1	43,9	16,7	7,6	0,6
GPC21	GP21	3	GP	GPC	257	16-SEP-12 3:49:10PM	-23,4923	15,0412	4,2	18,4	39,0	15,6	21,6	1,2
GPC23	GP23	5	GP	GPC	259	16-SEP-12 4:03:53PM	-23,4723	15,0408	0,0	0,0	2,0	38,0	59,3	0,7
GPC24-1	GP24 CP	2	GP	GPC	260	16-SEP-12 4:09:00PM	-23,4634	15,0401	4,7	17,2	43,7	21,8	11,8	0,6
GPC25	GP25	4	GP	GPC	261	16-SEP-12 4:11:32PM	-23,4632	15,0401	1,2	4,2	20,6	35,8	37,9	0,3
GPC26	GP26	5	GP	GPC	262	16-SEP-12 4:14:57PM	-23,4633	15,0399	1,2	3,9	12,9	30,6	50,0	1,4
GPC27	GP27 CP	3	GP	GPC	263	16-SEP-12 4:16:41PM	-23,4635	15,0397	5,2	19,2	35,6	21,3	17,9	0,8
GPC28	GP28	4	GP	GPC	264	16-SEP-12 4:24:49PM	-23,4634	15,0396	2,6	8,3	28,4	27,5	30,4	2,9
GPS10	GP10	5	GP	GPS	245	16-SEP-12 11:34:43A	-23,5552	15,0558	1,0	2,9	10,7	31,1	51,6	2,7
GPS12	GP12	5	GP	GPS	249	16-SEP-12 12:07:41P	-23,5240	15,2040	0,6	1,9	10,5	32,7	52,8	1,6
GPS14	GP14	5	GP	GPS	251	16-SEP-12 1:35:00PM	-23,5617	15,0891	0,0	0,2	3,3	19,9	71,1	5,5
GPS16	GP16	5	GP	GPS	255	16-SEP-12 3:30:24PM	-23,5250	15,0408	0,1	1,0	6,9	32,8	56,9	2,4
GPS3	GP3	5	GP	GPS	104	12-SEP-12 1:11:43PM	-23,0502	14,6098	0,8	2,7	15,2	26,7	50,7	3,9
GPS31	GP31	5	GP	GPS	TOC	16-SEP-12 4:35:14PM	-23,4402	15,0406	0,3	2,0	7,5	18,2	66,9	5,1
GPS4	GP4	5	GP	GPS	105	12-SEP-12 1:36:47PM	-23,0384	14,6175	1,4	4,6	12,3	25,5	51,8	4,4
GPBL32	H2	4	GP	GPBL	21	09-SEP-12 4:24:04PM	-23,49616	14,98526	8,2	14,6	10,9	13,2	52,8	0,3
GPC33	TS2-17	5	GP	GPC	97	11-SEP-12 1:28:13PM	-23,35278	14,88888	0,0	1,0	5,8	18,6	65,7	9,0
GPS34	H1	5	GP	GPS	21	09-SEP-12 4:24:04PM	-23,49616	14,98526	0,0	0,1	5,4	30,1	58,7	5,8
GPS35	338	5	GP	GPS		2013-03-28 12:05	-23,3350	14,8307	0,0	0,3	6,9	29,7	60,1	3,0
GPS36	TS2-18	5	GP	GPS	98	11-SEP-12 1:29:46PM	-23,35262	14,88889	0,0	0,3	8,8	28,3	57,4	5,2
GPS37	TS 5-12	5	GP	GPS	150	13-SEP-12 12:30:52P	-23,592230	15,074640	0,0	0,0	4,8	29,9	60,4	4,9
GPC38	J1	5	GP	GPC	23	09-SEP-12 5:04:26PM	-23,44315	14,95851	0,0	0,6	8,0	40,1	50,0	1,3
GPS39	330	5	GP	GPS	330	2013-03-28 09:46	-23,34535	14,82244	0,1	1,4	8,1	30,8	56,4	3,1
GPS40	TS5-13	5	GP	GPS	151	13-SEP-12 12:47:41P	-23,585550	15,074670	0,1	1,4	6,0	26,6	62,2	3,6
GPC50	J2	5	GP	GPC	23	09-SEP-12 5:04:26PM	-23,44315	14,95851	0,2	1,2	8,1	23,5	56,9	10,2
GPS41	326B	5	GP	GPS		2013-03-27 12:24	-23,6039	15,1917	0,2	1,3	9,3	33,6	53,8	1,9
GPS42	331	5	GP	GPS	331	2013-03-28 10:03	-23,34572	14,82253	0,2	1,6	7,8	30,6	57,7	2,0
GPC43	TS2-13	5	GP	GPC	93	11-SEP-12 1:10:24PM	-23,35446	14,88636	0,3	2,2	14,4	23,6	59,4	0,0
GPS44	326A	5	GP	GPS		2013-03-27 12:24	-23,6039	15,1917	0,7	1,7	9,6	31,1	53,7	3,2
GPS45	327	5	GP	GPS		2013-03-27 12:42	-23,5856	15,2263	1,2	3,5	10,5	19,8	62,8	2,2
GPC24-2	GP24 MATRIX	4	GP	GPC	260	16-SEP-12 4:09:00PM	-23,4634	15,0401	2,0	7,1	21,0	24,5	42,7	2,7
GPC46	SALT SPRING 5	3	GP	GPC	270	17-SEP-12 9:40:15AM	-23,5108	15,0652	4,7	18,5	33,8	13,7	26,2	3,1
GPC47	I1	1	GP	GPC	22	09-SEP-12 4:44:23PM	-23,48255	14,98008	11,4	38,7	36,3	7,1	5,2	1,3
GPC48	SOUT 2	4	GP	GPC	226	15-SEP-12 4:08:08PM	-23,52796	15,02041	3,7	14,0	24,7	16,5	37,0	4,1
GPC49	SOUT 1	2	GP	GPC	224	15-SEP-12 4:04:03PM	-23,52843	15,02132	6,4	28,3	34,8	9,5	16,5	4,5
ID	KHOMMABES SILT	5	ID	ID			-23,5357	14,9961	0,3	2,2	14,1	25,9	57,5	0,0
RAC1-1	TS3-1	6	RT1	RAC	106	12-SEP-12 2:13:01PM	-23,18173	14,64606	0,0	0,0	2,4	7,4	90,1	0,1
RF1-10	TS3-10	2	RT1	RL	114	12-SEP-12 3:24:21PM	-23,18418	14,64129	2,7	14,8	61,5	8,9	12,1	0,0
RF1-12	TS3-12	3	RT1	RL	118	12-SEP-12 3:40:24PM	-23,18438	14,63918	1,8	9,2	48,4	28,8	11,8	0,1
RF1-2	TS3-2	3	RT1	RL	107	12-SEP-12 2:29:40PM	-23,18319	14,64356	1,7	9,3	48,8	19,1	21,1	0,0
RF1-3	TS3-3	1	RT1	RL	108	12-SEP-12 2:34:05PM	-23,18324	14,64352	4,2	23,8	65,7	6,1	0,2	0,0
RF1-4	TS3-4	1	RT1	RL		12-Sep-12	-23,18350	14,64247	4,7	28,2	61,2	4,5	1,3	0,1
RF1-5	TS3-5	3	RT1	RL	111	12-SEP-12 2:52:02PM	-23,18349	14,64227	1,5	7,8	43,2	28,6	18,9	0,1
RF1-6	TS3-6	4	RT1	RL	112	12-SEP-12 3:02:40PM	-23,18403	14,6416	0,9	4,2	33,5	33,5	27,4	0,5
RF1-7	TS3-7	3	RT1	RL	112	12-SEP-12 3:02:40PM	-23,18403	14,6416	1,0	3,6	40,9	37,4	17,0	0,2
RF1-9	TS3-9	6	RT1	RL	113	12-SEP-12 3:14:24PM	-23,18398	14,64149	0,2	1,6	2,0	4,3	92,0	0,0
RFBL1-8	TS3-8	4	RT1	BL	112	12-SEP-12 3:02:40PM	-23,18403	14,6416	0,4	2,8	25,3	38,6	32,6	0,3
RF1-15	349	6	RT1	RL	349	2013-03-29 12:20	-23,185	14,6406	0,0	0,1	2,9	6,3	90,5	0,2
RF1-14	345	5	RT1	RL	345	2013-03-29 12:04	-23,1847	14,63942	0,8	4,5	18,3	9,5	67,0	0,1
RF1-16	350 CP	1	RT1	RL	351	2013-03-30 12:23	-23,18477	14,6415	3,6	21,1	65,9	6,3	2,6	0,4
RF1-13	344 CP	1	RT1	RL	344	2013-03-29 11:57	-23,18397	14,64152	2,4	13,9	67,8	12,0	3,8	0,1
RF1-17	352	4	RT1	RL	352	2013-03-29 12:30	-23,18479	14,642	0,5	3,1	28,8	38,2	29,3	0,1
RF2-12	TS4-12	6	RT2	RL	130	12-SEP-12 6:05:34PM	-23,28421	14,75237	0,0	0,0	2,3	9,2	88,4	0,0
RFBL2-6	TS4-6	5	RT2	BL	124	12-SEP-12 5:42:28PM	-23,28218	14,7551	0,3	3,0	18,8	26,1	51,6	0,1
RF2-8	TS4-8	5	RT2	RL	126	12-SEP-12 5:51:15PM	-23,28271	14,75454	0,6	3,3	18,0	29,7	48,4	0,0
RF2-9	TS4-9	4	RT2	RL	127	12-SEP-12 5:53:32PM	-23,28289	14,75389	1,0	6,0	27,3	20,8	44,8	0,0
RF2-14	TS4-14	4	RT2	RL	134	12-SEP-12 6:16:53PM	-23,28639	14,74886	1,5	7,7	29,8	19,3	41,4	0,3
RF2-3	TS4-3	4	RT2	RL	122	12-SEP-12 5:38:07PM	-23,28203	14,75549	1,1	5,5	30,4	28,5	34,1	0,5
RF2-15	TS4-15	4	RT2	RL	136	12-SEP-12 6:45:42PM	-23,28409	14,75272	0,3	2,3	21,1	38,8	37,4	0,2
RFBL2-11	TS4-11	4	RT2	BL	128	12-SEP-12 5:57:05PM	-23,28311	14,75358	0,4	2,8	23,5	36,5	36,2	0,6
RF2-5	TS4-5	3	RT2	RL	124	12-SEP-12 5:42:28PM	-23,28218	14,7551	1,7	9,5	38,6	23,9	26,3	0,0
RF2-4	TS4-4	3	RT2	RL	123	12-SEP-12 5:40:35PM	-23,28212	14,75533	1,8	9,0	43,8	23,6	21,7	0,2
RF2-7	TS4-7	3	RT2	RL	125	12-SEP-12 5:49:17PM	-23,28246	14,75482	1,8	9,5	45,3	22,4	20,6	0,4
RF2-2	TS4-2	2	RT2	RL	121	12-SEP-12 5:34:00PM	-23,2818	14,75586	1,7	9,1	54,6	24,9	9,4	0,3
RF2-1	TS4-1	2	RT2	RL	119	12-SEP-12 5:21:55PM	-23,27915	14,75899	2,8	14,1	60,0	13,1	9,9	0,1
RF2-16	TS4-16	1	RT2	RL	137	12-SEP-12 6:58:05PM	-23,28095	14,75785	3,1	18,6	68,8	7,4	1,9	0,2
RF3-6	336A	6	RT3	RL	336A	2013-03-28 10:38	-23,35146	14,82161	0,0	0,0	0,1	11,3	88,5	0,1
RAC3-3	334	6	RT3	RAC	334	2013-03-28 10:15	-23,34753	14,82253	0,0	0,0	0,9	1,9	97,2	0,0
RF3-1	332	6	RT3	RL	332	2013-03-28 10:07	-23,34607	14,82238	0,0	0,0	0,0	9,5	90,5	0,0
RAC3-5	335B	6	RT3	RAC	335B	2013-03-28 10:24	-23,35002	14,82215	0,0	0,0	0,0	6,8	93,2	0,0
RF3-4	335A	1	RT3	RL	335A	2013-03-28 10:24	-23,35002	14,82215	3,0	16,8	65,6	9,9	4,3	0,4
RF3-2	333 POC	1	RT3	RL	333	2013-03-28 10:10	-23,34633	14,82225	3,3	18,0	64,4	10,2	3,8	0,2

New ID	Sample Name	TYPE	Transect	LOCATION	Way point	Sampling date	Latitude	Longitude	<2 µm	2-10 µm	10-63 µm	63-125 µm	125-1000 µm	>1000 µm
RF4-16	TS2-1	2	RT4	RM	73	11-SEP-12 11:06:31A	-23,37224	14,87382	2,5	13,6	58,2	16,0	9,9	0,0
RF4-7	TS2-10	4	RT4	RM	88	11-SEP-12 12:37:46P	-23,36432	14,88389	0,7	4,1	29,2	27,1	38,8	0,1
RF4-6	TS2-11	6	RT4	RM	89	11-SEP-12 12:47:42P	-23,36135	14,88395	0,0	0,0	2,2	13,0	80,8	4,1
RF4-5	TS2-12	3	RT4	RM	91	11-SEP-12 12:52:13P	-23,36021	14,88373	3,4	15,0	40,4	12,9	28,0	0,3
RF4-3	TS2-14	4	RT4	RM	94	11-SEP-12 1:14:02PM	-23,35426	14,88672	1,0	4,3	29,2	27,1	38,4	0,1
RF4-2	TS2-15	4	RT4	RM	95	11-SEP-12 1:18:06PM	-23,35363	14,88777	0,7	3,2	30,7	31,9	33,5	0,0
RF4-1	TS2-16	6	RT4	RM	96	11-SEP-12 1:21:42PM	-23,35344	14,88801	0,0	0,0	2,7	13,0	84,1	0,2
RF4-15	TS2-2	2	RT4	RM	73	11-SEP-12 11:06:31A	-23,37224	14,87382	2,5	13,0	53,4	14,8	16,3	0,0
RF4-14	TS2-3	5	RT4	RM	75	11-SEP-12 11:24:39A	-23,37171	14,87478	0,0	1,2	9,0	17,8	72,0	0,0
RF4-13	TS2-4	4	RT4	RM	76	11-SEP-12 11:29:59A	-23,37128	14,87541	0,9	4,7	32,7	28,4	32,6	0,6
RF4-12	TS2-5	3	RT2	RM	77	11-SEP-12 11:36:02A	-23,37082	14,87604	1,4	6,9	45,0	28,3	18,1	0,4
RAC4-11	TS2-6	6	RT4	RAC	79	11-SEP-12 11:46:47A	-23,3699	14,87757	0,0	0,0	1,6	4,4	94,0	0,0
RF4-10	TS2-7	5	RT4	RM	81	11-SEP-12 12:05:29P	-23,36896	14,87992	0,3	2,9	22,3	23,0	51,5	0,0
RF4-9	TS2-8	5	RT4	RM	86	11-SEP-12 12:27:09P	-23,36631	14,88301	0,0	0,8	7,3	11,9	79,9	0,0
RF4-8	TS2-9	4	RT4	RM	87	11-SEP-12 12:30:37P	-23,36622	14,88321	1,3	6,7	28,0	22,3	41,7	0,0
RF5-1	K	3	RT5	RM	27	09-SEP-12 5:29:18PM	-23,41005	14,91952	1,7	8,2	48,1	29,9	12,0	0,1
RF5-2	L CP	3	RT5	RM	38	09-SEP-12 5:35:57PM	-23,41035	14,91874	1,8	7,9	41,0	31,2	17,9	0,2
RF5-3	L MATRIX	4	RT5	RM	38	09-SEP-12 5:35:57PM	-23,41035	14,91874	1,2	4,7	20,4	26,8	46,6	0,4
RF5-4	M	3	RT5	RM	42	09-SEP-12 5:58:09PM	-23,41423	14,91236	1,9	10,1	46,5	15,4	26,1	0,0
RAC5-5	N	6	RT5	RAC	43	09-SEP-12 6:01:30PM	-23,41443	14,91216	0,0	0,0	1,0	3,8	95,3	0,0
RF5-6	O	4	RT5	RM	60	09-SEP-12 6:07:36PM	-23,41552	14,91028	0,8	4,4	22,8	24,0	48,0	0,0
RF6-1	A1	3	RT6	RM	14	09-SEP-12 3:18:53PM	-23,50294	14,97504	1,5	7,6	48,7	24,9	17,2	0,1
RFBL6-2	A2	6	RT6	BL	14	09-SEP-12 3:18:53PM	-23,50294	14,97504	0,0	0,0	0,4	15,1	84,5	0,0
RAC6-3	B	6	RT6	RAC	15	09-SEP-12 3:26:21PM	-23,50329	14,97482	0,0	0,0	2,3	6,9	90,7	0,1
RF6-4	D1	3	RT6	RM	17	09-SEP-12 3:40:53PM	-23,50421	14,97429	1,5	7,4	48,4	28,0	14,8	0,0
RFBL6-5	D2	6	RT6	BL	17	09-SEP-12 3:40:53PM	-23,50421	14,97429	0,0	0,0	1,1	3,0	95,9	0,0
RF6-6	E	5	RT6	RM	18	09-SEP-12 3:45:31PM	-23,50421	14,9742	0,0	1,2	12,0	34,3	52,4	0,1
RF6-7	F	2	RT6	RM	19	09-SEP-12 3:51:55PM	-23,5037	14,9742	1,7	8,8	53,3	24,6	11,3	0,2
RF6-8	G1	4	RT6	RM	20	09-SEP-12 4:04:10PM	-23,50309	14,97446	0,5	3,1	26,2	34,6	35,3	0,3
RF6-9	G2	3	RT6	RM	20	09-SEP-12 4:04:10PM	-23,50309	14,97446	0,9	4,5	39,6	35,7	19,2	0,1
UNKNOWN	STRAT	2	RT6	UNKNOWN					1,8	8,5	56,1	25,9	7,5	0,2
FGP7-10	SOUT 10	5	RT7	RU	238	15-SEP-12 5:30:00PM	-23,53070	15,01704	0,1	1,5	9,4	15,3	73,8	0,0
RF7-11	SOUT 11	3	RT7	RU	242	15-SEP-12 5:50:20PM	-23,52994	15,01737	1,8	9,7	39,0	24,1	25,3	0,2
RF7-4	SOUT 4	6	RT7	RU	228	15-SEP-12 4:14:49PM	-23,52853	15,01937	0,1	1,2	2,3	8,9	72,8	14,7
RF7-5	SOUT 5	3	RT7	RU	230	15-SEP-12 4:33:56PM	-23,52869	15,01923	2,5	8,8	37,1	29,7	21,3	0,6
RF7-6	SOUT 6	4	RT7	RU	230	15-SEP-12 4:33:56PM	-23,52869	15,01923	1,1	4,0	27,9	35,4	31,1	0,4
RAC7-7	SOUT 7	6	RT7	RAC	233	15-SEP-12 4:55:37PM	-23,52902	15,01866	0,0	0,0	1,1	1,9	96,9	0,0
RF7-8	SOUT 8	5	RT7	RU	234	15-SEP-12 5:01:37PM	-23,52973	15,01807	0,0	1,2	8,5	18,3	71,9	0,0
FGP7-9	SOUT 9	5	RT7	RU	237	15-SEP-12 5:16:09PM	-23,53262	15,01671	0,0	0,2	6,4	16,0	77,4	0,0
RF8-1	TS5-1	2	RT8	RU	138	13-SEP-12 10:49:32A	-23,590420	15,071790	3,1	15,6	61,8	14,3	4,8	0,5
RAC8-10	TS5-10	6	RT8	RAC	147	13-SEP-12 12:13:16P	-23,592820	15,073930	0,0	0,0	0,0	1,9	98,1	0,0
RF8-11	TS5-11	5	RT8	RU	149	13-SEP-12 12:26:12P	-23,592380	15,074350	0,0	1,4	9,3	24,0	65,1	0,2
RFBL8-2	TS5-2	3	RT8	BL	138	13-SEP-12 10:49:32A	-23,590420	15,071790	1,5	7,4	47,4	29,8	13,7	0,2
RF8-3	TS5-3	4	RT8	RU	139	13-SEP-12 11:03:33A	-23,590340	15,072150	1,0	4,9	33,7	30,1	29,5	0,8
RF8-4	TS5-4	3	RT8	RU	140	13-SEP-12 11:07:17A	-23,590530	15,072330	1,6	7,5	42,9	25,2	20,9	1,9
RF8-5	TS5-5	4	RT8	RU	141	13-SEP-12 11:14:40A	-23,591120	15,072530	1,2	5,7	32,9	31,8	27,8	0,7
RF8-6	TS5-6	4	RT8	RU	142	13-SEP-12 11:21:43A	-23,591830	15,072750	0,2	2,2	24,4	36,3	36,3	0,5
RF8-7	TS5-7	4	RT8	RU	142	13-SEP-12 11:21:43A	-23,591830	15,072750	0,3	2,6	21,9	33,5	40,9	0,7
RF8-8	TS5-8	4	RT8	RU	144	13-SEP-12 11:58:19A	-23,593390	15,072010	1,4	7,2	32,1	9,4	49,8	0,0
RF8-9	TS5-9	3	RT8	RU	145	13-SEP-12 12:03:43P	-23,593430	15,073020	1,5	7,9	45,4	20,6	24,6	0,0
RF9-1	CT 1	5	RT9	RU	208	15-SEP-12 12:38:59P	-23,638490	15,184220	0,0	1,0	6,3	16,1	75,0	1,5
RF9-10	CT 10	3	RT9	RU	214	15-SEP-12 1:03:31PM	-23,639410	15,183710	0,9	3,7	38,0	37,0	20,1	0,3
RF9-11	CT 11 CRUST	2	RT9	RU	215	15-SEP-12 1:09:23PM	-23,639740	15,184120	1,8	9,4	60,0	23,0	5,7	0,1
RFBL9-12	CT 12	4	RT9	BL	215	15-SEP-12 1:09:23PM	-23,639740	15,184120	0,7	3,7	26,8	29,9	38,9	0,0
RF9-14	CT 13 A	4	RT9	RU	218	15-SEP-12 1:17:57PM	-23,640150	15,183980	0,8	3,5	31,0	37,5	26,8	0,3
RF9-15	CT 13 B	2	RT9	RU	218	15-SEP-12 1:17:57PM	-23,640150	15,183980	1,6	8,0	60,2	24,3	5,9	0,0
RF9-16	CT 14	5	RT9	RU	221	15-SEP-12 1:28:19PM	-23,640820	15,182570	0,0	0,9	6,7	21,4	71,1	0,0
RF9-13	CT 15	3	RT9	RU	222	15-SEP-12 1:35:15PM	-23,639930	15,183720	1,3	6,1	46,6	30,7	15,0	0,2
RF9-2	CT 2	4	RT9	RU	209	15-SEP-12 12:41:16P	-23,638590	15,184230	0,5	2,2	23,3	39,5	33,8	0,7
RF9-4	CT 4	5	RT9	RU	210	15-SEP-12 12:48:48P	-23,638740	15,183880	0,2	1,8	15,8	35,5	45,7	1,0
RF9-5	CT 5	5	RT9	RU	210	15-SEP-12 12:48:48P	-23,638740	15,183880	0,0	0,8	4,8	18,7	73,2	2,5
RAC9-6	CT 6	6	RT9	RAC	211	15-SEP-12 12:53:42P	-23,638940	15,183740	0,0	0,0	2,4	7,5	90,2	0,0
RF9-7	CT 7	5	RT9	RU	212	15-SEP-12 12:58:47P	-23,639060	15,183610	0,0	1,0	9,7	34,8	53,8	0,6
RF9-8	CT 8	5	RT9	RU	213	15-SEP-12 1:01:30PM	-23,639190	15,183570	0,0	0,2	5,8	33,9	60,1	0,0
RF9-9	CT 9	5	RT9	RU	214	15-SEP-12 1:03:31PM	-23,639410	15,183710	0,0	0,6	5,1	21,2	73,0	0,0
RF9-17	Oswater 1	2	RT9	RU	207	15-SEP-12 12:16:32P	-23,63265	15,17076	5,5	21,7	42,0	15,7	14,0	1,1
RF9-18	OSWATER 2 ALL	4	RT9	BL	207	15-SEP-12 12:16:32P	-23,6327	15,1708	1,3	6,7	23,3	16,3	48,8	3,7
SS	336B	6		SS	336B	2013-03-29 10:38	-23,35155	14,82161	0,0	0,0	0,0	0,0	100,0	0,0
UNKNOWN	TYRE STOFF A	3	UNKNOWN	UNKNOWN					2,4	5,7	36,8	36,1	19,0	0,0
KH	Khomas Hochland	4	VAR	HIGHLAND	367	2013-04-03 10:12	-22,53627	16,9413	0,6	5,1	28,2	19,8	44,1	2,2

Note that the sample names were changed to make the analysis and discussion les confusing.

8.6 Cluster summary statistics

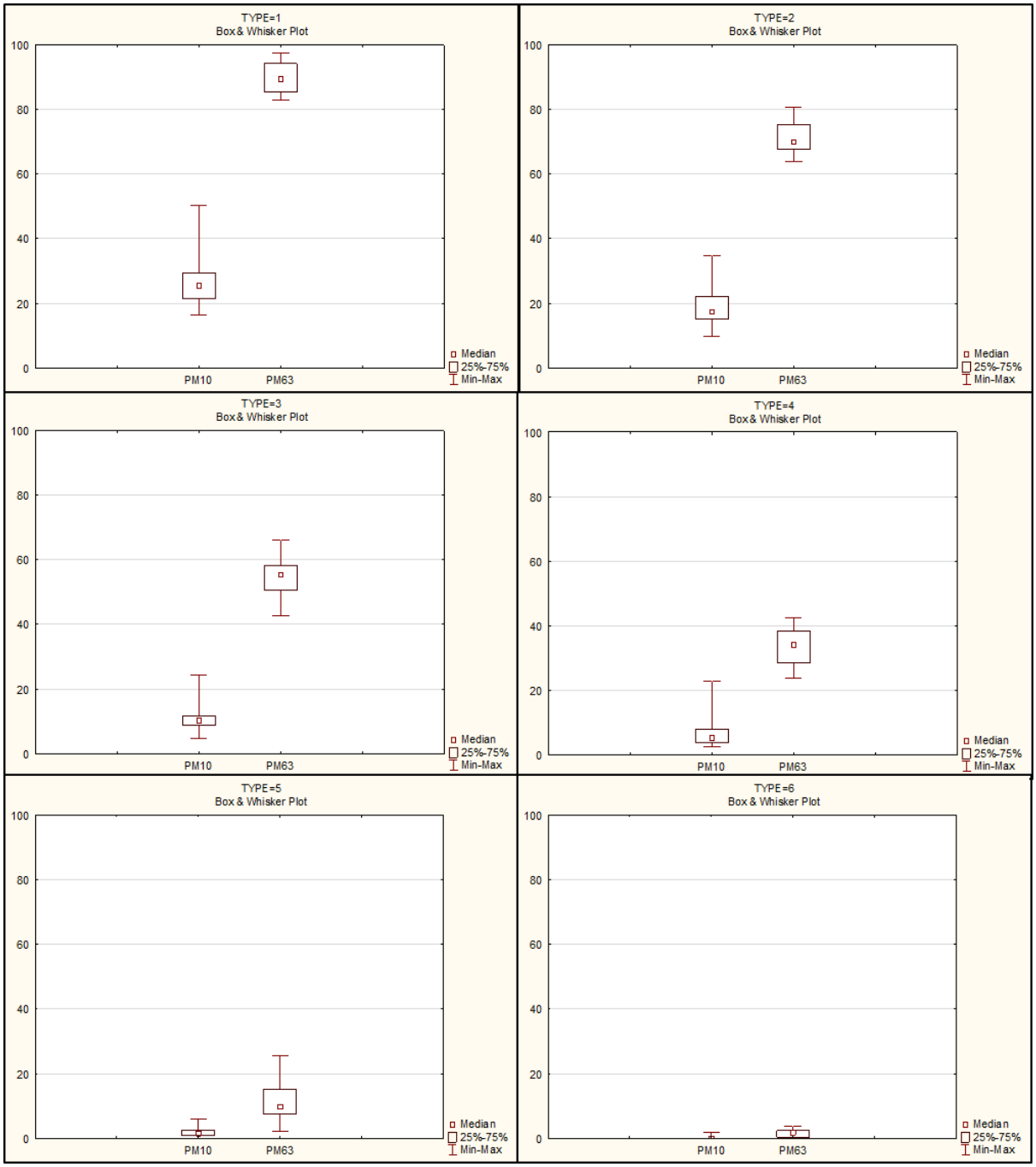

8.7 Acid fumigation-dry combustion method.

The acid fumigation-dry combustion method is the method used to measure organic carbon in the University of Stellenbosch, Department of Soil Science (Dr A.G. Hardie, personal communication, 18/09/2013). Contact details: aghardie@sun.ac.za.

This method involves grinding the sample very finely, after which it is wetted to gravimetric water holding capacity. The samples is placed in a sealed chamber (like a desiccator) with a beaker of concentrated HCl and allowed to react for 3-7 days to slowly dissolve the carbonates. The sample is then dried at 40°C and then analysed with a dry combustion CN analyser. The CN analyser combusts the sample at 1800°C in the presence of a catalyst and the CO_2 evolved is measured using gas chromatography. It is not advisable to add the HCl to the sample directly as it can result in the loss of organic carbon. This is due to hydrolysis reactions and therefore results in the removal of not only the carbonates.